ELECTROCHEMICAL CHLORIDE EXTRACTION TO HALT CORROSION OF REINFORCEMENT

MOHAMMAD BIN ISMAIL

Doctor of Philosophy

ASTON UNIVERSITY

May 1998

ASTON UNIVERSITY

ELECTROCHEMICAL CHLORIDE EXTRACTION TO HALT CORROSION OF REINFORCEMENT

Mohammad bin ISMAIL **Doctor of Philosophy 1998**

ABSTRACT

This thesis presents results of experiments designed to study the effect of applying electrochemical chloride extraction (ECE) to a range of different hardened cement pastes. Rectangular prism specimens of hydrated cement paste containing sodium chloride at different concentrations were subjected to electrolysis between the embedded steel cathodes and external anodes of activated titanium mesh. The cathodic current density used was in the range of 1 to 5 A/m^2 with treatment periods of 4 to 12 weeks. After treatment, the specimens were cut into sections which were subjected to pore-solution expression and analysis in order to determine changes in the distribution of free and total ionic species. The effect of the ECE treatment on the physical and microstructural properties of the cements was studied by using microhardness and MIP techniques. XRD was employed to look at the possibility of ettringite redistribution as a result of the accumulation of soluble sulphate ions in the cement matrix near the cathode during ECE.

Remigration of chloride which remains after the ECE treatment and distribution of other ions were studied by analysing specimens which had been stored for several months, after undergoing ECE treatment. The potentials of the steel cathodes were also monitored over the period to detect any changes in their corrosion state.

The main findings of this research were as follows:

- ECE, as applied in this investigation, was capable of removing both free and bound chloride. The removal process occurred relatively quickly and an equilibrium between free and bound chlorides in the specimens was maintained throughout. At the same time, alkali concentrations in the pore solution near the steel cathode increased. The soluble sulphate ionic concentration near the cathode also increased due to the local increase in the pH of the pore solution.
- ECE caused some changes in physical and microstructural of the cement matrix. However these changes were minimal and in the case of microhardness, the results were highly scattered. Ettringite in the bulk material well away from the cathode was found not to increase significantly with the increase in charge passed.
- Remigration of chloride and other ionic species occurred slowly after cessation of ECE with a resultant gradual increase in the Cl^-/OH^- ratio around the steel.
- The removal of chloride from blended cements was slower than that from OPC

KEY WORDS: Electrochemical Chloride Extraction, Electromigration, Remigration, Corrosion, Passivation, Durability.

ACKNOWLEDGMENTS

The author is deeply indebted to Professor C.L.Page under whose supervision this research project was conducted, and whose knowledge, expertise, guidance and support are greatly appreciated.

Thank you to Universiti Teknologi Malaysia and the Government of Malaysia which provided funding and financial support for this research at Aston University.

Thanks also to the technical staff in the Civil Engineering Department, in particular C.J.Thompson, Dr. M.Page, Dr. Li, P.Green and W.Curtis for their assistance with laboratory work.

I would like to thank my friends and colleagues G.Abdelaziz, G.Chadbourn, D.Anstice, G.Seneviratne, P.Purnell and my fellow Malaysian friends, for their stimulating discussions, motivation, assistance and humor during the course of this research.

I am particularly grateful to my friend Dr. G.Sergi for his constructive criticism and patience in reading through this thesis.

The author appreciates very much the support given by his wife Sarah and children Husna, Hanif, Harish and Hana' for their loving and moral support and encouragement throughout his stay at Aston. Finally the author wishes to express his sincere appreciation to his mother, Sakdiah and his late father, Ismail who value knowledge in its true sense. It is to them this thesis is dedicated.

GLOSSARY OF ABBREVIATIONS

C_3A	-	Tricalcium Aluminate ($3CaO.Al_2O_3$)
$Ca(OH)_2$	-	Calcium Hydroxide
C_4AF	-	Tetracalcium Aluminoferrite ($4CaO.Al_2O_3.Fe_2O_3$)
Cl^-	-	Chloride Ion
Cl^-/OH^-		Chloride to hydroxyl ion ratio
CP		Cathodic protection
C_2S	-	Dicalcium Silicate ($2CaO.SiO_2$)
C_3S	-	Tricalcium Silicate ($3CaO.SiO_2$)
C-S-H	-	Calcium Silicate Hydrate ($CaO.SiO_2.H_2O$)
E	-	Ettringite ($C_3A.3CS.H_{32}$)
ECE	-	Electrochemical Chloride Removal
Hk	-	Hardness Knoop
GGBS	-	Ground Granulated Blast Furnace Slag
K^+	-	Potassium Ion
MIP	-	Mercury Intrusion Porosimetry
Na^+	-	Sodium Ion
NaCl	-	Sodium Chloride
OH^-	-	Hydroxyl Ion
OPC	-	Ordinary Portland Cement
PFA	-	Pulverized Fuel Ash
PSD	-	Pore Size Distribution
RH	-	Relative Humidity
SO_4^{2-}	-	Sulphate Ion
W/C	-	Water Cement Ratio
XRD	-	X-Ray Diffraction

TABLE OF CONTENTS

PAGE

LIST OF TABLES

LIST OF FIGURES

CHAPTER 1

INTRODUCTION

1.1 INTRODUCTION

Concrete was originally a Latin word "Concretus" meaning compounded. This compound consists of a graded range of stone aggregate particles bound together by hardened cement paste. The use of concrete as a construction material has been traced back several thousand years to the ancient Egyptians, the Greeks and the Romans. The composition of early concrete was based on lime, and later the Romans developed pozzolanic cement and lightweight concrete based on pumice [Davey, 1961 and Neville, 1995]. During the Norman period structures such as the Reading Abbey and the foundations to Salisbury Cathedral were constructed from concrete. In 1756 Eddystone lighthouse was rebuilt by Smeaton by mixing pozzolana with limestone containing a considerable proportion of clay material. James Parker developed Roman cement by calcining nodules of argillaceous limestone. Joseph Aspdin took out his patent for 'a superior cement resembling portland stone' used for concrete to construct the Thames Tunnel in 1824. The use of reinforcement in concrete is variously attributed to William Wilkinson, who first patented the method of producing reinforced concrete for a concrete beam in 1854, Lambot in 1855 for ferrocement boats, Monier in 1867 and to Hennebique in 1897 who built the first reinforced concrete frame building in Britain at Weaver's Mill, Swansea.

Today, reinforced concrete is widely used throughout the world as a major material of construction. The aqueous environment in concrete is alkaline in nature due to the presence of the hydroxides of sodium, potassium and calcium produced during hydration. The concrete cover provides a physical barrier to many of the aggressive agents which can attack the reinforcing steel. In this environment the steel is passive and, should small breaks occur in its protective oxide film, they are soon repaired. Two ways in which this passivity can be destroyed are by carbonation, whereby the concrete's alkalinity is reduced due to neutralisation with atmospheric carbon dioxide and sulphur dioxide [Strecker, 1987] or by depassivating anions such as chlorides which

able to reach the steel [Hansson, 1984]. Once the passivity is destroyed the steel is open to corrosion.

Corrosion of reinforcement is one of the major factors in the deterioration of reinforced concrete. In North America alone the estimated cost of restoration of structures suffering from corrosion of reinforcement is in the order of ten billion dollars [Hansson and Hansson, 1993]. In the UK, the work has been estimated to be equivalent to 10% of the cost of new concrete construction or £500 million. Similar figures have been found in Europe but the situation is worse in the Middle East due to more severe conditions [Society for the Cathodic Protection of Reinforced Concrete, Report No.001.95]. Knowledge on methods to stop corrosion from occurring is therefore valuable and contributes to world needs.

Repair to concrete suffering from corrosion of reinforcement may take various forms. The traditional patch repair, which involves the removal of the contaminated concrete and its replacement with a repair material, has proved in many cases to be ineffective [Thompson, 1991]. Chlorides which are left in the unrepaired section could develop what is known as incipient anode activation [Vassie, 1984]. Incompatibility of the repair material with the original concrete could result in shrinkage which could then lead to further chloride penetration [Keer et al., 1990]. In addition in cases where extensive treatment is required and where the provision of temporary support is necessary high cost could be incurred [Wallbank, 1989].

Cathodic protection has been used successfully on reinforced concrete structures for the last 20 years. This electrochemical technique depresses the potential of the reinforcing steel throughout the structure to a level at which pitting corrosion of the metal is suppressed. To achieve this, an electrical contact has to be made between reinforcement and an external anode which is placed at the surface of the concrete. The current density normally used in this treatment is less than 20 mA/m^2. The disadvantage of this method is that it has to be kept in place for the remaining lifetime of the structure, which is expensive and difficult to maintain.

A new approach is electrochemical chloride extraction (ECE), sometimes known as desalination. This method is similar to CP but the treatment is temporary and completed

in a relatively short time. Electrochemical chloride extraction, will be discussed in detail in the remaining parts of this thesis.

1.2 BACKGROUND OF THE PROBLEM

The electrochemical extraction of chloride ion is being used increasingly in chloride contaminated concrete [Miller, 1990 and Bennett et al., 1994]. A direct current is applied between the reinforcement and a temporary external electrode (anode) in electrolytic contact with the concrete. The reinforcement is connected as the cathode. When the current is induced, the negatively charged ions (chloride, hydroxyl and sulphate) migrate towards the anode and at the same time positively charged ions (sodium, potassium, calcium and magnesium) migrate towards the steel cathode. The combination of the electromigration of the positively charged ions and the production of hydroxyl ions at the cathode by the following cathodic reaction, increase the alkalinity around the steel,

$$2H_2O + 2e^- = H_2 \uparrow + 2OH^-$$

Since the objective of ECE is to remove chloride from chloride contaminated reinforced concrete in a short period of time, it is necessary to apply a current density much greater than that which is used for CP systems. Typical current densities used are in the region of 1-5 A/m^2 which are applied for periods of a few weeks.

The introduction of new remedial technique in itself becomes a source for future problems. Possible side effects, therefore, require detailed evaluation [Page, 1992]. For instance hydrogen embrittlement phenomena, particularly on prestressed structures, may occur due to the intense level of cathodic polarisation. Another possible side effect may be the modification in the composition of the cement paste near the reinforcement due to the high alkalinity caused by the cathodic reaction and the electromigration of alkali metal ions from the surrounding matrix towards the cathode. This modification in the composition of the cement paste matrix around the reinforcement could result in the reduction of bond strength at the steel/concrete interface [Rasheeduzzafar et al., 1993

and Ueda et al., 1995]. Furthermore, accelerated alkali aggregate reaction could occur if potentially susceptible aggregates are present in the mix [Sergi et al., 1991, Ali and Rasheeduzafar, 1993 and Page and Yu, 1995(a)].

Another aspect that was raised by Page et al., [1994] is the degradation of the cement matrix caused by the release of sulphate ions due to cathodic polarisation. Electromigration of sulphate ions away from the cathode towards the bulk of the material may eventually cause them to be redeposited as secondary ettringite, an expansive reaction which could cause some local cracking of the matrix.

Very important fundamental questions regarding the efficiency of chloride removal beyond the reinforcement depth or the possibility of corrosion re-initiation after the remigration of the remaining chlorides remain unanswered and require further research.

1.3 SCOPE OF INVESTIGATION

The aims of the investigation were:

1. To determine the effectiveness of ECE in removing chloride over a range of current densities and time periods.
2. To look at the possibility of side effects such as paste softening and secondary ettringite formation caused by the ECE process.
3. To confirm passivity of the steel reinforcement after ECE and study the possibility of subsequent remigration of chlorides to the steel reinforcement which may lead to further corrosion.

Emphasis was placed on the cement paste near the reinforcement which can be influenced from the production of hydroxyl ions by cathodic reaction and the electromigration of Na^+ and K^+ ions toward the reinforcement. The gradual accumulation of sodium and potassium around the steel may soften the cement matrix. Particular attention was paid to the sulphate ions to look at the problem of secondary ettringite formation following their release from the cement hydrates.

A fundamental question vital for the success of the ECE treatment is how stable the passivity of the reinforcement is after the treatment. This is likely to be linked to the speed of chloride ion remigration to the surface of the embedded steel and therefore both of these aspects were looked at in detail.

1.4 PLAN OF PRESENTATION

This thesis is divided into seven chapters, followed by references and appendices. The appendices are numbered in accordance with the chapter. Chapter 1 is the introduction and deals with, factors that might contribute to the deterioration of concrete, options for repair and the scope of research. The literature review is in Chapter 2. Chapter 3 describes the materials and analytical techniques used in the work. The experimental work is described in chapters 4, 5 and 6. Chapter 4 deals with the investigation of the ionic redistribution during ECE. The ionic species looked at were chloride, sodium, potassium, hydroxyl and sulphate ions. Chapter 5 looks at the effect of ECE and the resulting migration of ions on the physical properties of cements such as microhardness, pore structure distribution (PSD) and accumulation of ettringite and chapter 6 looks at the remigration of chloride ions, the effect of retreating specimens after storage for 9 months and passivation of the steel cathode after ECE.

Chapter 7 relates all the findings in this research and draws general conclusions with regard to the ECE process. Finally an outline of further areas of research is presented.

CHAPTER 2

REVIEW OF LITERATURE

2.1 INTRODUCTION

Most metals are not found in nature as pure materials. They are combined with other elements such as oxygen, forming compounds called ores. To obtain metal from ores the compound is subjected to extreme heat to break the chemical attractions between the elements. However, the metal extracted tends to revert to its native form by the processes of oxidation and corrosion.

Corrosion is an electrochemical process which involves the passage of electricity in the metal, which behaves as a mixed electrode, and through the surrounding medium. The medium surrounding the metal generally consists of moisture and soluble salts which conduct the electric current flow between the anode and cathode sites on the metal. This medium is called an electrolyte. The anodic reaction is the dissolution or loss of metal ions whilst the cathodic reaction is normally the chemical reduction of dissolved oxygen.

Even though the procedure for the construction of reinforced concrete buildings and structures is bound by codes of practice and technical rules, deterioration due to corrosion of reinforcement is escalating. The corrosion of steel in concrete is initiated by factors such as chloride contamination and carbonation.

The slow build up of chemicals locally can affect the chemical state at the steel-concrete interface. The change of the environment within the concrete permits the movement of electrons within the reinforcement. The flow of this current will then initiate corrosion. The speed of the corrosion process will depend on the potential difference between the anodic and the cathodic sites, the resistivity of the electrolyte and the availability of the reactants such as oxygen and water.

2.2 PROTECTION OF REINFORCEMENT BY CONCRETE

Concrete offers good chemical and physical protection to the reinforcement against corrosion. The highly alkaline environment in concrete forms a stable thin continuous passive ferric oxide film on the surface of the steel (for details see section 2.3). Also good quality concrete, of good compaction and curing results in low permeability and high electrical resistivity. This will minimise the ingress of corrosion inducing species via the aqueous phase and restrict the flow of corrosion current. Portland cement in its unhydrated form consists basically of the compounds shown in Table 2.1

When cement is mixed with water a series of complicated hydration reactions occur which gradually lead to the formation of a hardened mass. The most important hydration reactions are those involving C_3S and C_2S which are converted to a gel of tiny particles of calcium silicate hydrates (CSH) of ill-defined composition and structure, and to calcium hydroxide in the form of crystals of portlandite [Lea, 1970]. Diamond [1976], estimated that in a fully hydrated cement paste CSH gel forms 70% of the weight of solid material and $Ca(OH)_2$ about 20%. The remaining compounds produced by other phases (about 7% in total) are calcium aluminate trisulphate hydrate (ettringite) and calcium aluminate mono sulphate hydrate.

The pore solution pH of concrete made from the most common portland cements is normally in the range of 13-14 [Page & Treadaway, 1982]. The sodium hydroxide and potassium hydroxide originating from the Na_2O (approximately 0.15% by weight) and K_2O (approximately 0.5-1.5% by weight) in the cement increase the pH of the pore fluid above the pH value associated with saturated $Ca(OH)_2$ solution (i.e. approximately 12.4). At this pH level, the chemical reactions that occur on the steel surface quickly lead to a condition in which the steel is passivated.

Apart from the passivation environment provided by concrete towards the reinforcement, concrete also protects the reinforcement against the ingress of corrosion inducing agents. Good quality concrete should be dense and virtually impermeable. It can be assessed from the various tests such as water absorption, water permeability, chloride diffusion and oxygen and carbon dioxide diffusion and penetration. The details

of the testing and the criteria of assessment of good quality concrete can be found in Concrete Society Technical Report [1985] on "Permeability of Concrete and its Control", the summary of which is shown in Table 2.2

The factors that contribute to the permeability of concrete include depth of cover, type and quality of aggregate, type of cement, cement content, water cement ratio and variables from manufacturing such as mixing uniformity, degree of compaction and curing adequacy [Page, 1991(a)].

2.3 PASSIVITY OF THE REINFORCEMENT

Corrosion is an electrochemical process where metal is anodically oxidised to form a soluble species (e.g: $Fe \rightarrow Fe^{2+} + 2e^-$). The electrons released in this process flow through the metal to cathodic sites where they are consumed by a reduction reaction (e.g: $1/2O_2 + H_2O + 2e^- \rightarrow 2OH^-$). The process is then completed by the electromigration of ions through the electrolyte in order to maintain electro-neutrality [Page, 1988].

However, electrochemical reactions ($2Fe + 3H_2O = Fe_2O_3 + 6H^+ + 6e^-$) can also lead to the formation of an insoluble protective film γ-Fe_2O_3 on the surface of the metal. This film can reduce the corrosion rate to insignificant levels and this is generally the case when steel is embedded in good quality concrete. This condition is known as passivity and the layer is known as a passive film which is of the order of some nanometers thick and is composed of a cubic form of ferric oxide maintained on the metal surface [Hancock & Mayne, 1958]. The passive layer is not perfect and breaks are continually occurring. However, they are normally quickly repaired thus restoring the integrity of the film to ensure that loss of iron is insufficient to cause any significant reduction in the cross-sectional area of the steel.

If the dissolved oxygen level in the pore solution becomes depleted such as in some waterlogged or buried concretes, then the passive film can break down and uniform dissolution of the steel occur. Under these situations the soluble $FeO.OH^-$ species is formed. However the dissolution process is cathodically restrained by the same lack of

dissolved oxygen and therefore it occurs at a very slow rate [Arup, 1983]. The information about the relationship between the passivity and pH (environment) can best be seen from the potential-pH diagram for the Fe/H_2O system at 25°C or Pourbaix diagram as shown in Figure 2.1.

This simplified diagram for iron in water has been construed as approximating the state of the steel surface in uncontaminated concrete. The specific information in the diagram is restricted to reactions between the metal, its ions, oxides, hydroxides and water. If ions such as chlorides are introduced to the system, they will affect the corrosion and passivity domains of the metal. The change in Potential-pH diagram due to the presence of chloride is as shown in (Figure 2.2) where passivity is divided into three zones; perfect passivity, imperfect passivity and pitting. The passive layer in the zone of perfect passivity is stable and localised breakdown of the film is quickly repaired. In the pitting zone the environment is conducive for initiation and propagation of pits. In the zone of imperfect passivity, new pits will not form but any existing pits will continue to grow. [Page, 1997(a)]

2.4 CHEMICAL ATTACK IN CONCRETE

Lack of durability in concrete can be caused by external agents arising from the environment or by internal agents within the concrete. These causes can be categorised as physical, mechanical and chemical. Physical causes arise from the action of frost and from differences between the thermal properties of aggregates and the cement paste matrix whilst mechanical causes are associated mainly with abrasion [Strecker, 1987]. Attack by sulphate, acids, sea water and chloride can be categorised as chemical attack. This project will concentrate only on degradation related with chloride.

Chloride may be introduced into concrete in several ways. It may be added as an admixture (accelerator) in concrete or during mixing where contaminated water and aggregates are used. In the U.K., the most important mode of introduction is by penetration from the environment as in the cases of structures exposed to a marine environment or to de-icing salts in the winter.

2.4.1 Corrosion Reaction and Corrosion Model

The electrochemical reactions that occur as a result of the breakdown of passive oxide film by chloride ions are illustrated in Figure 2.3 and are summarised below.

(i) Anodic Reaction (oxidation)

$$Fe \rightarrow Fe^{2+} + 2e^{-} \quad (2.1)$$

(ferrous ion pass into the concrete pore solution at the anode)

(ii) Cathodic Reaction (reduction of oxygen)

$$1/2O_2 + H_2O + 2e^{-} \rightarrow 2OH^{-} \quad (2.2)$$

(the free electrons in the metal produced by the anodic reaction combine with water and dissolved oxygen in the pore water to produce hydroxyl ions)

(iii) Secondary Reactions at the anode site

$$Fe^{2+} + 2OH^{-} \rightarrow Fe(OH)_2 \text{ (ferrous hydroxide)} \quad (2.3)$$

$$4Fe(OH)_2 + O_2 + 2H_2O \rightarrow 4Fe(OH)_3 \text{ (ferric hydroxide)} \quad (2.4)$$

$$2Fe(OH)_3 \rightarrow Fe_2O_3.H_2O + 2H_2O \text{ (hydrated ferric oxide (rust))} \quad (2.5)$$

(ferrous hydroxide becomes ferric hydroxide and then hydrated ferric oxide or rust)

The formation of corrosion product around the corroded steel will increase the volume of the steel up to four fold [ACI 222R-85]. However, Broomfield [1997] suggested that the volume of the steel might swell up to ten times when ferric oxide hydrates and becomes porous. This process will induce stresses around the reinforcement. Since concrete is weak in tension the stresses can cause cracking and spalling of the cover.

The process of corrosion involves two stages known as initiation period (t_0) and propagation period (t_1). The model was first proposed by [Tuuti, 1982]. The initiation period is when the reinforcement is still in a passive condition because chloride has not reached the threshold level for corrosion whereas the propagation period is when the corrosion has initiated and is proceeding. This model is shown in Figure 2.4

2.4.2 Corrosion Initiation

The corrosion initiation period (t_0) for reinforcement in chloride contaminated concrete is a function of several parameters including:

(a) the chloride penetrability of the concrete

(b) the chloride binding capacity of the cement

(c) the critical chloride content

(d) the condition of the reinforcement/ concrete interface.

2.4.2.1 Chloride Penetration into concrete

The mechanism of ingress of chloride into concrete can be due to permeation of salt solution, capillary absorption of chloride containing liquid and diffusion of free chloride ions.

Permeation may become important for the ingress of chlorides if the penetrating liquid carries chloride ions, e.g. dissolved salts such as in sea water or from industrial processes [Rilem Report 12, 1995]. This mechanism is only relevant for cases such as marine structures under a high hydrostatic pressure or seepage of solutions through retaining structures.

The ingress of chloride due to capillary action of the pore system absorbing a chloride containing solution is a convective flow process. The absorption process is considered as the major cause of chloride contamination of concrete that is subjected to wetting and drying. During wetting periods the surface layers absorb the chloride solution. When the surface is dry the water evaporates leaving the salt in the pore system of the near surface region. The salt concentration in the pore system increases after repeated wetting and drying .

The diffusion of chloride ion into concrete is caused by gradients of the chloride concentration. Sufficient moisture is needed to provide a continuos liquid path in the capillary pore system in order for the chloride ions to penetrate the matrix. Moisture and temperature are two factors that affect the diffusion [Rilem Report 12, 1995]. The diffusion process of chloride into concrete can be described using a solution of Fick's second law of diffusion [Cussler, 1984]. This is based on the error function [Browne,

1982] where stationary conditions are assumed and the time dependent chloride binding effect of the concrete is neglected.

Depending on the exposure condition as well as on the moisture content of the concrete element these individual mechanisms may act simultaneously; they may prevail in sequence during consecutive periods of time; or one of them may be the exclusive transport mechanism.

Models based on Fick's laws of diffusion have been developed [Grace 1991, Wood 1994, Bamforth 1996]. By modelling the concrete as thin elements it is possible to model diffusion of any chloride profile and vary the surface chloride concentration and chloride diffusion coefficient of each element with time and or depth into concrete. The knowledge of chloride concentration with depth at a specific time is important to estimate the time to corrosion initiation of the reinforcement.

2.4.2.2 Chloride Binding by Cement

Chloride may be present in concrete in several states [Buenfeld, 1986]:

(a) Chloride strongly bound by C_3A hydrates and C_4AF hydrates mainly in the form of calcium chloroaluminate (Friedel's salt)

(b) Chloride loosely bound (immobilised) by calcium silicate hydrates and

(c) Free chloride ion in solution within the pore space.

The extent of chloride binding by cement, as summarised by Arya et al. [1990], depends on factors such as cement type, cement extenders, cement content, water cement ratio, hydration time, curing temperature, percentage of chloride present and associated cation. However, the most important parameter is the cement type which relates to the C_3A content and degree of hydration on exposure to chloride. The proportion of bound chloride increases with increased C_3A content which binds chloride by forming chloro-aluminate hydrate, $3CaOAl_2O_3.CaCl_2.10H_2O$, at a temperature between 20-25°C [Roberts, 1962; Holden et al., 1983; Rasheeduzzafar et al., 1992]. The chloride binding capacity of cements is reduced in high temperature environments and Hussain &

Rasheeduzzafar [1993] and Masslehuddin [1994] found higher chloride concentrations in their specimens after exposure to temperatures of up to 70°C.

Blending compounds such as ground granulated blast furnace slag (ggbs) or fly ash (pfa) used in OPC mixes may also increase the binding capacity for chloride [Diamond, 1981, Holden et al., 1983, Byfors, 1986, Rilem Report 12, 1995] because they effect both the uptake of the chloride ion by chemical reactions as well as the adsorption at the internal surface area. Increasing levels of Silica fume (SF) additions to OPC, however, reduces the chloride binding capacity [Page, 1983; Byfors, 1986]. Their results indicate that increasing the SF content added to cement paste could lead to a progressive increase in the chloride ion, introduced during mixing, found in the pore solution. Page and Vennesland [1983] who analysed data from DTA coupled with TG analyses, indicate that increasing the content of SF reduced systematically the quantity of $Ca(OH)_2$ and also caused the diminution in the quantity of calcium chloro-aluminate hydrate. SRPC cements with low C_3A content also reduce the chloride binding capacity [Arya et al., 1990].

Arya et al. [1990], also showed, however, that for chloride derived externally as for the case of structures in service, SRPC gives almost identical results to that of OPC. The level of C_3A had little effect on the binding of chloride introduced after 2 days of hydration. Water/cement ratio and curing (hydration) time also had little effect but the level of binding increased with exposure time and chloride ionic concentration of the external solution. The types of chloride also had a significant impact on the binding process, $CaCl_2$ allowing a greater amount of chloride to combine compared to KCl or NaCl [Rilem Report 12, 1995].

It is generally recognised that only free chloride ions in concrete initiate corrosion of the steel reinforcement [Hope et al., 1985; Buenfeld, 1986 and Rilem Report 12, 1995]. Both free and bound chlorides, however, exist simultaneously to maintain an equilibrium [Hannson & Berke, 1988]. Concrete which can bind more chloride, for the same concentration gradient of free chloride, will allow less chloride diffusion into the structural element, hence a longer period before corrosion initiation can take place.

2.4.2.3 Critical Chloride concentration

The rate of corrosion of reinforcement in concrete will depend on the amount of chloride present. It is accepted that a threshold or critical amount of chloride to initiate corrosion exists. Its value is normally expressed as a percentage of the total chloride by weight of cement, which is the sum of the free chloride, the chemically bound chloride and the adsorbed chloride. The method of obtaining the total chloride has been incorporated in standards such as BS 1881: part 124, 1988 Testing of Hardened Concrete. Determining the free chloride content by expression of the pore solution from samples where much of the free water has evaporated may not always be possible [Arya & Newman, 1990].

By understanding the inhibitive action of the alkalis within concrete and the fact that free chloride ions break down the reinforcement passivity another threshold for reinforcement corrosion initiation can be found, viz. the Cl^-/OH^- ratio as was first suggested by Haussman [1967]. The Cl^-/OH^- ratio he found for steel in a saturated calcium hydroxide solution was 0.6 over a pH range of 11.6 -12.4. Page & Treadaway, [1982] pointed out that such a ratio was not applicable in the case of concrete as no account was taken of the buffering properties of the cement matrix or of the diffusion characteristics of the concrete. The pH of the pore solution in concrete is also higher, in the range of 13-14. Lambert et al., [1991] found that corrosion of steel in good quality concrete occurred once the Cl^-/OH^- ratio exceeded approximately 3. The factors affecting chloride binding, diffusion and penetrability characteristics of concrete and exposure condition will all be inter-related such that no one threshold Cl^-/OH^- ion ratio could ever be expected. It is a difficult task to establish a chloride content below which a risk of corrosion is negligible, which is appropriate for all mix ingredients and under all exposure conditions.

Glass & Buenfeld [1997], however suggest that chloride threshold levels are best presented as total chloride contents expressed relative to the weight of cement due to the fact that bound chloride presents a corrosion risk, an effect which may be due to its contribution to the reservoir of available chloride at the steel concrete interface. A

summary of chloride threshold levels cited by Glass & Buenfeld [1997] is given in Table 2.3.

2.4.2.4 Condition of Reinforcement Concrete Interface

It is good construction practice to ensure that steel reinforcement is fully covered by concrete. As suggested by Page [1982], this thin layer is composed of portlandite ($Ca(OH)_2$) with inclusions of CSH gel to form at the steel cement matrix interface. This provides significant corrosion protection by restraining or buffering the lowering of the pH of the pore solution in the pitting process. Yonezawa et al. [1988] confirms the 'quasi-buffering action' of portlandite crystals. They found that a higher Cl^-/OH^- ion ratio was required to initiate corrosion of the steel than in solutions. Good adhesion between the steel and concrete is essential. The formation of voids due to poor adhesion denies the 'quasi-buffering action' at the steel concrete interface and promotes corrosion [Yonezawa et al., 1988; Mays, 1992].

2.5 MECHANISM OF THE PASSIVE FILM BREAKDOWN

If a sufficient chloride ion concentration is present, the passivity of reinforcement can be destroyed, leading to corrosion. The effect of chloride on reinforcement passivity can be described by three theories [ACI Committee 222R-85, 1985]

(a) The Oxide Film Theory:

This theory postulates that chloride ions penetrate the oxide film on the steel through pores or defects in the film. Alternatively the chloride ions may "colloidally disperse" the oxide film.

(b) The Adsorption Theory:

Chloride ions are adsorbed on the metal surface in competition with dissolved oxygen or hydroxyl ions. The chloride ions promote the hydration of the metal ions and thus facilitates the dissolution of metal ions.

(c) The Transitory Complex Theory:

This theory postulates that chloride ions form a soluble complex (iron chloride) with ferrous ions, which then diffuses away from the anodic sites. Thereafter, the

complex decomposes, iron hydroxide precipitates, and the chloride ions are free to transport more ferrous ions from the anode.

This problem, however, is still not entirely resolved and subject to much debate in the literature [Burstein, 1994]. Page [1998] attributed the passive film breakdown to several factors such as the increase in Cl^-/OH^- ratio near the metal surface, environmental factors such as temperature, oxygen availability and material variables (e.g. steel surface condition, chloride binding and buffering capacity of cement, voids at steel/concrete interface) and steel potential gradients if the steel is embedded in concrete of variable levels of chloride contamination.

2.5.1 Pitting Corrosion Initiation

Pitting corrosion of reinforcement is a stochastic process. Corrosion is initiated at sites with the lowest level of protection. Thus areas of limited hydroxyl ion availability such as voids at the reinforcement/concrete interface or where the portlandite layer is separated from direct contact with the bare steel surface by thick oxide scales are likely to be the sites at which corrosion can initiate given sufficient chloride ion concentration at that site [Treadaway, 1991].

Pitting is a process whereby intense anodic dissolution of metal occurs over a very small area. Galvele [1981], and Alvarez & Galvele [1984] describe pitting as the theory of localised acidification. When breakdown occurs in the passive film, chloride ions cause the metal to dissolve and form Fe^{2+} ions which then rapidly hydrate to form $Fe(OH)_2$ and hydrogen ions. Therefore, the immediate area near to the site of breakdown is acidified. The process of acidification promotes the oxidation of the metal to form Fe^{2+} ions and thus the corrosion process is accelerated locally. The illustrated mechanisms are shown in Figure 2.5

2.5.2 Corrosion Propagation

The corrosion propagation phase (t_1) is the time from when corrosion products form to the stage where they generate sufficient stress to crack or spall the concrete cover or when local attack on reinforcement becomes sufficiently severe to impair structural integrity.

The environmental conditions in which corrosion of reinforcement will initiate its propagation will depend on electrochemical, chemical and physical conditions including:

(a) The availability of oxygen and water

(b) Polarisation of the anodic process

(c) The chemical condition within pits

(d) The resistance between the anodic and cathodic sites

(e) The potential difference between anodic and cathodic sites

2.5.2.1 Oxygen availability

Figure 2.6, known as an Evans Diagram, shows the effect of decreasing oxygen availability to the reinforcement surface and increasing cathodic polarisation in a chloride environment. In the high pH environment of concrete, the predominant cathodic reaction is the reduction of oxygen. The availability of oxygen is, therefore, important. The polarisation of the oxygen reduction reaction will contribute substantially to the overall corrosion process, by influencing the corrosion current/rate (I_{corr}) and the corrosion potential (E_{corr}).

When the oxygen supply is good, the oxygen reduction cathodic reaction will occur and the corrosion potential E_3 is developed corresponding with corrosion current rate I_3. When oxygen access to the cathodic area is reduced, cathodic polarisation of the corrosion process of both potential and current drop to E_2 and I_2. A Further drop in oxygen results in a more negative corrosion potential (E_1) and a slower rate of corrosion (I_1). The corrosion potential (E_2), is termed the pitting potential. Potentials more positive than this point result in an increase in the corrosion rate. Hence in marine

structures, corrosion problems commonly occur in the splash zone where oxygen and chloride are present in high concentrations [Page, 1997(b)].

2.5.2.2 Polarisation of the Anodic Process

Since the overall corrosion process involves anodic and cathodic activity, consideration should be given to the anodic process. Figure 2.7 shows the conceptual effect of increasing chloride concentration on the rate of corrosion. When chloride is increased, the range of potential of passivity is decreasing. When there is no chloride in the concrete the passive current I_5 corresponds to the passive potential E_5, with the range of potential between point b and E_5. When the chloride content is gradually increased the corrosion potential decreases from E_{4p} through E_{3p} and E_{2p} to E_{1p}. The corrosion current (rate) similarly decreases from I_{4p} to I_{1p}. Therefore the range of potential passivity is decreased. This is an illustration of the corrosion process being under anodic control.

The abundance of chloride will transform the zone of film breakdown into an acidic chloride-rich solution which causes the anode activity of the metal to increase locally and develop into a pit. The pit will grow in size locally and can penetrate the metal [Page 1997(b)].

2.5.2.3 Pit Propagation

For a pit to remain active the following conditions are required [Rilem 1988].

(a) sufficient concentration of chloride ions at the pits

(b) recycling of chloride ions during the corrosion process

(c) diffusion of chloride ions from the bulk concrete to the pit

(d) acidity development within the pit

(e) cathodic process happening elsewhere on the steel surface

(f) electrolytic path between cathode sites and pit has continous link

During chloride-induced pitting corrosion, it is sufficient to consider that chloride encourages dissolution of metal to form iron (II) oxidation state ions. These metallic ions combine with chloride to form intermediate corrosion product such as $FeCl_2$ (Iron II chloride) or FeOCl (Iron II oxychloride), which are stable in acidic conditions. They will hydrolyse rapidly in an alkaline or neutral environment to form iron hydroxides, liberating the chloride ions and also releasing the hydronium ion (H_3O^+) from water [Treadaway, 1991]. The liberation of hydronium ions within the pit locality creates more acidic conditions which are favourable for corrosion, and high corrosion rates are generated. Also this acidic condition increases the solution stability of iron (II) compounds which enhance the mobility of the products of corrosion and faciliting migration further from the corrosion site. This effect can induce cracking within the cover of the concrete. From this phenomenon it is understood that pitting corrosion is self-supporting by creating conditions more favourable to propagation as it propagates, especially in the development of acidity within the pit and the recycling of chloride ions during the corrosion process. The schematic diagram of the reaction is shown in figure 2.8.

2.5.2.4 Resistance between Anodic and Cathodic Sites

The corrosion process involves the flow of electrons through the metal (which should not be a problem) and ionic current flow through the electrolyte. The flow through the electrolyte may be restricted by the internal resistance (resistivity) which exists between the anodic and cathodic sites. This restriction will reduce the current flow and hence the rate of corrosion.

The Evans diagram shown in Figure 2.9 shows the effect of electrolytic resistance on the corrosion current. From the figure, when the anode/cathode resistance increases, the flow of the corrosion current decreases from I_{corr} to I_{R4}. The resistivity of concrete is affected by factors such as moisture content, ionic content of the pore solution and concrete quality [Treadaway, 1991].

2.5.2.5 Potential Difference between Anodic and Cathodic Sites.

A corrosion cell can be formed when a potential difference occurs on the reinforcement between two electrically connected sites. The potential difference can develop due either to a variation in the metal or in the electrolyte as is the case of chloride contamination.

One practical example of chloride induced reinforcement corrosion exists where a high degree of cathodic polarisation is accompanied by severely localised attack. This occurs in severely chloride contaminated concrete which has a high moisture content and therefore oxygen diffusion to the reinforcement is limited [Treadaway, 1991]. In this condition current flow can occur over large distances making a large cathode available such that while cathodic efficiency on a unit area basis of reinforcement surface is low, the combined effect over large areas can lead to high current flow at the anode, and additionally to potentials polarised to low negative values [Treadaway, 1991].

Pitting is highly likely in these circumstances and will be limited to a few anodic sites of high activity where corrosion will be intense and a deep penetrating attack can occur. The importance of this corrosion situation is that little precipitation of corrosion product will occur and therefore, the typical development of cracking and spalling of cover concrete will be minimised.

2.6 PREVENTION AND REHABILITATION TECHNIQUES FOR CHLORIDE-INDUCED CORROSION

As discussed in chapter 1, repair to structures deteriorated due to chloride induced reinforcement corrosion can be very expensive. It is, therefore, prudent to take some measures during the design of a structure to prevent or reduce the risk of corrosion of the reinforcement. According to Slater [1983] and Strecker [1987] this can be done by concrete modification, reinforcing steel modification and cathodic protection. For rehabilitation measures of existing structures, methods that are popular and available commercially include patch repair and removal of chloride contaminated concrete, cathodic protection and electrochemical chloride removal.

2.6.1 Concrete Modification

2.6.1.1 Quality, cover and water/cement ratio

By following the recommendation in the code of practice and technical notes and practising the correct procedures in design and construction according to the environmental conditions, the design life of a structure can normally be achieved. The water/cement ratio should be within the specification and as low as possible. Compaction should be carried out in a proper way to ensure good consolidation and to avoid segregation. Concrete cover should be adequate and uniform throughout the structure. In cases where improved performance is required or where external factors such as chloride contamination are likely to play a significant part, other measures may need to be considered.

2.6.1.2 Decreasing permeability of concrete

The basic first step approach to control the permeability of concrete should be in the mix design and the placement itself. The other approaches can be divided into either application during construction of the structure such as the use of latex modified concrete or application after the structure has undergone some service life, such as the use of extremely low water/cement ratio overlay material or of a top coat. Both of these techniques are useful in slowing down the ingress of chloride as well as oxygen [Strecker, 1987]

2.6.2 Reinforcing Steel Modification

Modification which can normally be carried out on the reinforcement is in the form of coatings. The most common are coatings with fusion bonded epoxy and galvanised coatings [Strecker, 1987]. Special site precautions must be taken on both of these methods when constructing the cages. The bend radii of the bar should be within the prescribed limits. However both of these techniques have problems, zinc corrodes over time and is only expected to be passive at a pH below about 12.5 and it will tend to dissolve as the pH increases above this level [Roetheli et al., 1932]. Epoxy coating has

been reported to disbond from the reinforcing bar, even in zones where corrosion did not occur. This happens particularly on structures exposed to sub-tropical marine environments [Smith et al., 1993]. Stainless steel and bronze has been tried for reinforcement, but the high cost implied has made them impracticable.

2.6.3 Surface Treatment

The application of a surface coating is only suitable and reliable for a newly built structure. When the concrete already shows signs of deterioration and enough salt is present at the reinforcement, application of a coating is considered to be too late and is unlikely to prevent further deterioration. The application of a coating can basically slow down the rate of deterioration in three different ways [Strecker, 1987]. (a) by increasing the resistance of the concrete to chloride penetration. (b) by increasing the resistance of the concrete to carbon dioxide penetration and (c) by reducing the moisture content of the concrete.

To resist salt penetration, the coating should be impermeable and waterproof as the salt is dissolved in the water. Any coating, therefore that can form a coherent waterproof barrier is able to reduce penetration of salty water into the concrete. Examples of this are epoxy, Methyl methacrylate, Moist-cured urethane and Alkyl-alkoxy silane [Mallet, 1994].

It is important to note that the build up of water-vapour pressure behind the coatings can cause the coating to peel off unless the adhesion to the surface is very good. It is possible to overcome or reduce this problem by using a priming coating which penetrates into the surface of the concrete, but the water in the surface pores can reduce the degree of impregnation. The water therefore has to be displaced by heating or soaking with impregnant.

2.6.4 Patch Repair

This method requires the cracked, spalled or delaminated concrete to be removed. The bars are cleaned and extra steel is added if required. The removed concrete is then replaced with either concrete or repair mortar. To prevent further contamination by chloride the new surface is often coated with a surface coating. This method may appear easy and cheap but unless all the significantly contaminated material is removed even in regions away from the active corrosion area, corrosion will be initiated in the area around the repair [Thompson, 1989]. This is because initially, the anodic zone sacrifically protects the surrounding areas which contain smaller amounts of chloride. Once fresh non-contaminated material replaces the contaminated area this protection is removed and the surrounding areas become the new anodes. This incipient anode formation can be avoided if most of the chloride-contaminated concrete is removed a process which inevitably adds to the cost. This method also requires the structure to be assessed periodically for load bearing capacity and safety, hence it is not always economic.

2.6.5 Cathodic Protection

Cathodic protection was first employed to suppress the corrosion of a British ship hull by Sir Humprey Davy in 1824. Since then it had been used in many situations such as for a buried pipelines and submerged coastal and offshore structures. Its first application above ground was on a bridge deck concrete structure by the California Department of Transportation in 1973 [Stratful, 1974].

The basic mechanism of corrosion is illustrated in Figure 2.10 with the development of anodic and cathodic sites. Cathodic protection alters this situation by providing electrons from an external source (a dc power supply) via an external anode installed at the surface of the concrete. The flow of electrons between this anode and the reinforcing steel turn the corroded sites into cathodes, hence corrosion is suppressed. The term used for this process is called "impressed current cathodic protection system". This process is illustrated in Figure 2.11.

Various control criteria for cathodic protection were suggested including achieving sufficiently negative steel potentials in the range of -650mV and -1135mV (CSE) [Mallet, 1994]. However the difficulty in measuring absolute potential and the worry of overprotection on some parts of the structures because of differences in concrete resistivity has made this criterion inappropriate. The most accepted criterion is now based on a potential shift of 100 mV to 150 mV [Broomfield, 1997]. The current density applied normally is between 5 to 20 mA/m^2 at about 2 to 10 volts to each square metre of concrete surface, so a power of 100 watts will protect 2500 m^2 to 10000 m^2 [Report No. SCPRC/001.95].

For achieving satisfactory results, the anode system needs to be carefully designed and the steel reinforcement needs to be electrically connected. The anode system must satisfy several criteria such as durability, aesthetics, increase in dead weight, vandal resistance and cost. The two most popular anode systems, are a conductive paint overlay or a noble metal oxide coated titanium mesh covered in a cementitious overlay.

Cathodic protection was shown to be a successful option for repair [Boam, 1989], the only concern raised being about the continuous maintenance of the system which can be difficult and costly. Cathodic protection can be used either as a repair technique or installed on a new construction to prevent corrosion from occurring.

Another form of cathodic protection which can be cheaper to install and maintain, is by connecting the steel reinforcement to a metal which is higher in the electrochemical series of metals than steel, such as magnesium, aluminium and zinc. The metals gradually dissolve over a period when connected to the steel reinforcement and this kind of mechanism is termed "sacrificial anode system".

2.6.6 Electrochemical Chloride Extraction

Electrochemical chloride extraction (ECE) is also sometimes called Electrochemical chloride removal (ECR) or desalination. This system is similar to CP except that a higher current density is used for a limited time period.

2.6.6.1 Principle of Electrochemical Chloride Extraction

ECE is a short term process, whereby a dc electric field is applied between the reinforcing steel and a temporary anode/electrolyte system attached to the exterior surface of the concrete. Under the action of the electric field, the negatively charged chloride ions move along the current flow lines from the reinforcement, representing the cathode, towards the external anode system where they can be removed. The schematic process of ECE is shown in Figure 2.12. The following reaction will happen at the anode:

$$2OH^- = 1/2O_2 + H_2O + 2e^- \quad (2.6)$$

$$H_2O = 1/2O_2 + 2H^+ + 2e^- \quad (2.7)$$

$$2Cl^- = Cl_2 + 2e^- \quad (2.8)$$

and at the same time hydroxyl ions are generated around the reinforcement due to electrolysis:

$$1/2O_2 + H_2O + 2e^- = 2OH^- \quad (2.9)$$

$$2H_2O + 2e^- = H_2 + 2OH^- \quad (2.10)$$

This enables repassivation of the steel surface if the chloride content can be reduced below the critical value.

The speed of ionic migration in concrete depends very much on the volume of pores (which exist mainly in the cement matrix) as well as their geometry and distribution which is due to w/c ratio, compaction, curing and type of concrete. It is this variation in the microstructure of the cement matrix that results in a different speed of chloride extraction from case to case. The movement of ions by diffusion and convection, as

compared to migration, is slow at the relatively high current density employed and so can be neglected [Andrade et al., 1994].

Chloride ions are transported through the concrete along streamlines that have been formed by the applied field, therefore, the streamline distribution is an important parameter to consider. Figure 2.13 shows a schematic representation of the streamline pattern in an inhomogenous field with equal resistivity between steel reinforcement and concrete surface. The force acting on the ions is stronger on the shorter streamlines with higher current so the speed of ionic migration is highest in the zone directly above the reinforcement and lesser as the lateral distance from the reinforcement increases. The removal of chloride is therefore, very slow from the area between two levels of reinforcement and very little from behind the reinforcement.

In view of the above principle, designing an ECE system related to the electrical resistance between the surface of the concrete and the reinforcement and the resistance on the surface itself is important. This is to ensure that a relatively equal level of chloride is removed from all areas of the concrete because the current will flow through the area of lowest resistance. It is a mistake to assume that the resistivity of the surface and the cover depth of the concrete is uniform as local damage to the integrity of reinforced concrete could result and leave significant amounts of chloride (still present) in the adjoining areas [Walker, 1994]. This is because the total resistance between the concrete surface and the reinforcement is lower in the corroding zone, hence the corroding zone will receive a greater percentage of current. Marine structures are a clear example of situations where the resistivity can be significantly different varying from low in the tidal zones to medium and high in the atmospheric zone. Such a structure would need to be divided into zones to enable different levels of treatment to be set [Collins & Farinha, 1991 and Polder & Hondel, 1992].

Prior to the installation of the ECE system, checks need to be carried out on the concrete surface as well as on the reinforcement. The concrete surface has to be checked for any signs of cracks that penetrate the concrete, for spalling and for lamination. Leakage could result in partial short circuits during the ECE process and the entire current could flow here [Gjerp and Miller, 1990]. Therefore, cracks and other defects must be sealed before ECE is applied. The reinforcement has to be electrically

connected. Where steel reinforcement is electrically discontinuous, stray current corrosion can occur under the influence of the impressed current [Collins & Farinha, 1991].

The most frequently used solutions for outer electrolytes are saturated calcium hydroxide, sodium borate, sodium hydroxide and tap water. When an alkaline solution is used, the OH^- ions present at the anode according to equation (2.6) are converted into oxygen and water molecules hence the electrolyte pH decreases. Water, however, decomposes at the anode and oxygen gas and hydrogen ions are formed according to equation (2.7). The pH of the electrolyte shifts to the acidic range because the H^+ ions migrate towards the negative pole and run against OH^- and Cl^- ions which move in the opposite direction. The OH^- ions are neutralised to water and hydrochloric acid is formed with the chloride ions discharged at the anode to form chlorine gas as shown in equation (2.8). The pH of the electrolyte should be kept above 7 to avoid the formation of chlorine gas which is a health hazard and an acidic electrolyte could also etch concrete [Broomfield, 1997].

A proprietary system for ECE treatment was developed in Norway [Broomfield, 1997] consisting of shredded paper and water sprayed onto the surface to form a wet "papier mache". The mesh anode is then fix to the surface on wooden batons before another layer of "papier mache" is applied. Steel mesh has been tried but is not very popular because it can be consumed during treatment and stains the concrete surface [Broomfield, 1997].

The current is applied for the desired length of time. When the treatment is complete, the current is switched off and the anode system is removed. The treated surface is cleaned and a surface coating is applied, if necessary, to avoid further ingress of chloride.

2.7 DEVELOPMENT, TRIALS AND APPLICATION OF THE ECE

Electrochemical chloride extraction was first tried in the USA for the Battele Columbus corporation, Ohio from 1973 to 1975 for the Kansas Department of Transportation [Lankard et al., 1975; Slater et al., 1976 and Morrison et al., 1976]. These studies were oriented towards development of a rapid technique to remove chloride from bridge decks in approximately 12 to 24 hours in order to avoid disruption of traffic flow.

Up to 100V DC was used in the laboratory investigations to reduce the chloride content of the concrete to below 0.02% in 48 hours or less. For the field trial on a bridge deck, maximum chloride removed from around the steel was 90% by applying up to 100A cathodic current over an area of 3.7 m^2 (i.e. current density of 27A/m^2 of concrete surface) for 24 hours. The potential measurements which were carried out up to three months after the treatment showed that all the steel was passive compared to 55% that had been corroding before the treatment. Platinised titanium was used for the external anode, and an ion exchange resin in the OH^- form in saturated calcium hydroxide solution was used as the electrolyte surrounding the anode.

Morrison et al.[1976] used a much higher voltage of 220V. Copper wire was used as an anode material to prevent chlorine gas evolution. Distribution of streamlines in concrete as a factor of chloride removal efficiency was discussed where he found that chloride removal was very little from behind the reinforcing bar. The drawbacks of a very high current density included a rise in the concrete temperature up to 52°C and an increase in porosity and permeability of the concrete.

In the late 1980's, a version of the ECR process was patented in Norway [Vennesland & Opsahl, 1986). The process has been offered commercially in Europe by the Norwegian group and is known as NORCURE™. As described by Miller [1989], in this approach the applied treatment current is limited to 1A/m^2 of concrete surface making treatment times correspondingly longer. The external anode can either be a standard reinforcement net or activated titanium mesh which is installed on to wooden battens bolted to the concrete. The electrolyte is a cellulose fibre material containing $Ca(OH)_2$ solution sprayed on to the surface to completely cover the net. The electrolyte in this form is capable of being used on both vertical and soffit surfaces. In theory this

approach makes such treatment feasible on most structures which have suffered from chloride ingress [Farinha & Peek, 1991]. A diagram of an installation is shown in Figure 2.14.

Manning & Ip [1993] reported results of three structures which had been treated using the NORCURE™ method. They found that for Pier S19 of the Burlington Bay Sky Way, 42-87% of chloride was removed after 0.77A/m^2 of current was induced for 8 weeks. The chloride ion concentration profile which was measured again after one year showed no significant increase. The pier of Credit View Road Overpass which was treated for 8 weeks using a current density of 0.85A/m^2 had up to 70% of its chloride removed. In both structures, the anode consisted of steel mesh encased in an electrolyte of cellulose fibre moistened with lime water.

The anode blanket system for the abutment of Montreal River Bridge consisted of a sandwich of a thick layer of highly absorbent material in contact with concrete, a geotextile material, a titanium mesh anode and a high strength geotextile material, to hold the other materials in position. Lithium borate, known to be an inhibitor to alkali silica reaction, was added to the electrolyte because the structure contained reactive aggregates. The treatment took place over a 22 to 25 day period. This shorter period was due to the higher current density which was applied. Analysis of the data is incomplete. However, measurement of the electrolyte concentration of the early samples showed a rapid increase in chloride content and a reduction in lithium ion content during the first days of the treatment.

Manning & Ip [1993] also suggested that the maximum voltage applied is limited by the electrical codes to 30 or 50V and the current density on the concrete surface in the range of 1 to 4 A/m^2. The total charge passed should be 600 to 1200Ah/m^2 and treatment time approximately 10 to 80 days. Polder & Hondel [1992] however, suggested that the maximum applied current density could be up to 5A/m^2 with treatment duration varying from 3 weeks to 3 months.

As part of the Strategic Highway Research Program (SHRP) in the USA ECE methods were studied in greater detail between 1988-1993. The problems studied include the efficiency of the method, bonding between steel and concrete, cracking in concrete and

hydrogen embrittlement [Bennett et al., 1993 a,b]. SHRP recommends the use of an activated titanium grid as the anode material, 0.2M sodium borate as electrolyte and 0.2M lithium borate for concrete containing alkali-sensitive aggregate and a current density between 1-5 A/m^2 and a DC voltage not more than 50V [Meitz, 1997].

In Australia, a significant amount of chloride was removed from a bridge deck pier in Sydney Harbour. Chloride concentrations were reduced to below 0.05% by weight of concrete. Results after 16 months showed that, the chloride concentration in the atmospheric zone remained as low as recorded immediately after chloride extraction but the chloride concentration in the tidal/splash zone had returned to the pre-treatment concentration [Collins & Kirkby, 1992].

Elsener et al. [1992], reported results on a subway in Switzerland which was treated using the ECE process. They found that 40% to 50% of acid soluble chloride was removed after eight weeks induced by a current density of between 0.3 to $0.75A/m^2$ of concrete surface. The potential mapping carried out after 5 months showed that corrosion was still occurring in a small number of areas. These areas were treated again 9 months after the first treatment and a further 50% of chloride was removed. Elsener et al. [1992] suggest that the components of bound chloride and free chloride in the pore solution are in chemical equilibrium; by removing the free chloride and waiting a sufficient time, bound chloride is dissolved until a new equilibrium is reached. There is however, no evidence to support their suggestion which is in dispute with findings discussed in chapter 4.

Application of ECE on a large scale in the U.K. on precast concrete houses and a car park was successful. $900m^2$ of concrete surface could be treated at a time and a guarantee of 20 years was given to the client to prove how confident the operators were [Parker & Hayward, 1995]. The anode used was a non sacrificial rhodium and iridium oxide coated titanium mesh, enclosed within fibreglass tanks filled with water. This trial used a 240V, 13A supply system compared to a 240V, 60A which is popularly used. $1A/m^2$ of current was induced for a duration of 4 weeks.

2.8 AREA OF POSSIBLE RESEARCH

So far ECE has been used successfully in many parts of the world with application varying from quays, office buildings, road bridges, parking garages, housing and industrial plants [Miller, 1994]. As with any new technique, questions regarding possible deleterious effects have been raised in many instances. The important points are: (a) Factors affecting the efficiency of the chloride removal process and possible re-initiation of corrosion. (b) The effect of current on bonding between steel and concrete. (c) Alkali-silica reaction.

2.8.1 Removal Efficiency and Corrosion Re-initiation

The cost factor has always been the main criterion for choosing the repair technique. A rapid and less destructive technique with reasonable cost will of course be popular. With ECE the easiest way to expedite the rehabilitation process is by increasing the current density induced. As reported above, the highest limit of current that caused no defect to the structure so far is $5A/m^2$ [Polder & Hondel, 1992]. Furthermore, Bennett & Schue [1990] in their conclusion said that the current efficiency for chloride removal is independent of current density, but varies with chloride concentration and is higher at 80^oC than at lower temperatures. Practical conditions will however limit the allowable temperature increase.

The fraction of the total current carried by a specific ion is defined as its transference number, t which is

$$tCl^- = \frac{\text{amount of current carried by chloride } (ICl^-)}{\text{total current } (I_{tot})}$$

Electrolytes in which the concentration of other mobile ions is high will reduce the current carried out by the chloride ion hence the efficiency is reduced.

The degree and effect of remigration of chloride after treatment is still unclear up to now. Chloride ions can only be removed if an electric field exists between them and the temporary surface anode. Therefore, chlorides in concrete beyond the reinforcement depth or between widely spaced bars, will not be moved during the ECE process. These chloride ions can then back-diffuse into areas where chloride has been extracted whereby increasing the risk of re-initiation of corrosion [Green, 1991]. Elsener et al. [1992] discussed the possible existence of a free to bound chloride equilibrium which could have serious long term effects on the durability of the treated concrete and on the efficiency of this system to remove chloride which penetrate beyond the reinforcement. It was suggested that the treatment may need to be run twice. The applied current can be stopped after some period of treatment to allow bound chloride to be released into the matrix which can then be removed by the second treatment. Green [1991], further suggested that the current can be induced intermittently. The rest period is still not clearly indicated. Other factors such as initial chloride distribution, cement type and water cement ratio could also contribute to the efficiency of the system [Tritthart a&b, 1989].

2.8.2 The Effect of Current on Bond Strength

Application of a high current in ECE treatment can lead to loss of bond between steel and concrete. This problem has been the subject of research by many researchers. Locke et al. [1983] studied the effect of an impressed cathodic current of approximately $0.03 A/m^2$ of steel surface area on the bond strength for a period of 5 years. After 2 years a significant loss in bond was found as compared to the control specimens. After 4 years 20% in bond reduction was found where the sample was treated with approximately $1200 Ah/m^2$. Rasheeduzzafar et al. [1993] found up to a 33% decrease in bond strength for a charge of $5426 Ah/m^2$ of steel surface in studies involving deformed steel bars.

The bond strength decrease is due to changes in the composition in the hardened cement matrix such as accumulation of alkali hydroxide around the cathode which may soften the binder matrix.

Studies by Nustad & Miller [1993] on smooth steel bars showed a loss in bond strength of 60-70% at charge levels of up to 5000Ah/m^2 but the bond strength increased again after the charge level increased to about 12000Ah/m^2. Ueda et al. [1995] found quite a significant loss in bond strength when the total current density was less than 10000Ah/m^2. He, however, observed that the bond strength of some specimens was restored after 10080Ah/m^2 of total charge was applied. He explained that this phenomenon was due to the secondary cathodic reactions,

$$4H_2O + 4e^- \rightarrow 2H_2 + 4OH^-$$

which occur at the cathode due to the lack of oxygen around the steel bar. When the total current density becomes large, the cement paste hardens again owing to the consumption of moisture in the softened cement paste. Buenfeld & Broomfield, [1994] carried out studies on uncorroded plain round bars embedded in normal and contaminated concrete. Prior to ECE, the bond strength of the specimens containing chloride was around 57% higher than for specimens not containing chloride, as a result of corrosion. The enhanced bond strength of the chloride specimens was largely eliminated by 2 weeks of ECE although results were not clear beyond 2 weeks. This initial drop in bond is attributed to the removal of corrosion product which was supported by visual evidence.

Page [1992], cited that the data recorded by Locke et al.[1983], on bond strength measurements show large scatter. In their work, Sergi and Page [1992] found a small but significant reduction in micro hardness was seen when small current densities were applied therefore, Page [1992] concluded that moderate levels of cathodic protection are unlikely to cause any significant degradation of bond strength. However, the use of high currents in ECE is likely to cause quite a significant reduction in bond strength.

Reduction in bond strength may be attributed to the factors below [Page, 1992 and Walker, 1994]:

* Hydrogen gas evolution
* Thermal cracking

* Iron and corrosion product dissolution
* Paste softening
* Reduction of frictional forces.

2.8.2.1 Hydrogen Gas Evolution

As discussed in section 2.4.1, the dissolved oxygen in the electrolyte is reduced to hydroxyl ions. Due to the high current densities used and the limited diffusivity of oxygen through hardened cement paste, the reaction is very quickly stifled by the lack of oxygen. The majority of the current is therefore passed by a second reaction; the evolution of hydrogen by the reduction of the water.

$$2H_2O + 2e^- = H_2 \uparrow + 2OH^-$$

The hydrogen gas which is formed at the cathode will try to diffuse through the pores to the surface of the concrete. Bursting forces will be induced in concrete around the steel if the rate of hydrogen evolution is greater than the rate at which it can disperse. If this bursting pressure exceeds the tensile strength of the concrete, cracking will occur and the steel/concrete bond will be reduced [Ali & Rasheeduzzafar, 1991 and Polder, 1994]. Not many publications exist which discuss the aspect of reduction in bond strength due to hydrogen evolution.

2.8.2.2 Thermal Cracking

Due to the high resistivity of concrete, the high current applied will convert to heat energy which can subsequently cause expansion in concrete. Tensile stresses induced by the expansion of concrete may result in micro cracking. Miller [1994] cited the work by Taywood Engineering that no significant increase in micro cracking was found after the concrete had undergone ECE with a current density of $1A/m^2$ of concrete surface for 40 days. However Miller cited Karlsson [1990] who found an increase in micro cracking after concrete with a high salt content was treated with higher charges for a duration of treatment of 8 weeks.

2.8.2.3 Iron and Corrosion Product Dissolution

At high pH values $FeO.OH^-$ species are formed [Pourbaix 1966] which is soluble and, according to Walker [1994] leads to a space between the steel and the hardened concrete which will result in a reduction in bond strength.

2.8.2.4 Paste Softening

When the current is induced in the ECE process the positive ions Na^+ and K^+ accumulate gradually around the steel bar. These ions combine with OH^- to form NaOH and KOH which are believed to be detrimentally incorporated into the CSH gel and cause soluble silicates to be formed [Locke et al., 1983]. It has been proposed by Page et al. [1994], who observed an increase in sulphate around the cathode, that the stability of the sulpho and chloro-aluminate compound could be weakened by high concentration of alkalis.

Microhardness profiles have been determined by Sergi & Page [1992] for cement paste specimens containing steel cathodes polarised at $5mA/m^2$ and $20mA/m^2$ for 100 days. They have observed a small reduction in hardness in a zone extending less than 1 mm from the steel for the sample treated using $20mA/m^2$. Ueda et al., [1995] found a reduction in hardness up to 6 mm from the cathode by using $5A/m^2$ of current density with total current density $6720Ah/m^2$. However, Bertolini [1993] and Page et al. [1994] found that it was not possible to establish statistically significant changes in hardness for a distance 0.1 mm from the steel after polarising specimens up to 12 weeks at current densities in a range $5mA/m^2$ to $5A/m^2$. This they concluded, may not be typical behaviour of cement matrices in general and further work is needed to clarify the possible influences of differences in mineralogy and pore structure [Page et al. 1994].

An additional effect that also warrants detailed study is the fate of the sulphate ions that enter the pore solution paste in the vicinity of the steel cathode [Bertolini et al., 1996]. When they migrate towards the bulk material of lower pH, it may cause them eventually

to be deposited as secondary ettringite. This expansive reaction might cause a local disruption of the matrix.

2.8.2.5 Reduction of Frictional Forces

Sodium hydroxide and potassium hydroxide are formed at the reinforcement steel cathode. These low-density alkali hydroxides may precipitate around the steel at the cathodes and locally disrupt the interfacial bond [Ali & Rasheeduzzafar, 1991]. Page [1995(b)], however, disagrees with this idea since sodium and potassium hydroxide are highly soluble in water. Nustad [1992], suggests a "soapy film" theory where sodium and potassium hydroxide are hydrophilic and form a wet soapy film on the surface of the steel to reduce frictional force. Such a soapy film was observed after specimens were broken up after treatment.

2.8.2.6 Alkali Aggregate Reaction

The electromigration of the positive ions Na^+ and K^+ towards the cathode which combine with the OH^- ions modify the local composition of the cement paste and can result in an increase in the risk of expansive alkali aggregate reaction. Certain siliceous aggregates are unstable in alkaline conditions. These unstable aggregates exhibit slightly acidic characteristics which react with the hydroxyl ion, attacking some silicon-oxygen bonds and forming a hydrous silicate gel [Hobbs, 1988]. The gel will expand by imbibition of water and induce forces which may lead to cracking of the concrete and, in severe cases, to structural damage. This type of reaction can take place at the steel surface region, and have a deleterious effect on the strength of the concrete at the concrete interface [Sergi et al., 1991 and Locke, 1983].

Miller [1994] suggested that ASR would not necessarily occur by the application of ECE and cited the work carried out by Bennett & Schue [1990] and Natesaiyer [1990] but Page & Yu [1995] found that ECE did promote ASR in their study on concrete containing Thames valley flint aggregate and calcined flint aggregate. Sergi et al. [1991]

found some significant expansion in similar calcined flint aggregate concrete but by using cathodic protection-type current densities.

Table 2.1: Main Compounds in Portland Cement

Name of Compound	Oxide composition	Abbreviation
Tricalcium Silicate	$3CaO.SiO_2$	C_3S
Dicalcium Silicate	$2CaO.SiO_2$	C_2S
Tricalcium Aluminate	$3CaO.Al_2O_3$	C_3A
Tetracalcium Aluminoferrite	$4CaO.Al_2O_3Fe_2O_3$	C_4AF

Table 2.2: Typical Values of Concrete Permeability and Related Properties.

Test Method	Units	Concrete Permeability/ absorption/ diffusion		
		Low	Average	High
Intrinsic permeability k	m^2	$< 10^{-19}$	$10^{-19} - 10^{-17}$	$>10^{-17}$
Coefficient of permeability to water	m/s	< 10-12	$10^{-12} - 10^{-10}$	$> 10^{-10}$
Coefficient of permeability to gas	m/s	$< 5 \times 10^{-14}$	$5 \times 10^{-14} - 5 \times 10^{-12}$	$> 5 \times 10^{-12}$
ISAT 10 min	$mL/m^2/s$	< 0.25	0.25 - 0.50	> 0.50
30 min		< 0.17	0.17 - 0.35	> 0.35
1 h		< 0.10	0.10 - 0.20	> 0.20
2 h		< 0.07	0.07 - 0.15	> 0.15
Figg water absorption 50 mm (Dry concrete)	s	> 200	100 - 200	< 100
Modified Figg air permeability (Ove Arup) -55 to -50 kPA	s	> 300	100 - 300	< 100
Water absorption 30min	%	< 3	3 - 5	> 5
DIN 1048 depth of penetration (4 days)	mm	< 30	30 - 60	> 60
Oxygen diffusion coefficient 28 days	m^2/s	$< 5 \times 10^{-8}$	$5 \times 10^{-8} - 5 \times 10^{-7}$	$> 5 \times 10^{-7}$
Apparent chloride diffusion coefficient	m^2/s	$< 1 \times 10^{-12}$	$1 - 5 \times 10^{-12}$	$> 5 \times 10^{-12}$

Table 2.3: Threshold chloride content

Total Chloride wt% cem.	Free Chloride Mole/l	[Cl]:[OH]	Exposure	Sample	Reference
0.17 - 1.4			Outdoors	structure	Stratful et al. [1975]
0.2 - 1.5			Outdoors	structure	Vassie [1984]
0.5 - 0.7			Outdoors	concrete	M. Thomas [1996]
0.25 -0.5			Laboratory	mortar	Elsener and Bohni [1986]
0.3 - 0.7			Outdoors	structure	Henriksen [1993]
0.32 - 1.9			Outdoors	concrete	Treadaway et al. [1989]
0.4			Outdoors	concrete	Bamforth and Chapman-Andrews[1994]
0.4	0.11	0.22	Laboratory	paste	Page et al. [1986]
0.4 - 1.6			Laboratory	mortar	Hansson and Sorensen [1990]
0.5 - 2			Laboratory	concrete	Schiessl and Raupach [1990]
0.5			Outdoors	concrete	Thomas et al. [1990]
0.5 - 1.4			Laboratory	concrete	Tuuti [1993]
0.6			Laboratory	concrete	Locke and Siman [1980]
1.6 - 2.5		3 - 20	Laboratory	concrete	Lambert et al. [1991]
1.8 - 2.2			Outdoors	structure	Lukas [1985]
	0.14 - 1.8	2.5 - 6	Laboratory	paste/mortar	Pettersson [1993]
		0.26 - 0.8	Laboratory	Solution	Goni and Andrade [1990]
		0.3	Laboratory	paste/solution	Diamond [1986]
		0.6	Laboratory	solution	Hausmann [1967]
		1 - 40	Laboratory	mortar/solution	Yonezawa et al. [1988]

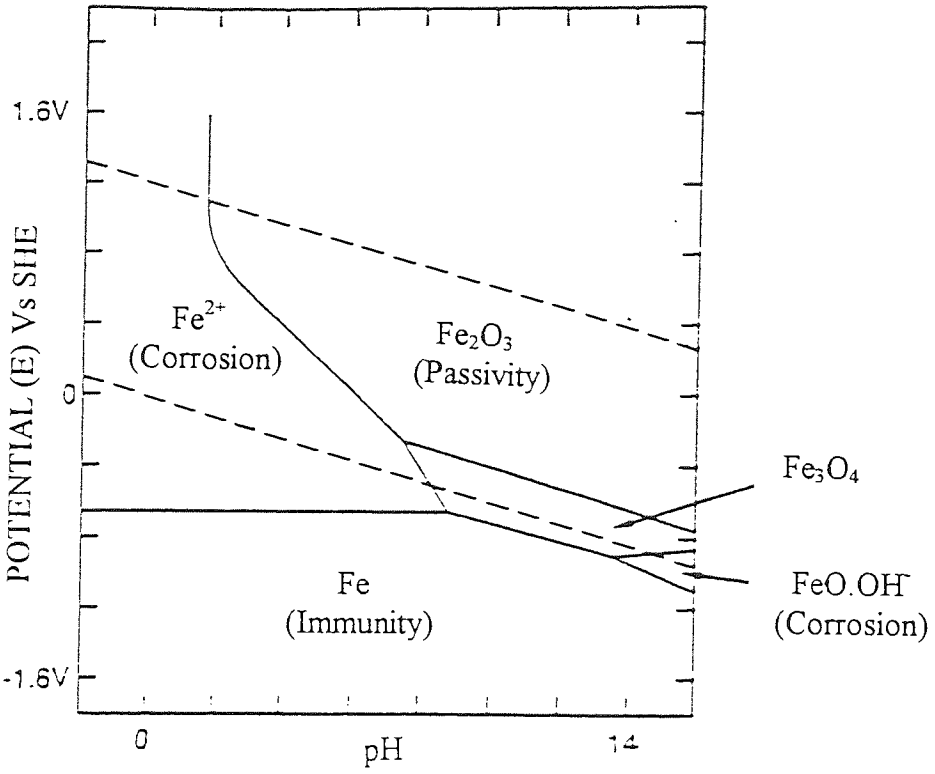

Figure 2.1: Simplified Equilibrium Potential-pH diagram for iron in water [Pourbaix, 1966]

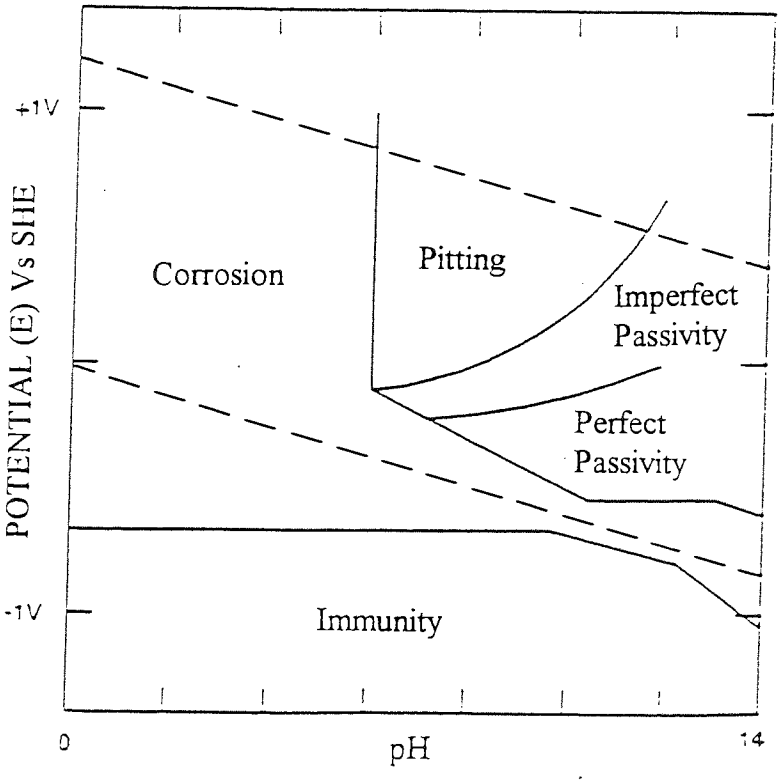

Figure 2.2: Experimentally derived Potential-pH diagram for iron in 0.01M Aqueous Chloride Solution [Pourbaix, 1974]

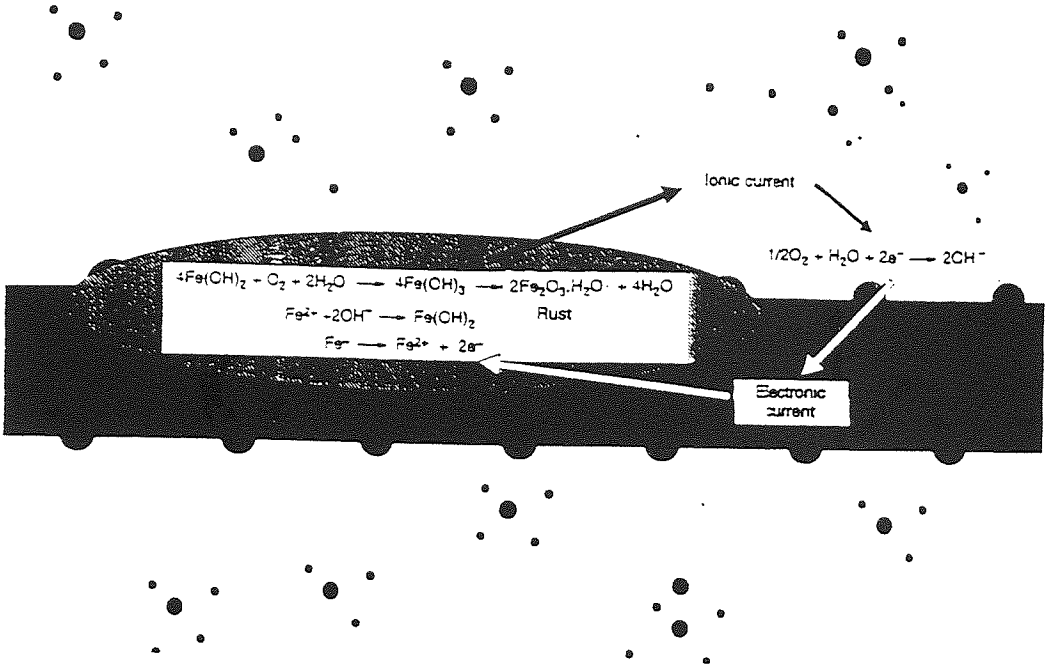

Figure 2.3: The corrosion reactions on steel [Broomfield, 1997]

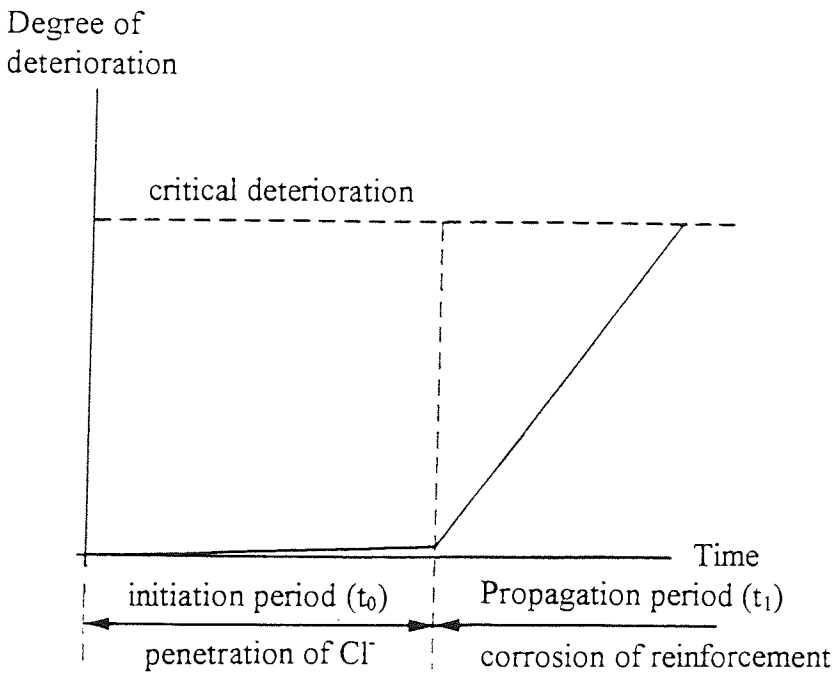

Figure 2.4: Model for corrosion of reinforcement in concrete [Tuutti, 1982]

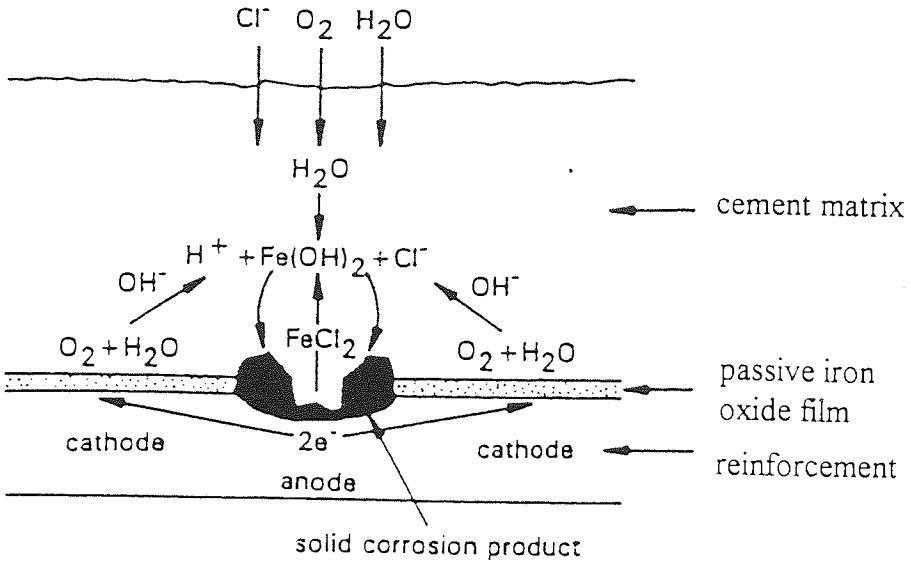

Figure 2.5: Corrosion cell for chloride-induced pitting corrosion [Rilem Report. 1995]

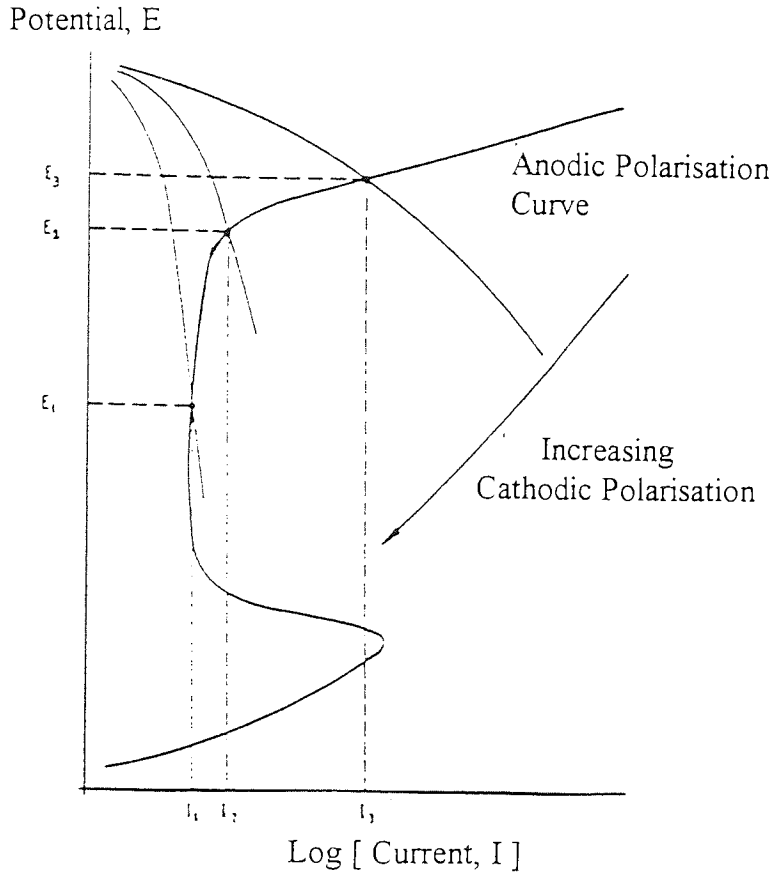

Figure 2.6: Evans diagram showing effect of increasing oxygen availability and increasing cathodic polarisation on a pitting anode [Treadaway 1991]

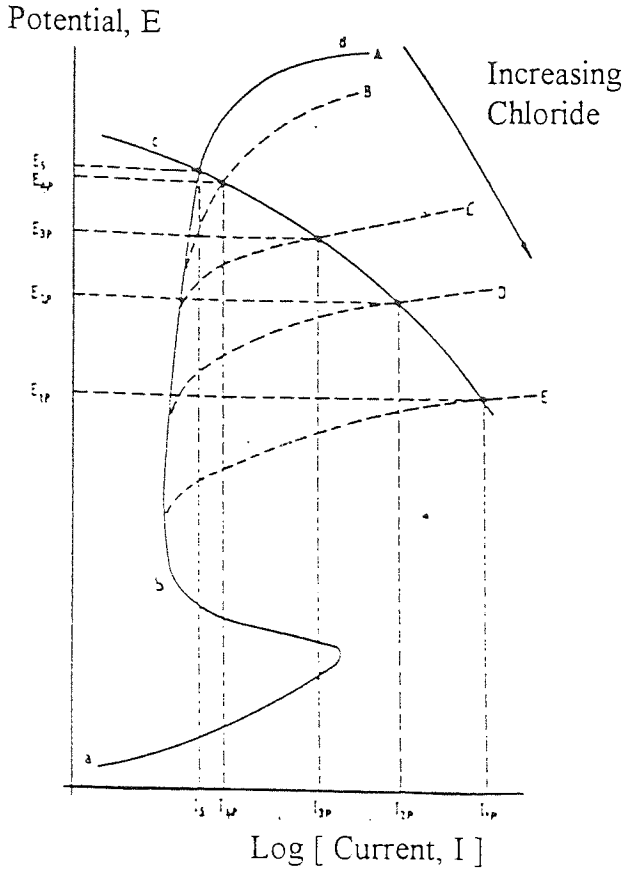

Figure 2.7: Evans diagram of influence of increasing chloride content on corrosion rate of steel in concrete [Treadaway, 1991]

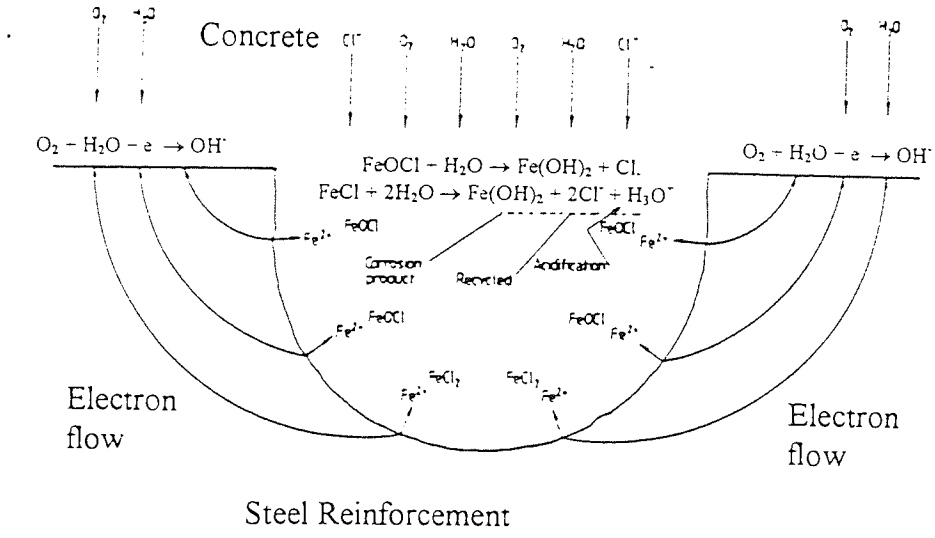

Figure 2.8: Schematic diagram of reactions within a propagating pit [Treadaway 1991]

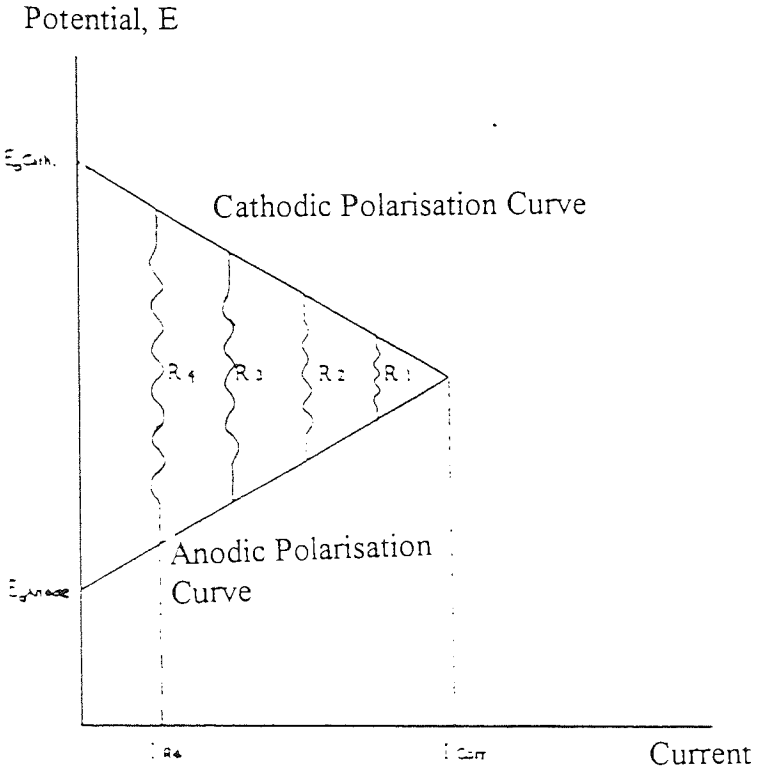

Figure 2.9: Evans diagram indicating effect of increasing anode/ cathode resistance on corrosion rate [Treadaway, 1991]

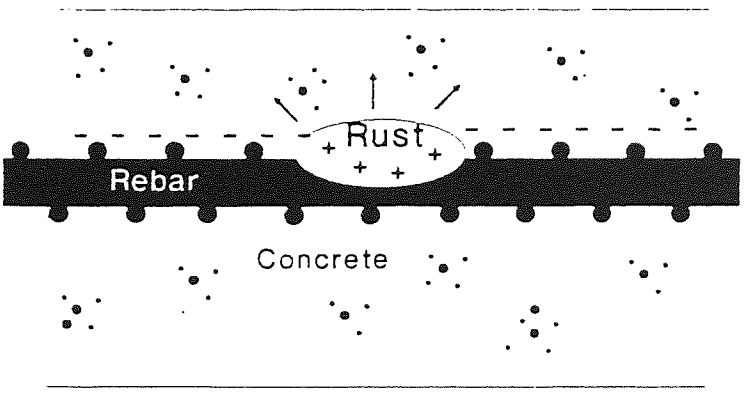

Figure 2.10: Corrosion proceeds by forming +ve and -ve areas on steel [SCPRC/001.95]

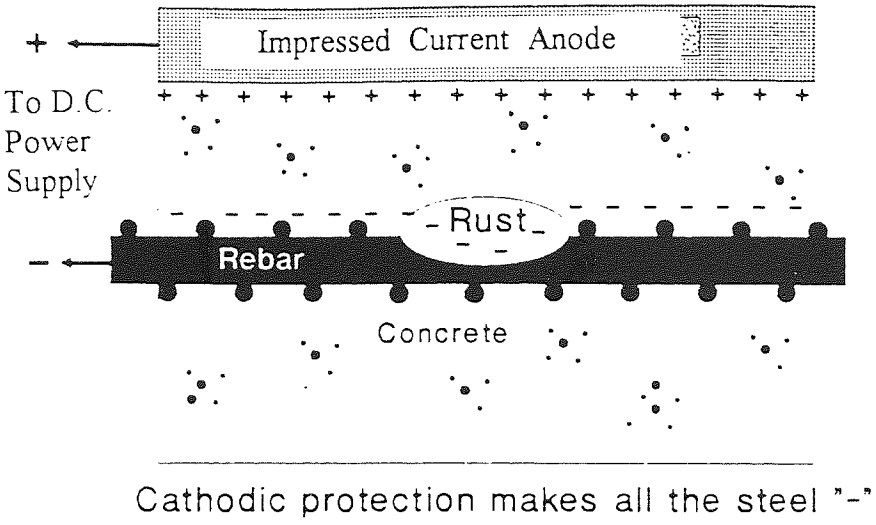

Figure 2.11: How impressed current cathodic protection stops corrosion [SCPRC/001.95]

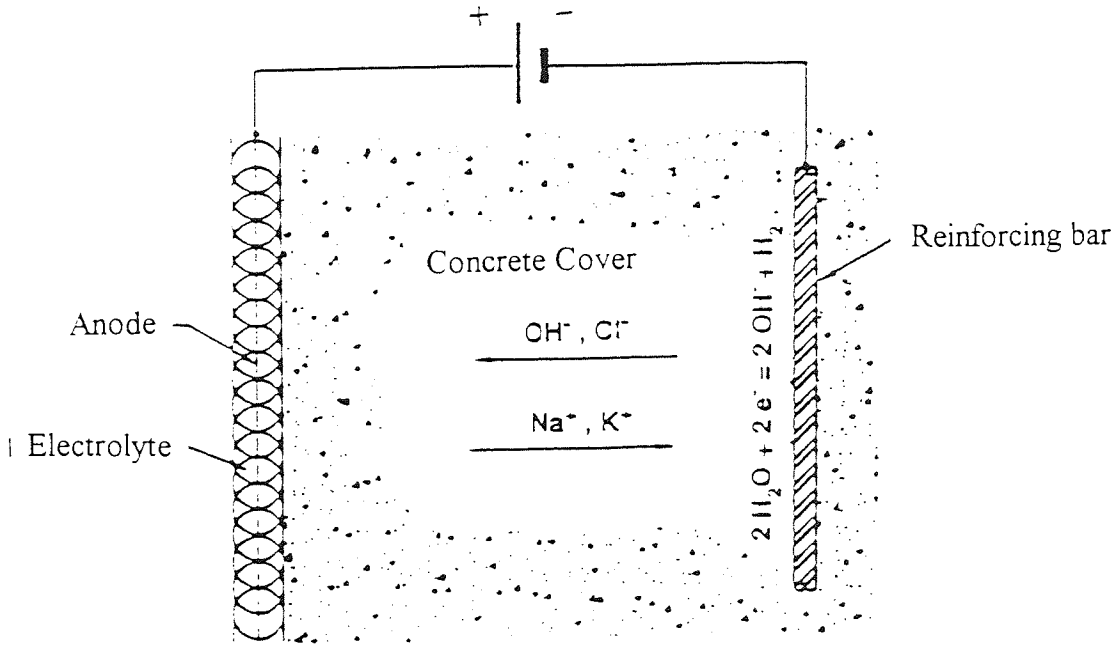

Figure 2.12: Principle of electrochemical chloride extraction [Polder et al. 1995]

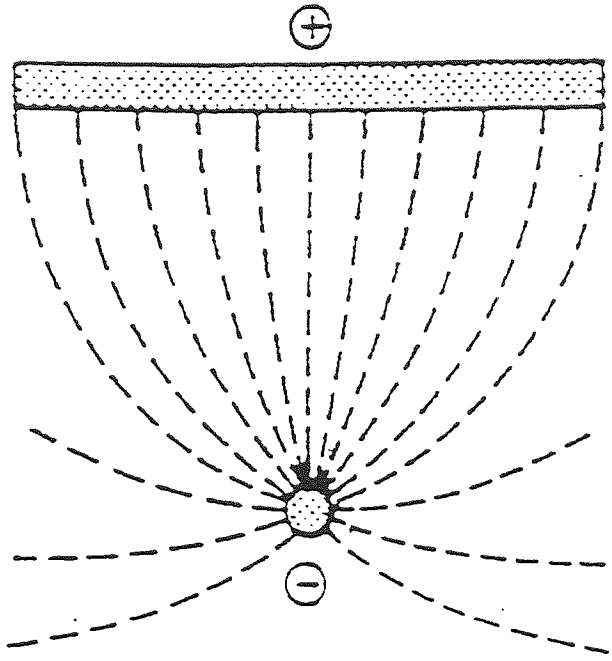

Figure 2.13: Streamlines in an inhomogeneous field between bar and surface [Elsener 1990]

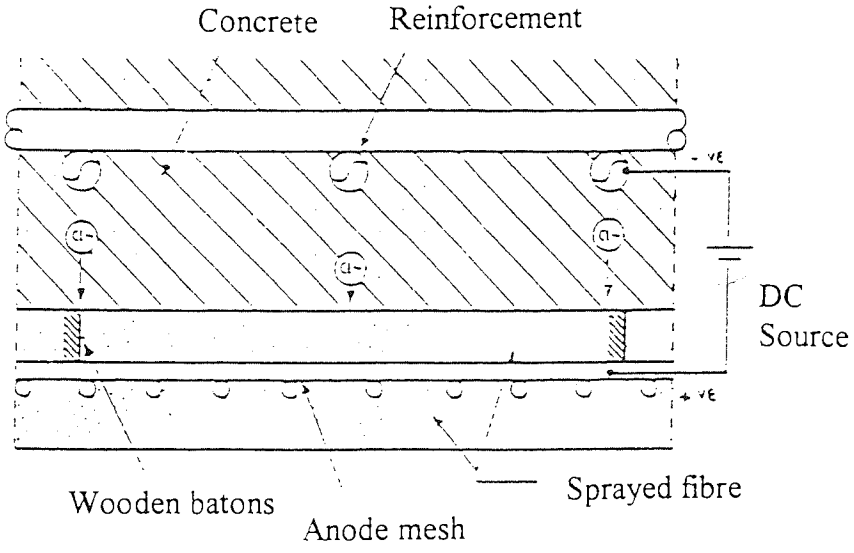

Figure 2.14: Schematic installation of ECE using cellulose fibre as an electrolyte [Collins & Kirby, 1993]

CHAPTER 3

MATERIALS, PREPARATION OF SPECIMENS AND EXPERIMENTAL TECHNIQUES

3.1 INTRODUCTION

This chapter describes the materials used, the preparation and production of specimens and the experimental techniques in conducting the research.

3.2 MATERIALS

3.2.1 Ordinary Portland Cement

The cement used throughout this research was a standard Ordinary Portland Cement (OPC) complying with BS 12, 1978. The chemical composition of the cement and the content of different phases as calculated with the use of Bogue's Formulae is shown in Table 3.1.

3.2.2 Cement Replacement Materials

Two cement replacement materials, namely Pulverised-Fuel Ash (PFA) and Ground Granulated Blast Furnace Slag (GGBS) were used when blending was required. The chemical compositions of the cement replacement materials are given in Table 3.1

3.2.3 Sodium Chloride

Analytical reagent grade sodium chloride (99.5% NaCl) was used in this research which was dissolved in the water during mixing.

3.2.4 Steel Plate

Mild steel plate was used for the cathode with the chemical composition as shown in Table 3.2 and a mixed metal oxide activated titanium mesh was used as an external anode.

3.3 PREPARATION OF SPECIMENS

3.3.1 Cement Paste

The cements were sieved through a 150 μm mesh to ensure homogeneity and to avoid the presence of the coarse unhydrated cement particles in the mix. Blended cement was prepared by adding OPC to PFA and GGBS accordingly and mixing manually to get a proper blended cementitious material. Chloride was dissolved as NaCl by weight of cement in the mixing water. The detail of mixing of chloride and preparation of specimens is explained in section 4.2.1.2

3.3.2 Steel Plate

The cathode consisted of a 35 mm x 35 mm steel plate which was cut from 1 mm thick steel. A 4 mm diameter steel rod was fixed at the centre of the plate by spot welding. An electrical wire was then soft soldered at the top of the rod.

The surface of the steel cathodes were first cleaned by sand blasting and then by wiping with an acetone-imbibed tissue. The clean plates were then stored in a desiccator for a few days. A slurry of cement and styrene-butadiene rubber (SBR) was used to mask the lower part of the rod and the region of the plates where crevice attack might occur. Heat-shrink tubing was used to cover the upper part of the rod. One side of the plate was fully masked with a combination of SBR-modified slurry used as a first and top coat and a layer of sealocrete epoxy resin as the second coat in order to prevent current from generating from that face. The specimens were then cured in a desiccator for three days.

3.4 TEST TECHNIQUES AND PROCEDURES

3.4.1 Pore Solution Expression

A high pressure pore solution expression device was first used by Longuet et al.[1973] and developed by Diamond [1981] and Page[1983]. The determinations of the ionic constituents in cement pastes, mortars and concrete has been made possible by the ability of this device to remove capillary pore solutions by pressure.

The pore solution expression device consists of four main sections viz, support cylinder, platen, die body and piston assembly as shown in Figure 3.1. PTFE spray is applied to the cylinder and piston to minimise the friction between the cylinder surface and the paste. A PTFE disc is inserted between the piston and the cement paste (specimen) to seal the whole diameter of the die to prevent liquid from escaping upward.

Since the specimens were of rectangular form, the edges had to be trimmed a little before being inserted in the cylinder. Pressure was then applied slowly at a rate of 0.3kN/s. The solution was then drawn through the outlet tube and stored in sealed plastic vials to prevent it from being exposed to air. The pressure applied to the piston stopped automatically after reaching a maximum load value of 600 kN. The parts were then cleaned with water and acetone and sprayed with PTFE solutions before re-using for the next specimens.

3.4.2 Pore Solution Analysis

The expression of each batch of sample would take around 30 minutes. The OH^- ionic concentration of the first sample was determined by titration analysis while waiting for the second sample undergoing the expression process. The procedure was followed for each batch of specimens until all the samples were finished. Analysis to determine Cl^-, K^+, Na^+ and SO_4^{2-} ionic concentrations were carried out within a week of expression.

3.4.2.1 Hydroxyl Ions

The hydroxyl ionic concentration was measured by titration. 0.1ml sample of pore solution made up to 1ml with de-ionised water was neutralised with 0.01M Nitric acid, using phenolphthalein as a pH indicator.

The pH of the solution was then calculated from the hydroxyl concentration. The calculation is as below and detailed in Appendix A.

$$pH = -\text{Log}_{10}[H^+]$$
$$pOH = -\text{Log}_{10}[OH^-]$$
$$pH + pOH = 14$$
$$pH = 14 + \text{Log}_{10}[OH^-]$$

3.4.2.2 Chloride ions

The chloride concentration was determined by spectrophotometer which measured the absorbance at 460 nm according to Vogel [1978]. The pore solution first had to be diluted by taking 0.1 ml of the solution and making it up to 250 ml in a standard flask. 2ml of saturated mercuric thiocynate in ethanol, and 2ml of 0.25 molar ferric ammonium sulphate $[Fe(NH_4)(SO_4)_2.12H_2O]$ in 9M nitric acid were added to 10 ml of this solution. Chloride ions displace thiocynate ions which, in the presence of iron(III) ions form a highly coloured complex.

$$2Cl^- + Hg(SCN)_2 + 2Fe^{3+} \rightarrow HgCl_2 + 2[Fe(SCN)]^{2+}$$

The intensity of a beam of monochromatic light is thus related to the concentration of the absorbing substance it passes through. Chloride concentrations were estimated from a calibration curve constructed from standard chloride solutions against absorption as shown in Appendix B.

3.4.2.3 Sodium, Potassium and Calcium Ions

The concentration of the alkali ions, sodium, potassium and calcium were measured by flame emission spectrometry according to Vogel [1978]. The same diluted pore solution as prepared for the chloride test was used. The solution was then poured in a small beaker so that a thin tube could draw it to the flame photometer which atomised and sprayed the liquid over a flame.

When a solution containing a metallic salt is introduced into the flame, it glows transmitting a light of a specific set of wavelengths. A filter is placed in front of the flame allowing only light of the required wavelength to pass through. This enables the concentration estimation of each ionic species by relating the intensity of the light to the ionic concentration. Prior to measurement, a calibration curve using standard solutions has to be produced as shown in Appendix C.

3.4.2.4 Sulphate Ions

The sulphate concentration was determined by spectrophotometer which measured the absorbance at 530nm. Sulphate ions in a range 2-400mg/l may be readily determined by utilising the reaction between barium chloranilate with sulphate ions in an acid solution to give barium sulphate and the acid-chloranilate ion:

$$SO_4^{2-} + BaC_6Cl_2O_4 + H^+ = BaSO_4 + HC_6Cl_2O_4^-$$

The amount of acid chloranilate ion liberated is proportional to the sulphate-ion concentration. The reaction is carried out in 50% aqueous ethanol buffered at a pH of 4. The pH of the solution governs the absorbance of chloranilic acid solution at a particular wavelength; chloranilic acid is yellow, acid-chloranilate ion is dark purple, and chloranilate ion is light purple. At pH 4 the acid-chloranilate ion gives a broad peak at 530nm, and this wavelength is employed for measurements in the visible region.

0.5 ml sample of pore solution was mixed with 2.5ml of buffer solution (pH = 4) and 12.5ml of ethanol. It was diluted with de ionised water to 25ml and 0.08g barium chloranilate was added. After shaking the flask for 10 minutes the solution was filtered to remove barium sulphate and the excess of barium chloranilate and the absorbance value of the filtrate was measured at 530nm against a blank prepared in the same manner [Vogel, 1978]. A calibration curve had first to be constructed using standard potassium sulphate solutions as shown in Appendix D.

3.4.3 Evaporable Water

It is important to determine the bound and free amount of water present in cement in order to express ionic species as free or total amounts present in the paste as a fraction of the unhydrated cement.

Small fragments of about 2 g of hydrated cement were weighed in a platinum crucible immediately after crushing. It was then heated in an oven at 105°C until a steady weight was obtained. It was then transferred to a furnace at 950°C for 30 minutes after which the weight was recorded.

The loss on ignition was determined according to the method given in the British Standard [1970]. About 1g of unhydrated cement was weighed in a platinum crucible before and after heating at 950°C and the loss of mass was reported as a percentage of the weight at 950 °C.

The Evaporable water was then calculated in grammes of water per gram of unhydrated cement after correction for ignition loss and for admixtures, since NaCl was added in the mix. The following equation was used for the calculation of Evaporable water:

$$\text{E.W.}(\%) = \frac{W_0 - W_{105}}{W_{950}} * (100 - i + a)$$

Where

E.W. = evaporable water (% weight of cement)

W_0 = weight of hydrated cement (g)

W_{105} = weight at 105°C (g)

W_{950} = weight at 950°C (g)

i = loss on ignition (% weight of cements)

a = total admixtures (% weight of cement)

Example of calculation of evaporable water is shown in Appendix E

3.4.4 Total Chloride and Alkali Analysis

A sample of cement powder collected during cutting was dissolved in acid for analysing chloride and alkali content. About 0.5g of cement powder which had undergone a dried process at 105°C for 12 hours was placed in a glass beaker. 50 ml of 20% nitric acid was then added. The mixture was placed over a flame and boiled for a few minutes. Once cooled, this solution was filtered and transferred to a standard flask and diluted to 500 ml.

The analysis of chloride, sodium and potassium were the same as described for the pore solution. The total chloride was then calculated as follows:

$$\text{Total Chloride (mM } Cl^-\text{/g cem)} = \frac{\text{Conc. of Chloride in Solution (mM/l)} * \text{Dilution}}{\text{Weight of sample at 950 °C (g)} * 1000}$$

3.4.5 Microhardness Measurement

In order to determine whether softening of the cement paste had occurred during polarisation in the cathodic region, micro-hardness measurements were carried out. For each current density and duration of polarisation, two samples were taken for the micro-hardness measurement. These two samples were then cut in the middle across the cathode so that the measurement could be carried out on the surfaces.

3.4.5.1 Microhardness Determination

Microhardness is a well established technique for measuring the hardness of a material which is defined as a ratio of applied load (g) to the projected area of impression (mm^2). It consists of driving a diamond shaped indenter into the surface using a known load and measuring the size of indentation [Lysaght & DeBellis, 1969 and John, 1993]. The diamond indenter is either of a Knoop or Vickers shape. This technique was adopted for the hardness of cement materials using a Buehler Micromet 4 fitted with a Knoop indenter designed to give a long thin impression on the surface. Figure 3.2 shows the Knoop indenter and the indentations formed by the indenter.

To increase the visibility of the surface indentation under the microscope, the specimens were ground flat using water as the lubricant, polished to 9μm with alumina and ethanediol and polished with a diamond paste down to 1μm. Application of an ink on the specimens surface improved the image of the indentation. A constant load of 100g was applied for 30s to make an indentation on the polished surface of the specimen. The indentation length was then marked and the microhardness reading was recorded in Knoop hardness (Hk) according to John [1993]:

$$Hk = \frac{10P}{7.028l^2}$$

where P is the applied load (g) and

l is the measured length of long diagonal (mm)

3.4.6 Determination of Pore Size Distribution

A mercury intrusion porosimeter (MIP) has been employed to determine the distribution of pore size in hydrated cements by measuring the volume of mercury penetrating a sample. Small fragments of hydrated cement paste of about 30 mg were placed in a bottle containing propan-2-ol for 1 week. The idea is to remove all non-chemically bound water from the specimens. The specimens were then dried in a cool air using a

hair drier and placed in a desiccator. The desiccator was evacuated for a week to remove the alcohol.

About 25 mg of the sample was taken for mercury intrusion measurement where a pressure was applied to drive the mercury inside the pores. The pressure at which mercury enters pores of a given size may be calculated from the Washburn equation [Winslow & Diamond, 1970]

$$P = \frac{-4\gamma \cos\theta}{d}$$

Where P is the applied pressure (N/m^2)

d is the pore diameter (m)

γ is the surface tension of the mercury (N/m)

θ is the contact angle between mercury and the material (117°)

The assumed contact angle was based on earlier work by Winslow and Diamond [1970]. Penetration volume is then plotted against pore diameter which is translated from pressure. This technique is useful to compare different type of cements or similar cements but subjected to different treatments.

3.4.7 Identification of Cement Hydrate Phases

The technique adopted to determine the changes in cement phases due to ECE treatment was X-Ray Diffraction (XRD).

3.4.7.1 X-Ray Diffraction Analysis

A 'Philips' X-Ray diffractometer (with CuKα radiation) was used for the analysis of powdered cement specimens. An electronic counter tube was used to measure the intensity of the x-ray reflections. The counter tube is rotated at twice the speed of the specimens in order to receive the reflected rays. This is shown in Figure 3.3. A trace in intensity (I) is recorded against the Bragg angle (θ) from which the d value can be

determined. The reflection of X-rays of a specific wavelength should be in accordance with Bragg's law

$$n\lambda = 2d \sin\theta$$

where n is the order of reflection (1,2 etc)

λ is the wave length of the x-ray

d is the spacing of the crystal plane

θ is the angle of the incidence or reflection of the x-ray beam.

3.4.8 Potential Measurement

Electrochemical measurement was used to assess the condition of the steel in the specimens. It involves measuring the steel half-cell potential which is the potential difference between the steel and a reference cell which is placed on the cement surface. A saturated calomel electrode was used as the reference cell. A high impedance digital voltmeter was used to collect the data.

Table 3.1: Chemical analysis of OPC cement (% weight)

PROPERTY	OPC	PFA	GGBS
a: Chemical Composition, %			
CaO	65.3	1.45	40.09
SiO_2	20.6	48.2	35.51
Al_2O_3	5.32	32.2	12.59
MgO	1.2	0.66	9.110
SO_3	3.03	0.52	0.150
Na_2O	0.09	2.58	0.540
K_2O	0.75	0.98	0.240
LOI	0.77	3.84	1.170
b: Bogue Compound, %			
C_3S	61.14		
C_2S	13.02		
C_3A	9.74		
C_4AF	7.84		

Table 3.2: Chemical composition (%) of mild steel plate

C	Si	Mn	P	S	Cr	Mo	Ni	Al	Cu	Sn	Fe
0.06	0.01	0.29	.004	.030	0.04	0.01	0.03	.012	0.02	0.05	bal.

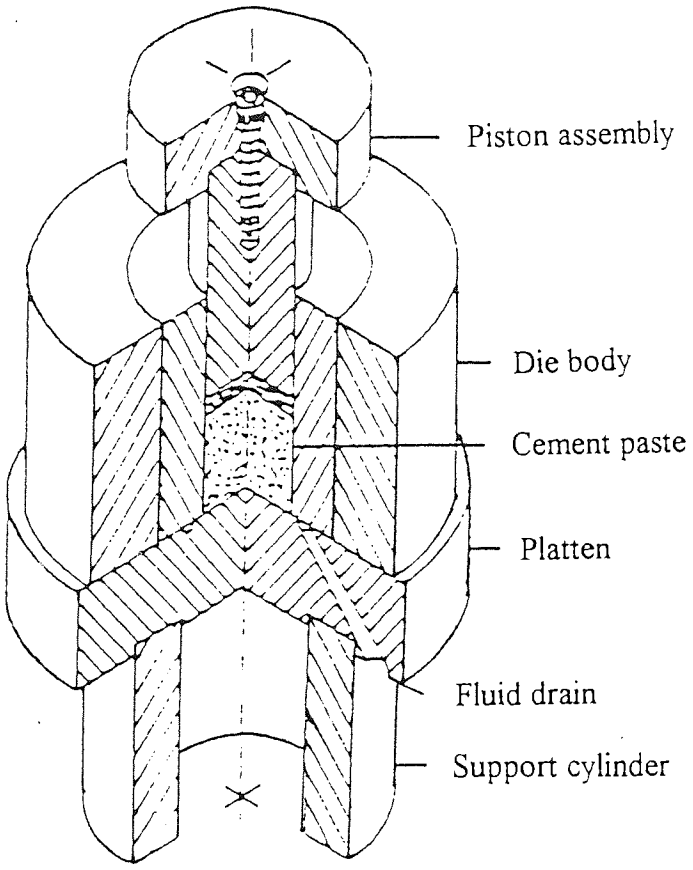

Figure 3.1: Pore expression device. (After Barneyback & Diamond, 1981)

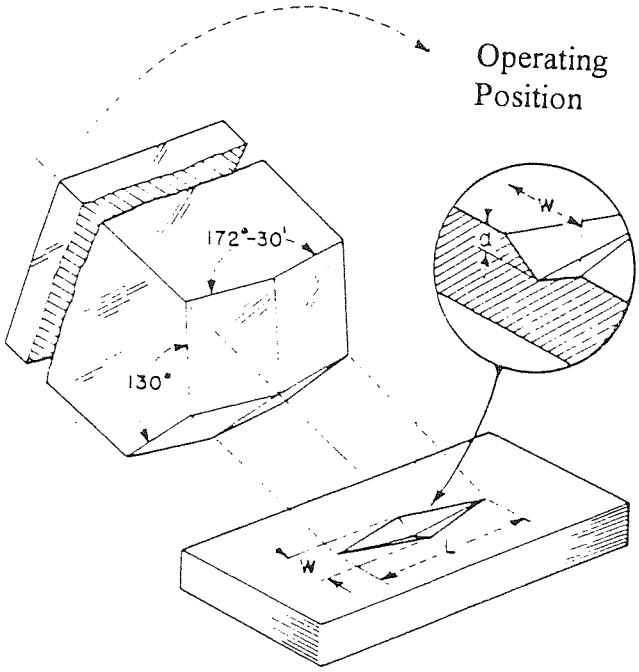

Figure 3.2: Knoop indenter and the Indentation formed (After Lysaght & DeBellis, 1969)

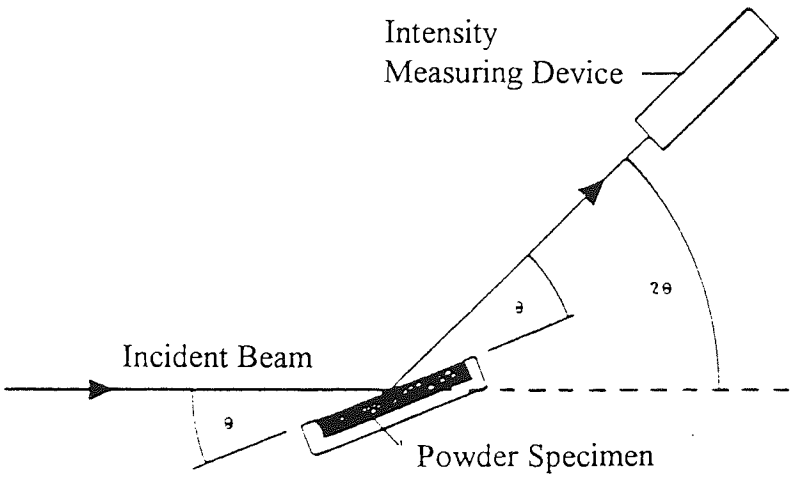

Figure 3.3: Geometric arrangement of the x-ray diffractometer

CHAPTER 4

IONIC REDISTRIBUTION DURING ECE

4.1 INTRODUCTION

Corrosion of reinforcement in concrete due to chlorides is a world-wide problem. Cast-in chlorides which were previously added to the concrete mix as an additive to accelerate the hydration process have now been banned by codes of practice in many countries. However, such a measure is still unable to stop chlorides from entering concrete from external sources such as deicing salts which are applied during the winter. Consequently, structures such as bridges, buildings close to traffic movement and car parks which are exposed to salt spray are still susceptible to chloride contamination. Marine structures, especially in the tidal and splash zones, are also prone to chloride ingress. The wetting and drying process associated with such exposure, accelerates the ingress of chloride into the concrete cover.

When chlorides reach the reinforcing steel, the passive oxide layer, which was formed as a result of the high alkalinity of the concrete, is destroyed. The breakdown of this protective layer can lead to the formation of pits which can generate expansive corrosion products that induce cracking and ultimately spalling of the concrete cover. Deterioration due to corrosion of the reinforcement can be very costly to repair [Page, 1992].

Apart from conventional patch repair techniques which, if not carried out adequately, can lead to incipient anode formation, other appropriate repair methods, which can be grouped under electrochemical rehabilitation techniques, are cathodic protection (CP) and electrochemical chloride extraction (ECE). CP depresses the electrode potential of the reinforcement to a level where pitting corrosion is suppressed and has been practically and successfully used. A drawback with CP lies with the continual maintainance of the system throughout the service-life of the structure and the long term durability of the anode system.

A new technique, now available in the market, is ECE sometimes known as desalination. Although this technique existed as early as the 70's, unsuccessful trials with current densities which were too high, made it unpopular until the late 80s when control on the voltage (not more than 50V) and current density (not more than 5 A/m^2) was applied [Bennett & Schue, 1993]. In this technique, a large cathodic current density is applied through the concrete between the polarised reinforcing steel and an extended anode positioned at the surface for a period of a few weeks. The chloride ions will migrate towards the anode and alkali ions will move in the opposite direction towards the cathode. ECE will not only remove the chloride in the concrete but will also restore the alkalinity around the reinforcement

Today the use of ECE is growing quite extensively [Mc Farland, 1995]. However, as with all new techniques, further research needs to be carried out in order to understand and to improve the system. Problems related to the efficiency of the system, especially with regard to the removal of bound chlorides, and possible side effects which can be caused by the migration of alkalis towards the cathode (reinforcement), the generation of hydroxyl ions around the cathode and the movement of sulphate ions still need to be researched further

The aim of the work described in this chapter was to study experimentally ionic redistribution near the cathode and in the bulk after the application of ECE to hardened cement paste at up to 5 A/m^2 current densities and for periods of up to 12 weeks. The work also enabled study of the effectiveness of the system to remove chloride at variable current densities and time periods and the likelihood of an equilibrium relationship between free and bound chloride even after treatment. This study also looked at the relationship between pH and sulphate ionic concentration and the ionic redistribution in other types of cements than Portland cement.

4.2 MATERIALS AND EXPERIMENTAL SETUP

In this experimental study, the specimens were of two categories. 'Profile-specimens' were specimens in which the initial chloride concentration profile was artificially set according to predictions based on Fick's second law as detailed in section 4.2.1.2. In these samples only OPC cement was used. The other samples known as 'bulk-specimens' consisted of three types of cements, viz. OPC, PFA (70% OPC + 30% PFA) and GGBS (65% OPC + 35% GGBS). In these samples, 1% chloride by weight of cement was dissolved as NaCl in the mixing water and added to the paste during the mixing giving a uniform chloride distribution. The chemical compositions of the cement and the cement replacement materials were as reported in Table 3.1. The content of different phases as calculated with the use of Bogue's Formulae are also shown in Table 3.1. Mild steel plate was used for the cathode with the chemical composition as shown in Table 3.2. A mixed metal oxide activated titanium mesh was used as the external anode.

4.2.1 Preparation, Production and curing of specimens

4.2.1.1 Steel Plate

The preparation of the steel plate was described in section 3.3.2. The diagram of the plate is as shown in Figure 4.1.

4.2.1.2 Modelling of Cement Paste

Before casting, a calculation has been made to model the actual ingress of chloride into concrete. This calculation is based on a solution to Fick's second law of diffusion as follows,

$$C_x = C_0 [1 - \text{erf}(y)] \quad \text{with } y = x/(2 (D.t)^{1/2})$$

where

C_x is the chloride content at depth x (m) after time t (s)

C_0 is the notional surface chloride level

D is the apparent diffusion coefficient (m^2/s)

For this research C_0 was taken as 2% and C_x at x = 55 mm (position of steel cathode) as 0.4%. The result of the full calculation is shown in Table 4.1

Nine batches of an Ordinary Portland Cement paste, each batch containing one of the calculated chloride levels were produced with 0.5 water cement ratio. The different concentrations of chloride 0, 0.2, 0.3, 0.4, 0.6, 0.8, 1.1, 1.5 and 1.8 % as NaCl by weight of cement, were first dissolved in the mixing water which was added to the pre-weighed cement and mixed manually for 5 minutes. The fresh cement pastes were then cast in specially made plastic moulds with dimensions of 50 x 50 x 100mm. The mould was then vibrated for 1 minute on a vibrating table for compaction. In the case of the paste containing 0.4% chloride by weight of cement, six steel plates were immersed in the mix fixed to the mould by special plastic holders. The plates were arranged so that they were perpendicular to the longest dimension of the specimen.

4.2.2 Curing, Cutting and Sticking of Specimens

After casting, the moulds were covered with plastic to avoid water evaporation and stored at room temperature in a high humidity room. The specimens were demoulded after 18 hours and then wrapped in cloths soaked with water and stored in an air tight bag for 1 week in a container of 100% RH. The specimens were then cut into slices about 13 mm thick by using a diamond-tipped clipper. The surfaces were then ground so as to produce smooth and perfectly flat surfaces using a grinding machine. The final thickness of the slices was about 10 mm. Cement slurry was spread on the surfaces of the pre-wetted individual slices to make them electrolitically continuous with each other, taking care not to trap any air bubbles. The individual slices containing one of the different chloride contents were then laminated together in increasing order of concentration and stored for another seven weeks in a container with RH of 100%. The arrangement of the slices is as shown in Figure 4.2. The final dimension of the specimen was 50 x 50 x 90 mm.

Bulk-specimens were continuously cured for eight weeks without involving any cutting and cementing procedures.

4.2.3 Galvanostatic Polarisation

At the end of the curing period, the specimens were prepared for polarisation as shown in Figure 4.3. Each specimen was wrapped in a cloth leaving one face uncovered for applying the anode. The specimens were fixed to the wall of a specially constructed reservoir. Pressure was applied on the 'rear' face of the specimen by a screw in a way that ensured that an area of the front exposed surface was in contact through the window with the solution. Silicone rubber sealant was placed at all the contact edges between the specimen and the wall of the reservoir. Anodes, 50 x 50 mm, were cut off from an activated titanium mesh and positioned in the reservoir at the end of the exposed face of the specimens. About 5 litres of solution consisting of saturated calcium hydroxide was then introduced into the reservoir. Six specimens were placed in each reservoir with their long dimensions parallel to each other and at equal distances apart sharing the same solution.

The steel plates (cathodes) were connected to the negative pole of the galvanostat, whilst the titanium anodes were connected to the positive pole of the galvanostat. The specimens were left in a high humidity room.

For the profile-specimens three different cathodic current densities of 0, 1, and 5A/m^2 of steel surface were applied. Each current density was applied to a group of six specimens individually. The value of 0 A/m^2 was set as a control, 1 A/m^2 is the typical value used for desalination purposes and 5 A/m^2 is the level proposed by Polder & Hondel [1992] and Bennett & Schue [1993] as the upper limit for the current density in desalination. The polarisation periods were 4, 8 and 12 weeks. Table 4.2 summarises the different polarisation levels and periods and shows the total charge circulated.

For bulk-specimens only a single current density (5 A/m^2) was used and the treatment was set for 12 weeks.

4.2.4 Chemical Analysis of Hardened Cement Paste and its Pore Solution

To evaluate the concentration profiles of chloride, sodium, potassium and sulphate ions in the cathodic region, chemical analysis was carried out. The free ionic concentration in the pore solution and the total content in the hardened cement paste were determined. Hydroxyl ionic concentration was determined from the pore solution.

4.2.4.1 Sample Preparation

After every polarisation period, all the specimens were disconnected from their wiring system and sealed in a small polythene bag. Two specimens were set aside for microhardness testing and the remaining four specimens for chemical analysis. The specimens for chemical analysis were dry-sliced into sections at regular intervals (10mm) parallel to the steel plates with the use of a mechanical hacksaw as illustrated in Figure 4.4. Corresponding sections from the four specimens were grouped and stored in sealed polythene bags inside a plastic container. The samples were then pressed in the pore expression device. The dimensions and cutting arrangement for bulk-specimens are as shown in Figure 4.5.

4.2.4.2 Pore Solution Expression

Each sample, made up of equidistant slices from the four specimens, was inserted in the pore expression device shown in Figure 3.1. A PTFE disc was inserted between the piston and the cement paste specimen to seal the whole diameter of the die and prevent liquid from escaping upward. A load was then applied slowly at a rate of 0.3 kN/s. The solution was then drawn through the outlet tube and stored in sealed plastic vials to prevent it from being exposed to air. A detailed description of the pore solution device was given in section 3.2.3 and the chemical analysis procedure for ions was discussed in section 3.2.4.

4.3 RESULTS AND DISCUSSION

4.3.1 Free Ionic Concentration Analysis of Profile-Samples

Figure 4.6 shows the ionic concentration profile determined on profile-specimens which were exposed to the ECE solution for one of the three periods but were not subjected to polarisation. The setup of the specimen was similar to the treated specimens and the samples were analysed after 4 weeks, 8 weeks and 12 weeks. Each point represents the value determined from the pore solution extracted from four equidistant slices from the steel cathode. The points are plotted at a distance corresponding to the middle of these slices.

A significant drop in the value of ionic concentrations was observed near the surface (x = 5 mm) as shown in Figure 4.6. This is due to leaching of ions occurring near the surface which was in contact with the electrolyte. Other than that, there was no obvious difference with time of exposure, except perhaps an overall reduction in the OH^- concentration.

Figure 4.7 shows the ionic concentration profiles determined on specimens treated using $1A/m^2$ current density analysed after 4, 8 and 12 weeks. The ionic concentration gradients in Figure 4.7 do not look very different to those in Figure 4.6 apart from a small overall increase in OH^- concentration and an overall small drop in chloride concentration particularly close to the surface. Even after 12 weeks, the $1A/m^2$ current density used was not very effective in removing chloride from the specimens. No real increase in concentrations of Na^+ and K^+ ions near the cathode were observed.

Figure 4.8 which depicts the ionic concentration gradient of specimens subjected to $5A/m^2$ current density for up to 12 weeks, shows some interesting results. The gradients of all the ions altered even after four weeks of polarisation. The hydroxyl ionic concentration increased up to 520mM/l resulting in a higher pH value close to the cathode. The sodium and potassium ionic concentrations were also affected by the polarisation. The attraction of the sodium and potassium ions to the cathode and their repulsion from the anode produced S-shaped curves as shown in Figure 4.8a. The

reduction of overall chloride concentration at this stage (4 weeks) was still relatively small.

Ionic concentration profiles after 8 weeks of polarisation as shown in Figure 4.8b, show further changes. The OH^- ions concentration had increased up to 660 mM/l which resulted in a pH of 13.82. The chloride concentration overall dropped quite significantly near the cathode as well as near the surface. Increase in positive ions (Na^+ and K^+) near the cathode was also significant. Furthermore, the reduction in the concentration of alkalis close to the surface was more pronounced due to electromigration.

Figure 4.8c shows the ionic concentration profile after 12 weeks of polarisation. For the alkali ions and OH^- ions, the drop in concentration after about 30 mm from the steel cathode is more pronounced than the increase near the cathode. Near the anode, the OH^- ionic concentration decreased substantially due to the acidity produced during the anodic reaction. However, its level at the cathode did not show any further increase whilst those of Na^+ and K^+ continued to increase.

Hydroxyl ions are produced as a result of the cathodic process as shown in reaction (2.9) and (2.10) in section 2.6. From reaction 2.9, the existing oxygen is used up to form OH^- ions at the cathode. As the amount of oxygen arriving at the steel surface is less than that required by the reaction, reaction (2.10) predominates where the formation of OH^- ions and gaseous hydrogen occur simultaneously with the decomposition of water. Positively charged ions Na^+ and K^+ move to the cathode and form sodium hydroxide and potassium hydroxide with the hydroxyl ions. The production of hydroxyl ions occurring continously at the cathode would normally result in an increased concentration of OH^- ions even though the negatively charged ions, OH^- and Cl^-, migrate away from the cathode. This is because for every OH^- or Cl^- ion that leaves, a new OH^- ion is formed [Tritthart, 1996]. The fact that the OH^- concentration did not appear to increase near the cathode at 12 weeks can be explained by the very large increase in the $SO_4^=$ content as will be discussed in section 4.3.1.2, which maintained the necessary charge balance.

Despite the relatively large volume of saturated $Ca(OH)_2$ solution in the reservoir (5 litres per 6 specimens) and the frequent stirring (3-4 times a week) the pH of the solution was reduced gradually to neutral or even acidic values as low as pH 4. Initially, consumption of OH^- ions would have been occurring (eq. 2.6) but as the pH was lowered the electrolysis reaction (eq 2.7) would have become more prominent producing H^+ ions. The positively charged H^+ ions would migrate towards the cathode under the influence of the applied current. When H^+ ions meet OH^- ions which move in the opposite way, neutralisation occurs to form water. Furthermore, when H^+ ions meet Cl^- ions migrating from the cement paste hydrochloric acid is formed, therefore, the pH value of the electrolyte drops into an acidic range as the treatment continues. Contact between the acidic electrolyte and the cement close to the surface can lower the OH^- ionic concentration. Chloride ions arriving at the anode can discharge as chlorine gas at a pH of about 4 or lower as shown by reaction (2.8).

In contrast with the alkali metal and hydroxyl ions, the concentration of chloride ions was reduced significantly in the vicinity of the cathode as well as in the bulk. The reduction in the chloride concentration was caused by electromigration towards the external anode. The effects of polarisation time on the changes of free chloride concentration are shown more clearly in Figure 4.9. From the figures, it can be seen that chloride concentration tended to decrease with increasing polarisation time. This indicates that free chloride ions were removed constantly from the paste by migration under the applied current.

Considerably more chloride was lost from near the surface (anode) compared to near the cathode owing to the initial chloride concentration profile. This could have been facilitated by the decrease in the concentration of the OH^- ions near the anode. As discussed in section 2.8.1 the chloride tranference number t_{Cl} is defined as the amount of DC current carried by the chloride ions I_{Cl} in relation to the total current I_{tot} ($t_{Cl} = I_{Cl}/I_{tot}$). The chloride transference number depends on the chloride concentration and on the concentration of other ions present in the pore solution especially OH^- ions and alkali ions [Elsener & Bohni, 1994]. However, since negatively charged ions are attracted to the anode, only OH^- ions need to be considered [Tritthart, 1996]. As the concentration of OH^- ions decreases near the anode, less current is tranferrered by the

OH^- ions allowing a greater proportion of current to be tranferred by the Cl^- ions. The lower the OH^- ionic concentration is, the higher the chloride transference number becomes resulting in more efficient removal of the chloride ions.

As would be expected, Figure 4.9 shows that the 5 A/m^2 current density managed to extract chloride more effectively compared to the 1 A/m^2 current density.

4.3.1.1 Ionic Movement with circulated charge

Figure 4.10 shows ionic concentrations in the pore solution of hardened cement paste within a distance of 0 to 5 mm from the steel cathode as a function of circulated charge. From this figure, it can be seen that hydroxyl, sodium and potassium ions increased in concentration as the charge increased. The increase in ionic concentration was much more pronounced after more than 3000 Ah/m^2 charge was passed. Chloride ions on the other hand decreased significantly beyond that figure. This confirms that for periods up to 12 weeks, 1 A/m^2 current density is not very effective in removing chloride when compared to 5 A/m^2.

A very high value of circulated charge results in elevated sodium, potassium and hydroxyl ionic concentrations near the cathode. The pH value, representing an average within a distance of 5 mm from steel plate was measured to be as high as 13.8. A higher pH value is expected very close to the cathode as will be discussed in section 4.3.4

4.3.1.2 Sulphate Ionic Concentration

The concentration of sulphate ions near the steel cathode is also presented in Figure 4.10. As was the case with the alkali and OH^- ions, its concentration increased with increasing circulated charge even though free sulphate ions are being driven away from the cathode by the applied electric field. This increase in sulphate concentration locally supports the argument of dissolution of sulphate ions from solid phases within the cement matrix (calcium sulphoaluminate hydrates) [Page et al., 1994].

Sulphate ionic concentration plotted against the hydroxyl ionic concentration on a logarithmic scale, shown in Figure 4.11, suggests an approximate linear relationship. Page et al., [1994] explained this in terms of solubility equilibria, which involve an exchange between sulphate and hydroxyl ions. Bertolini et al., [1996] referred to Damidot and Glasser [1993] who expected the following equilibria, if coexistence of the solid phase, ettringite, hydrogarnet and portlandite is involved.

$$3CaO.Al_2O_3.3CaSO_4.32H_2O = 2Ca^{2+} + 2Al(OH)_4^- + 3SO_4^{2-} + 4OH^- + 26H_2O \quad (4.1)$$

$$3CaO.Al_2O_3.6H_2O = 3Ca^{2+} + 2Al(OH)_4^- + 4OH^- \quad (4.2)$$

$$Ca(OH)_2 = Ca^{2+} + 2OH^- \quad (4.3)$$

These equilibria would give a relationship between sulphate and hydroxyl ions as expressed by

$$[\ SO_4^{2-}\ ] = K_1^{1/3}\ K_2^{-1/3}\ K_3^{-1}[\ OH^-\ ]^2$$

Whence, $$\text{Log}\ [\ SO_4^{2-}\ ] = 2pH + \text{Log}\ \{\ K_1^{1/3}\ K_2^{-1/3}\ K_w^{\ 2}\ \}$$

Where K_1, K_2 and K_3 are the solubility products of the phases referred to in equation 4.1, 4.2 and 4.3 and K_w is the ionic product of water.

The mechanism of sulphate attack can be divided into ettringite formation, gypsum formation and salt crystallization. All products occupy a greater space than the original compounds causing expansion, disruption and cracking. For gypsum and ettringite formation , the volume increases by about 1.2 to 2.5 times whereas the crystallization of $Na_2SO_4.10H_2O$ can cause expansion of about 4 to 5 times the original volume [Irassar et al., 1996]. As will be discussed in chapter 5, no evidence of ettringite formation was observed.

4.3.2 Total Content Analysis of Profile-Specimens

Figure 4.12 shows the total (acid soluble) profile concentrations of sodium, potassium and chloride ions of an untreated profile-sample exposed to the ECE solution for 4, 8 and 12 weeks. As with the pore solution results discussed in section 4.3.1, analysis

showed a slight change in chloride and alkali metal ionic concentrations near the surface of the specimens due to leaching. Overall, there were no other large changes.

With $1A/m^2$ current density, as shown in Figure 4.13, alkali metal ions show a slight increase in concentration near the cathode beginning from week 8. However, this increase was not very large even after 12 weeks of treatment. Chloride, in contrast with alkali metal ions, showed a slight reduction in concentration both in the vicinity of the cathode and near the surface especially after 12 weeks of polarisation.

Figure 4.14 depicts the total content of ions of specimens subjected to electrochemical treatment at $5A/m^2$. As was the case with the pore solution results in Figure 4.8, the changes in concentration were more pronounced. At 4 weeks the rise in concentration of Na^+ and K^+ ions near the cathode was already obvious and this trend continued after 8 and 12 weeks. The significant increase appeared to start at a distance of about 25 to 35 mm from the surface.

Chloride, decreased in concentration both near the cathode and in the bulk. This decrease in chloride content is shown more clearly in Figure 4.15 where comparison is made between the polarisation periods.

4.3.3 Equilibrium between Free and Bound Chloride

When chloride ingress into concrete occurs or when chloride is added to the concrete mix, cement hydrates bind a certain proportion of the chloride. This proportion of bound chloride varies according to the cement type [Rilem Report 12, 1995]. Bound chloride reaches a limit when the binding capacity of the cement is exausted. Any chloride added beyond this limit will remain free in the pore-solution [Page et al., 1991, Rilem Report 12, 1995]. This can be best explained from Figure 4.16. In the beginning of addition, if all the chloride is bound, the binding of chloride will follow the line of equality until it reaches point A, (maximum binding capacity). Further addition of chloride beyond the maximum binding limit will not increase the bound chloride but will remain free. In

reality, an equilibrium of free and bound chloride exists so that the bound chloride follows line B in Figure 4.16 and the free chloride follows line C.

When ECE was carried out, as shown in Figure 4.17, chloride concentration near the steel cathode (52.5mm from the surface) and in the bulk (35 mm from the surface) decreased with increasing charge passed. This indicates that chloride ions were removed constantly from the paste by electromigration. Figure 4.18 shows not only that free chloride was removed but also that the decomposition of the solid hydrates such as Friedel's salt (calcium chloroaluminate hydrate) and its subsequent removal had occurred. The speed of reduction of both the free and the bound chloride was quite fast as is evident in Figure 4.18. It can be seen that, Figure 4.18 looks very similar to Figure 4.16 where chloride is added, so it seems reasonable to assume that the same equilibrium of free to bound chloride is maintained during removal of chloride. If bound chloride is not removed, its concentration remain at a level close to the maximum binding capacity of the cement represented by line A in Figure 4.18. Also if the speed of removal is slow, the measured concentrations of bound chloride will fall close to the line of equality.

A plot of free chloride against bound chloride (Figure 4.19) resulted in a typical non linear curve which Sergi et al., [1992] approximated to a Langmuir adsorption isotherm indicating a stable equilibrium between free and bound chloride. Figure 4.20 is a plot of free chloride against total chloride at all depths and confirms that a binding capacity exists for the cement which can be approximated by the intercept of the rectlinear plot on the horizontal axis [Page et al., 1991(b)].

ECE proved to be effective in removing both free and bound chloride. However, not all chlorides were removed even at the higher charge conditions. This is likely to be related to the decreased relative concentration of chlorides to other anions causing a reduced efficiency of its removal. The consequence of chlorides left in the cement will be looked at again in chapter 6.

4.3.4 Ionic Concentration Profiles of Blended Cements subjected to ECE

Chemical analysis on the blended cements were carried out in the same manner as for the profile-specimens discussed above. The only difference was in the method of cutting where the distances were 5, 14, 23, 32, 41 and 50 from the surface. Figure 4.21 shows the concentration of hydroxyl ions in the cement analysed after the specimens were subjected to the ECE process for 12 weeks with 5 A/m^2 current density. From the figure, it can be seen that the hydroxyl ionic concentration in the vicinity of the cathode for OPC increased to 1400 mM/l, to 1200 mM/l for PFA and to 540 mM/l for GGBS.

The higher OH^- concentration of OPC in this study compared to that reported in section 4.3.1 is due to the thinner thickness of the sample analysed near the cathode where the higher hydroxyl ionic concentrations occur. This rise in OH^- concentration around the cathode results in a pH of more than 14 as shown in Figure 4.22. This is in agreement with results reported by Page et al. [1994] who analysed the cement very close to the cathode and with the pore solution study by Tritthart [1996]. This level of pH can be dangerous as it can trigger ASR in concrete which contains even mildly reactive aggregates which, under normal conditions, may be considered harmless [Page et al., 1994]. The pH of PFA cement was also elevated up to 14 near the cathode whilst the pH for GGBS cement increased only to 13.7.

Figure 4.23 and 4.24 show the free and total chloride concentration profiles. More chloride was driven out from the OPC specimens when compared to the blended cement specimens. It is known that blended cements containing slag or pozzolana limit chloride diffusion more effectively than OPC owing to a number of reasons such as fineness of pore structure, greater tortuosity and pore surface interactions [Page et al., 1981]. Similar mechanisms may restrict ionic migration to an extent even under the influence of an electric current. This is evident in Figure 4.25 and 4.26 for free and total sodium concentration and Figure 4.27 and 4.28 for free and total potassium concentration. Very little increase in the potassium ionic concentration near the cathode was observed for the GGBS cement specimen as shown in Figure 4.28.

The equilibrium of free and total chloride as discussed in section 4.3.3 is also evident in this case as shown in Figure 4.29. This figure again shows clearly that more chloride was removed from OPC compared to PFA and GGBS cements but, as all the points appear to lie on a single straight line, there is no evidence to suggest that the blended cements have a superior chloride binding capacity as suggested by Holden et al. [1983]. Rilem Report 12 [1995], explained that blended cements containing slag or PFA, lower the concentration of C_3A considered to be the most important compound for chemical binding of chloride ion to form Friedel's salt ($3CaO.Al_2O_3.CaCl_2.10H_2O$). On the other hand, however, these materials (slag and pozzolana) increase the formation of CSH and CSH-like phases which adsorb chloride due to surface forces and therefore retain more chloride in the sample. This is a more loosely form of bound chloride compared to chlorides bound by C_3A [Maslehuddin, 1994].

The relationship between sulphate concentration and pH is shown in Figure 4.30. The pH of OPC and PFA rose up to above 14. When the pH increased, the sulphate ionic concentration was elevated near the steel cathode.

4.4 CONCLUSIONS

From the study conducted in this chapter, it was found that ECE is capable of removing free and bound chloride quite effectively. More chloride is removed as the current or polarisation time is increased. An equilibrium between free and bound chloride is maintained when chloride is removed from the concrete. A reduction in the efficiency of chloride removal was observed as the concentration of chloride diminished owing to the resultant lower transference number.

A change in ionic concentration gradients resulted from the ECE process around the cathode; changes in concentration were more prominent after specimens had undergone longer treatment periods or were exposed to higher current densities. The combined effect of current density and polarisation time resulted in chloride ionic concentrations decreasing near the cathode because chloride was transported away from the cathode.

Conversely, hydroxyl ionic concentrations increased with increased polarisation near the cathode as a result of the cathodic process and the alkali ionic concentrations increased due to the electromigration process. The hydroxyl ionic concentration near the surface of the cements was depleted due to contact with the external electrolyte whose pH was reduced by the anodic reactions.

The sulphate ionic concentration also increased near the steel cathode as the hydroxyl concentration increased as a function of the circulated charge. The increase in concentration of sulphate ions locally is indicative of dissolution of sulphate ions from solid phases within the cement matrix

The removal of chloride ions was more effective from OPC when compared to blended cements. This is possibly related to the denser matrix in blended cements which lowers their permeability. It may also be due to the supposedly superior chloride binding capacity of the blended cements although, this was not found in these experiments.

Finally, it was shown that, it is possible to simulate the profile of chloride ingress in concrete exposed to a chloride laden environment by making a laminated sample, as described in section 4.1.1.2, with added chloride levels according to Fick's second law of diffusion. The evaluation of ECE techniques can then conveniently be conducted in the laboratory using small samples.

Table 4.1: Chloride concentration in each slice of cement

Slice No	x (mm)	y	erf (y)	1 - erf(y)	Cx	NaCl (% wt. of cem.)
1	5	0.080	0.09	0.91	1.80	3.0
2	15	0.25	0.28	0.72	1.50	2.5
3	25	0.41	0.44	0.56	1.10	1.8
4	35	0.58	0.59	0.41	0.80	1.3
5	45	0.75	0.71	0.29	0.60	1.0
6 (cathode)	55	0.91	0.80	0.20	0.40	0.7
7	65	1.10	0.87	0.13	0.30	0.5
8	75	1.24	0.90	0.10	0.20	0.3
9	85	1.41	1.00	0.00	0.00	0.0

Table 4.2: Galvanostatic polarisation: total charge circulated ($A.h/m^2$)

	Applied current density		
Polarisation Time	0 A/m2	1 A/m2	5 A/m2
4 Weeks		672	3360
8 Weeks		1344	6720
12 Weeks		2016	10080

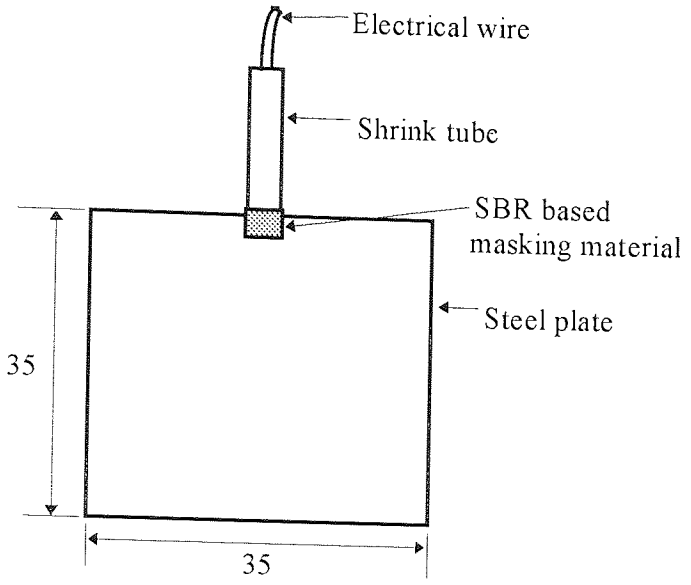

Figure 4.1: Steel plate (cathode)

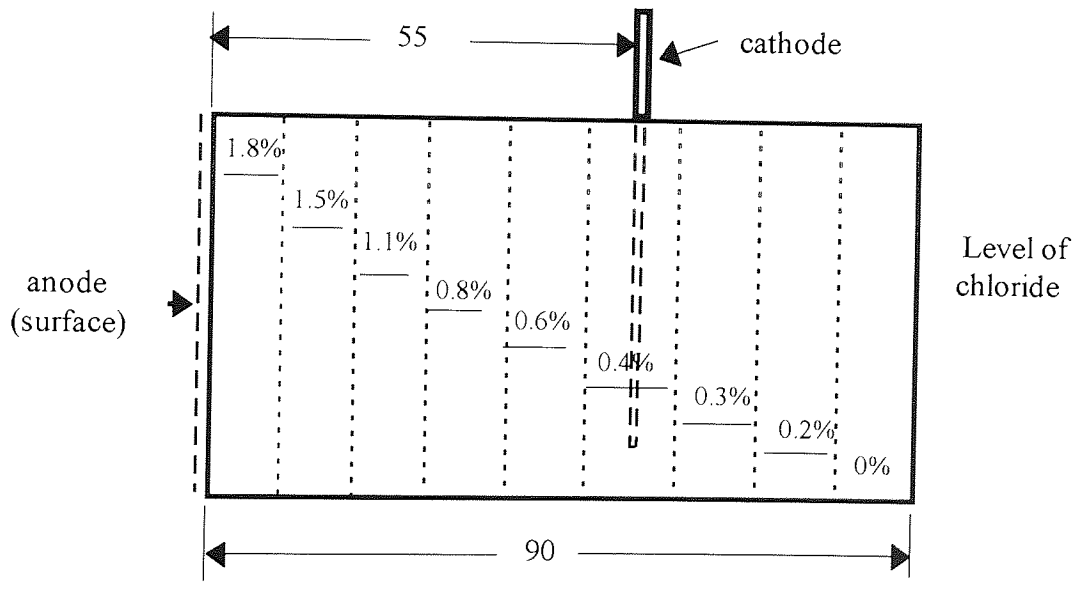

Figure 4.2: Arrangement of different slices of chloride concentrations

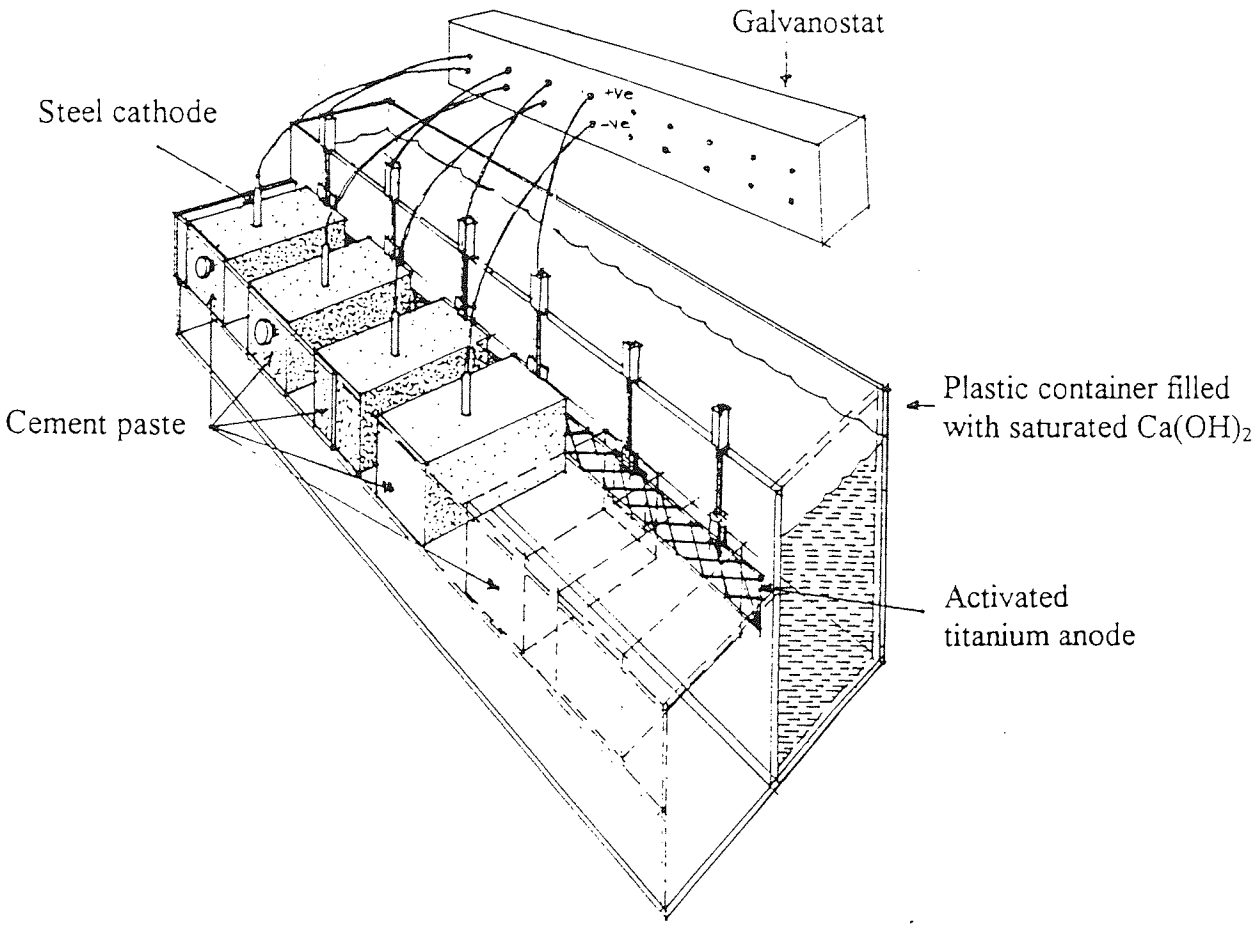

Figure 4.3: Setting-up of galvanostatic polarisation on specimens

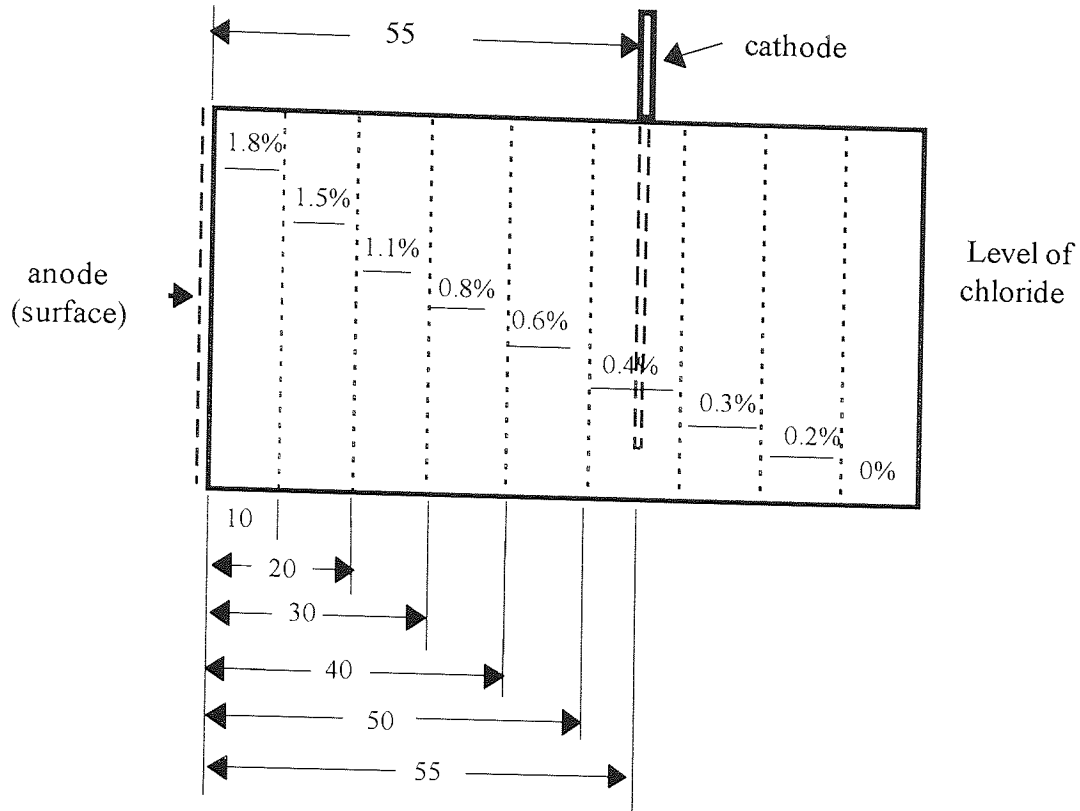

Figure 4.4: Arrangement of cutting of profile-plate specimens

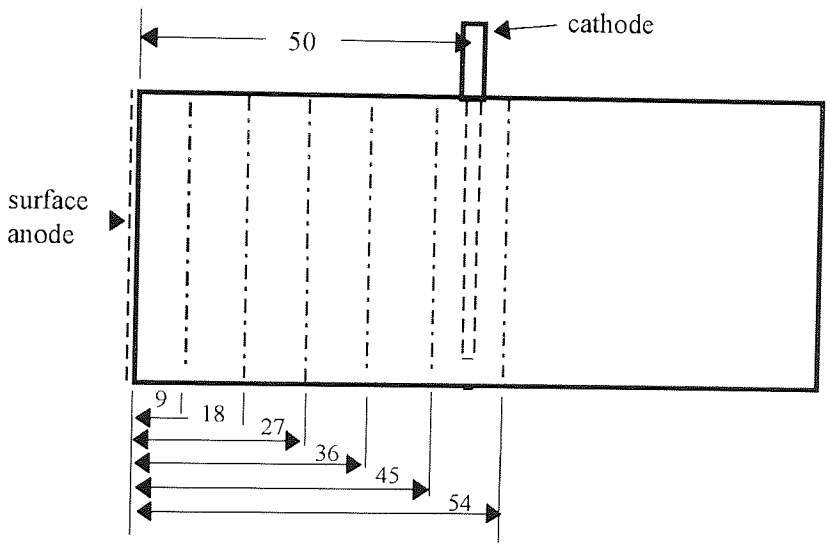

Figure 4.5: Arrangement of cutting of bulk-specimens

(a)

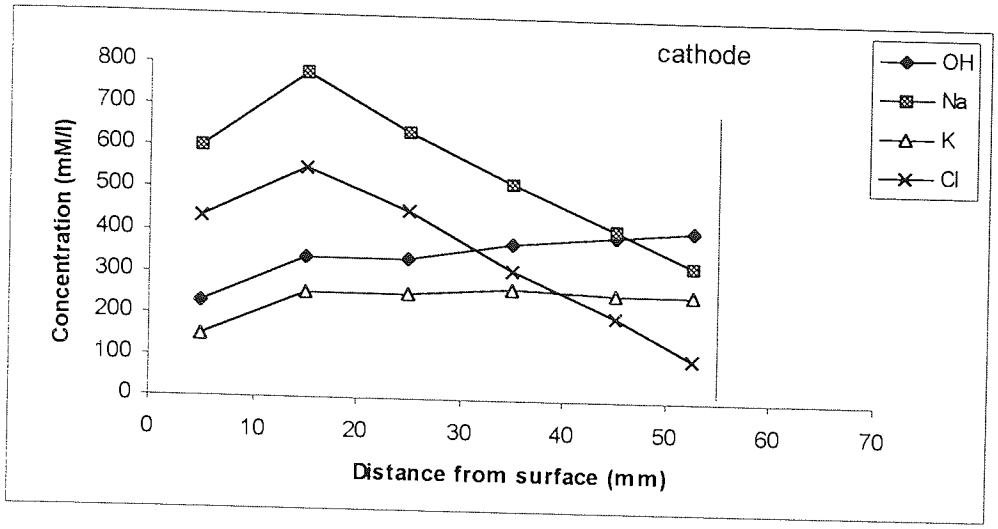

(b)

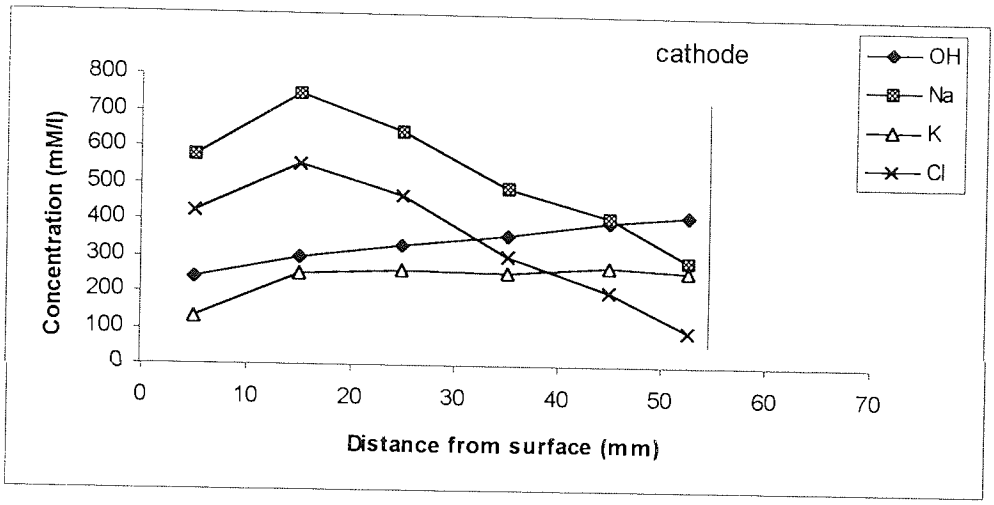

(c)

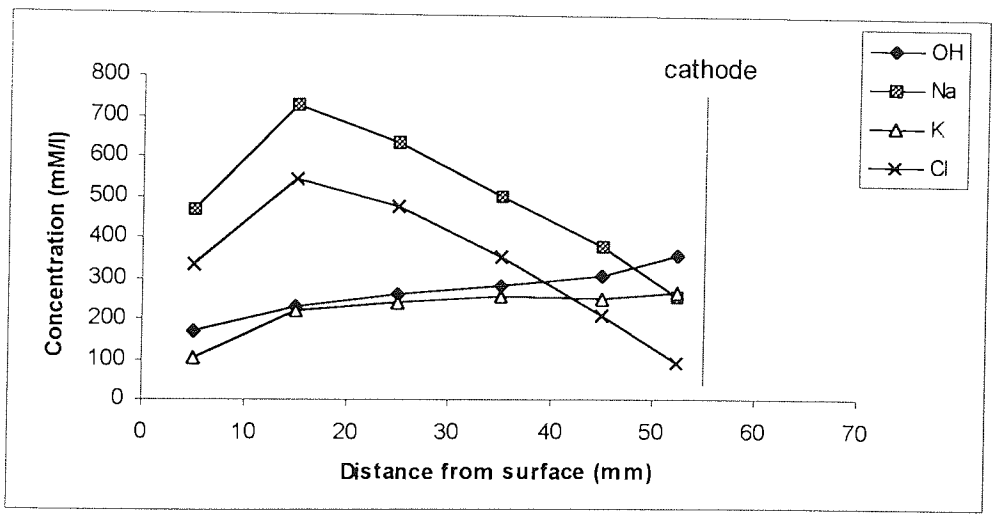

Figure 4.6: Ionic concentration profiles in pore solutions of cement paste subjected to electrochemical treatment at 0 A/m^2 (weeks of exposure (a) 4, (b) 8, (c) 12)

(a)

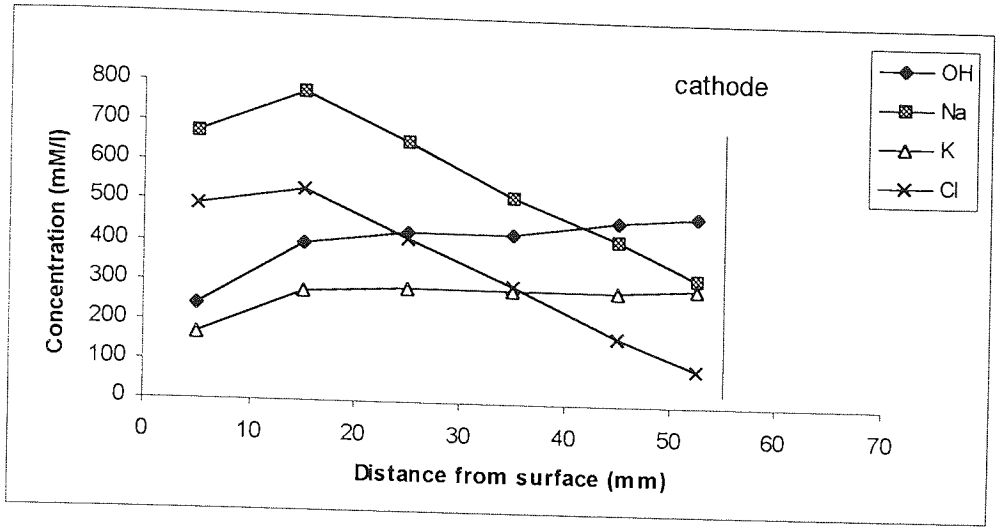

(b)

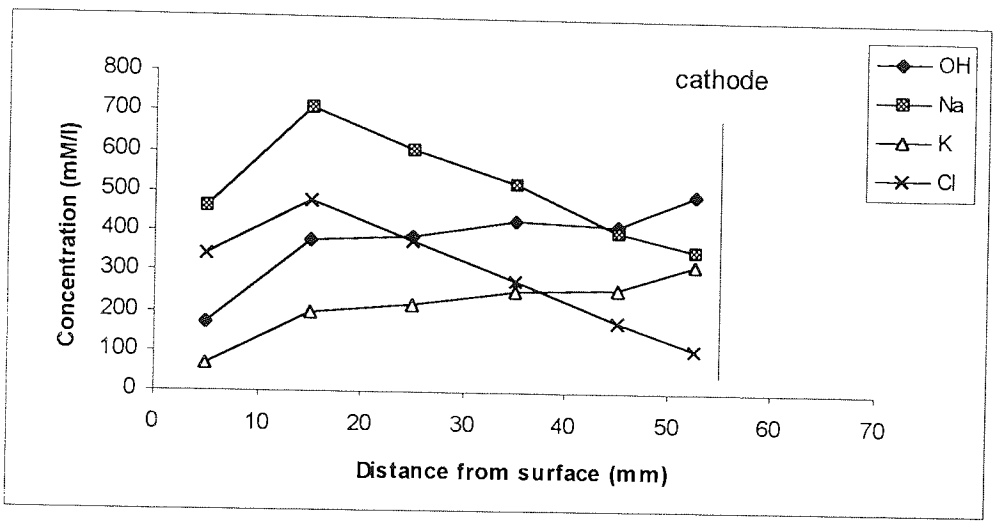

(c)

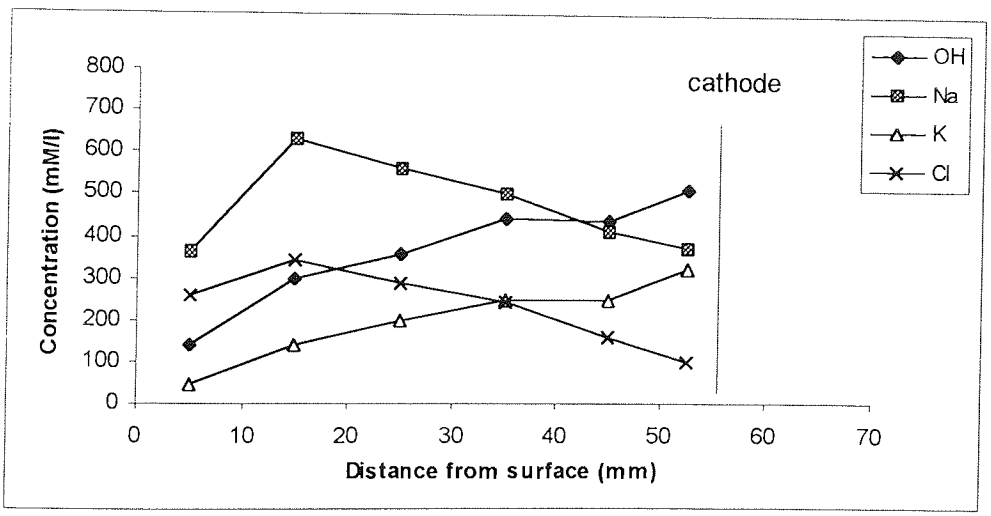

Figure 4.7: Ionic concentration profiles in pore solutions of cement paste subjected to electrochemical treatment at 1 A/m^2 (weeks of polarisation (a) 4, (b) 8, (c) 12)

(a)

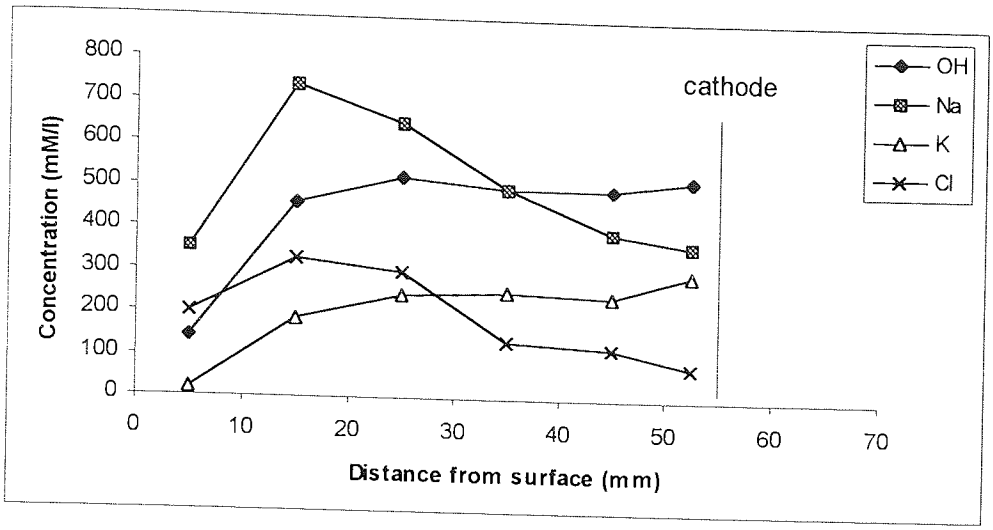

(b)

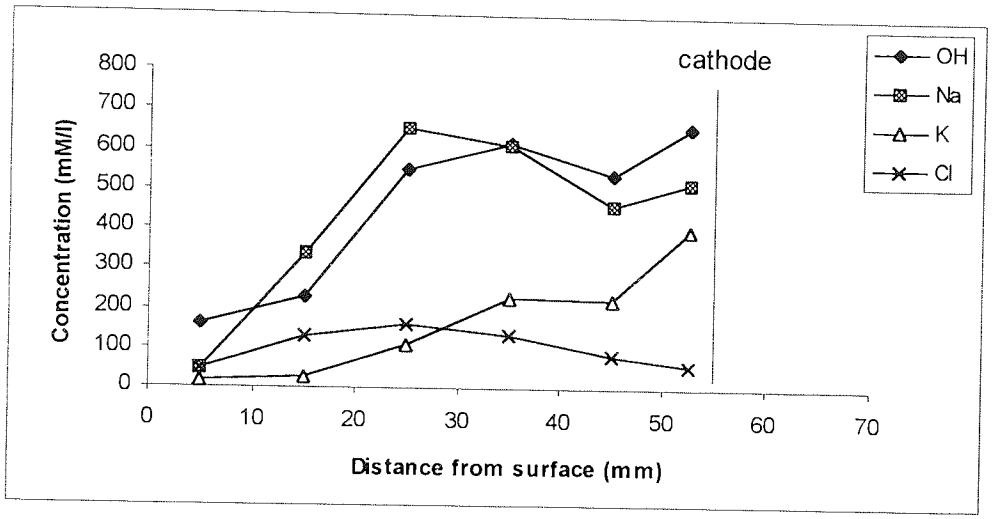

(c)

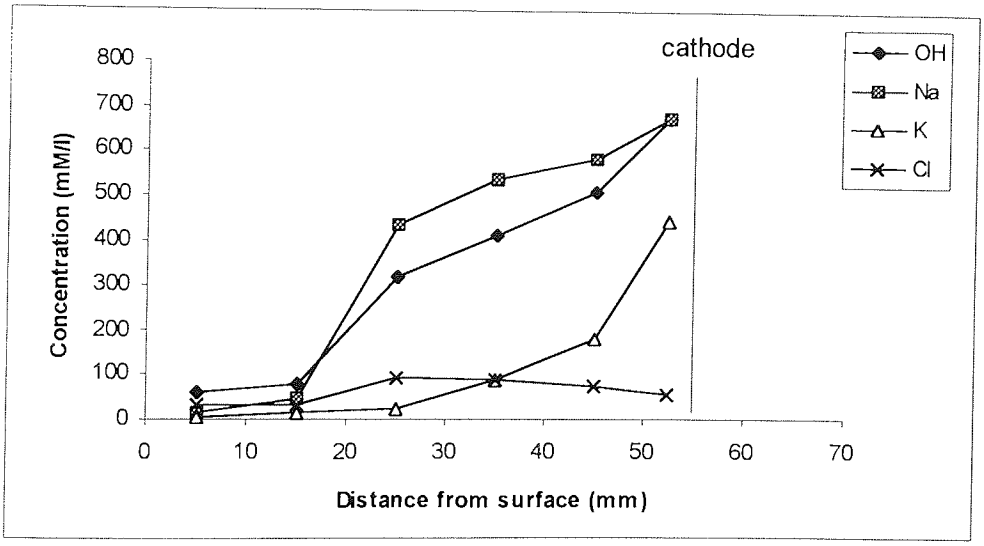

Figure 4.8: Ionic concentration profiles in pore solutions of cement paste subjected to electrochemical treatment at 5 A/m^2 (weeks of polarisation (a) 4, (b) 8, (c) 12)

(a)

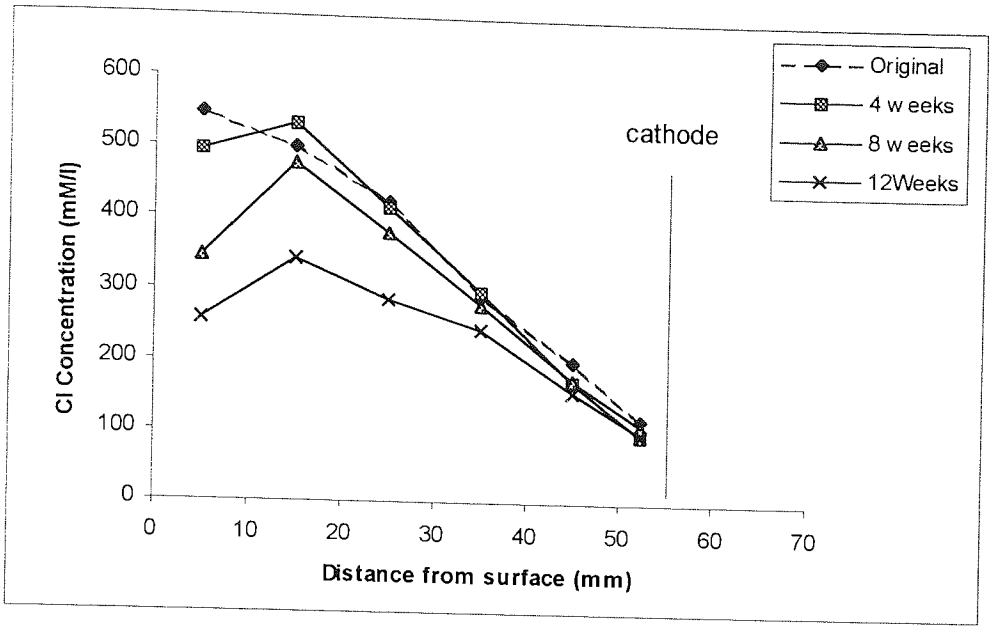

(b)

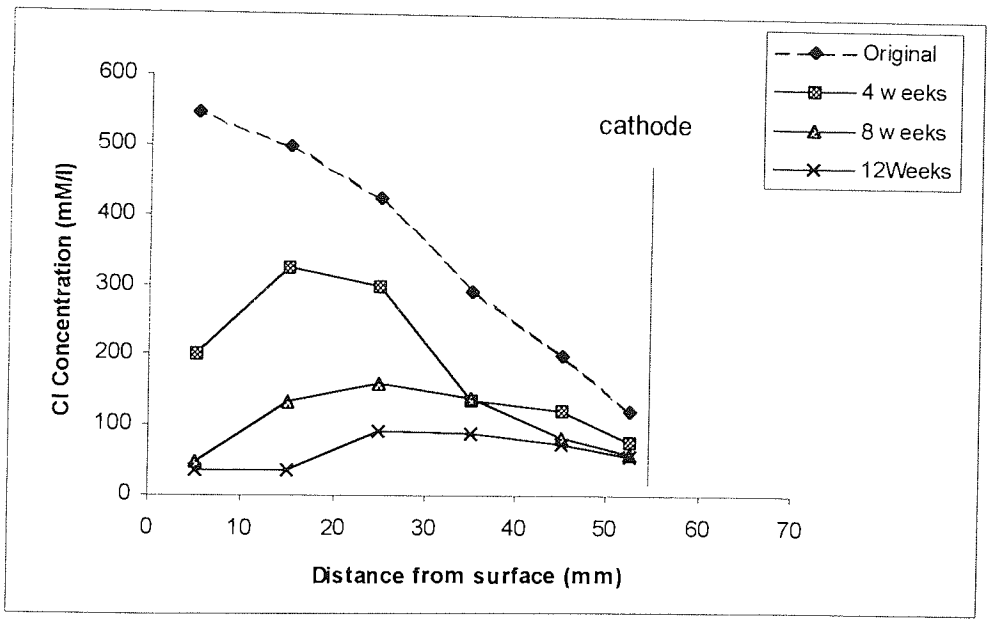

Figure 4.9: Chloride concentration profiles in the pore solutions after treatment at (a) 1 A/m^2 and (b) 5 A/m^2 (Original profile analysed after 8 weeks of curing)

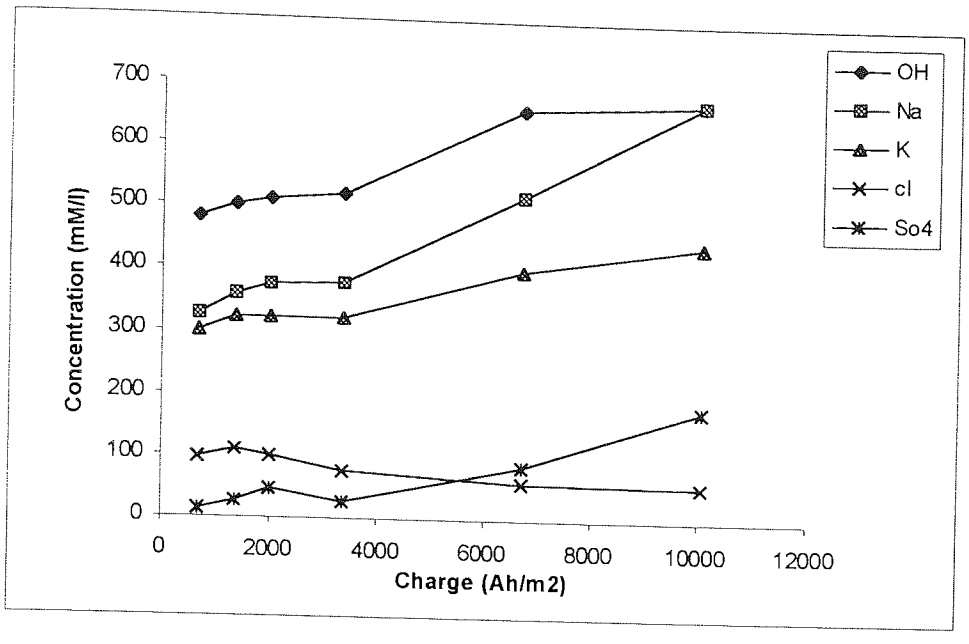

Figure 4.10: Ionic concentration in pore solution of hardened cement paste within a distance of 5 mm from steel cathode as function of circulated charge

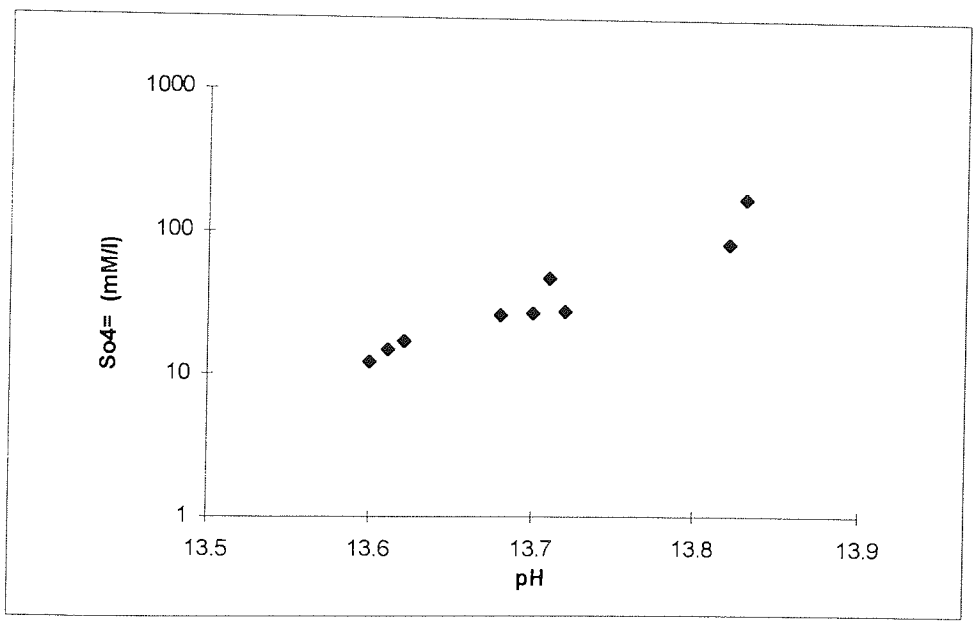

Figure 4.11: Sulphate ionic concentration in pore solution of hardened cement paste within a distance of 5 mm from steel cathode as a function of pH

(a)

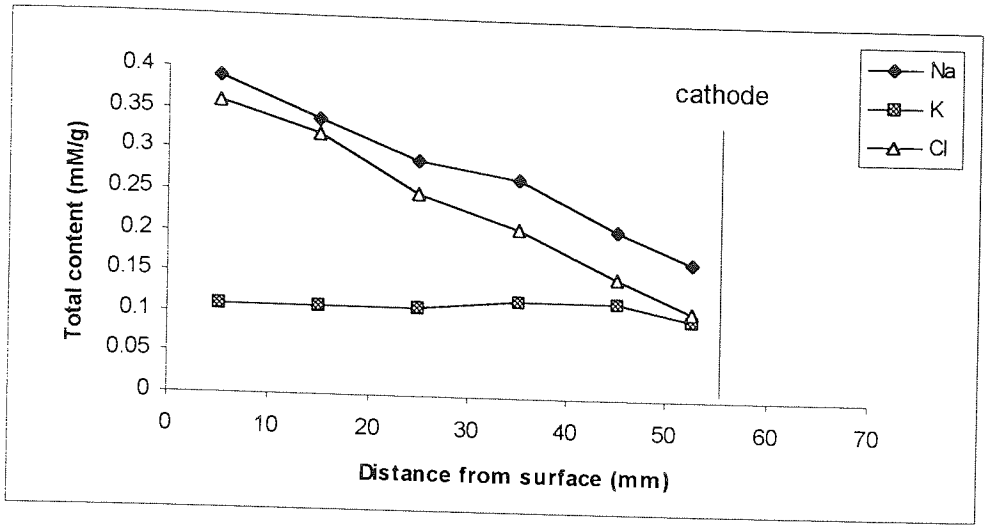

(b)

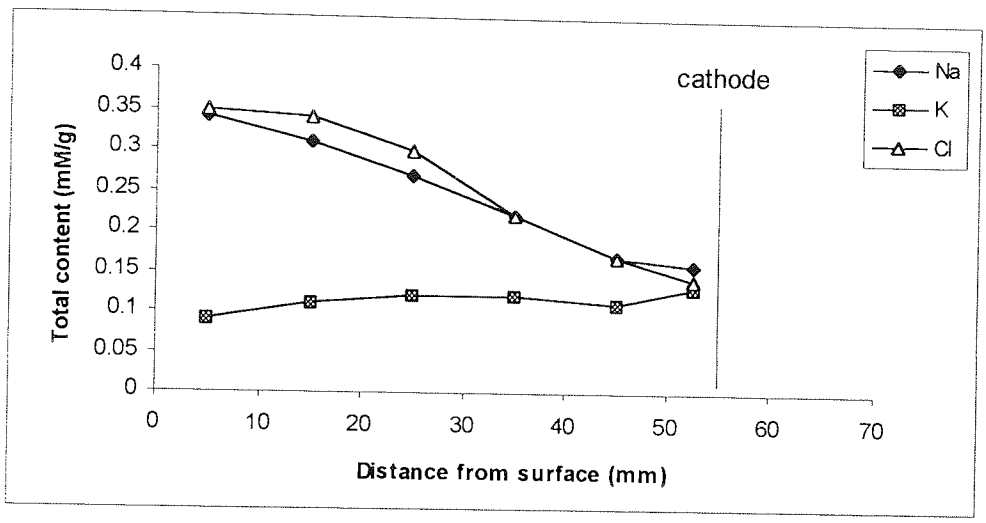

(c)

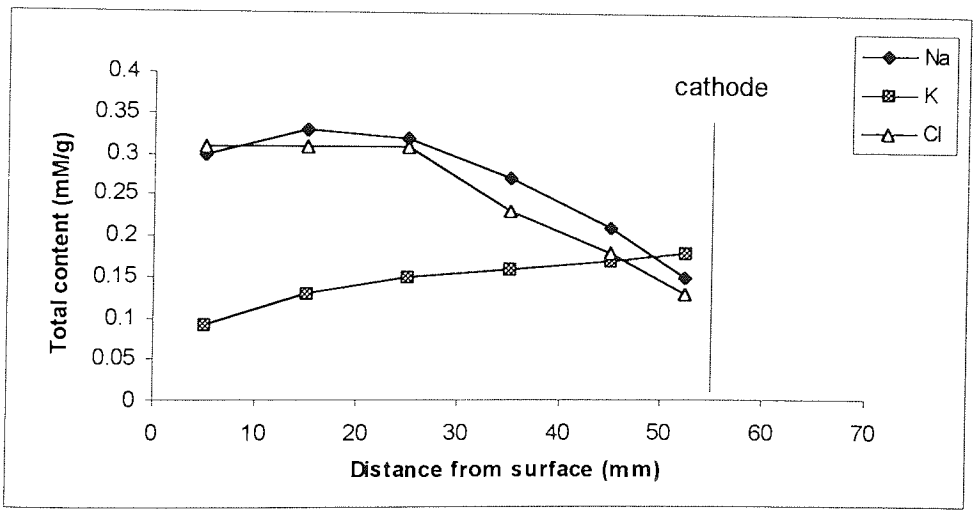

Figure 4.12: Chemical analysis on hardened cement paste subjected to electrochemical treatment at 0 A/m2 (weeks of exposure (a) 4, (b) 8, (c) 12)

(a)

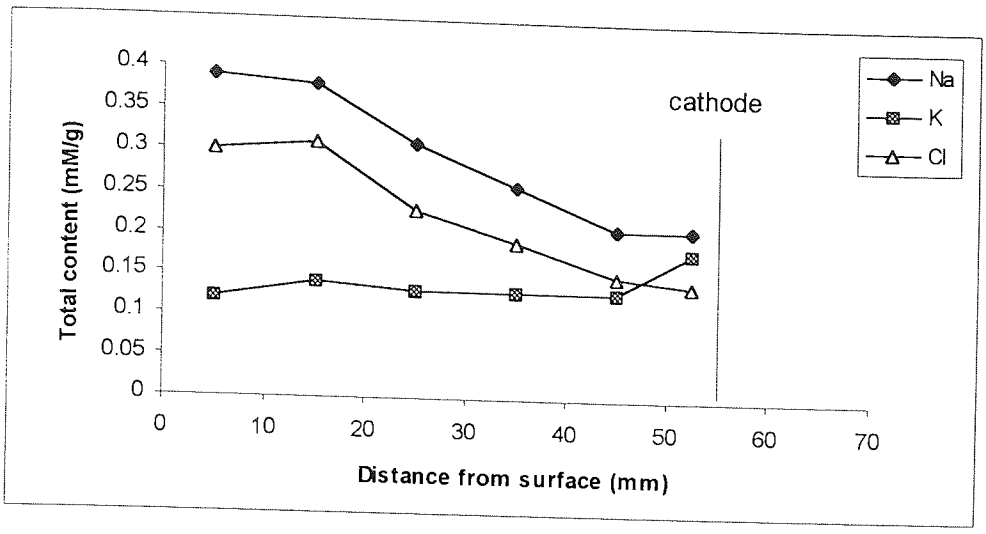

(b)

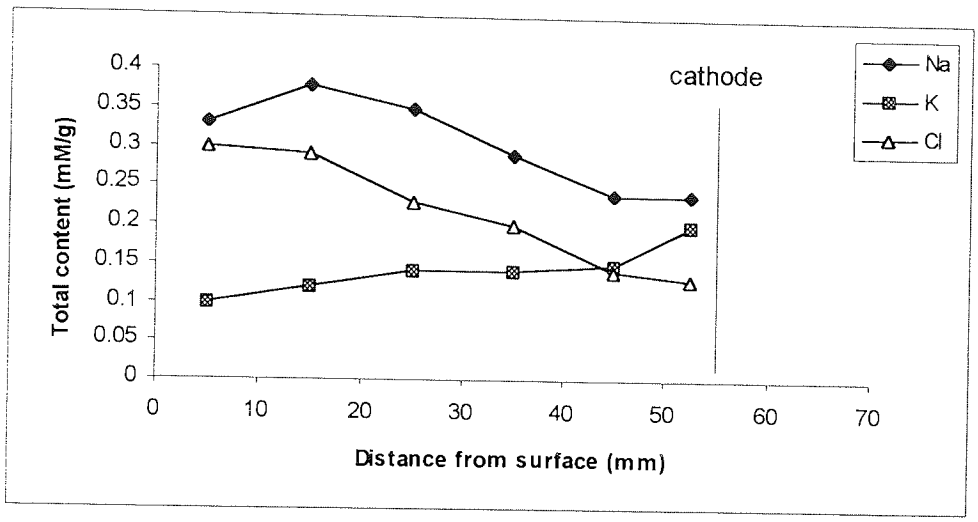

(c)

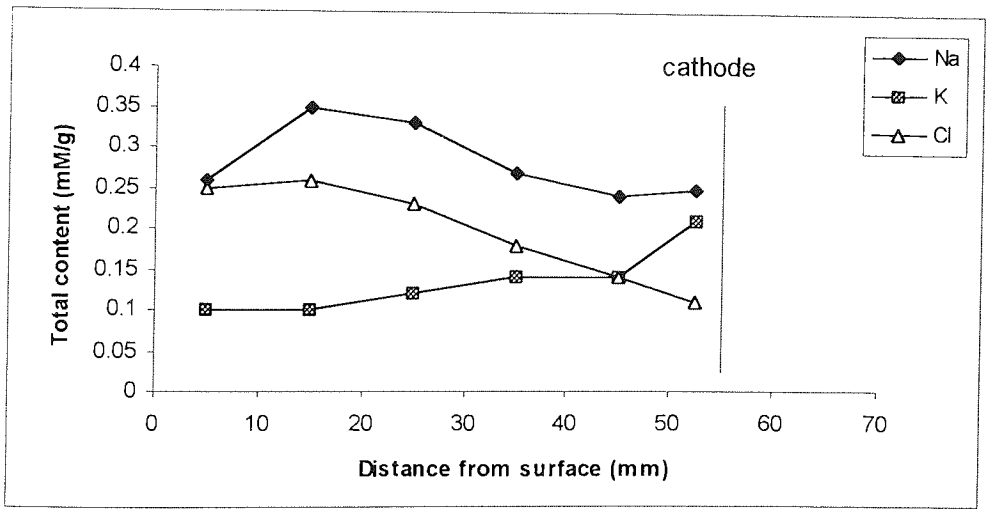

Figure 4.13: Chemical analysis on hardened cement paste subjected to electrochemical treatment at 1 A/m^2 (week of polarisation (a) 4, (b) 8, (c) 12)

(a)

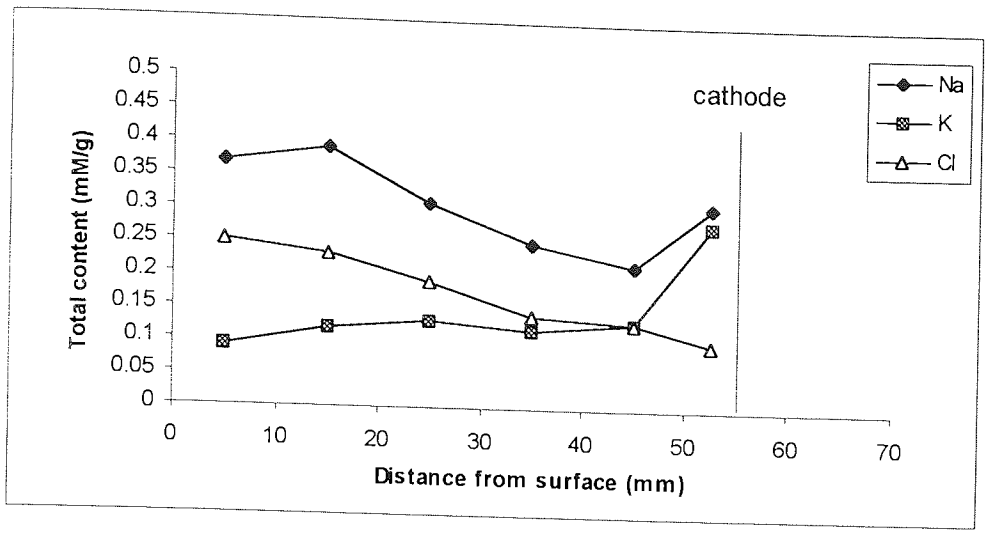

(b)

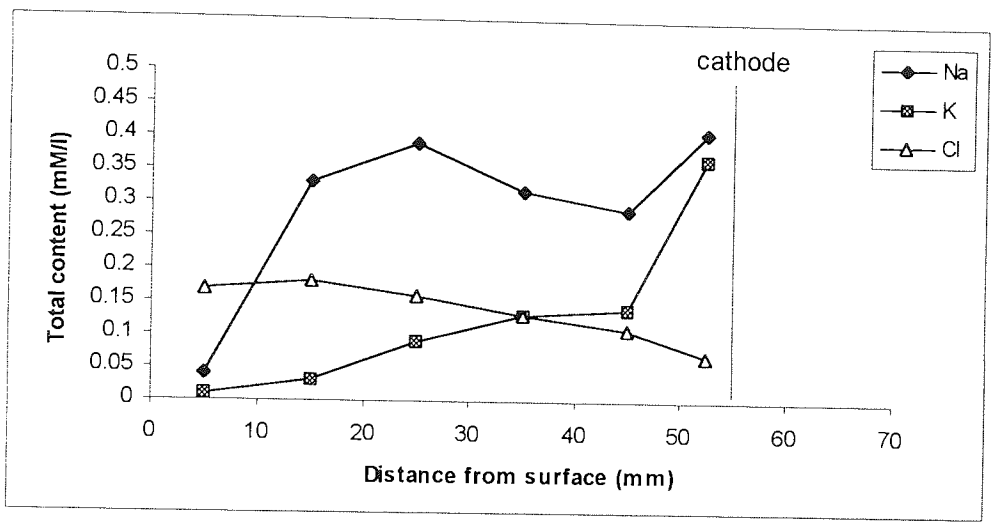

(c)

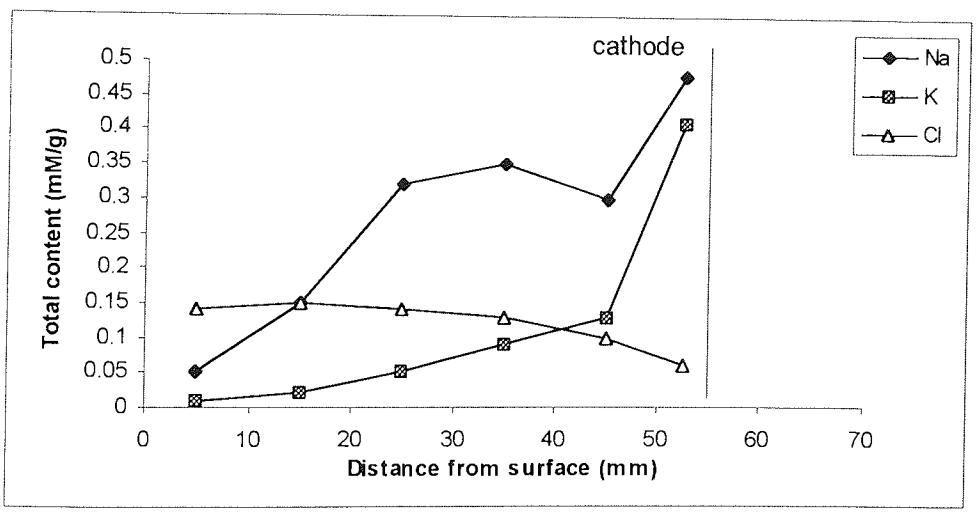

Figure 4.14: Chemical analysis on hardened cement paste subjected to electrochemical treatment at 5 A/m^2 (week of polarisation (a) 4, (b) 8, (c) 12)

(a)

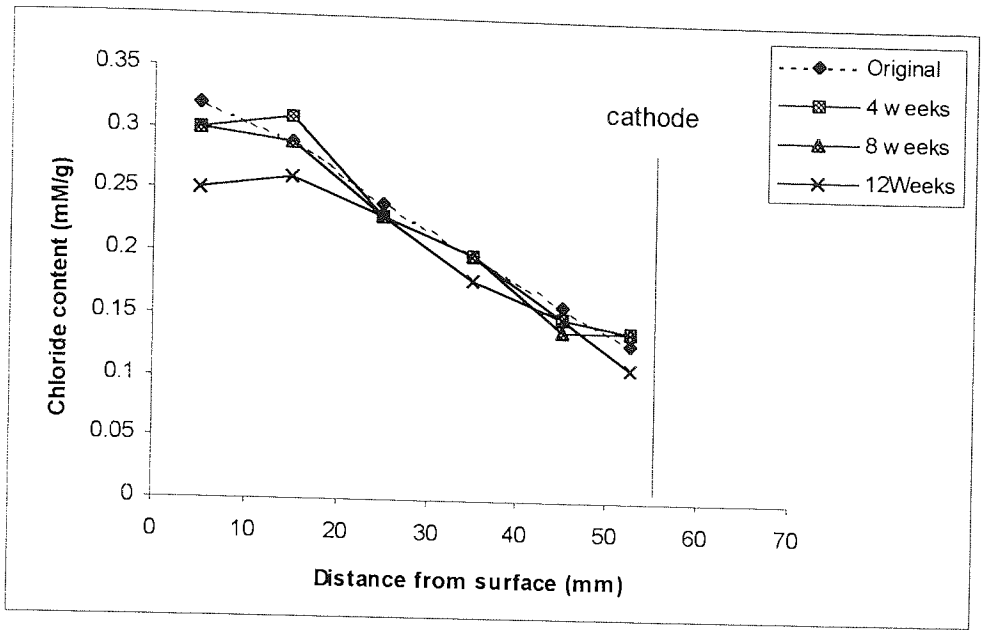

(b)

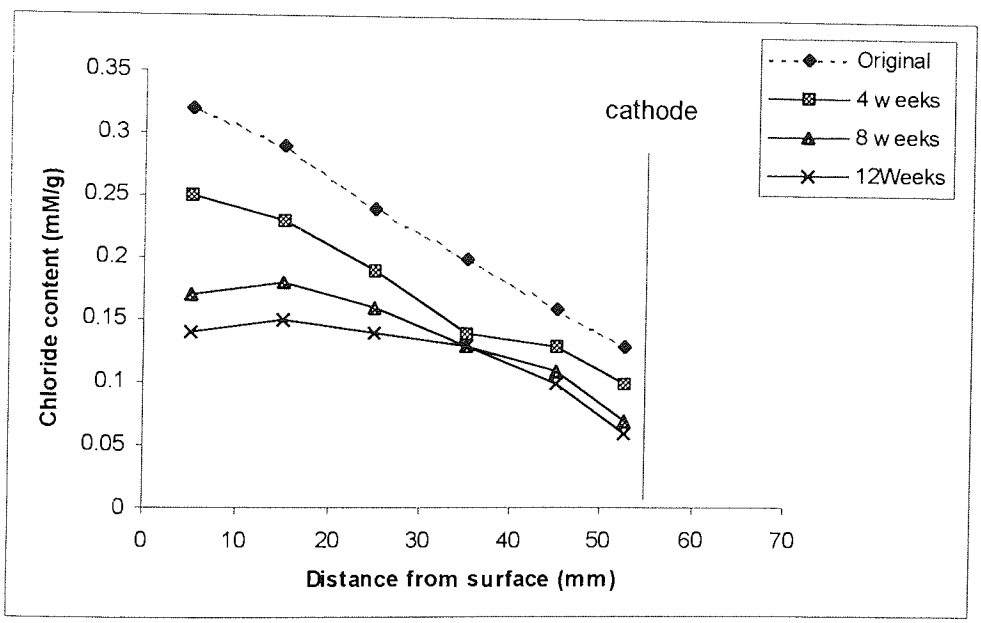

Figure 4.15: Total chloride profiles after treatment at (a) 1 A/m2, (b) 5 A/m2 (Original profile analysed after 8 weeks of curing)

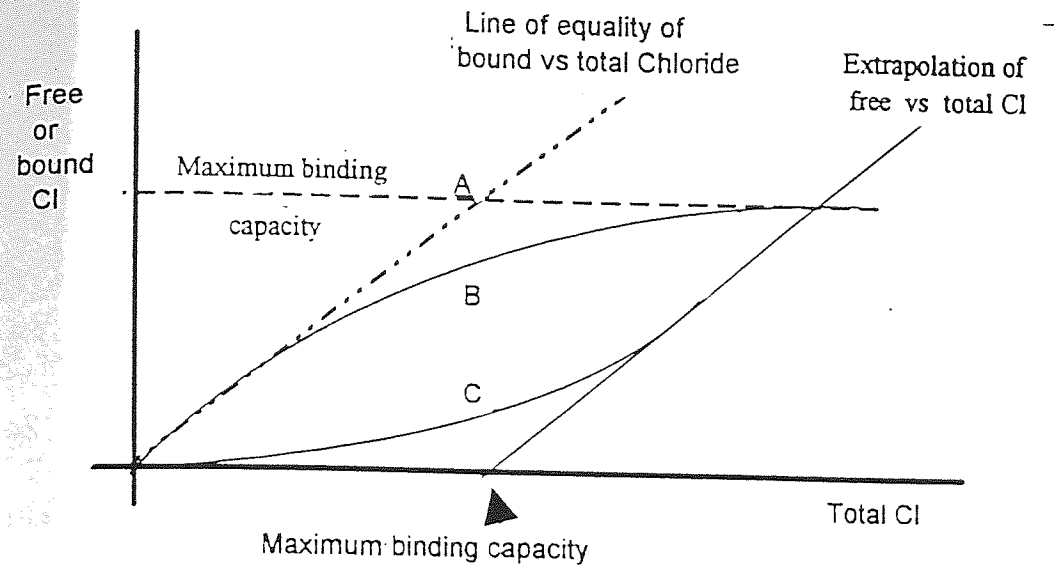

Figure 4.16: Relationship between bound and total chloride content

(a)

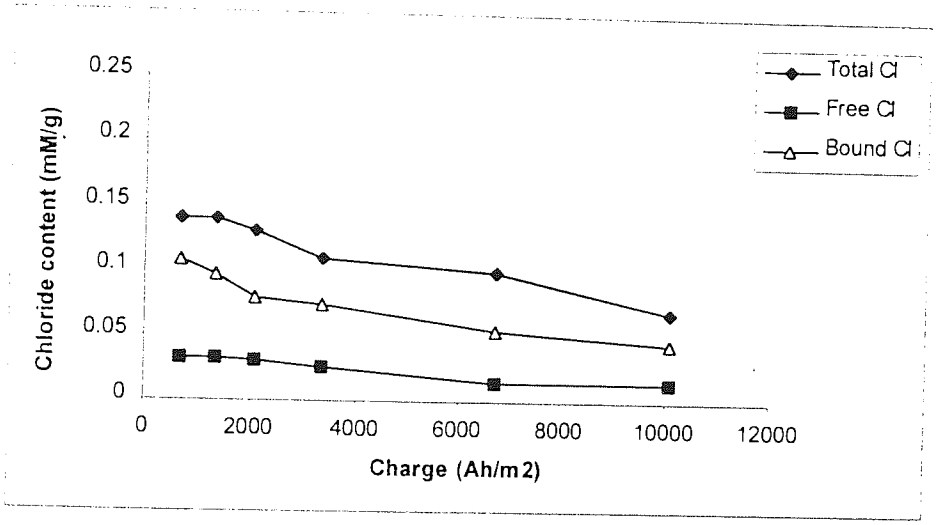

(b)

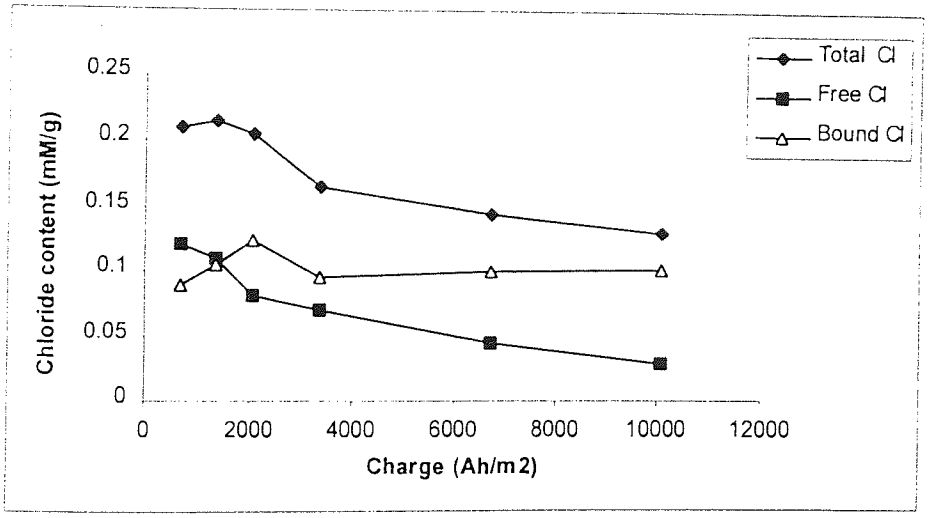

Figure 4.17: Total, free and bound chloride as a function of circulated charge
(a) near the cathode, (b) in the bulk

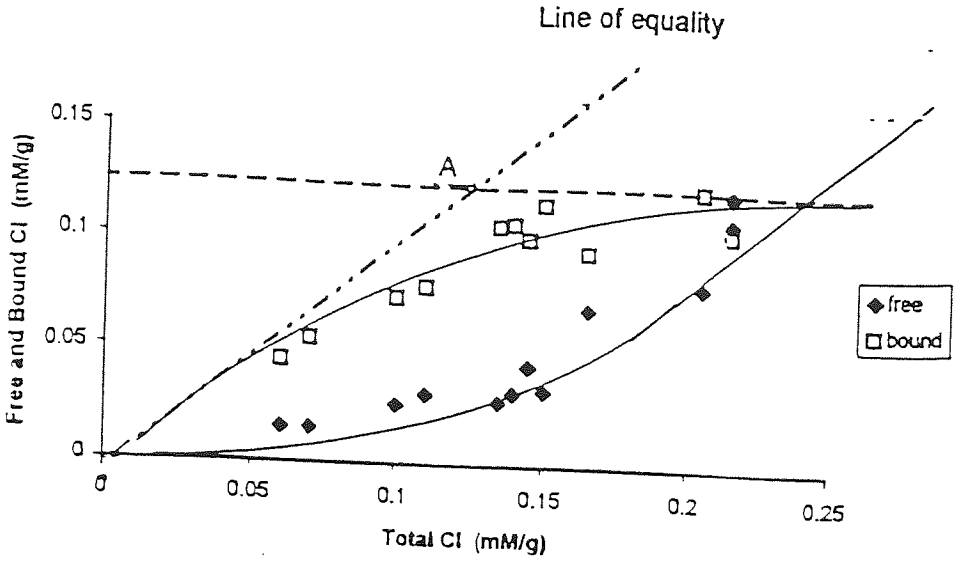

Figure 4.18: Relationship between free & bound chloride and total chloride content

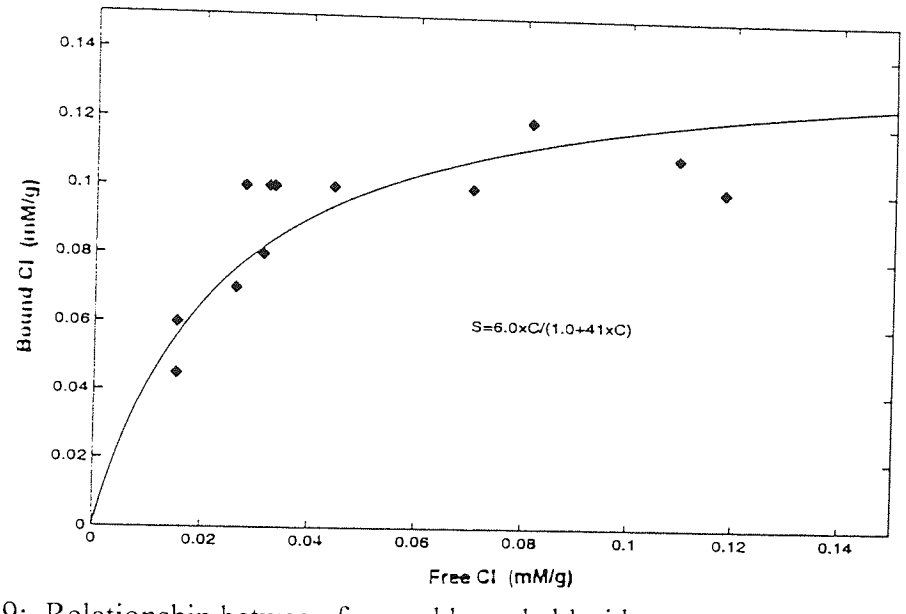

Figure 4.19: Relationship between free and bound chloride

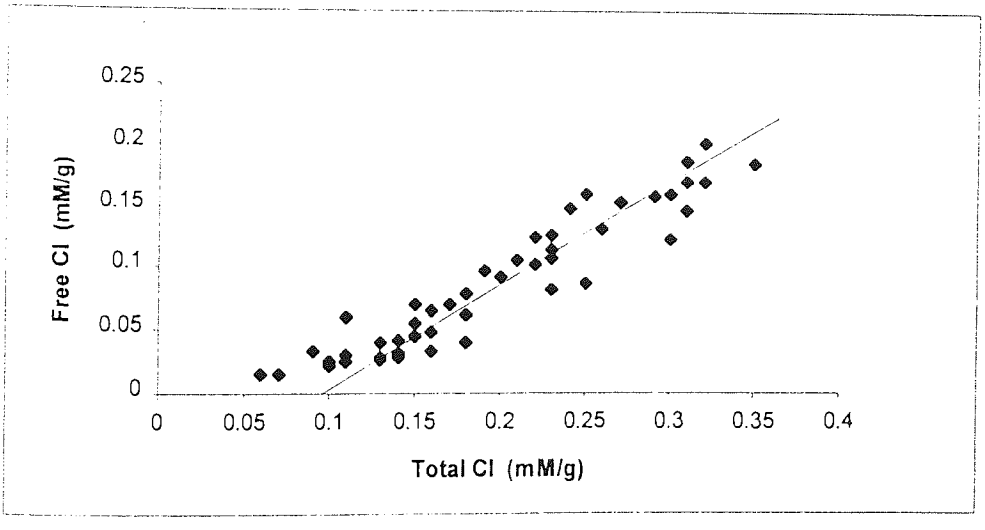

Figure 4.20: Free Cl content as a function of total Cl content

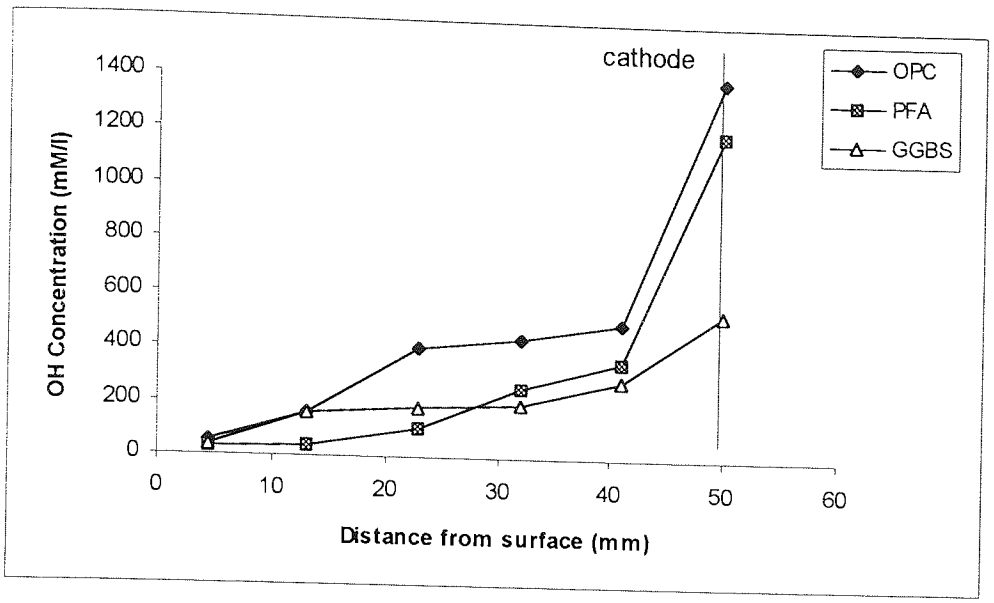

Figure 4.21: OH^- ionic concentration in different types of cements subjected to electrochemical treatment at 5 A/m^2 for 12 weeks

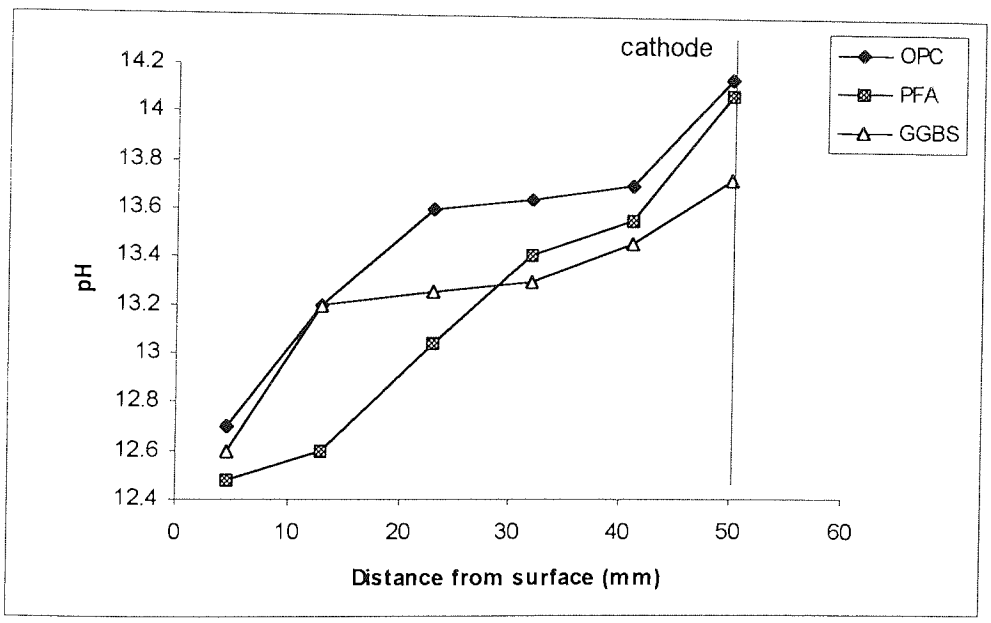

Figure 4.22: pH in different types of cements subjected to electrochemical treatment at 5 A/m^2 for 12 weeks

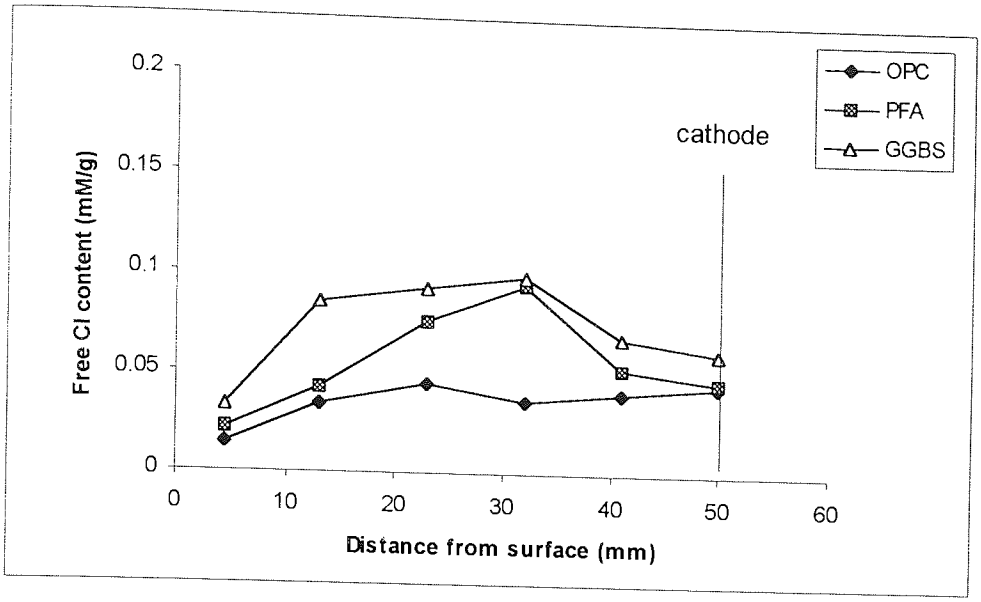

Figure 4.23: Free Cl^- ionic concentration in different types of cements subjected to electrochemical treatment at 5 A/m^2 for 12 weeks

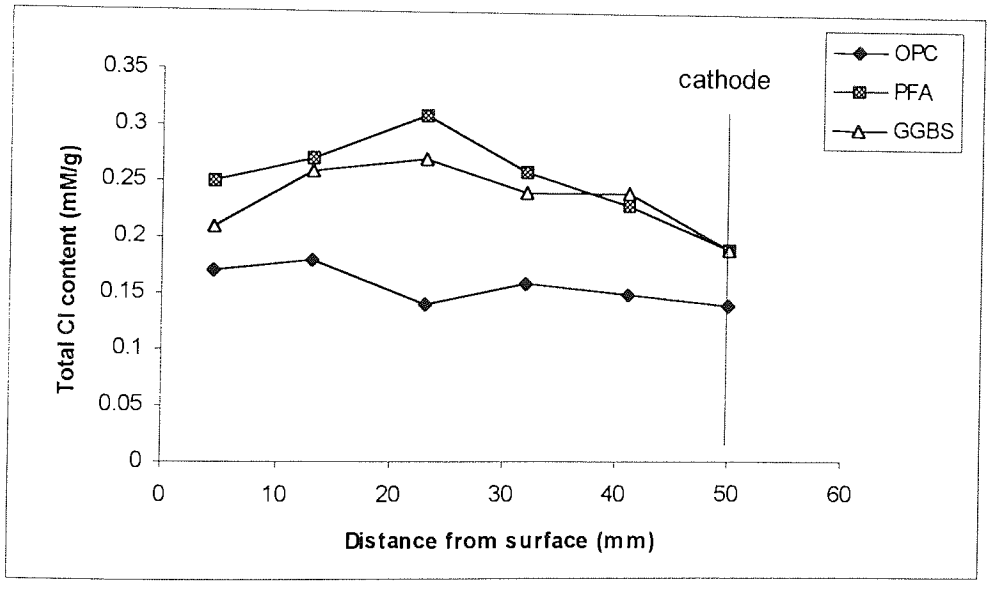

Figure 4.24: Total Cl^- content in different types of cements subjected to electrochemical treatment at 5 A/m^2 for 12 weeks

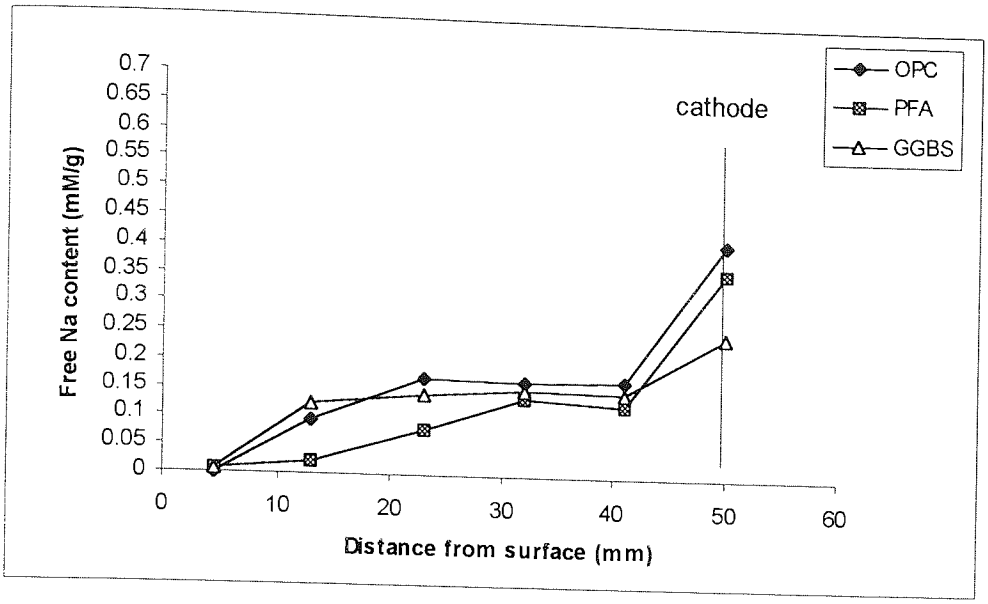

Figure 4.25: Free Na^+ ionic concentration in different types of cements subjected to electrochemical treatment at 5 A/m^2 for 12 weeks

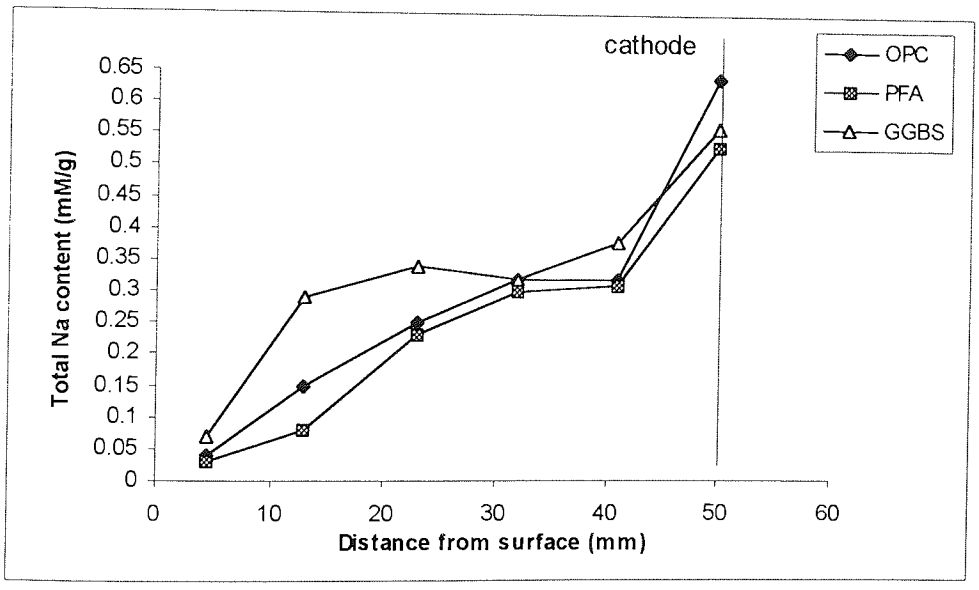

Figure 4.26: Total Na^+ content in different types of cements subjected to electrochemical treatment at 5 A/m^2 for 12 weeks

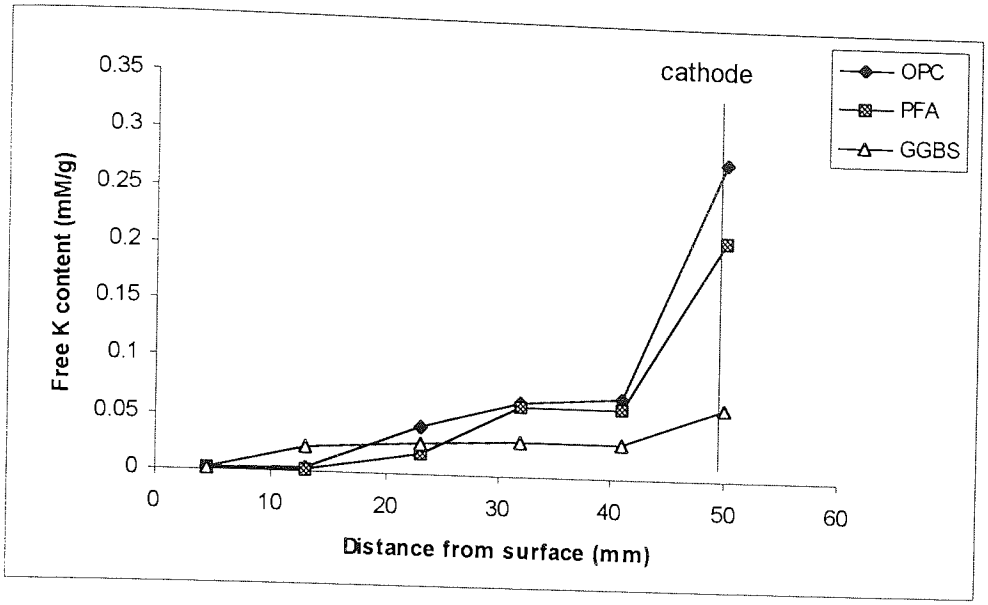

Figure 4.27: Free K^+ ionic concentration in different types of cements subjected to electrochemical treatment at 5 A/m^2 for 12 weeks

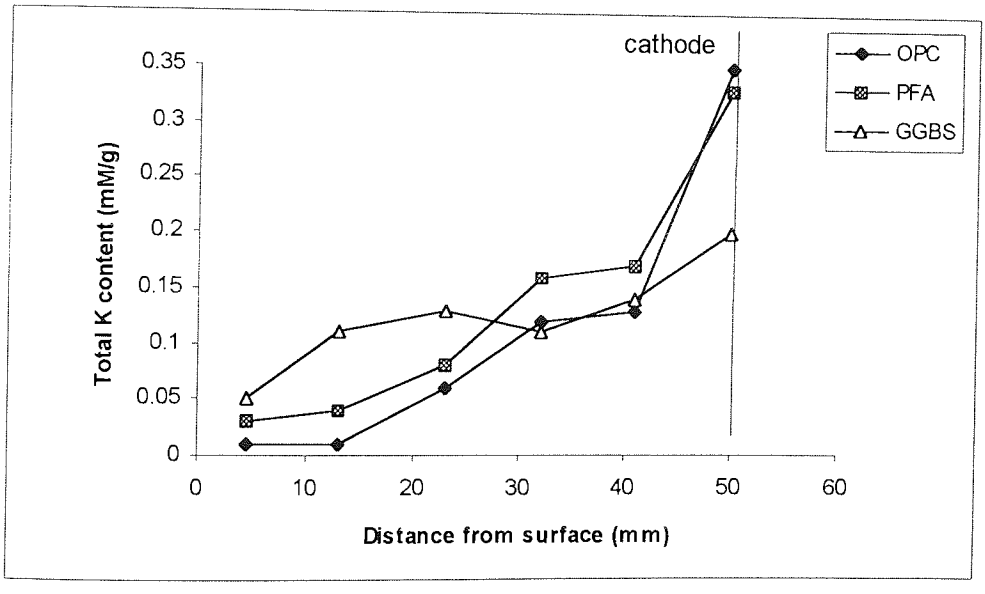

Figure 4.28: Total K^+ content in different types of cements subjected to electrochemical treatment at 5 A/m^2 for 12 weeks

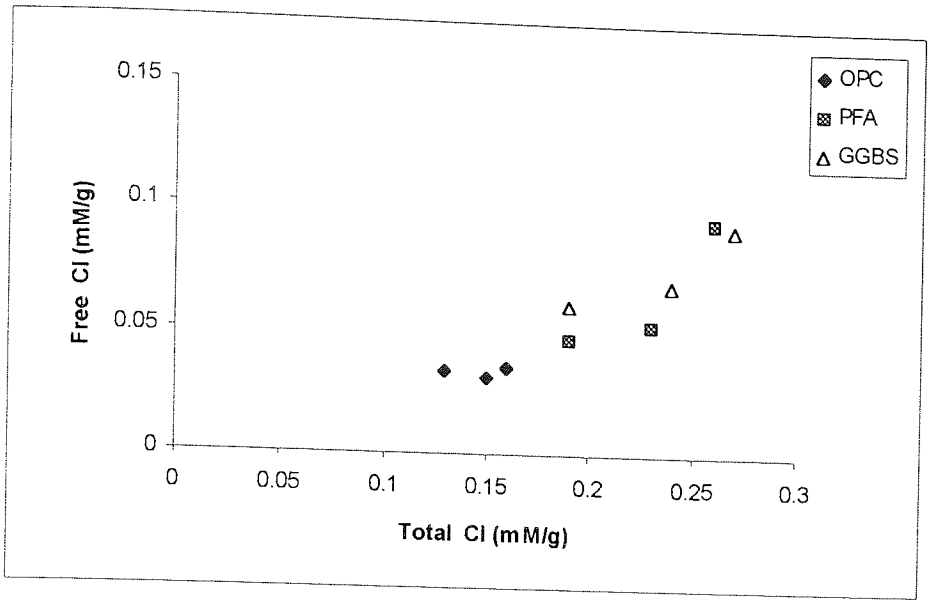

Figure 4.29: Free chloride content as a function of total chloride content

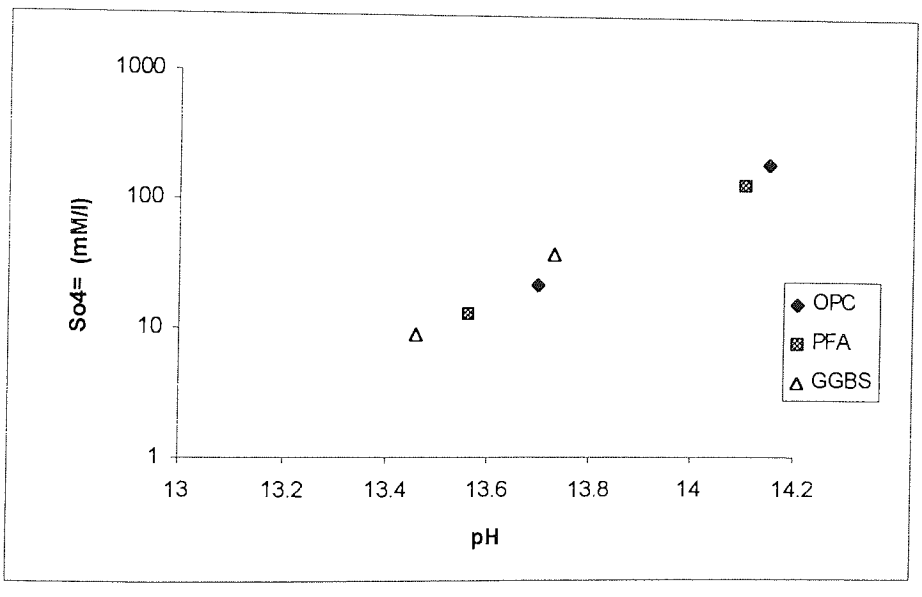

Figure 4.30: Sulphate ionic concentration in pore solution of hardened cement paste within a distance of 4.5 mm from steel cathode as a function of pH

CHAPTER 5

EFFECT OF ECE ON PHYSICAL PROPERTIES OF CEMENTS

5.1 INTRODUCTION

The use of a high current in the ECE treatment proved to be successful in removing chloride ions from the contaminated cement samples as discussed in Chapter 4. Negative ions (Cl^- and OH^-) moved away from the cathode towards the anode and positive ions (Na^+ and K^+) moved towards the cathode. This accumulation of alkalis around the cathode combined with the hydroxyl ions which are generated at the cathode during the electrochemical process to form alkali hydroxides have been suggested to cause softening in the cement matrix around the steel [Ali and Rasheeduzzafar 1993, Ihekwaba et al., 1996(a)]

A popular method to look at the softening of the cement binder around the reinforcement after the ECE process is by looking at the bond strength as explained in section 2.8.2. Various researchers [Nustad and Miller 1993, Ueda 1995, Ihekwaba et al., 1996(b)] have found that loss of bond between steel reinforcement and the cement binder was observed after specimens had undergone treatment of about 5000 Ah/m^2 charge. Another method, employed by Sergi and Page [1992], Bertolini et al. [1996], Page et al. [1994] and Ueda et al. [1995] is called the "microhardness" measurement technique. A small but statistically significant decrease in hardness of the hardened cement paste near the steel cathode (< 1 mm in distance) was observed by Sergi & Page [1992] when polarisation was applied simulating cathodic protection conditions (20 mA/m^2) for a period of 110 days. Ueda et al. [1995] who worked with ECE using $2.5A/m^2$ and $5A/m^2$ for periods up to 12 weeks also found a significant decrease in the microhardness of the cement binder near the steel cathode. Bertolini et al. [1996], however, found no significant difference between the cement hardness near the cathode compared statistically to the hardness in the bulk.

The aim of this chapter was to look at the physical and microstructural changes around the cathode due to ECE process. The technique of microhardness measurement was

employed in this study to determine any possible effect of paste softening caused by the ECE process. The results, reported in this chapter, were supported by mercury intrusion porosimetry (MIP). The two techniques (microhardness and MIP) complement each other and can detect changes in the pore-structure properties of the cements.

In chapter 4, the amount of sulphate ions was found to increase in the pore solution with increasing concentration of hydroxyl ions. An increased level of sulphate in the pore-solution of hardened cement paste could pose problems to the cement matrix in the form of ettringite which can expand up to 2-fold [Irassar et al., 1996]. The XRD technique was employed to trace the presence of ettringite in the cement matrix and determine the possibility of secondary ettringite formation after the application of ECE.

5.2 MICROHARDNESS MEASUREMENT

5.2.1 Sample Preparation

In order to determine whether changes had occurred in the properties of the hardened cement paste in the cathodic region such as softening during polarisation, microhardness measurements were carried out. For each current density and duration of polarisation, two samples were taken for the microhardness measurement. These two samples were cut in the middle at right angles to the cathode. Three out of the four resulting surfaces were then chosen for microhardness testing.

To increase the visibility of the surface indentation under the microscope, the cut surfaces were ground flat using water as the lubricant, polished to 9μm with alumina and ethanediol and polished with a diamond paste down to 1μm. Black ink was then applied on the polished surface to enhance the indentation image.

Microhardness was measured using a Buehler Micromet 4. Six different distances from the steel cathode were considered viz. 0.1, 0.5, 1, 2, 10 and 25mm. For a given distance ten readings were taken across the surface resulting in a total of 60 measurements on each of the specimens. The readings were taken around the middle part of the polished section, avoiding the edges.

5.2.2 Discussion of Microhardness Results on Profiled Specimens

5.2.2.1 Effect of Current Density

The effects of current density on the hardness of the cement matrix after ECE are shown in Figure 5.1, 5.2 and 5.3. All thirty readings taken for each depth of the three surfaces were averaged and represented by a single point on the curve. There were no obvious trends in softening of the matrix with regard to the current applied. All values lie between 25 and 40 Hk with considerable scatter in the microhardness readings. This made it difficult to judge any possible reduction in hardness in the cement matrix.

A statistical analysis which was carried out using a 't-test' to compare the mean of the microhardness reading around 0.1 mm distance from the steel cathode with regard to the change in current density shows that untreated and treated specimens gave an insignificant difference in hardness values. The comparison made between 1 A/m^2 and 5 A/m^2 current density also gave an insignificant difference for results at 4 weeks, 8 and 12 weeks. The results of the statistical analysis are tabulated in Table 5.1 and all microhardness reading are shown in Appendix G.

5.2.2.2 Effect of Duration of Treatment

The effects of the duration of treatment on the hardness of the cement matrix after ECE are shown in Figure 5.4, 5.5 and 5.6. There was no clear trend in softening of the matrix with regard to duration of treatment.

A statistical analysis carried out at a distance of 0.1 mm from steel cathode gave an insignificant difference for the mean of values for all durations of treatment when 5 A/m^2 current density was used. When comparisons were made for specimens treated with 1 A/m^2 current density between 4 and 8 weeks and 4 and 12 weeks, they also gave an insignificant difference.

Figure 5.7 and 5.8 compare the hardness value with circulated charge near the steel cathode and at 25 mm from the cathode. From Figure 5.7, the trend in hardness in the cement matrix appears to decrease near the cathode as the charge is increased. However, the decrease was very small. In the bulk, there was no significant change in hardness as shown in Figure 5.8.

5.2.2.3 Effect of Distance from Steel Cathode

A statistical analysis was also carried out to compare the difference in hardness in the cement matrix with distance. Two points were taken for this purpose, viz 0.1 mm from steel cathode and at distances greater than and equal to 10 mm from steel cathode. For $1A/m^2$ current density the difference was insignificant at 4, 8 and 12 weeks. A similar result (Figure 5.6) was found for the $5A/m^2$ current density, where again all three treatment periods gave an insignificant difference. This finding was similar to that of Bertolini et al., [1996].

5.2.2.4 Microhardness Measurement on Other Types of Cements

Figure 5.9, 5.10 and 5.11 show the microhardness measurement of bulk-specimens consisting of OPC, PFA and GGBS. Bulk-specimens were specimens where a constant 1% chloride in a form of NaCl by weight of cement was added during mixing. OPC (Figure 5.9) seems to follow the trend of the profile-specimens as described (in section 5.2.2.1). The hardness of cement matrix up to 1 mm from steel cathode appeared to be slightly less than the hardness in the bulk but it was shown statistically to be insignificant as shown in Table 5.4. Similarly, however, there appeared to be a reduced hardness compared to the untreated samples but could not be proven statistically as shown in table 5.4.

The microhardness profile of the treated PFA overlapped the untreated curve almost exactly as shown in Figure 5.10. As was the case with OPC, there appeared to be a small, but insignificant decrease in microhardness near the surface as shown in Table 5.4.

GGBS behaved in the opposite way as shown in Figure 5.11. The hardness of cement matrix near the cathode was somewhat higher (35 Hk) compared to (28 Hk) in the bulk. The overall trend of the untreated specimen was also similar. Apart from the small effects near the cathode, all three types of hardened cement paste had very similar microhardness values (Figure 5.12). Statistical test results are shown in Table 5.4.

5.3 MERCURY INTRUSION POROSIMETRY (MIP)

The MIP technique was used in the work described in this chapter to supplement the information obtained from microhardness measurements. The pore size distribution (PSD) in each of the cement pastes was examined after the specimens had undergone the ECE process. MIP was carried out only on specimens subjected to the higher charge which was considered to be the most likely to exhibit any variation in porosity.

5.3.1 Sample Preparation

After dry-cutting the specimens for pore solution analysis, fragmented samples from slices at 5, 35 and 52.5mm from the surface were taken for the MIP measurement. The specimen was broken into small pieces and then approximately 30 mg of fragments were placed in bottles containing propan-2-ol for 1 week. The idea was to remove any available water from the specimens. The specimens were then dried in a stream of cool air using a hair drier and placed in a desiccator. The desiccator was evacuated for a week to remove the alcohol. About 25 mg of each sample was used for mercury intrusion porosimetry, as described in section 3.4.6.

5.3.2 Discussion of MIP Results on Profiled-Specimens

Graphs of cumulative intrusion volume against log of pore diameter of the profile-specimens are shown in Figure 5.13-5.18. Figure 5.13 depicts the specimens which were not subjected to any treatment current. From the graph it can be seen that there was no variation in the pore size distribution at the three chosen distances from the surface (5, 35 and 52.5 mm).

Figure 5.14 represents the specimens which were subjected to a current density of 1 A/m^2 for a period of 12 weeks. A slight variation in the pore size distribution is seen when comparing the profiles obtained at the cathode, in the bulk and at the surface. The pore structure appeared to become overall tighter and the total porosity reduced with distance from the cathode. This phenomenon was more pronounced when 5 A/m^2 current density was used as shown in Figure 5.15. In this figure, it can be seen that the pore diameter at the anode, (5 mm from surface) is much finer compared to the cement matrix near the cathode (52.5 mm) and in the bulk (35mm). However, comparatively little variation in the pore size distribution between distances 35 and 52.5 mm from the surface was seen and the profiles overlapped for most part, suggesting that the ECE treatment does not seriously effect the cement matrix around the cathode.

Figure 5.16-5.18 compare pore size distributions at the three specific distances from the cathode after 12 weeks of ECE treatment at different current densities. At 52.5 mm from the surface as shown in Figure 5.16, the total porosity of the specimen treated with 5 A/m^2 was lower than that obtained for specimens treated with 1 A/m^2 which in turn was lower than that of the untreated specimens. The same was true for specimens taken from the surface (Figure 5.18). Very little difference was, however, found at a distance of 35 mm from the surface (Figure 5.17). From these figures, it is clear that even though the ECE treatment does effect the pore size distribution , the effect is very small.

Table 5.5 gives the total intruded volume of mercury, which represents the porosity of all the specimens which has undergone MIP treatment. The reduction in porosity with increasing current density is confirmed. Furthermore, for the treated profile-sample, it is

evident that the total porosity of the cement matrix near the cathode was higher than that of the matrix near the surface (anode). However, the difference was very small.

5.3.3 MIP on Other Types of Cements

Figures 5.19-5.21 show the MIP results of bulk-specimens consisting of OPC, PFA and GGBS. Each figure compares samples taken close to the steel cathode of treated and untreated specimens for each type of cement. For the OPC samples (Figure 5.19), it was clear that treated specimens were more porous than untreated specimens. The total porosity of the untreated specimens near the steel was 0.1096 cc/g compared to 0.1339 cc/g when treated with 5 A/m^2 current for 12 weeks. However, the blended cements behaved differently. The treated specimens were more dense than the untreated specimens. There was no obvious change in the pore size distribution when current was induced, as can be seen from the graphs shown in Figures 5.20 and 5.21, but the total intruded volume as shown in Table 5.5, indicates that the treated specimens were denser than the untreated specimens.

It was argued by Locke et al. [1983] that as the pH in the solution increases, the stability of the CSH gel decreases therefore becoming more soluble. This may possibly lead to more empty spaces and an increased porosity in the case of OPC. The fact that the trend was reversed for the blended cements suggests that either the gel formed in blended cements has different properties or that this explanation is an oversimplification.

5.4 IDENTIFICATION OF CEMENT HYDRATE PHASES

5.4.1 Introduction

A hypothesis was formed in chapter 4 that the dissolution of sulphate ions around the cathode may possibly result in ettringite formation due to their reprecipitation in the bulk away from the cathode. This formation of ettringite could increase the volume of cement matrix between 1.2 to 2.5 times and introduce unwanted expansive forces. It is,

therefore, important to trace this product after the specimens had undergone ECE treatment.

XRD was employed to look at the overall change in the cement phases but with particular attention at changes in the level of ettringite. Since the concentration of sulphate was only prominent in the specimens subjected to a 5 A/m^2 current density, only these specimens were chosen for the XRD tests. The XRD tests were conducted at two distances from the surface viz. 35 and 52.5 mm. For each distance 4 specimens were selected which were untreated or treated for 4, 8 and 12 weeks.

5.4.2 Profile-Specimens

Figure 5.22 and 5.23 show the XRD traces of profile-specimens. Figure 5.22 was obtained from samples close to the cathode (52.5 mm from surface) whereas Figure 5.23 represents samples at 35 mm from the surface. Particular attention was given to ettringite since it was the purpose of this research to study its existence and possible change in level after specimens had undergone ECE treatment. An example of identification of an XRD trace is given in Appendix H. $Ca(OH)_2$ was also determined to allow comparison of the ettringite content in different samples.

From Figure 5.22, it can be seen that ettringite peaks are present on all treated and untreated specimens. The highest peak from the figure was chosen and tabulated in Table 5.6. Another phase which was also identified for comparison in terms of intensity is calcium hydroxide. Table 5.6 shows that the ettringite content near the cathode was lowest at the highest charge. By determining the ratio of ettringite to $Ca(OH)_2$ peak heights and assuming that the $Ca(OH)_2$ content remained reasonably constant , it can be seen that there was a possible reduction of the ettringite phase near the cathode at treatments periods of 8 and 12 weeks, but no obvious difference in the bulk region. Further work would be necessary to establish this for all positions within the specimens.

5.4.3 Other Types of Cement

Figure 5.24 and 5.25 show the XRD curves for blended cements (PFA and GGBS). Observing Figure 5.24, the ettringite peaks appear not to change close to the steel cathode or at 23 mm distance from the surface. The $Ca(OH)_2$ peaks were much lower than for OPC because $Ca(OH)_2$ was being consumed by secondary pozzolanic hydration reactions. Both near the cathode and at distance 23 mm from the surface, the $Ca(OH)_2$ peaks increased somewhat after the specimens had undergone the ECE process.

GGBS also behaved in a similar way to PFA. Whereas the level of ettringite did not show any significant change, the $Ca(OH)_2$ peaks increased after treatment especially close to the cathode.

5.5 CONCLUSIONS

The major conclusion that can be drawn from this chapter is that reinforced concrete subjected to ECE can undergo some physical changes. However, these changes were found to be very small and unlikely to adversely effect the cement matrix in concrete being treated in this way.

No evidence of softening of the cement matrix around the cathode was found after the specimens had undergone ECE. The results showed considerable scatter and any changes could not be proven statistically.

The pore structure of the cements around the cathode, as determined by MIP did not appear to change substantially after ECE regardless of the value of current used. A slight increase in the total porosity was observed very close to the steel cathode for the OPC specimens. A slight decrease was , however, found for the blended cements, PFA and GGBS.

The ettringite content of the bulk material did not appear to increase with ECE treatment even though the pore solution sulphate ionic concentration increased when the hydroxyl ionic concentration increased especially near the cathode. It is unlikely,

therefore, that any volume increase associated with secondary ettringite formation could be expected following the ECE treatment.

Table 5.1: Results of statistical analysis on microhardness at 0.1mm from the cathode: Effect of current density

Time (Weeks)	C.d (A/m^2)	Observation (n)	Mean	Variance	Standard deviation	P (T<=t) two tail	Results
4	0	30	36.97	47.21	6.87	0.0002 < 2	Insignificant
	1	30	29.77	47.70	6.91		
	0	30	36.97	47.21	6.87	0.002 < 2	Insignificant
	5	30	31.13	49.98	7.07		
	1	30	29.77	47.70	6.91	0.45 < 2	Insignificant
	5	30	31.13	49.98	7.07		
8	0	30	38.20	102.86	10.14	0.39 < 2	Insignificant
	1	30	36.20	41.04	6.41		
	0	30	38.20	102.86	10.14	0.0014 < 2	Insignificant
	5	30	30.53	50.88	7.18		
	1	30	36.30	41.04	6.41	0.0017 < 2	Insignificant
	5	30	30.53	50.88	7.18		
12	0	30	36.47	187.77	13.70	0.04 < 2	Insignificant
	1	30	30.27	70.13	8.37		
	0	30	36.47	187.77	13.70	0.01 < 2	Insignificant
	5	30	27.80	89.68	9.47		
	1	30	30.27	70.13	8.37	0.29 < 2	Insignificant
	5	30	27.80	89.68	9.47		

Table 5.2: Results of statistical analysis on microhardness at 0.1mm from the cathode: Effect of duration of treatment

C.d (A/m^2)	Time (weeks)	Observation (n)	Mean	Variance	Standard deviation	P (T<=t) two tail	Results
1	4	30	29.77	47.70	6.91	0.0004 < 2	Insignificant
	8	30	36.30	41.04	6.41		
	4	30	29.77	47.70	6.91	0.8 < 2	Insignificant
	12	30	30.27	70.13	8.37		
	8	30	36.30	41.04	6.41	0.0028 < 2	Insignificant
	12	30	30.27	70.13	8.37		
5	4	30	31.13	49.98	7.07	0.74 < 2	Insignificant
	8	30	30.53	50.88	7.13		
	4	30	31.13	49.98	7.07	0.13 < 2	Insignificant
	12	30	27.80	89.68	9.47		
	8	30	30.53	50.88	7.13	0.21 < 2	Insignificant
	12	30	27.80	89.68	9.47		

Table 5.3: Results of statistical analysis on microhardness: Effect of distance from the steel cathode

C.d (A/m^2)	Time (weeks)	Distance (mm)	Mean	Variance	Standard deviation	P (T<=t) two tail	Results
1	4	0.1	29.77	47.70	6.91	0.03 < 2	Insignificant
		>= 10	33.48	68.02	8.25		
	8	0.10	36.30	41.04	6.41	0.55 < 1.9	Insignificant
		>= 10	35.15	135.72	10.72		
	12	0.1	30.27	70.13	8.37	.0007 < 1.9	Insignificant
		>=10	37.48	105.14	11.65		
5	4	0.1	31.13	49.98	7.07	.0008 < 1.9	Insignificant
		>= 10	37.70	114.86	10.34		
	8	0.10	30.53	50.88	7.13	0.011 < 1.9	Insignificant
		>= 10	35.38	106.99	10.25		
	12	0.1	27.80	89.68	9.47	0.003 < 2	Insignificant
		>=10	34.37	94.71	9.73		

Table 5.4: Results of statistical analysis on microhardness of Blended cements: Effect of distance and current density

Cement type	Distance (mm)	Current density	Mean	Variance	Standard Deviation	P (T<=t) two tail	Results
OPC							
treated	0.1	5 A/m^2	21.90	48.51	6.96	0.0009 <	Insignificant
	>= 10		27.18	37.68	6.14	2.0	
Untreated		0 A/m^2	29.87	77.20	8.79	0.0003 <	Insignificant
						2.0	
PFA							
treated	0.1	5 A/m^2	26.57	82.60	9.09	0.03 < 2	Insignificant
	>= 10		30.90	59.55	7.72		
untreated		0 A/m^2	27.20	43.13	6.57	0.76 < 2	Insignificant
GGBS							
treated	0.1	5 A/m^2	35.77	40.94	6.40	1.9x10-6	Insignificant
	>= 10		26.9	97.45	9.87	< 1.9	
untreated		0 A/m^2	29.53	82.19	9.07	0.003 < 2	Insignificant

Table 5.5: Effect of ECE treatment on Porosity of cement matrix after 12 weeks

Samples	C.d (A/m^2)	Time (Weeks)	Distance from surface (mm)	Total Porosity (cc/g)
Profile-plate Untreated	0	12	5	0.1332
			35	0.1267
			52.5	0.1276
Profile-plate 1 A/m^2	1	12	5	0.1107
			35	0.1152
			52.5	0.1193
Profile-plate 5 A/m^2	5	12	5	0.0950
			35	0.1167
			52.5	0.1096
OPC	0	12	50	0.1096
	5	12	50	0.1339
PFA	0	12	50	0.1769
	5	12	50	0.1678
GGBS	0	12	50	0.1777
	5	12	50	0.1442

Table 5.6: Effect of period of treatment on ettringite content and calcium hydroxide content at two positions from cathode (in term of the highest intensities) deduced from XRD diagram

Distance from surface (mm)	Period of treatment (weeks)	Ettringite content	$Ca(OH)_2$ content	Ettringite/$Ca(OH)_2$
52.5	Untreated	5	32.5	0.15
	4	8	39.5	0.20
	8	4.1	39	0.11
	12	2	22	0.09
35	Untreated	5	32	0.16
	4	3.6	20	0.18
	8	4	20.5	0.20
	12	3	18.5	0.16

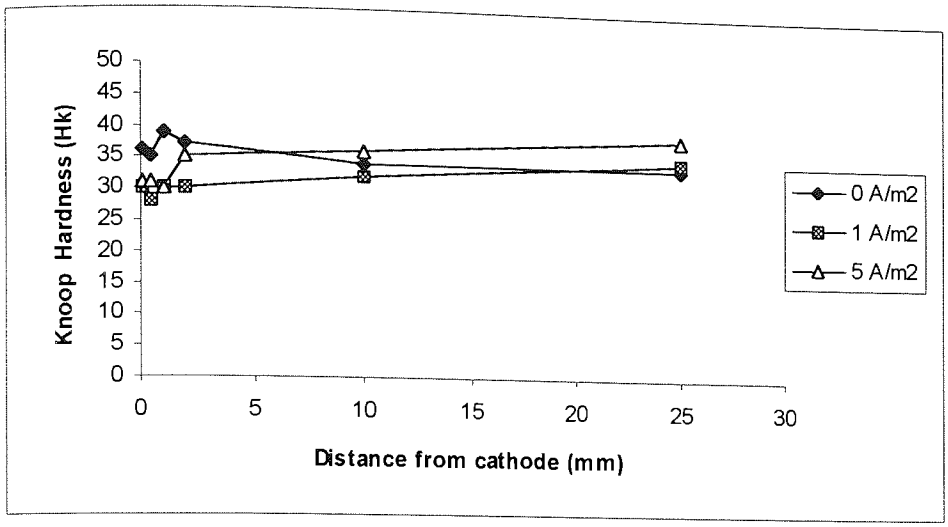

Figure 5.1: Microhardness profiles for specimens polarised for 4 weeks

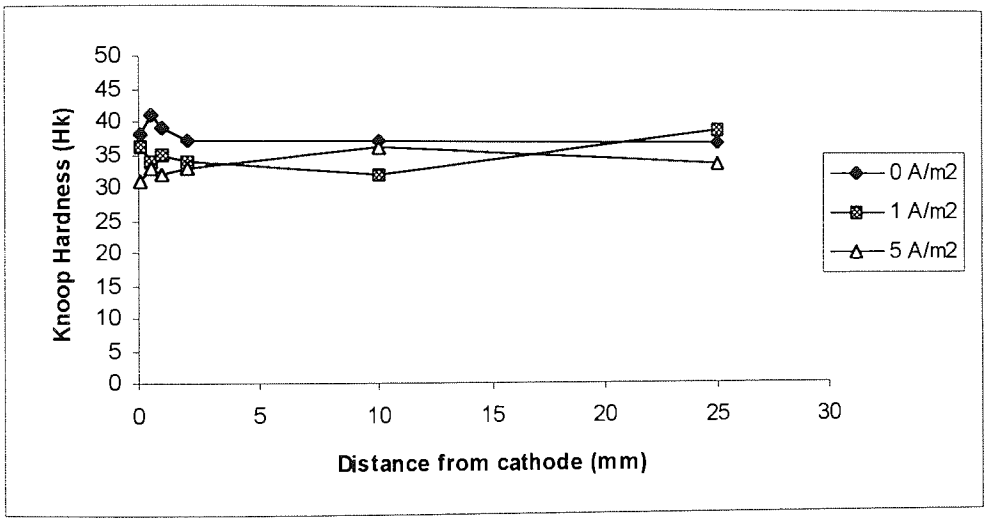

Figure 5.2: Microhardness profiles for specimens polarised for 8 weeks

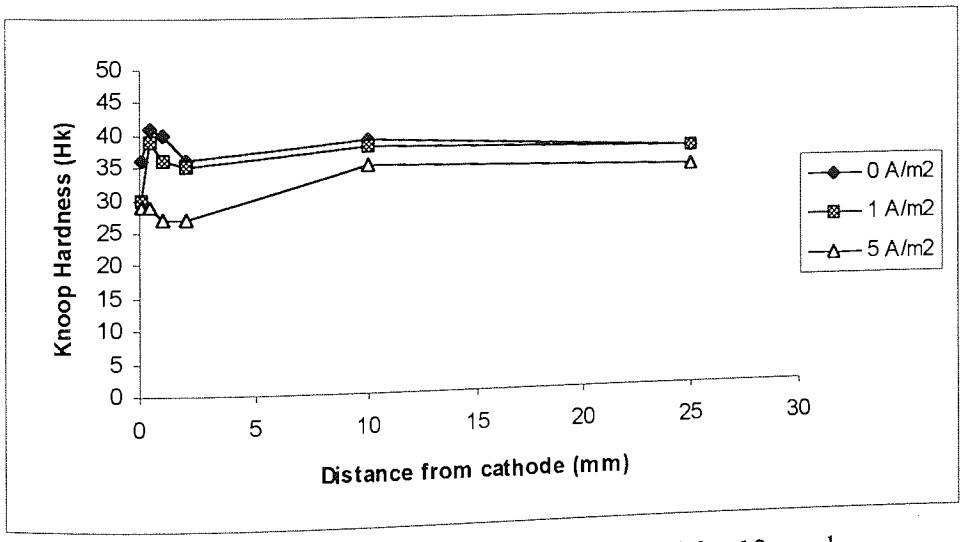

Figure 5.3: Microhardness profiles for specimens polarised for 12 weeks

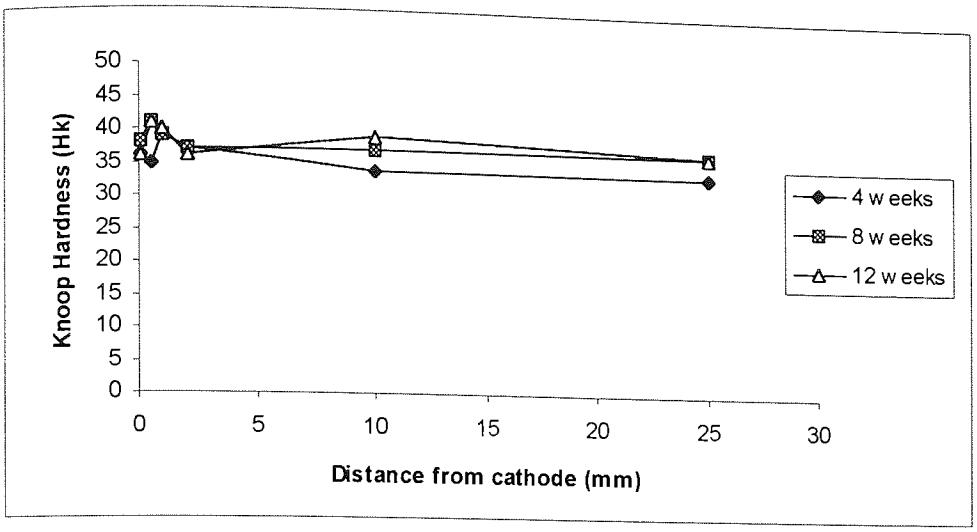

Figure 5.4: Microhardness profiles of specimens treated 0 A/m^2 current density

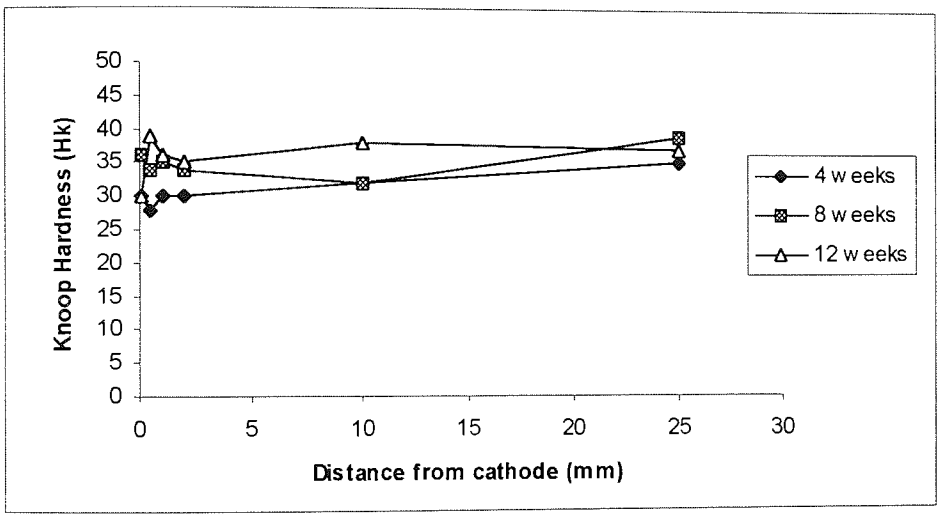

Figure 5.5: Microhardness profiles of specimens treated 1 A/m^2 current density

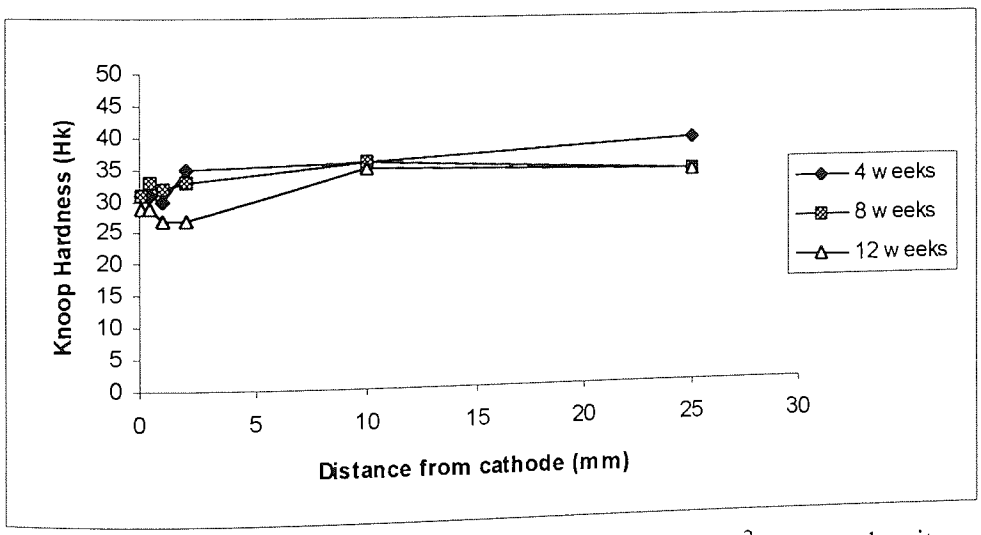

Figure 5.6: Microhardness profiles of specimens treated 5 A/m^2 current density

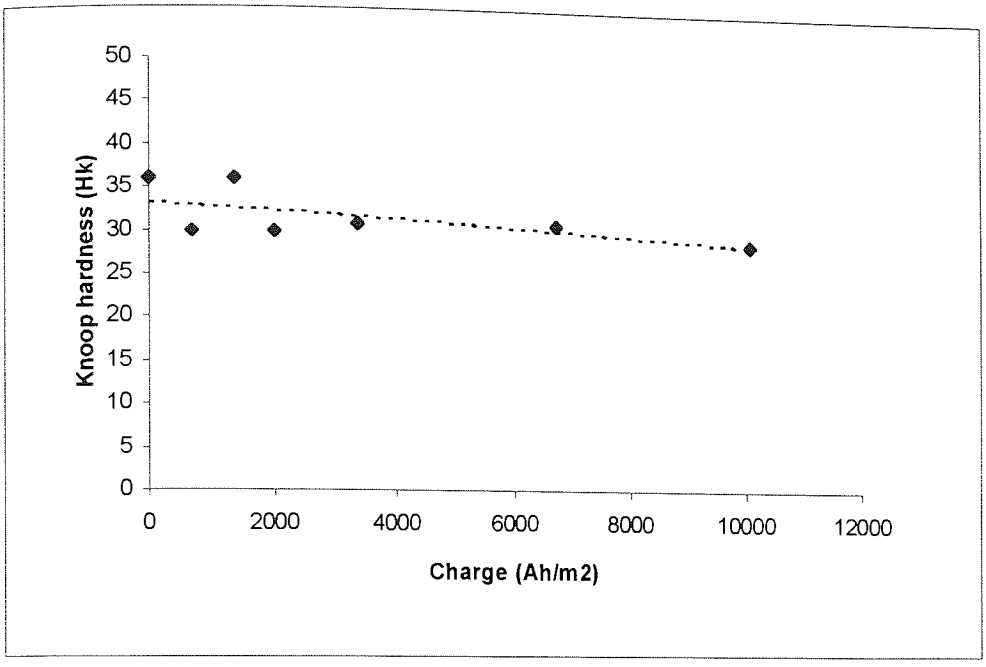

Figure 5.7: Microhardness of cement paste near the steel cathode as a function of circulated charge

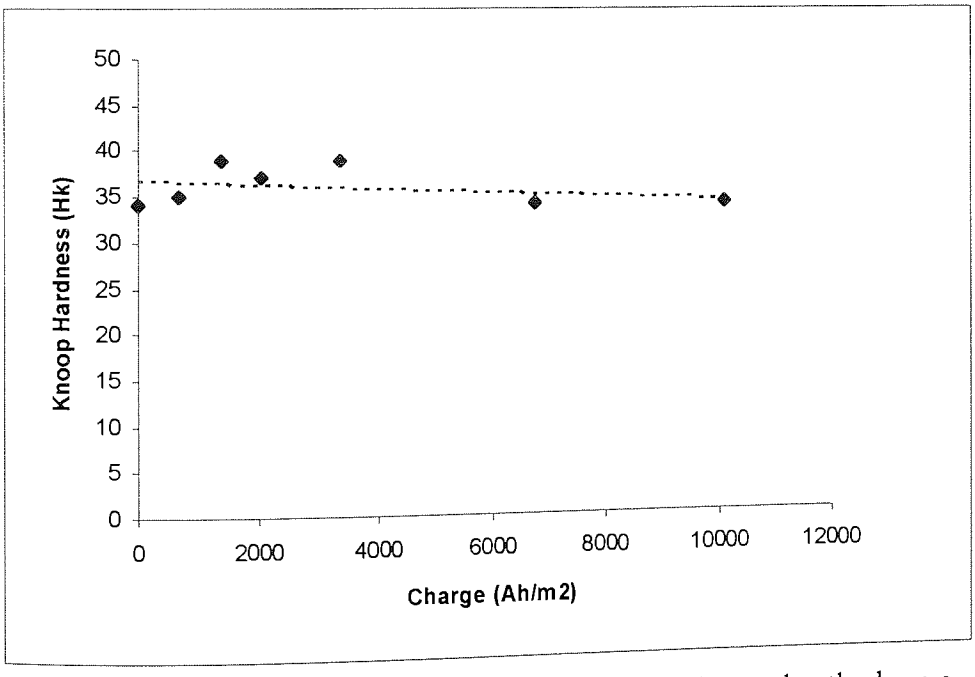

Figure 5.8: Microhardness of cement paste at 25 mm from the steel cathode as a function of circulated charge

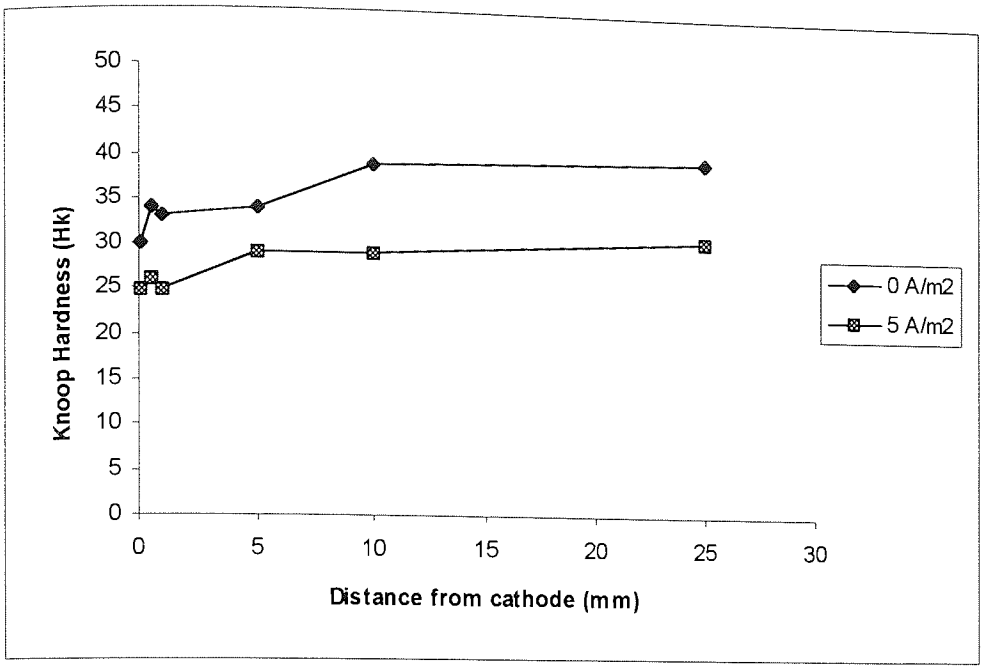

Figure 5.9: Microhardness profiles of OPC bulk-specimens polarised for 12 weeks

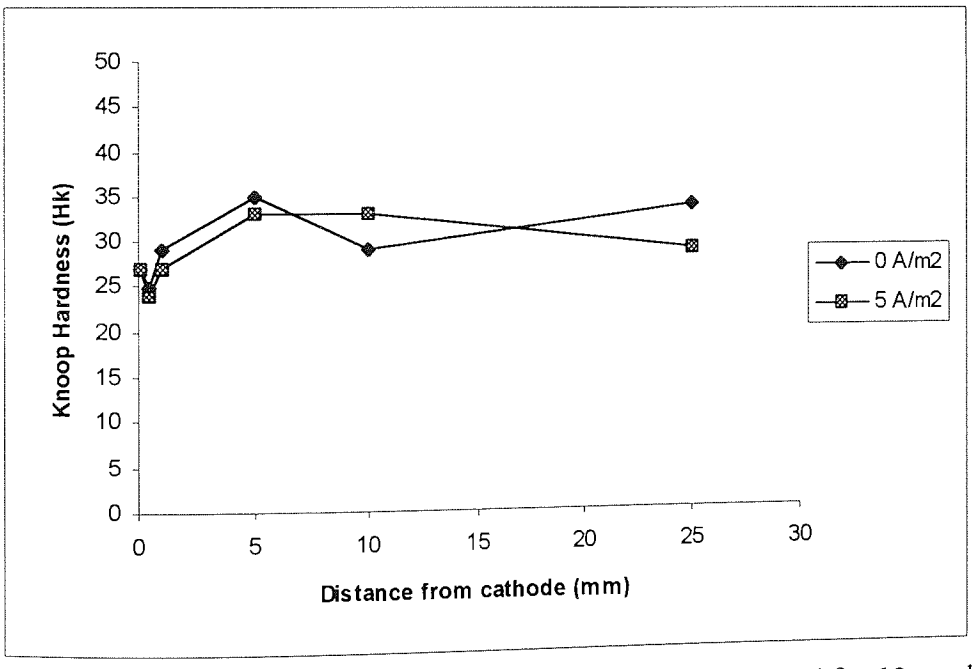

Figure 5.10: Microhardness profiles of PFA bulk-specimens polarised for 12 weeks

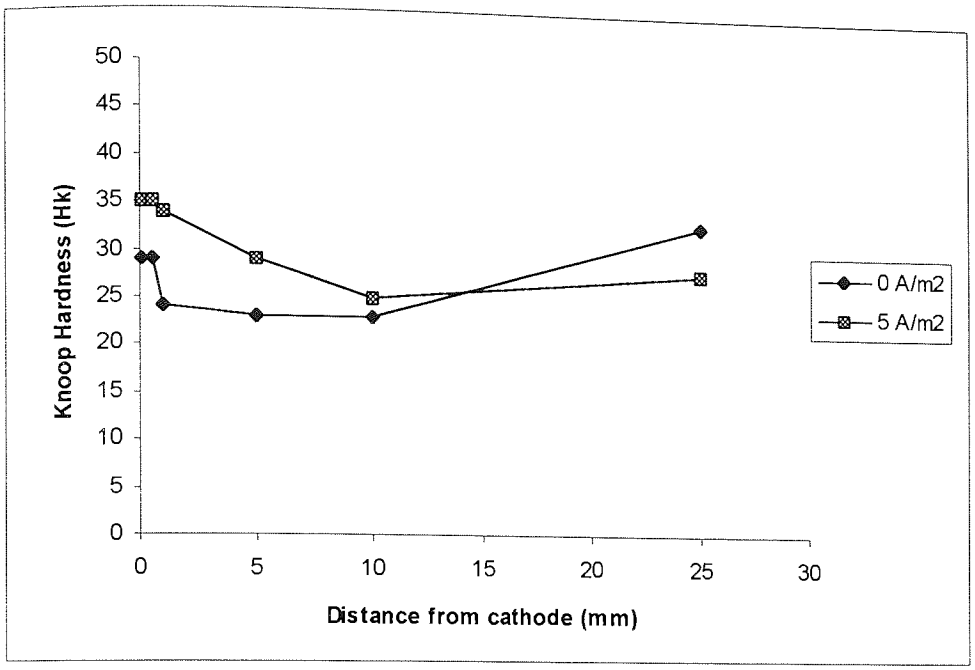

Figure 5.11: Microhardness profiles of GGBS bulk-specimens polarised for 12 weeks

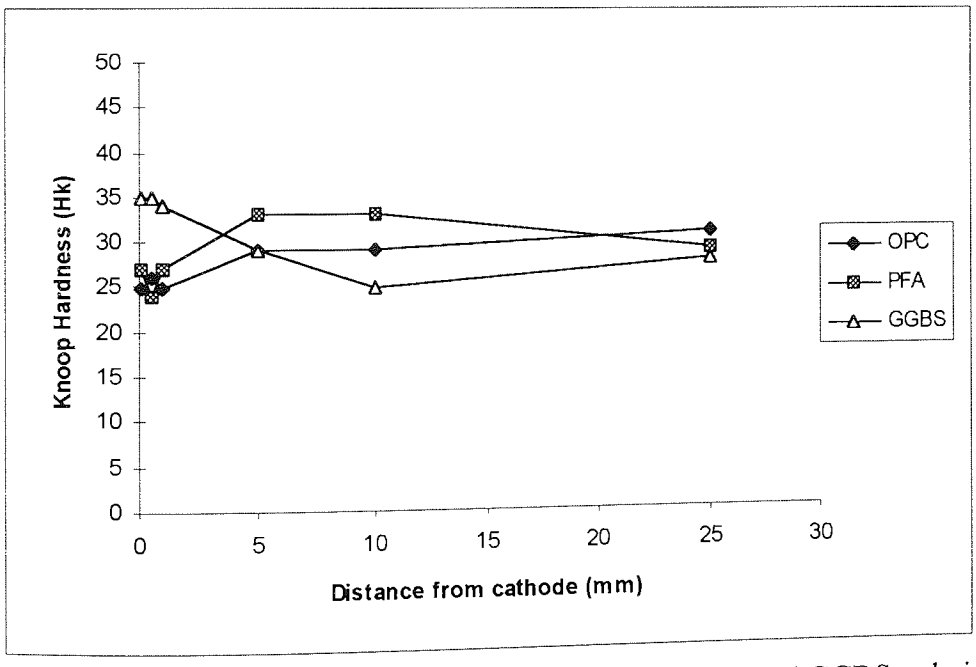

Figure 5.12: Comparison in microhardness between OPC, PFA and GGBS polarised for 12 weeks

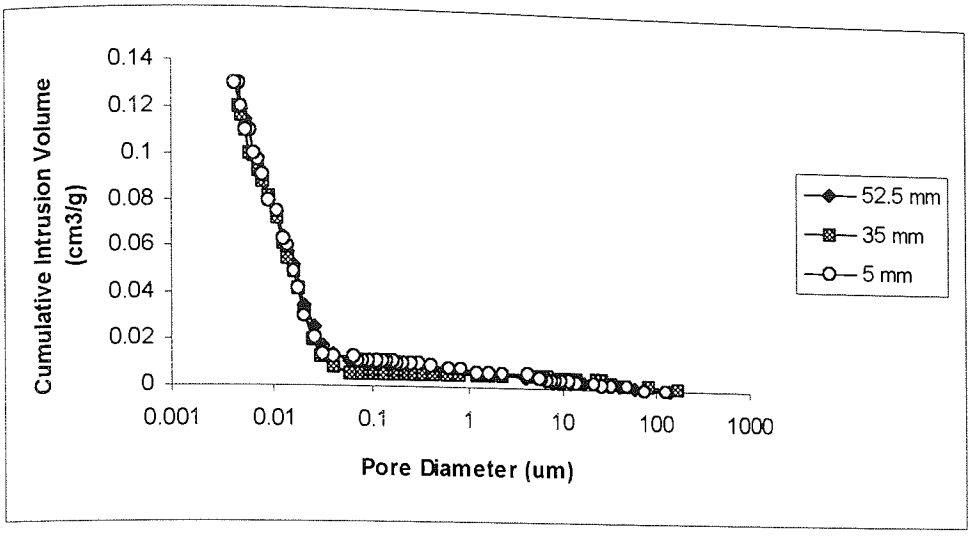

Figure 5.13: Cumulative pore size distribution of untreated specimens

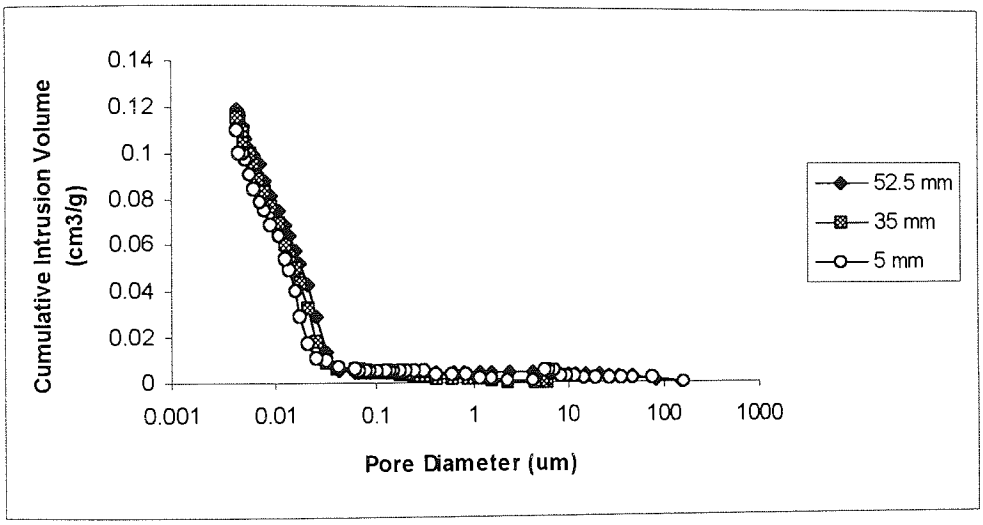

Figure 5.14: Cumulative pore size distribution of specimens polarised with 1 A/m^2 current density for 12 weeks

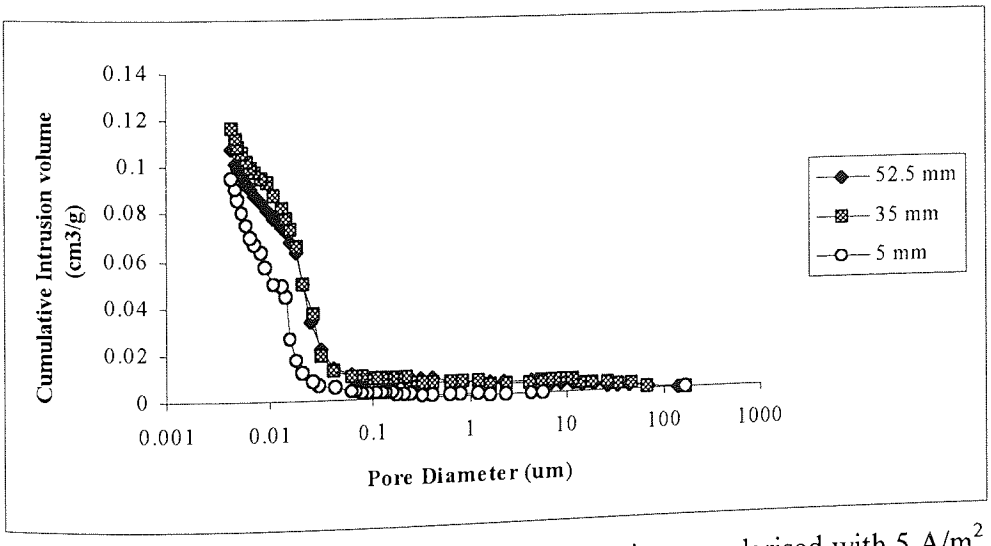

Figure 5.15: Cumulative pore size distribution of specimens polarised with 5 A/m^2 current density for 12 weeks

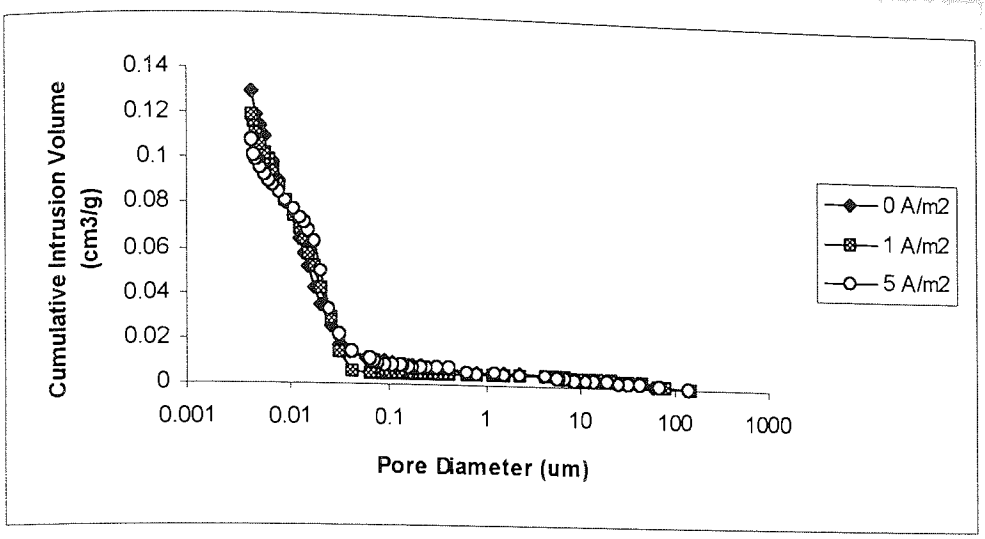

Figure 5.16: Cumulative pore size distribution of specimens polarised with different current density at 52.5 mm from the surface

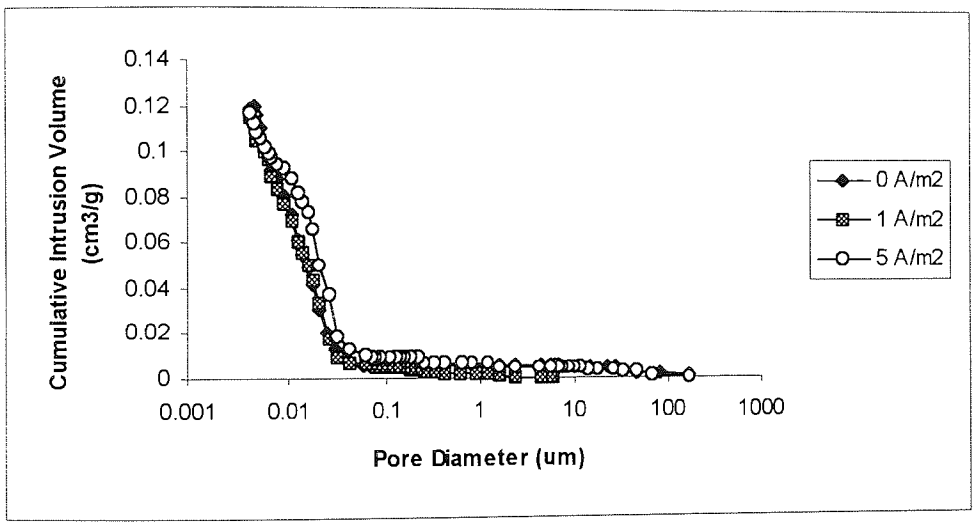

Figure 5.17: Cumulative pore size distribution of specimens polarised with different current density at 35 mm from the surface

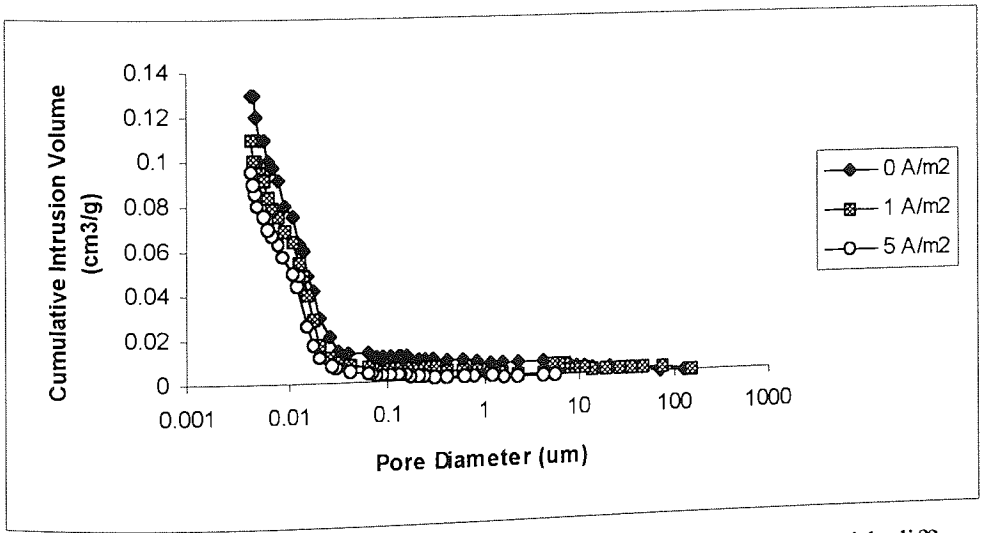

Figure 5.18: Cumulative pore size distribution of specimens polarised with different current density at 5 mm from the surface

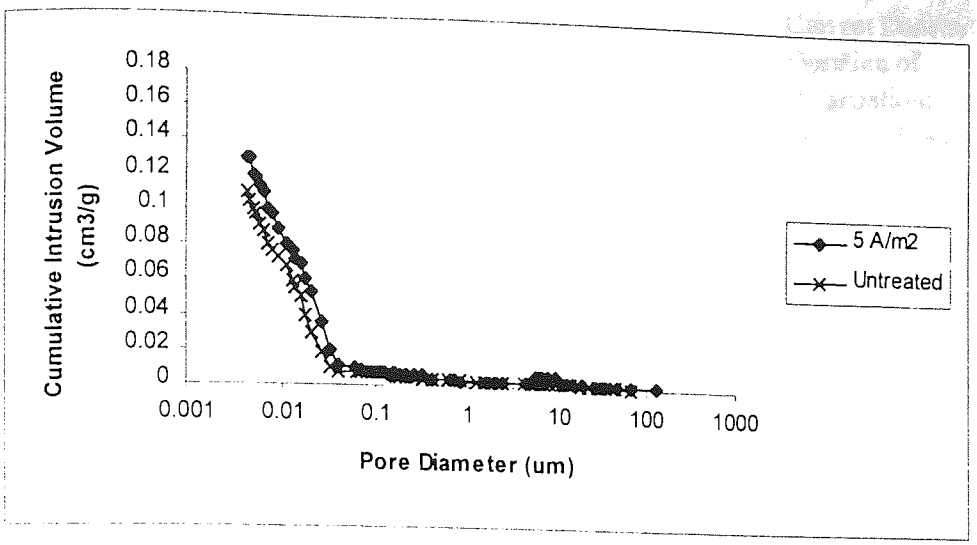

Figure 5.19: Cumulative pore size distribution of OPC specimens at 50 mm from the surface polarised with 5 A/m^2 current density for 12 weeks

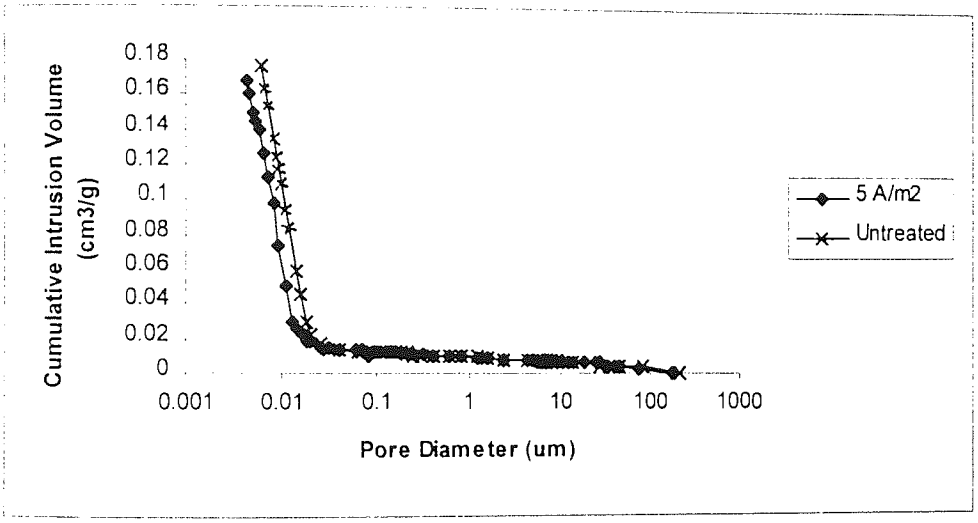

Figure 5.20: Cumulative pore size distribution of PFA specimens at 50 mm from the surface polarised with 5 A/m^2 current density for 12 weeks

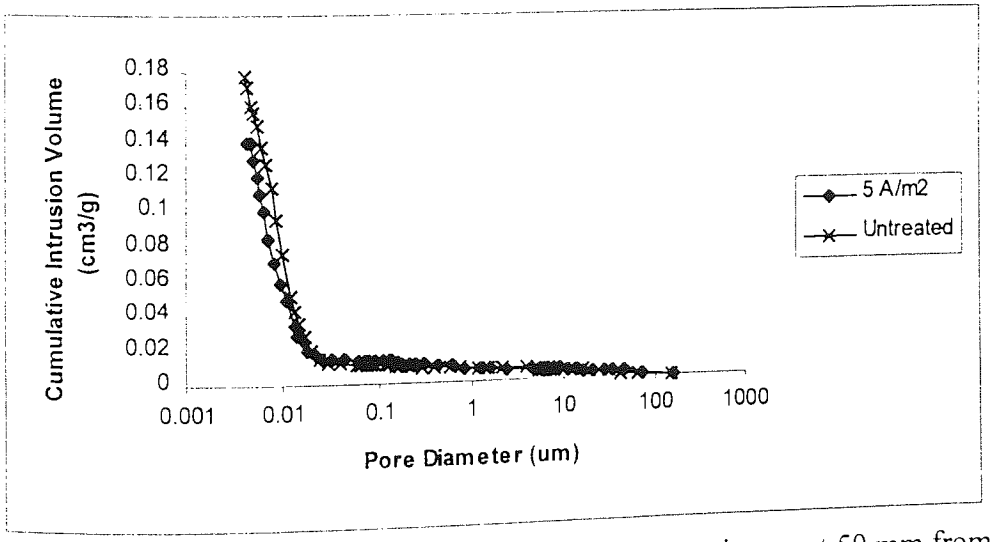

Figure 5.21: Cumulative pore size distribution of GGBS specimens at 50 mm from the surface polarised with 5 A/m^2 current density for 12 weeks

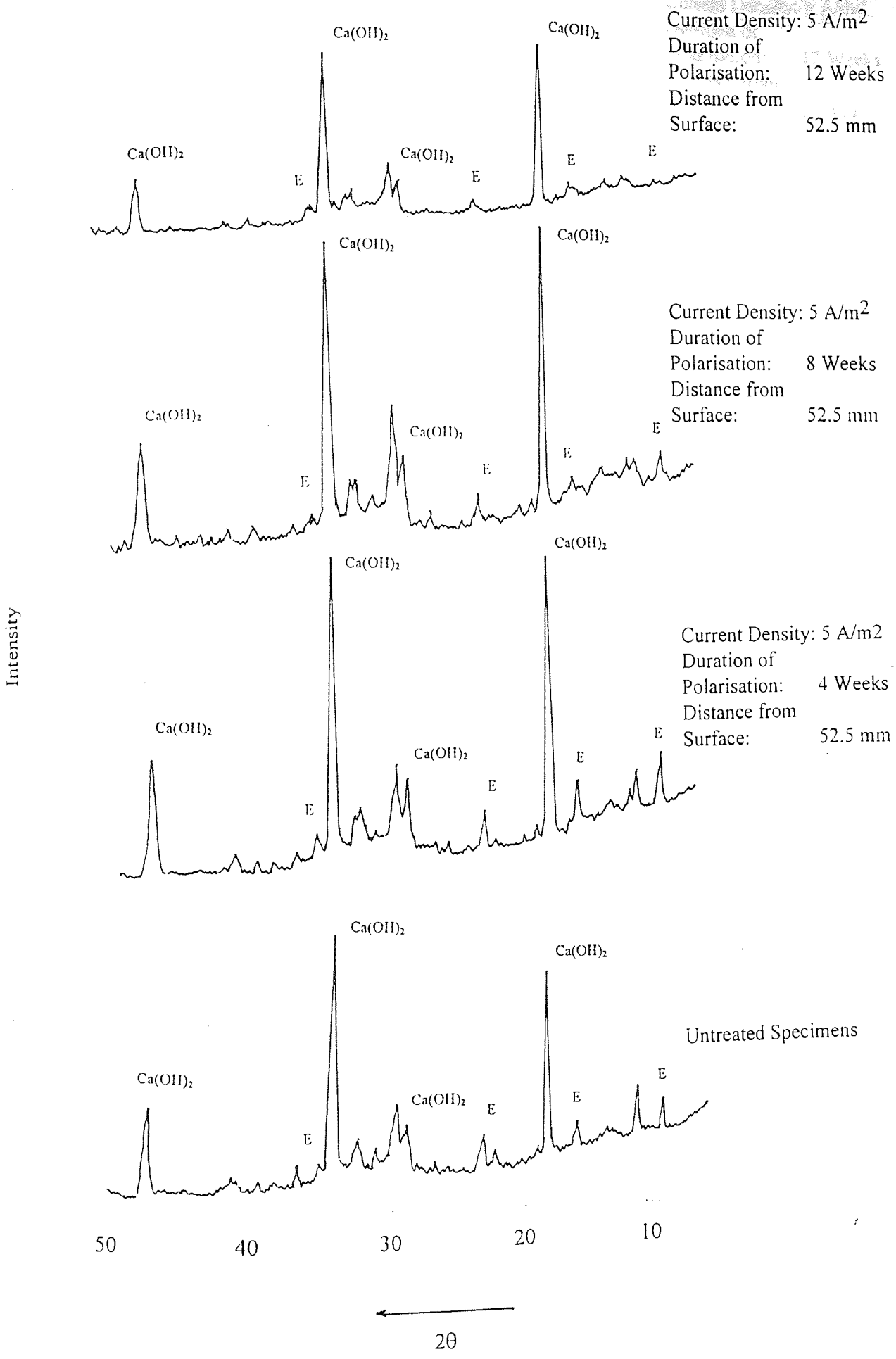

Figure 5.22: XRD traces of profile-specimens (near the cathode) treated with 5 A/m^2 current density for 4, 8 and 12 weeks

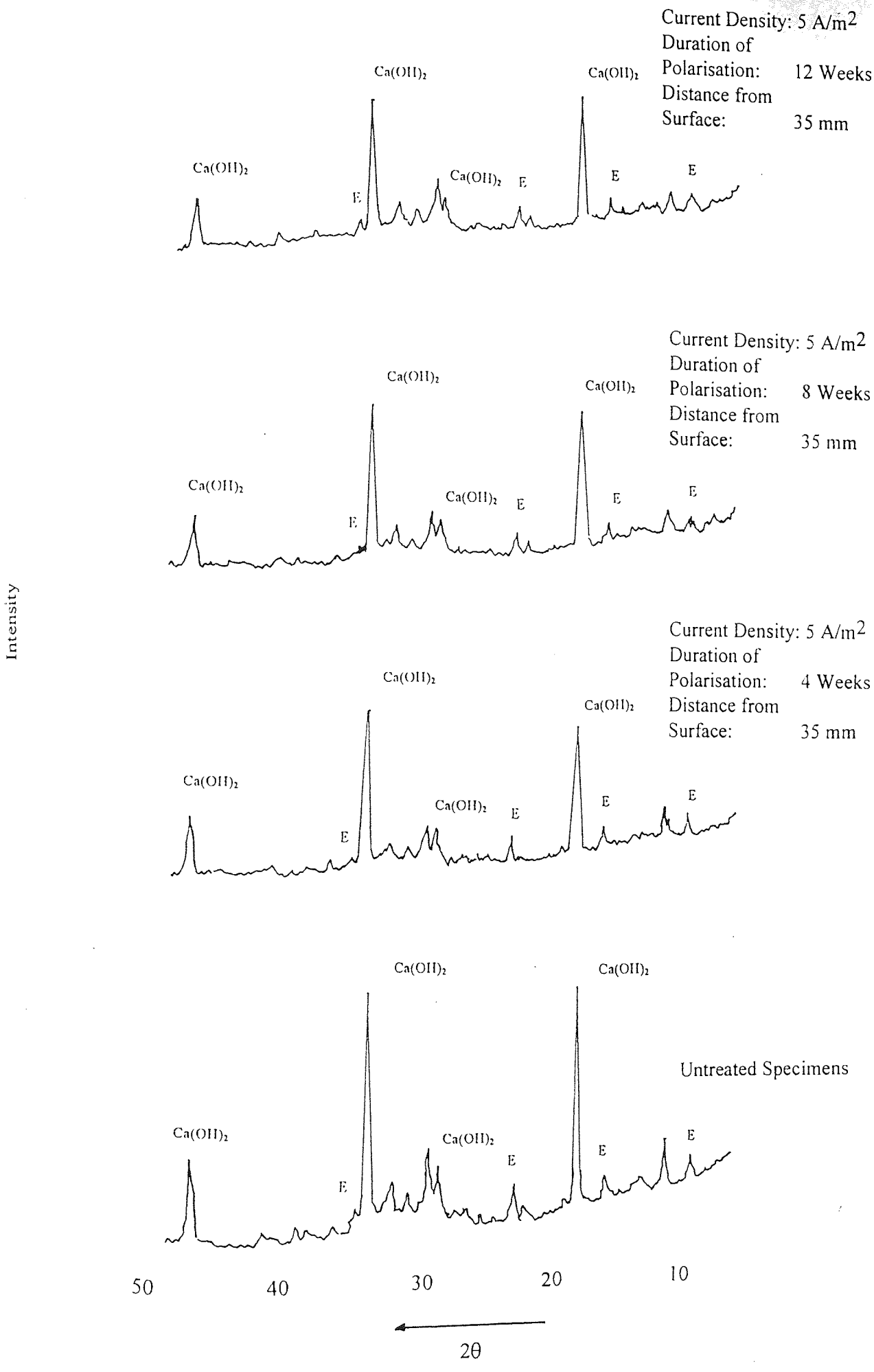

Figure 5.23: XRD traces of profile-specimens (35 mm from the surface) treated with 5 A/m^2 current density for 4, 8 and 12 weeks

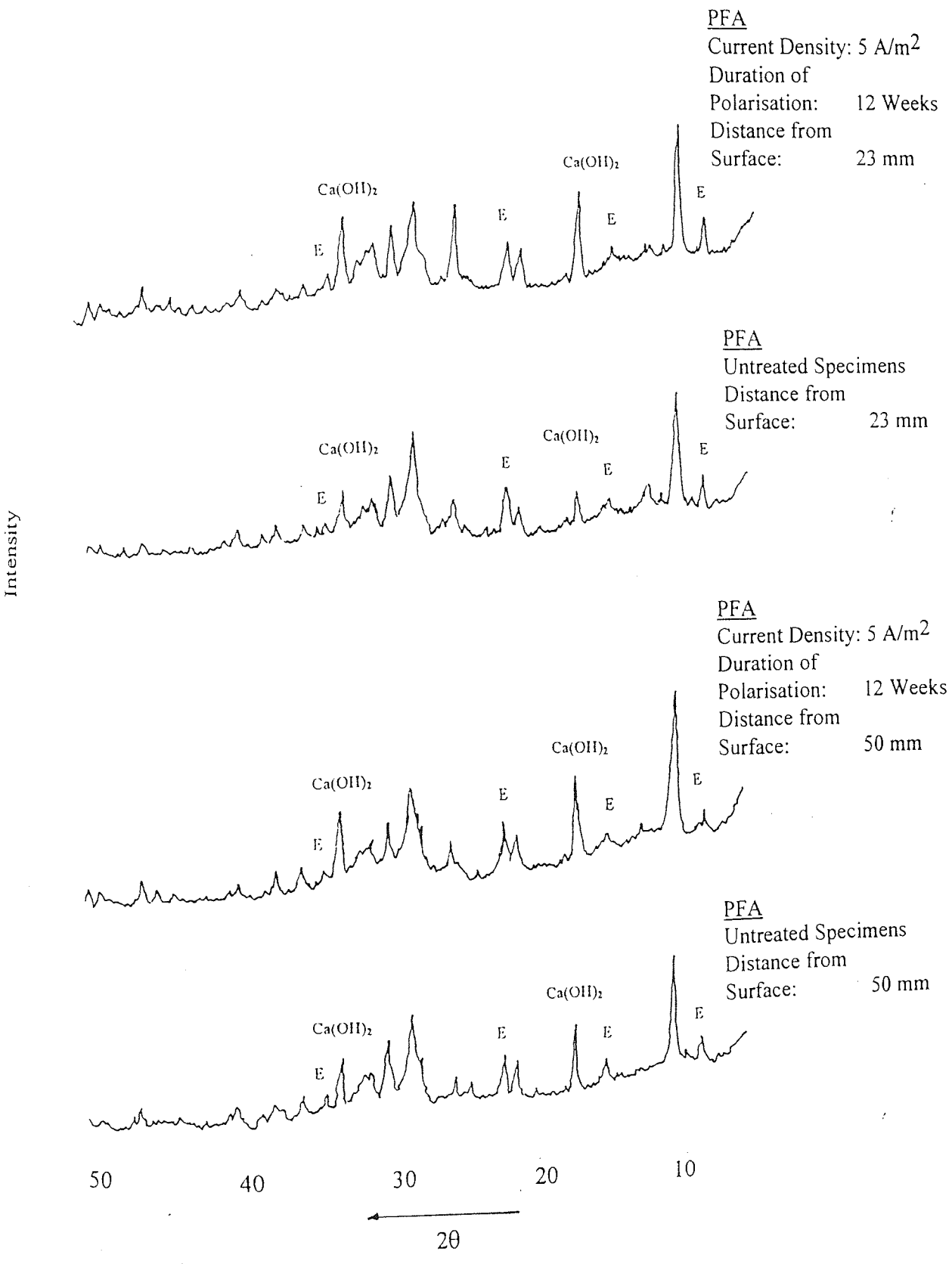

Figure 5.24: XRD traces of PFA specimens (near and at 35 mm) from the surface treated with 5 A/m^2 current density for 12 weeks

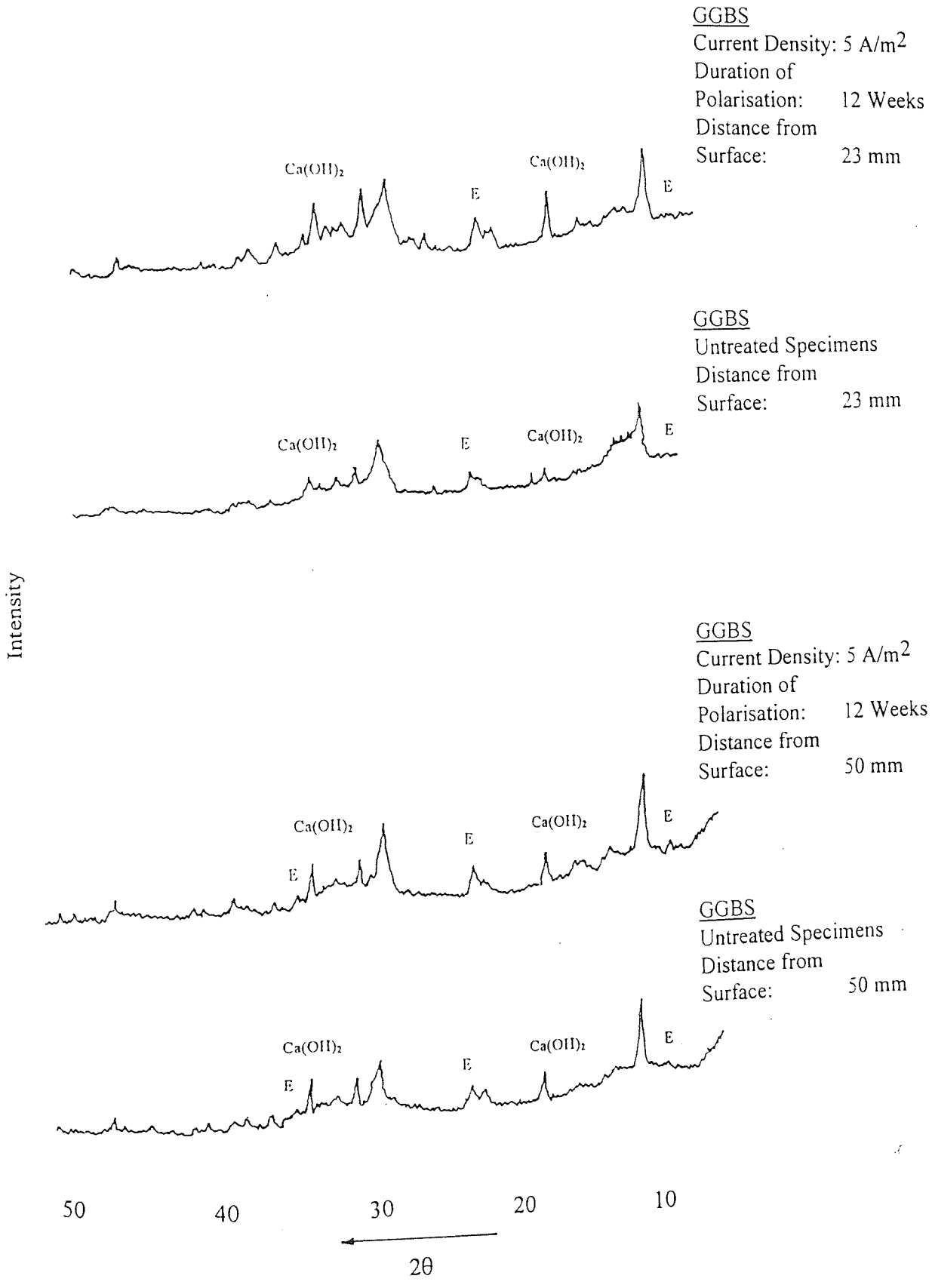

Figure 5.25: XRD traces of GGBS specimens (near and at 35 mm) from the cathode treated with 5 A/m^2 current density for 12 weeks.

CHAPTER 6

IONIC REMIGRATION AFTER ECE AND ITS EFFECT ON STEEL PASSIVATION

6.1 INTRODUCTION

In chapter 4, it was shown that ECE is capable of removing both free and bound chlorides available around the cathode but that complete removal is very difficult. Under normal polarising conditions some chloride still remains in the bulk. The possibility exists, therefore, that this chloride could re-migrate back to the cathode and, after a period of time cause depassivation of the steel. Furthermore, chloride that may have migrated or been present beyond the steel reinforcement is unlikely to be extracted effectively by the ECE process [Meitz, 1997]. These chloride ions can also diffuse back to the cathode. An understanding regarding the redistribution or remigration of chloride ions after ECE treatment is, therefore, extremely important in order to address and solve the problem effectively and to ensure that the steel remains in a passive state long after treatment.

The aim of the work described in this chapter was to study the remigration process by comparing experimentally the distribution of Cl^- and other ions (OH^-, SO_4^{2-}, Na^+, and K^+) immediately after treatment and after storage of the samples for a period of time. The work also attempted to look at the influence of ECE on ions beyond the steel cathode, and whether removal of chloride ions from this region is possible. The success of retreating already treated samples in order to remove more of the remaining chlorides was also looked at.

Removal of the chloride accompanied by the increase in the hydroxyl ionic concentration around the steel by the ECE process leads to passivation of the steel reinforcement. Owing to the strong polarising conditions of the process, however, the potential of the reinforcement can remain very low for a considerable time so success of the process may be difficult to detect. The potential (Ecorr) of the steel cathode was

monitored, for a period after ECE, therefore, in order to determine the extent of this gradual depolarisation effect.

6.2 MATERIALS AND EXPERIMENTAL SET-UP

Three types of specimen were prepared for this study namely profile-plate, bulk and profile-mesh specimens. 'Profile-plate' specimens, were prepared with an inbuilt chloride concentration profile calculated from Fick's 2nd law of diffusion and had a steel plate as the cathode. 'Bulk-specimens' had a constant concentration of 1% chloride by weight of cement and a steel plate as the cathode. For the bulk-specimens the current density used was $5A/m^2$ for the remigration study and $1A/m^2$ for the retreatment study. 'Profile-mesh' specimens also had an in-built profile but contained a mesh as the cathode.

Preparation, production and curing of the profile-plate cathode specimens was similar to the profile specimens described in chapter 4. The distance for each concentration level was measured from the exposed surface. The dimensions and cutting arrangement are as shown in Figure 6.1.

Preparation, production and curing of the bulk-specimens was also similar to the specimens described in chapter 4. Similarly, distance is measured from the surface (anode) and up to 40 mm behind the cathode. The dimensions and cutting arrangement are as shown in Figure 6.2.

Preparation of the profile-mesh specimens was similar to the profile-plate samples, apart from the level of chloride used and the dimensions of the paste. The concentration of chloride was once again calculated using Fick's 2nd Law. C_0 was assumed to be 5% and C_x , the concentration at the steel, was 1%. The higher level of chloride introduced in this case was to assess the capability of ECE to remove a significant level of chloride which may have penetrated beyond the reinforcement. The use of steel mesh as a cathode was to model to a certain extent, actual structural reinforcement. The mesh square spacing was around 8mm x 8mm as shown in Figure 6.3. The dimensions and

concentration levels of chloride are shown in Figure 6.4. The detailed calculation of the concentration profile of chloride is shown in Table 6.1.

6.2.1 Preparation of Steel Plate and Mesh

The cleaning and preparation of the steel plate was similar to that described in chapter 4, section 4.2.1.1. The steel mesh was cleaned by dipping in a sequence of baths. Six beakers were lined up and filled with different solutions, namely detergent, tap water, 20% hot HCl, tap water, de-ionised water and methanol. The steel mesh, after being cut to a size of 34 x 34 mm square, was dipped for a few seconds in each of the beakers to remove any rust, and grease available on the surface. The meshes were then dried and left in a desiccator prior to use.

6.2.2 Anodic Pre-treatment of Sample

Anodic pre-treatment was carried out on the profile-samples (both plate and mesh cathode) in order to induce corrosion to the steel. This process was carried out by holding the potential of the steel to + 300 mV (SCE) potentiostatically for a period of two weeks. The purpose of this pre-treatment was to ensure corrosion initiation of the steel prior to ECE treatment. A saturated calomel reference electrode (SCE) was used to determine the potential (Ecorr) of the embedded steel. Contact between the electrode and the specimens at a point immediately above the steel was achieved through a small moist cloth square. A digital voltmeter with an impedance greater than 10 Mohm was used to monitor the pre-set potential. About 2 weeks after pre-treatment, when Ecorr had stabilised, the specimens were set-up for ECE treatment.

6.2.3 Electrochemical Chloride Removal

For all of the specimens, the setting-up of each sample in the reservoir was similar to that already described in chapter 4 (section 4.2.3). A single current density viz. 5 A/m^2, was used. The duration of treatment was 2 months for the profile-specimens and 3 months for the bulk-samples.

Immediately after treatment, the potential (Ecorr) of the cathode was measured and the samples were then stored over water in a container having a relative humidity (RH) near 100%. Three specimens from each different sample type were taken for pore-pressing in order to extract the pore fluid. Prior to pressing, the samples were cut into sections as shown in Figure 6.1, 6.2 and 6.4 and equidistant sections of each specimens were grouped together and pressed in the pore-expression device. Chemical analysis of the hardened cement pastes and their pore solutions was carried out as described in Chapter 3. The pore-fluids were analysed for OH^-, Na^+, K^+, SO_4^{2-} and Cl^- ionic concentrations.

6.3 RESULTS AND DISCUSSIONS

This section discusses the ionic redistribution after ECE and ionic remigration after the specimens were kept for a period of time. Movement of ions behind the reinforcement and the behaviour of the steel potential (Ecorr) before and after ECE, are also discussed.

6.3.1 Ionic Remigration after ECE

Understanding of the remigration of ions after ECE treatment is very important in order to judge the effectiveness of the treatment. Two types of specimen were prepared for this investigation, namely profile-plate specimens and bulk-specimens.

Profile-plate specimens, which consisted of laminated cement pastes of different chloride concentrations, were assumed to simulate structures which have been exposed to a chloride-laden environment. These specimens had undergone potentiostatic pre-treatment to pre-corrode the steel cathode prior to ECE. Three specimens were analysed immediately after ECE and three more specimens were analysed 3 months after ECE.

Figures 6.5 and 6.6 show the free and total chloride concentration profiles respectively of untreated specimens, specimens analysed immediately after ECE and specimens analysed three months after ECE was completed. It can be seen from Figure 6.5, that after a significant drop in free chloride concentration due to ECE treatment, the concentration of chloride, increased somewhat after the specimens were left in a container at 100% RH for three months. This increase in concentration occurred over the whole depth of the specimens. Figure 6.6, which represents the total chloride, also shows some increase in the concentration of chloride near the cathode after the 3 month storage. At the anode the increase was not significant. Figure 6.7 which depicts the relation between the free and total chloride shows clearly that there were no significant increase in free chloride analysed after 3 months of storage.

Figure 6.8 and Figure 6.9 show the concentration profiles of free and total sodium in the untreated specimens, specimens analysed after ECE and specimens analysed three months after ECE was completed. From Figure 6.8, it can be seen that the sodium concentration profile has resulted in an S-type curve after ECE, showing clearly that an increase in concentration occurred close to the cathode and a reduction at the anode. This increase in concentration near the cathode was depleted after three months of storage which is contrary to what happened with the chloride. Total sodium, as shown in Figure 6.9 produced similar results to the free concentrations. At most of the depths within the cover the concentration of sodium after storage was higher than the concentration of specimens analysed immediately after ECE. Close to the surface of the specimens, the concentration remained very small.

Figure 6.10 and Figure 6.11 show the concentrations of the free and total potassium. As with the sodium, the potassium concentration increased close to the cathode after ECE, but dropped quite significantly after storage of the specimens for three months. Even

though the drop in the total potassium content close to the cathode was quite significant, the concentration level was still higher than it was before the treatment. At 30 mm from the surface, the increase in potassium concentration is not significant. The potassium concentration which was constant at the beginning had simply accumulated around the cathode and was reduced at the anode as a result of electromigration.

Analysis of the cement paste after the ECE treatment showed that the hydroxyl ionic concentration increased enormously to about 1020 mM/l near the cathode due to the cathodic process as shown in Figure 6.12. This increase in OH^- ionic concentration resulted in a pH of 14 as shown in Figure 6.13. However, after 3 months, the overall OH^- ionic concentration dropped, with the value around the cathode reduced to 520 mM/l. The pH returned to its pre-treatment level (>13) which is typical of the pore solution pH of non-carbonated portland cement.

In the bulk-specimens, which were stored for a much longer period and analysed 8 months after ECE was completed, an overall drop of about 60% in free chloride concentration within the cover (between cathode and anode) was observed. The chloride concentration increased again when analysed 8 months later as shown in Figure 6.14 and appeared to migrate from beyond the steel cathode. For total chloride, as shown in Figure 6.15, the increase around the cathode did not appear to be quite as significant as shown by the free chloride in Figure 6.14.

In chapter 2, (Figure 2.13), it was already discussed that chloride ions are transported out of the concrete following the streamlines formed by the applied field. The speed of the migration is, therefore, higher on the shorter streamline due to stronger forces acting on the ions viz. zone directly above the reinforcement. As the lateral distance from the reinforcement increases, the forces decrease resulting in fewer chloride ions being removed. It is therefore expected that slow removal of chloride ions from the area between two adjacent bars would occur and very little removal would be observed from behind the reinforcement. In this experiment, where small specimens were used with a steel plate as the cathode, the transportation of chloride ions out from behind the cathode (steel plate) towards the anode probably followed the streamlines shown in Figure 6.16.

Figure 6.14 gives an indication that chloride present behind the cathode (steel plate) was influenced by the ECE process. The chloride up to around 20 mm behind the steel appears to have been extracted towards the anode under the influence of the electrical field. A small peak was observed immediately after treatment which extended above the untreated level. Although the results were probably not accurate enough to be certain, the formation of this peak may have been caused by the movement of the chlorides from behind the centre of the steel plate away from the cathode following the streamlines as shown in Figure 6.16. The transported chloride from region A to region B, therefore, increased the amount of chloride there. These chlorides, however, redistributed themselves after eight months of storage and diffused towards the cathode replenishing the extracted chloride. The consequence of this was an increase in chloride concentration in the region between the cathode and the surface. The total chloride concentration profiles are somewhat different, particularly near the surface as shown in Figure 6.15. This is probably caused by a change in the binding capacity of the hardened cement as the surface is approached. Sodium and potassium concentrations were so low in this region (figure 6.18 and 6.20) that chloride must have been present as calcium chloride which, as will be discussed later, is bound more readily by the cement.

Overall, it is clear that ECE is capable of removing chloride from a small distance behind the reinforcement, up to 20 mm in this case. This finding supports what was found by Green et al., [1993] who conducted a study on concrete prisms. Their work also indicated that removal up to 20 mm behind the reinforcement is possible. Other researchers [Farinha & Peek, 1991; Hansson and Hansson, 1993; Tritthart, 1996; Stoop and Polder, 1996 and Arya et al., 1996] only expressed their view that ECE is capable of removing chloride within a close vicinity of the reinforcement without mentioning to what distance.

Figure 6.17 and 6.18 show the free and total sodium concentration profiles. A considerable amount of sodium was attracted towards the cathode forming a very clear peak. Sodium ions from within the cover zone also electromigrated beyond the cathode. After eight months of storage, the sodium concentration peak diminished and sodium ions redistributed themselves in both directions away from the cathode.

Figure 6.19 and 6.20, which depict the free and total potassium concentration profiles, also show similar peaks around the cathode and a drop at the anode after ECE. However, after 8 months of storage the peaks practically disappeared and potassium redistributed itself within the specimens going down to levels close to the original near the cathode, but remaining low near the surface.

Figure 6.21 shows the OH^- ionic concentration which increased enormously around the cathode as a result of the cathodic process and increased the pH to above 14 immediately after ECE as shown in Figure 6.22. The consequence of this high pH around the cathode as discussed in chapter 4, is that the sulphate ionic concentration increased due to solubility equilibria. This phenomenon is clearly shown in Figure 6.23. After eight months of storage, the OH^- ionic concentration around the cathode dropped following redistribution along the specimens, resulting in a concentration within the cover which was overall higher than the original level, with a pH of over 13.5.

As the concentration profiles of the individual ionic species need to satisfy an overall charge balance, a plot of $(\Sigma^+ - \Sigma^-)$ versus distance should, in theory, be a straight line with values close to zero. Figure 6.24 shows the actual values obtained for the untreated specimens and for specimens subjected to ECE and analysed either immediately after treatment or eight months after treatment. All three conditions appear to show an overall excess of cations. Near the surface, however, the charge balance is negative even after taking account of the increasing concentration of calcium as shown in Figure 6.25

As was discussed in chapter 4 (section 4.3.1), when the treatment was carried out for 12 weeks, the electrolyte became acidic leading to the formation of HCl which could then react with the $Ca(OH)_2$ in the external solution to form $CaCl_2$ as follows:

$$Ca(OH)_2 + 2HCl = CaCl_2 + 2H_2O$$

The very low concentrations of sodium and potassium in this region also suggests that some chloride may have been present in the form of $CaCl_2$. It is suggested from the literature that chloride in the form of $CaCl_2$ is bound more by the cement than NaCl

[Arya et al. 1990]. Also, Figure 5.15 in chapter 5 showed that the porosity at the surface was denser than at a position close to the cathode. This change in porosity may well be explained by the formation of $CaCl_2$ and its binding by the hardened cement leading to a denser matrix in the surface region. Figure 6.26 also suggests a change at the anode as the binding capacity of the cement paste in the anodic region appears to have been increased significantly.

An attempt was made to replot Figure 4.15 showing the ratio of chloride removed from the original constant level as shown in Figure 6.27. This figure shows a hump developing with time around the middle part of the specimens. This shape indicates that little chloride was removed from the bulk area and most was lost from around the cathode and from the surface. This figure, apart from suggesting that ECE does not achieve complete removal of the chloride, also shows that following the ECE treatment, a concentration gradient of chloride develops which would necessitate its diffusion towards the steel cathode as well as to the surface.

The chloride left behind the cathode (reinforcement) would also move towards the steel for the same reason which would inevitably result in an increased concentration of chloride in the vicinity of the steel. Stoop & Polder [1994], who observed the chloride around the rebar of a concrete prism exposed outdoors for over 1 year after ECE, found that the concentration increased near the steel.

The increase in the chloride concentration after storage of the bulk-specimens was higher than in the profile-plate specimens. This was probably due to the remigration of the higher level of chloride behind the cathode.

The period taken by the chloride to diffuse and over what distance depends on a number of parameters such as volume and diameter of the capillary pores of the concrete, the extent of the dryness of the pores and the extent of chloride binding by the cement [Meitz, 1997]. The wet condition experienced by these specimens even during the three months storage (see Figure 6.28), can allow the chlorides to diffuse easily within the pores and replenish the removed chloride, even after only three months, as shown in this chapter.

The bound chloride concentrations measured after 3 months, as shown in Figure 6.26, are in line with the bound chloride levels measured immediately after ECE between the steel and up to a distance of 30 mm from the cathode. A similar trend is observed for free chloride and the overall results are consistent with the results obtained in chapter 4 (Figure 4.18). Figure 6.26 also shows that at positions close to the surface indicated as the anodic region in the figure, both free and bound chlorides do not follow the equilibrium line and can probably be explained by the change of sodium chloride to calcium chloride and the accompanying change in the chloride binding capacity, as explained earlier.

Figure 6.29 illustrates the bound chloride in the bulk-specimens away from the surface of the after-storage specimens compared to the untreated and just treated specimens. It indicates once again, that there is no obvious detectable increase in the binding capacity of the bulk-specimens similar to that shown by the profile-plate specimens.

In the profile-mesh specimens, which resemble structures which have been subjected to heavy chloride ingress where the chloride has already penetrated beyond the reinforcement, the movement of chloride up to 20 mm behind the cathode was as shown in Figures 6.30 and 6.31. There is no doubt that the chloride in front of the cathode was removed extensively but it seems that the removal of chloride from behind the cathode, was not very effective. This lesser affected distance of chloride removal compared to the bulk-specimens could be attributed to the shorter treatment period of 8 weeks compared to 12 weeks for the bulk-specimens.

It is worth mentioning here that the spacing between the wires making up the mesh used in this research was around 8 mm. This relatively small spacing may allow chloride available in between the wires to be electromigrated by the influence of the electrical current. In actual structural reinforcement bars, which can be several centimetres apart, chloride which is available between this large spacing may not be influenced at all by the current and could remain in the concrete, subsequently diffusing to the steel.

The movement of free and total sodium and potassium are shown in Figure 6.32 to 6.35. In each case, a peak was formed around the cathode due to the accumulation of either sodium or potassium ions as a result of the electromigration process.

Figure 6.36 shows the concentration of hydroxyl ion. Around the cathode, the hydroxyl ionic concentration increased as a result of the cathodic process. This increase in hydroxyl ion concentration results in an increase in pH as shown in Figure 6.37. As with the other two types of specimens, near the surface the pH decreased but behind the reinforcement it remained high.

6.3.2 Ionic Redistribution After Retreatment

In chapter 4 it was found that a $1A/m^2$ current density was too low for achieving significant extraction of the chloride. Some of the bulk specimens in this chapter were polarised using only $1A/m^2$ current density for 12 weeks (Figs. 6.38 to 6.45). The level of extracted chloride was only about 20 % (Fig. 6.38) compared to 60 % at a $5A/m^2$ current density (Fig. 6.14). These specimens were then stored for 9 months in a container with a 100% RH environment.

After 9 months of storage, the specimens underwent a second treatment using a similar current density for another 8 weeks. It was found that this second treatment managed to extract a further 25 % of free chloride from the specimens compared to the levels achieved after the first treatment, as shown in Figure 6.38.

However, the overall reduction in total chloride was very low as shown in Figure 6.39 and occurred only up to 30mm from the cathode. It is likely, that the chloride concentration had already increased by diffusion from beyond the steel after the specimens were kept for 9 months as shown before by the profile-plate specimens which were analysed 3 months after completion of ECE treatment and the bulk-specimens which were analysed after 8 months.

The results of free and total sodium are shown in Figure 6.40 and 6.41. As expected, electromigration moved the Na^+ ions towards the cathode following the first treatment. After 9 months of storage, the peak at the cathode would have been reduced because the sodium ions redistributed themselves in the specimen as was shown by the profile-plate and bulk-specimens discussed in section 6.3.1. However, after retreatment, the peak formed again but the overall concentration level was reduced possibly because of leaching by condensation on the surface of the specimens during their long storage period. Similar phenomena were also indicated by the free and total potassium as shown in Figures 6.42 and 6.43 as well as for the OH^- and pH as shown in Figures 6.44 and 6.45.

6.3.3 Steel Passivation

Figure 6.46 shows the change in potential (Ecorr) of the steel before and after the specimens were subjected to ECE. After 40 days of monitoring, the potential of the steel was found to be fairly stable (point A). The specimens were then anodically polarised potentiostatically to +300mV for two weeks in order to encourage corrosion of the steel (point B). After that, the specimens were disconnected and left for another two weeks in the container. The potentials of the steel specimens were monitored to ensure that they were corroded before they were ready for ECE treatment (point C). The potential recorded after potentiostatic polarisation indicated that the steel plates were actively corroding. Some of the specimens were broken open to look at the state of the steel and were found to be corroded. The current density used for ECE was 5 A/m^2 and the duration of treatment was eight weeks. Immediately after ECE, the potential of the steel recorded was -849 mV (SCE) (point D) which is highly negative showing that the steel had not yet depolarised.

Concrete Society Technical Report No 36, [1991] noted that if the potential of the steel in concrete is reduced to a value lower than -750mV (SCE) by cathodic protection, further corrosion activity is unlikely. This negative potential however, depolarised quickly. In three days, the potential rose up to -179mV (SCE) (point D to E). The steel potential was then monitored for a further period shown in the graph as E and F. It

was found that the potential became less -ve and settled at about -120 mV. This indicates that the steel lay in the potential range where passivation can occur [Green et al., 1993]. Potential monitoring, which was carried out up to 100 days after ECE, indicates that the steel remained passive throughout this period. The potential had actually become more noble than before the ECE treatment. Although depolarisation for these specimens occurred fairly quickly owing to their small size, potential measurements on large structures should be conducted at least two months after the ECE treatment to allow the arrival of oxygen to the rebar and the re-establishment of the equilibrium pore pH in the concrete adjacent to the rebar.

As discussed in section 6.3.1 and as shown in Figure 6.12, analysis of the cement paste after the ECE treatment, showed that the hydroxyl ionic concentration increased enormously around the cathode. This increase in the OH^- ionic concentration helps to repassivate the corroded steel and restore the protective environment in the vicinity. When the specimens were cut and broken into pieces to analyse for ionic concentration, it was found that the cathodes were covered with a slimy black layer likely to be magnetite, a low oxygen corrosion product.

Furthermore, the reduction in the chloride concentration around the steel will enhance the passivation of the cathode. A SHRP research programme showed that even with a modest removal of chloride and the concentration still above the threshold value for steel corrosion, ECE treatment gave a very low corrosion rate and a very passive half cell potential which lasted more than five years without reactivation [Bennett and Schue, 1993]. This could possibly be due to a high pH around the steel which favours passivity of the steel environment. Analyses which were carried out three months after ECE in the profile-plate specimens, showed that the hydroxyl ionic concentration dropped close to the original level near the cathode and diminished in value as the surface was approached. The pH of the bulk specimens after 8 months of storage, however showed a high value well above 13.5 as shown in Figure 6.22 and considerably higher than the original pre-treatment value. It is likely that the pH of the pore solution would depend on the migration of other ions in the system as a charge balance needs to be maintained.

The bar charts in Figure 6.47 show a very slow increase in chloride and a large drop in the OH^- ionic concentration at the steel after storage which resulted in an increase in the [Cl^-/OH^-] ratio. This ratio was, however, considerably lower than the original value. Table 6.2 gives the comparison on the Cl^-/OH^- ratio before and after treatment and after storage. It is clear from this table, that the Cl^-/OH^- ratio increases in the vicinity of the cathode. However, on longer storage periods (bulk-specimens) the value closer to the surface and at a distance behind the cathode is reduced so the ratio appears to be moving towards a constant value for all depths as shown in Table 6.2. The Cl^-/OH^- ratio of the profile-plate specimens after three months was 0.11 which is well below 0.22, the critical threshold ratio for corrosion of steel in cement paste as shown in Table 2.3. The Cl^-/OH^- ratio of the bulk-specimens at the cathode after eight months was 0.27. Although this appears to be quite high, it is unlikely to lead to corrosion of the steel as no corrosion was observed originally when the Cl^-/OH^- ratio was 0.97 (Table 6.2). It was for that reason an anodic potentiostatic current was applied to some specimens in order to corrode the steel prior to ECE. Table 2.3 shows the confused picture with regards to the Cl^-/OH^- ratio required for corrosion of steel in concrete and no information is available for in-situ concrete. Although it may be possible to determine how the critical Cl^-/OH^- ratio may increase with time after ECE, it will be difficult to predict with certainty whether this can lead to further corrosion of the steel. Predictions may, therefore, be limited to the kind suggested by Armstrong et al., [1996] that the chloride content would take around 25 years for its concentration to reach double the after treatment value at the depth of the reinforcement.

6.4 CONCLUSIONS

Work in this chapter reaffirmed the conclusion made in chapter 4 that ECE not only removed the free chloride but also the bound chloride and maintained an equilibrium between the free and the bound chloride states. A significant level of chloride, however, remained in the specimens after ECE.

Around the outer surface of the specimens the chloride equilibrium was altered because of physical and chemical changes in the cement paste. Transformation of NaCl to $CaCl_2$

may have occurred which was accompanied by a denser cement matrix in this region and resulted in a higher chloride binding capacity of the cement paste.

It was found that ions present behind the cathode up to a distance of 20mm were influenced by the current applied during ECE. Thus, chloride ions in this zone behind the cathode were extracted by following the streamlines which were formed by the applied field towards the anode. Chloride present beyond this zone was available, however, to diffuse back to the steel.

Alkali metal ions (sodium and potassium) which were attracted towards the cathode under the influence of the current were also able to electromigrate to the cathode and beyond. The peak, formed around the cathode, diminished as the ions redistributed themselves with time.

As well as the removal of chloride, ECE also capable of restoring passivity in the steel cathode, which was previously corroded, by increasing the pH value in the immediate vicinity of the steel. This is because of the overall effect of reducing the Cl^-/OH^- ratio, a parameter that indicates the corrosiveness of the concrete pore solution.

It is recommended to allow sufficient time (of the order of 2-3 months) after ECE treatment of a reinforced structure for a potential survey in order that the polarisation effects on the steel are removed and the results become reliable.

A retreatment process does not appear to be necessary if the correct current density is applied within the required time of treatment.

Table 6.1: Chloride concentration in each slice of cement of 'profile-mesh' specimens

Slice No	x (mm)	y	erf(y)	1-erf(y)	Cx	NaCl (%wt. of cem.)
1	5	0.101	0.11	0.89	4.44	7.3
2	15	0.304	0.33	0.67	3.36	5.6
3	25	0.506	0.53	0.47	2.36	4.0
4	35	0.709	0.69	0.32	1.58	2.6
5	45	0.911	0.80	0.20	0.99	1.6
6	55	1.113	0.88	0.12	0.58	1.0
7	65	1.316	0.94	0.06	0.31	0.5
8	75	1.518	0.97	0.03	0.17	0.3
9	85	1.721	1	0	0	0

Table 6.2: Ratio of Cl^-/OH^- immediately after ECE and after storage

Profile-plate specimens				Bulk-specimens			
Dist. from surface (mm)	Untreated specimens	After ECE	3 months after ECE	Dist. from surface (mm)	Untreated specimens	After ECE	8 months after ECE
55 (cathode)	0.23	0.05	0.11	86	1.05	0.80	0.67
45	0.38	0.10	0.19	77	1.05	0.71	0.60
35	0.55	0.16	0.25	68	0.98	0.68	0.54
25	0.82	0.31	0.37	59	0.99	0.38	0.43
15	0.99	0.58	0.48	50 (cathode)	0.97	0.09	0.26
5 (surface)	1.10	0.34	0.63	41	0.95	0.24	0.22
				32	0.99	0.24	0.26
				23	1.05	0.33	0.33
				14	0.95	0.64	0.41
				5 (surface)	1.05	0.89	0.48

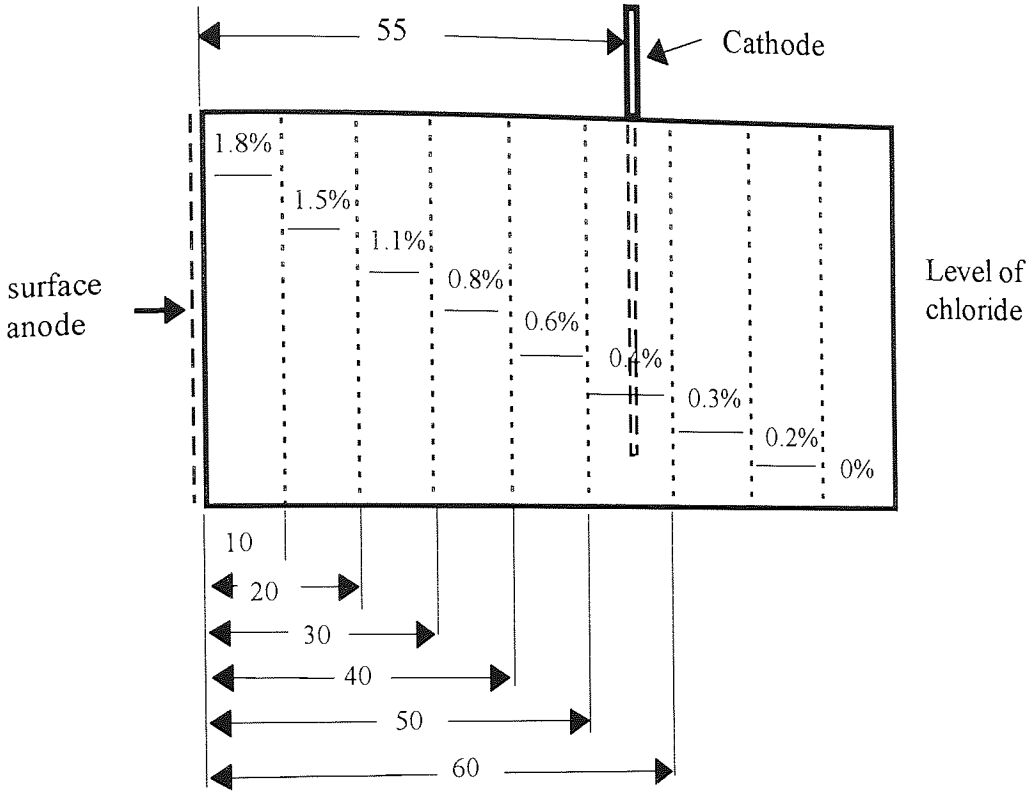

Figure 6.1: Arrangement of cutting of profile-plate specimens

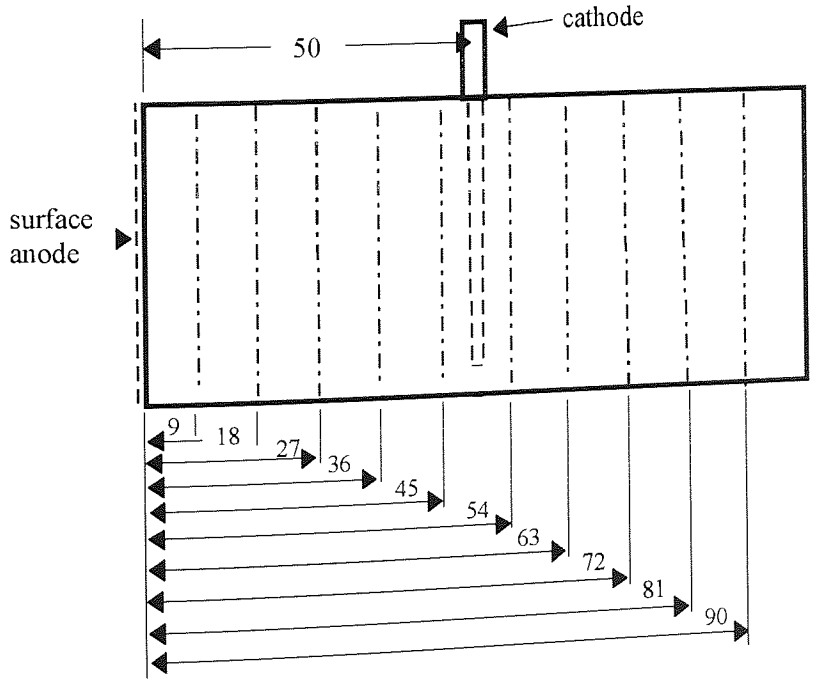

Figure 6.2: Arrangement of cutting of bulk-specimens

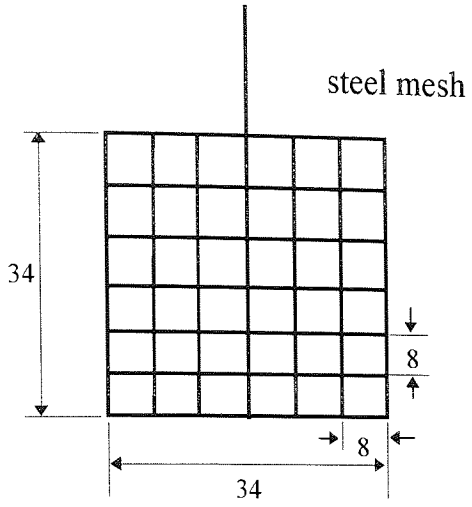

Figure 6.3: Steel Mesh (cathode)

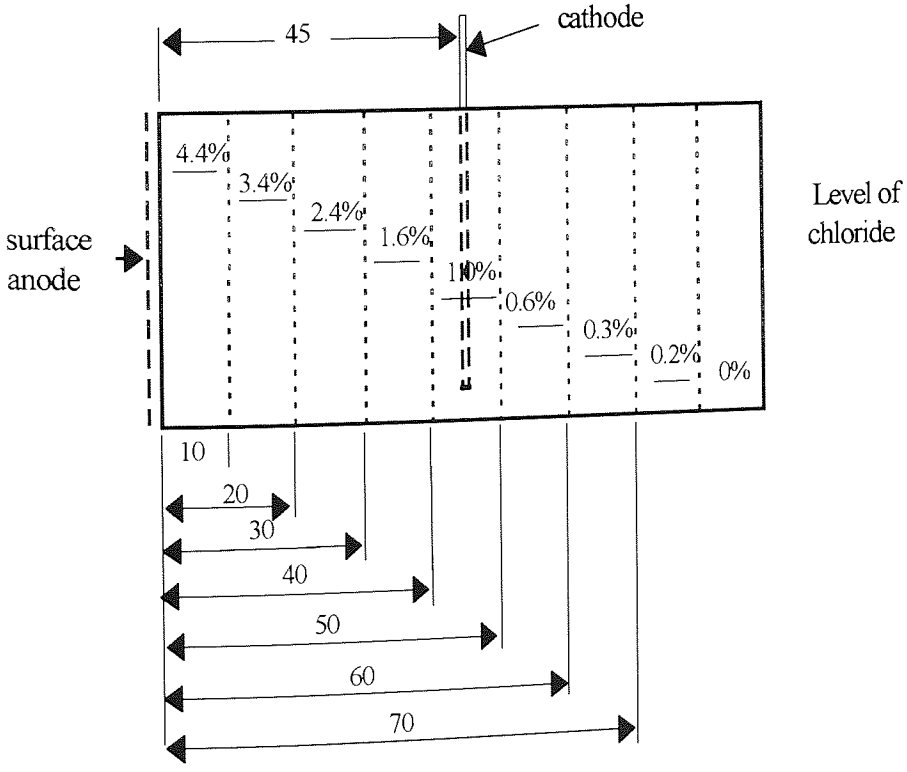

Figure 6.4: Arrangement of cutting of profile-mesh specimens

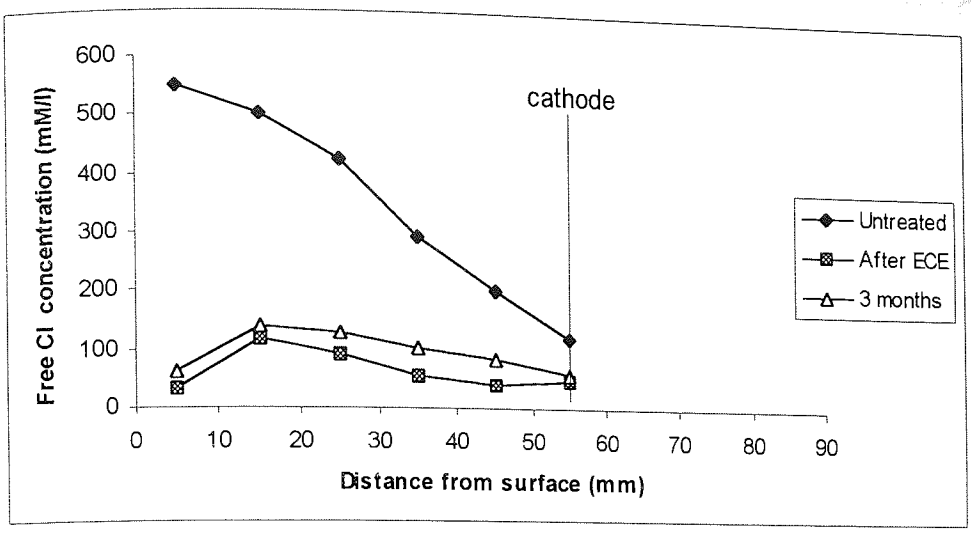

Figure 6.5: Free chloride concentration profile in pore solution of profile-plate specimens polarised at 5 A/m^2 for 8 weeks and after storage of 3 months

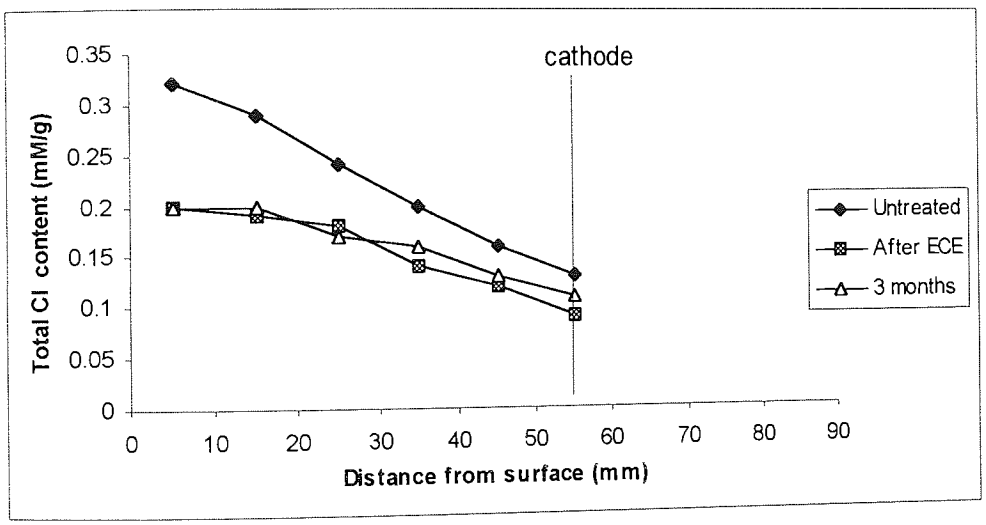

Figure 6.6: Total chloride content in hardened cement paste of profile-plate specimens polarised at 5 A/m^2 for 8 weeks and after storage of 3 months

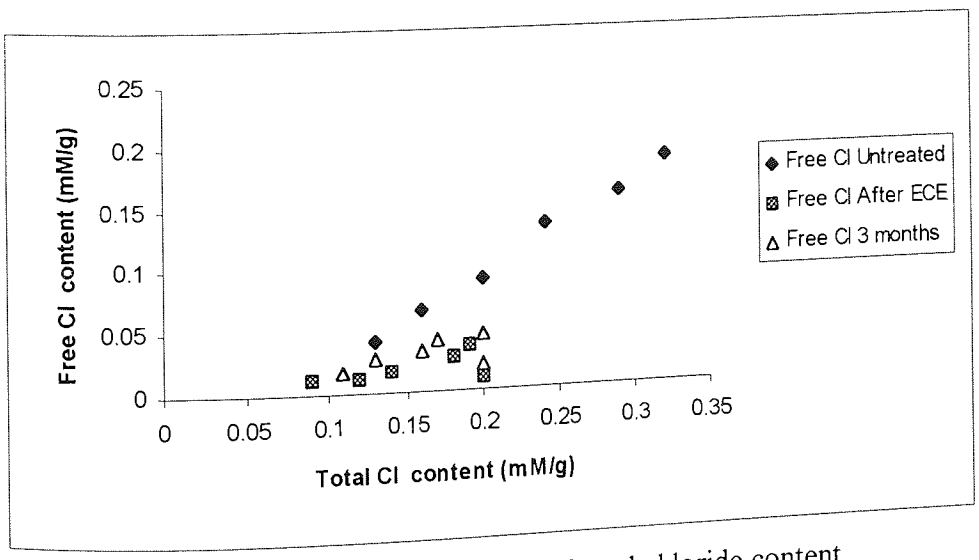

Figure 6.7: Free chloride content as a function of total chloride content

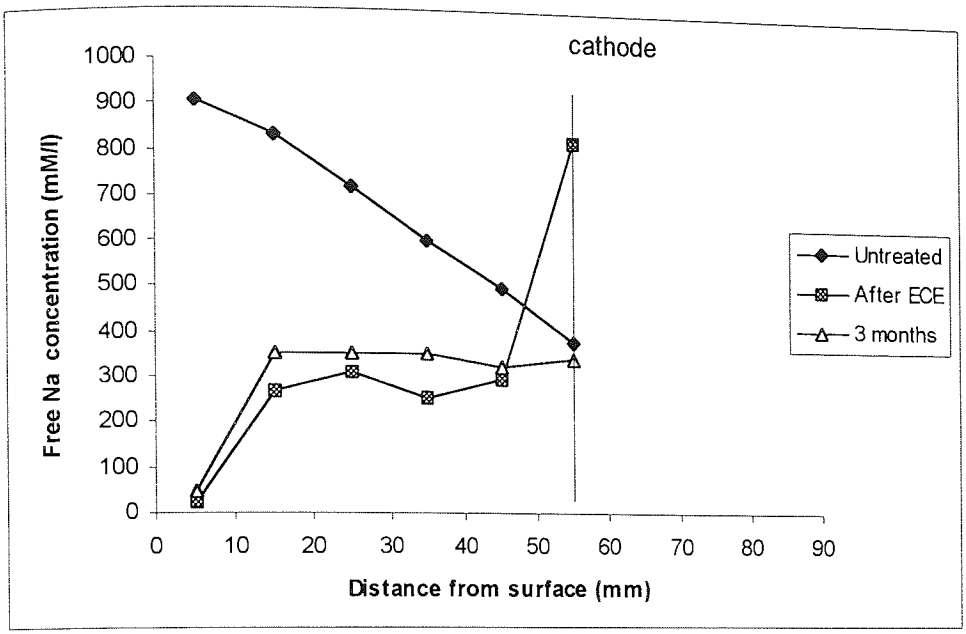

Figure 6.8: Free sodium concentration profile in pore solution of profile-plate specimens polarised at 5 A/m^2 for 8 weeks and after storage of 3 months

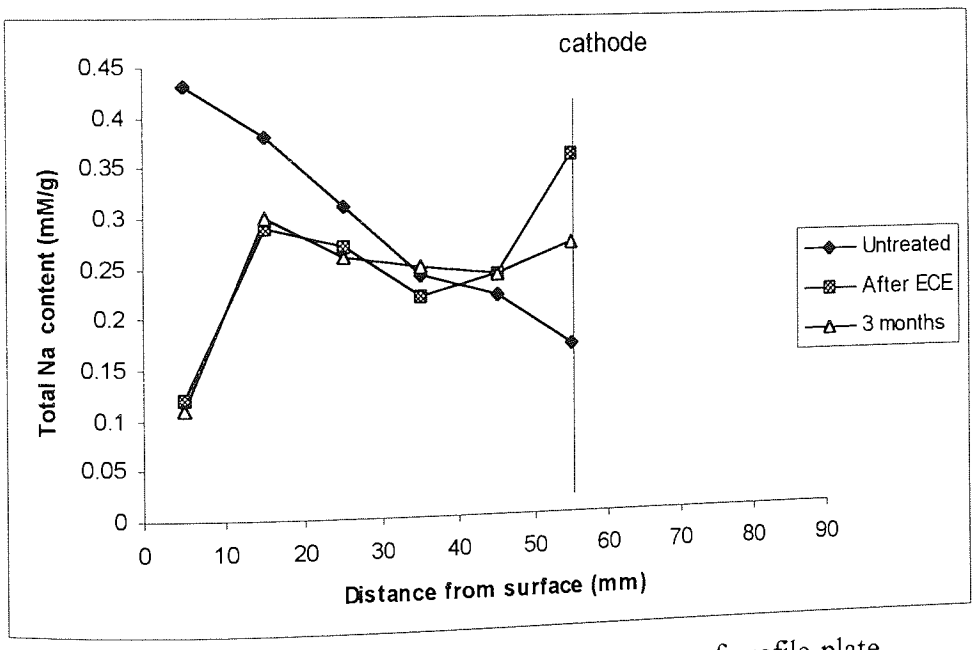

Figure 6.9: Total sodium content in hardened cement paste of profile-plate specimens polarised at 5 A/m^2 for 8 weeks and after storage of 3 months

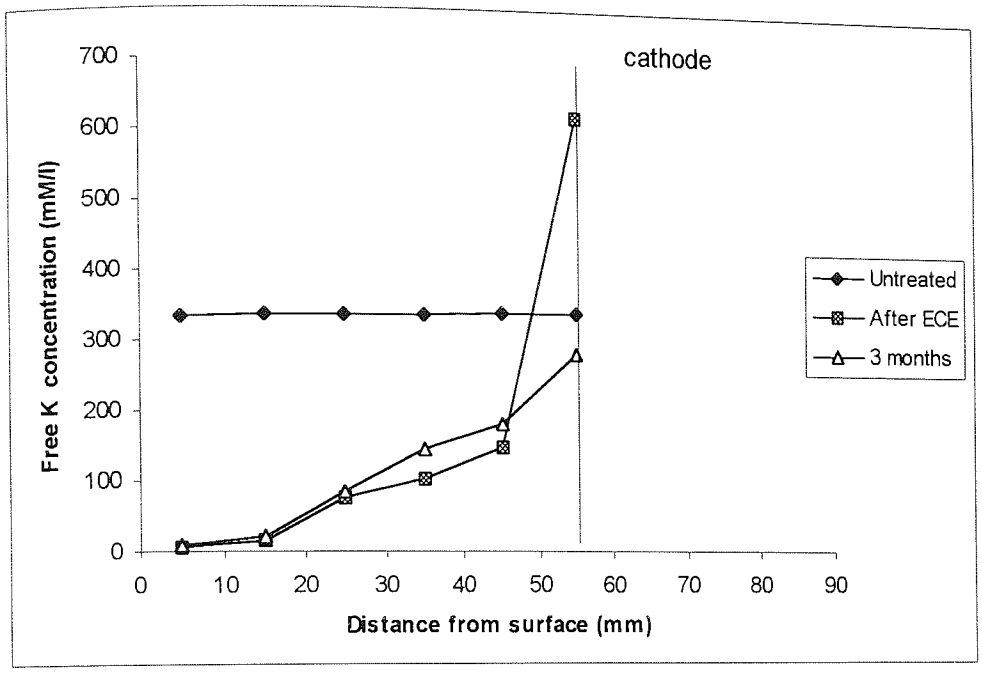

Figure 6.10: Free potassium concentration profile in pore solution of profile-plate specimens polarised at 5 A/m^2 for 8 weeks and after storage of 3 months

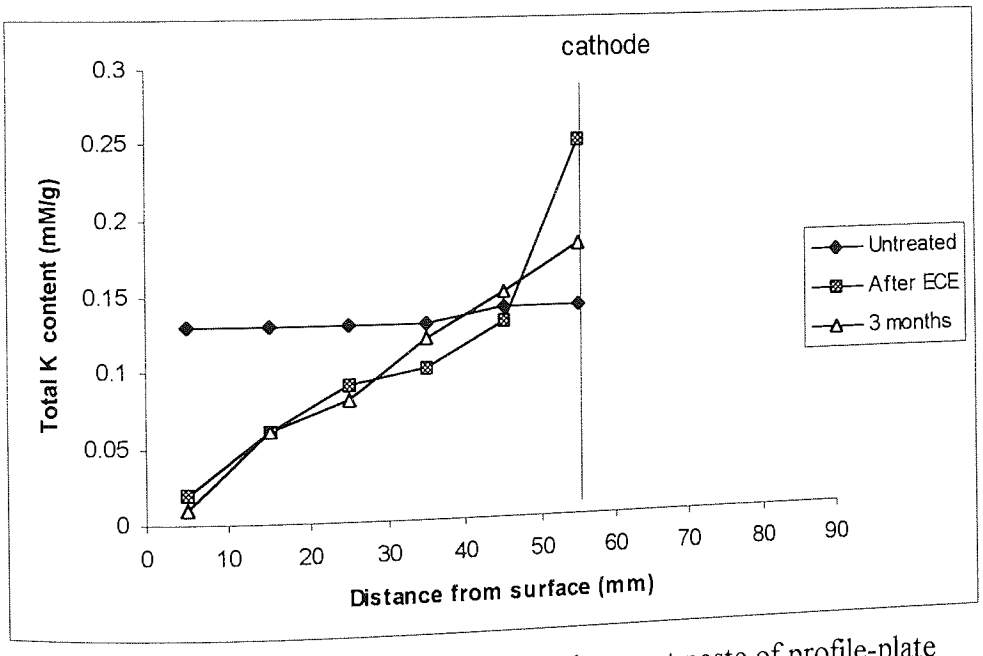

Figure 6.11: Total potassium content in hardened cement paste of profile-plate specimens polarised at 5 A/m^2 for 8 weeks and after storage of 3 months

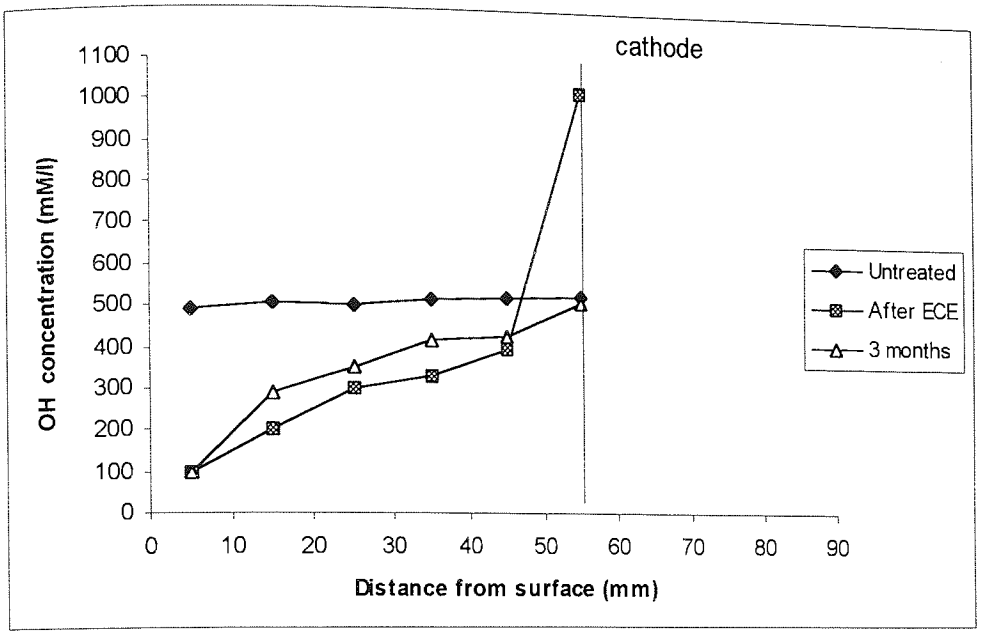

Figure 6.12: OH^- ionic concentration profile of profile-plate specimens polarised at $5A/m^2$ for 8 weeks and after storage of 3 months

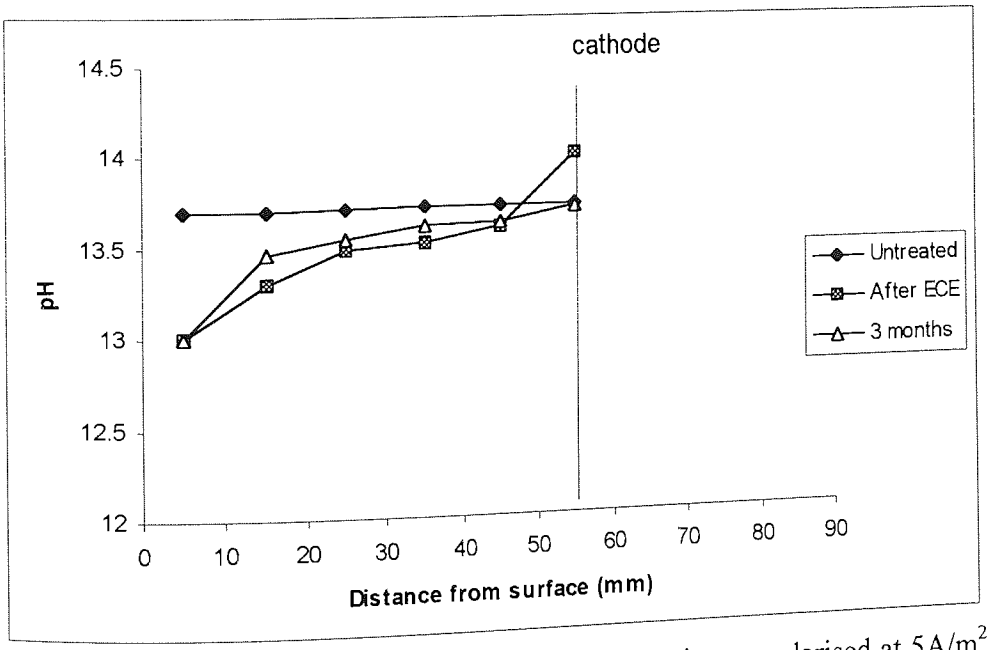

Figure 6.13: Pore solution pH profile of profile-plate specimens polarised at $5A/m^2$ for 8 weeks and after storage of 3 months

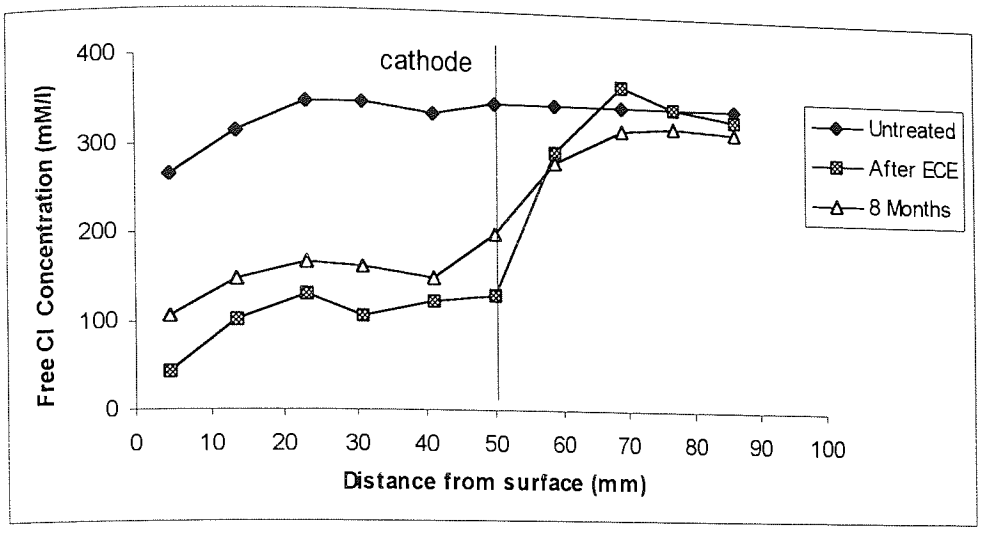

Figure 6.14: Free chloride concentration profile in pore solution of bulk-specimens polarised at 5 A/m^2 for 12 weeks and after storage of 8 months

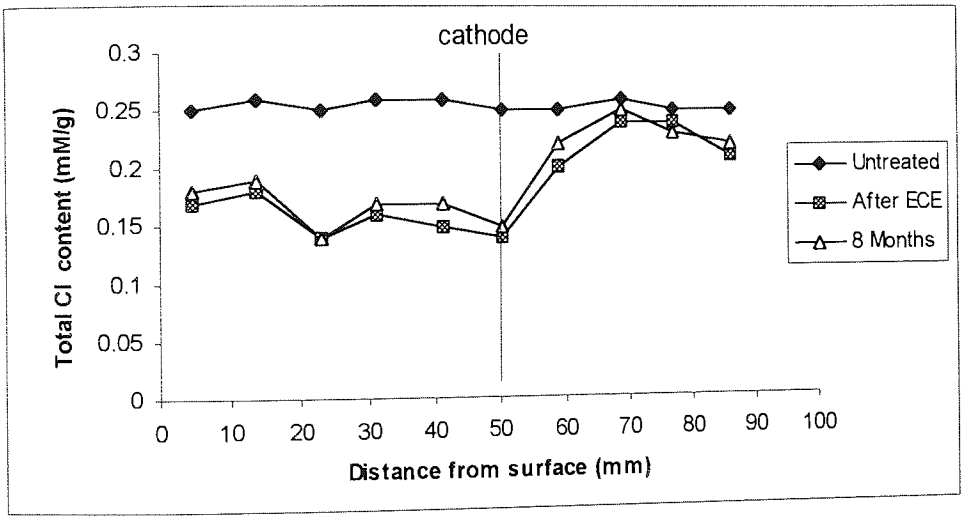

Figure 6.15: Total chloride content in hardened cement paste of bulk-specimens polarised at 5 A/m^2 for 12 weeks and after storage of 8 months

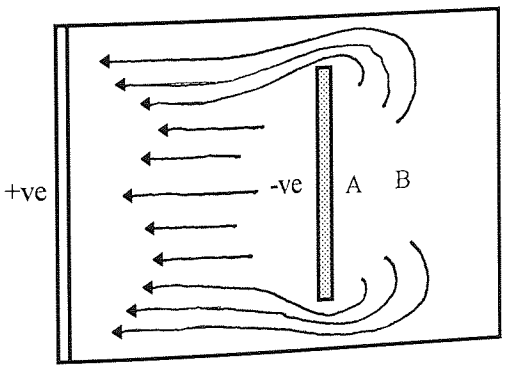

Figure 6.16: Streamlines field between cathode and anode at the surface

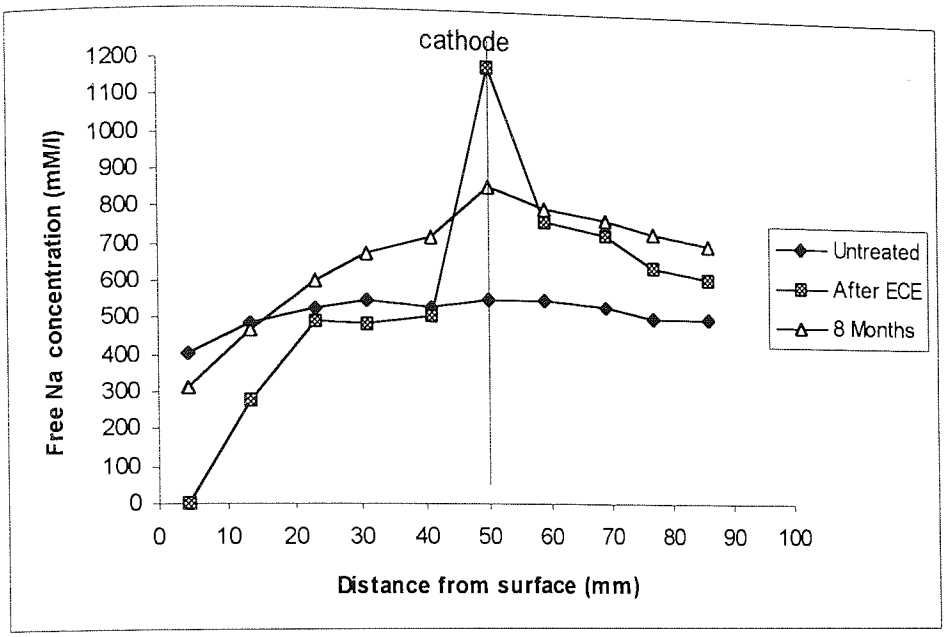

Figure 6.17: Free sodium concentration profile in pore solution of bulk-specimens polarised at $5A/m^2$ for 12 weeks and after storage of 8 months

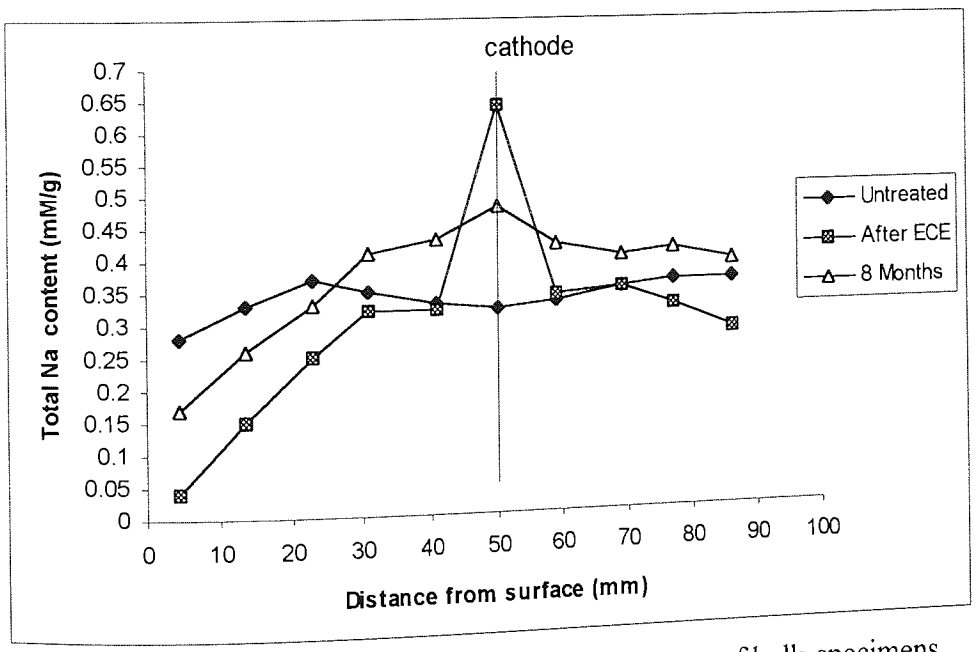

Figure 6.18: Total sodium content of hardened cement paste of bulk-specimens polarised at $5A/m^2$ for 12 weeks and after storage of 8 months

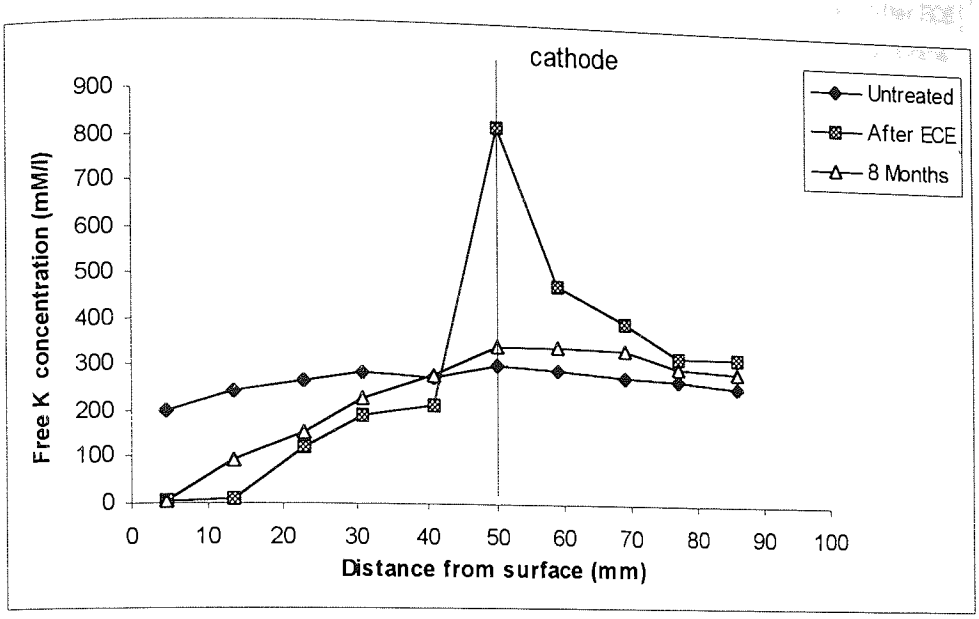

Figure 6.19: Free potassium concentration profile in pore solution of bulk-specimens polarised at $5A/m^2$ for 12 weeks and after storage of 8 months

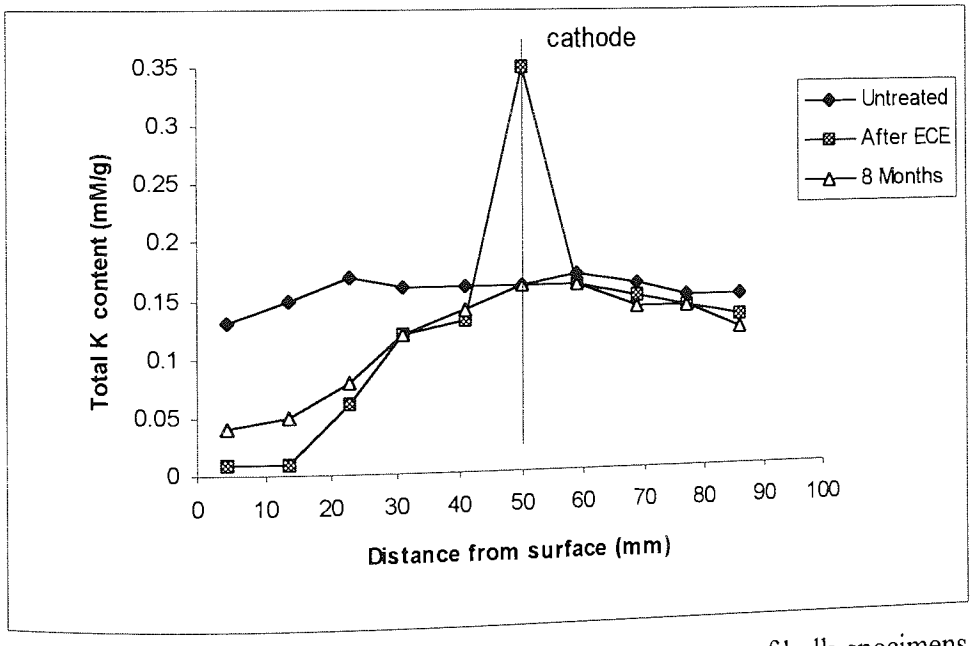

Figure 6.20: Total potassium content in hardened cement paste of bulk-specimens polarised at 5 A/m^2 for 12 weeks and after storage of 8 months

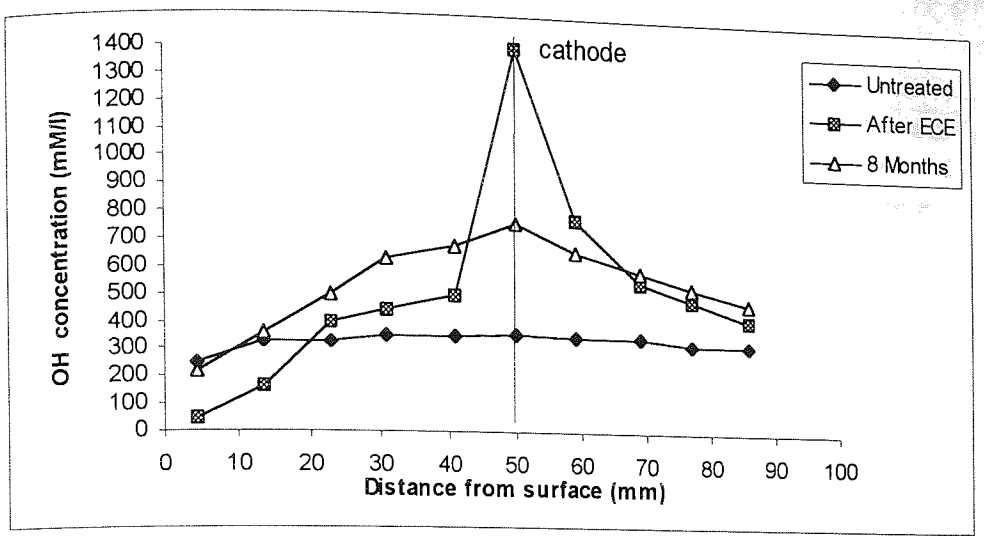

Figure 6.21: OH ionic concentration profile in pore solution of bulk-specimens polarised at 5A/m^2 for 12 weeks and after storage of 8 months

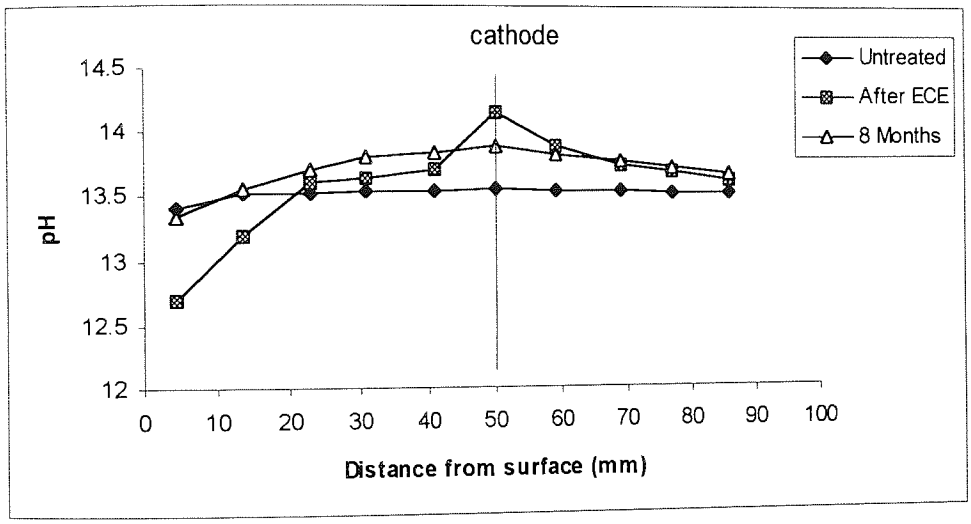

Figure 6.22: Pore solution pH profile of bulk-specimens polarised at 5A/m^2 for 12 weeks and after storage of 8 months

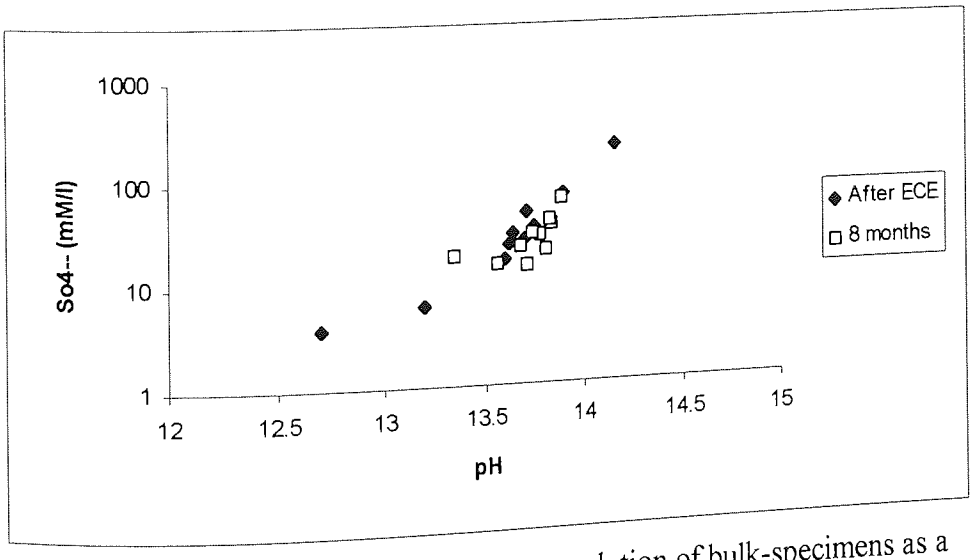

Figure 6.23: Sulphate ions concentration in pore solution of bulk-specimens as a function of pH

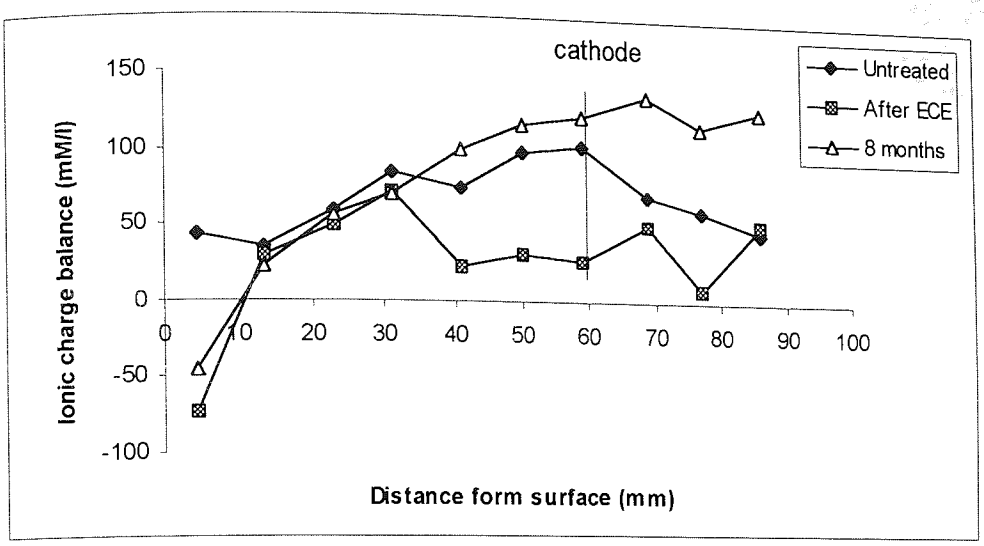

Figure 6.24: Ionic charge balance along depth of specimen

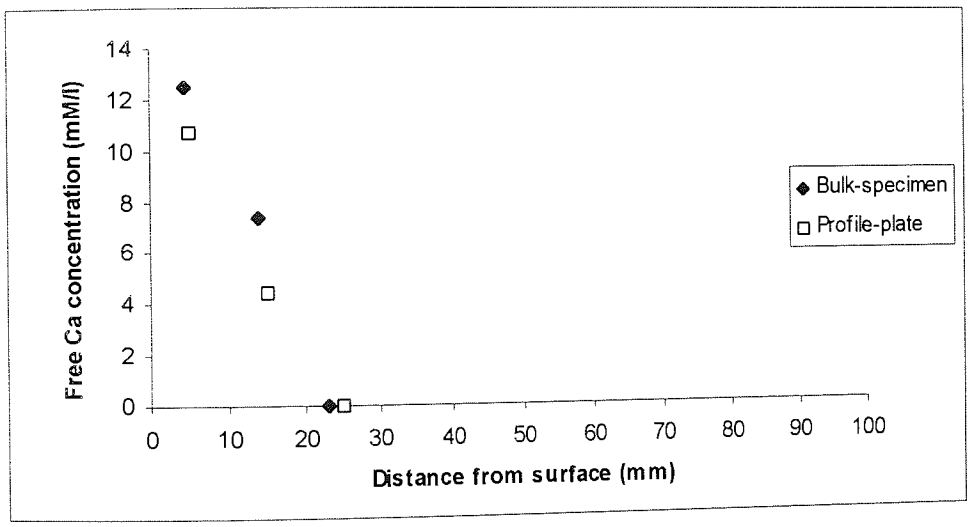

Figure 6.25: Free calcium concentration profile in pore solution of bulk-specimens and profile-plate specimens

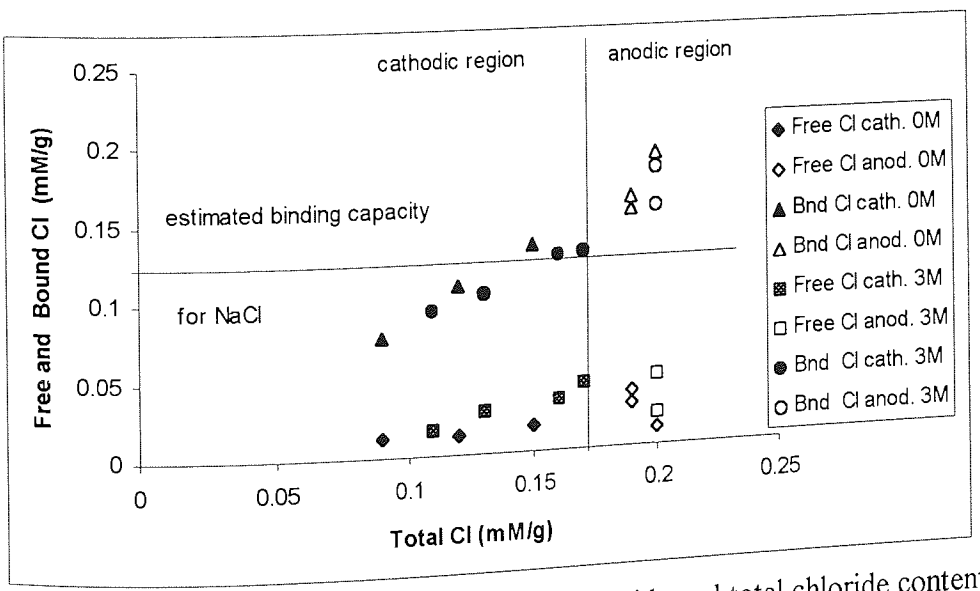

Figure 6.26: Relationship between free & bound chloride and total chloride content of profile-plate specimens

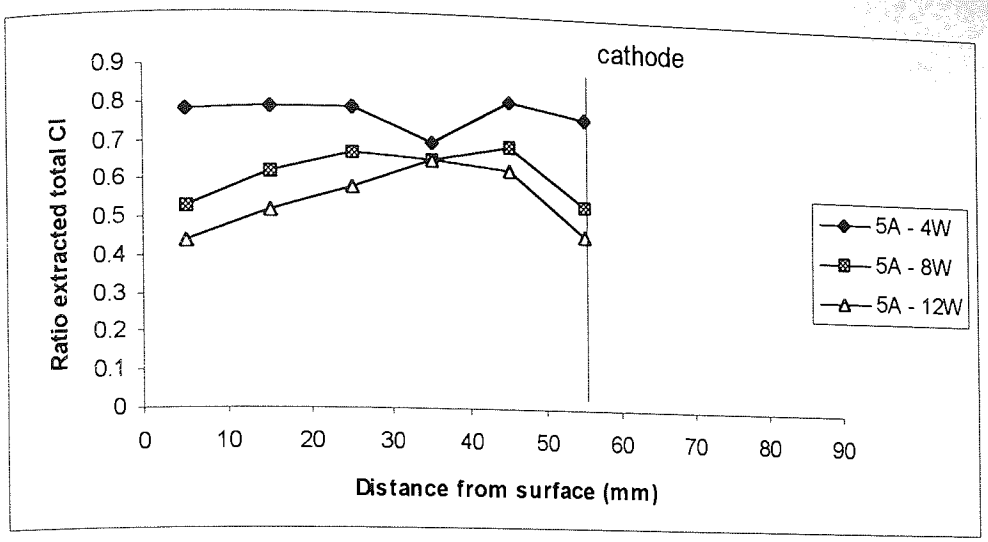

Figure 6.27: Ratio of extracted total chloride from the original profile

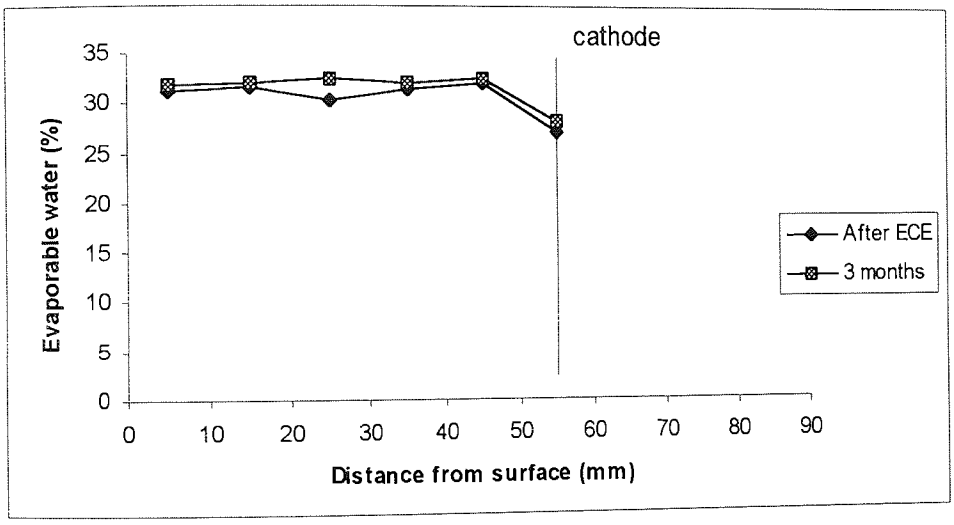

Figure 6.28: Evaporable water of profile-plate specimens polarised at 5 A/m^2 for 8 weeks and after storage of 3 months

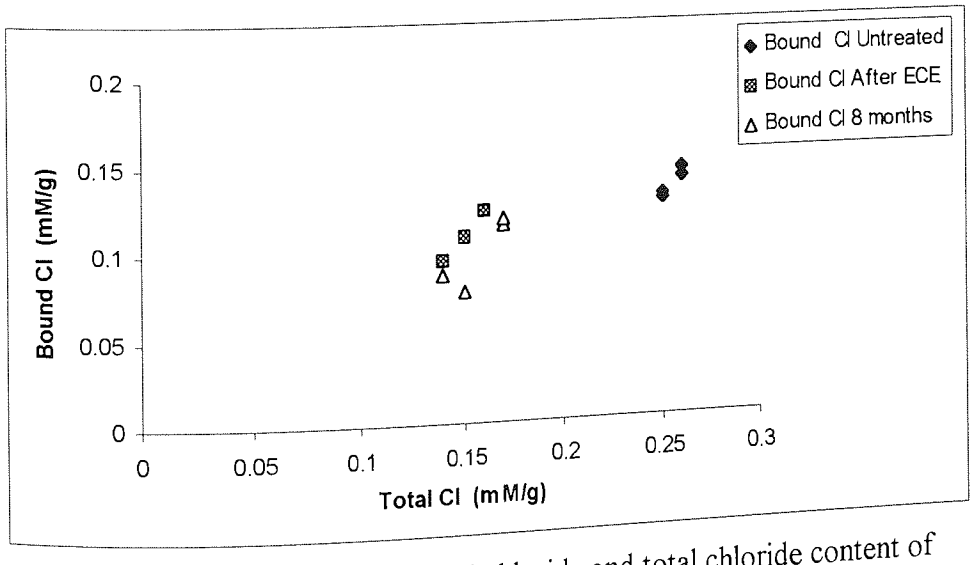

Figure 6.29: Relationship between bound chloride and total chloride content of bulk-specimens

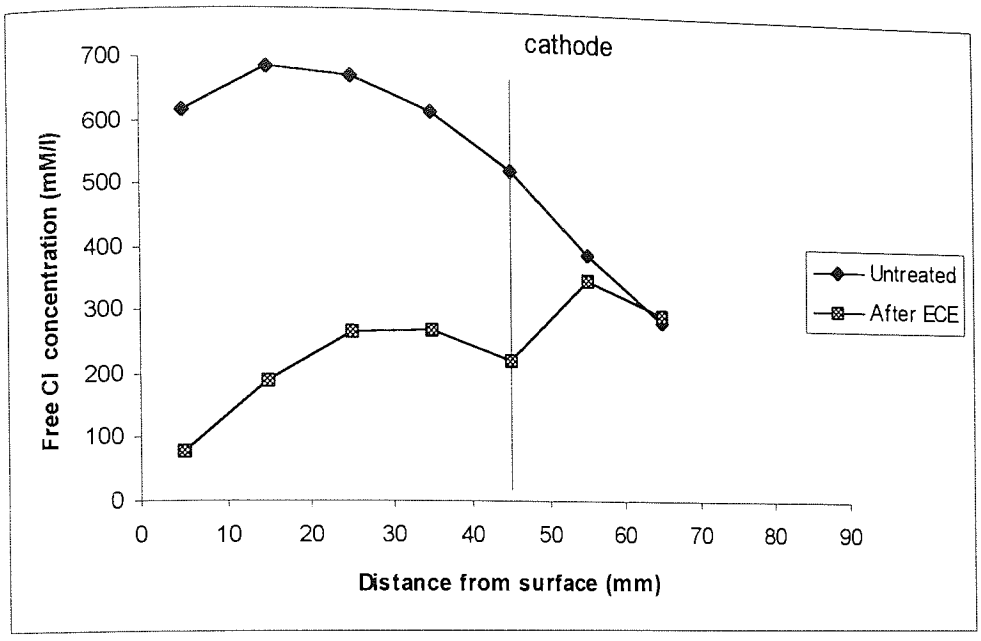

Figure 6.30: Free chloride concentration profile in pore solution of profile-mesh specimens polarised at 5 A/m^2 for 8 weeks

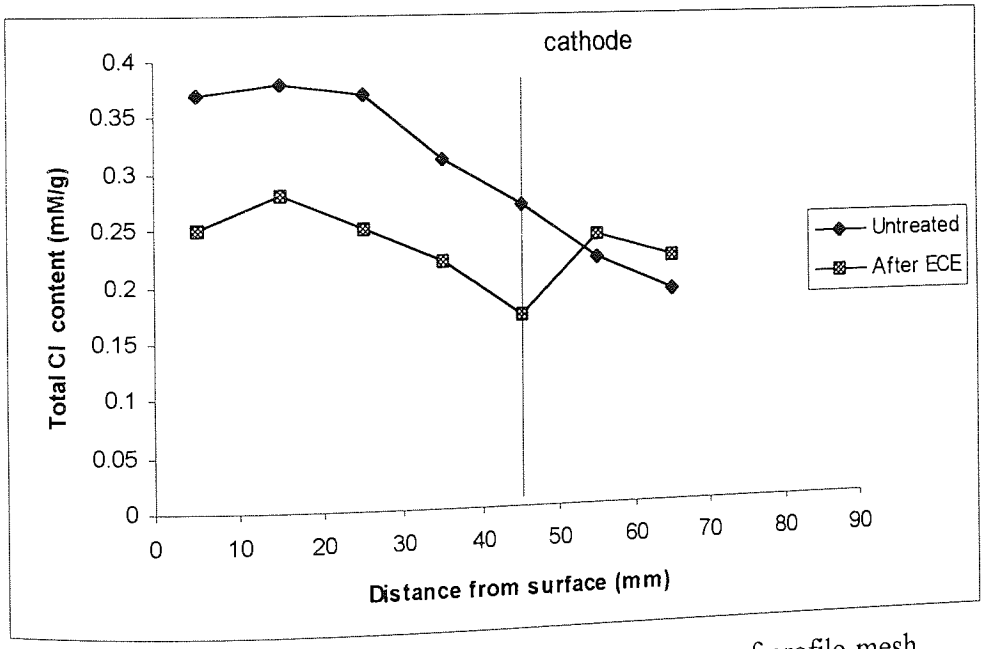

Figure 6.31: Total chloride content of hardened cement paste of profile-mesh specimens polarised at 5 A/m^2 for 8 weeks

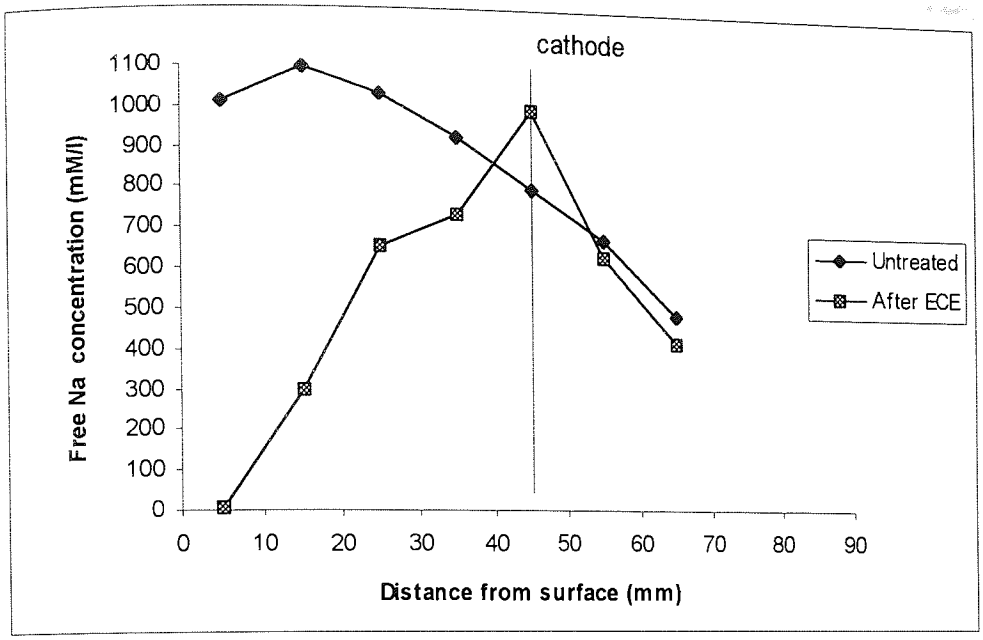

Figure 6.32: Free sodium concentration profile in pore solution of profile-mesh specimens polarised at 5 A/m^2 for 8 weeks

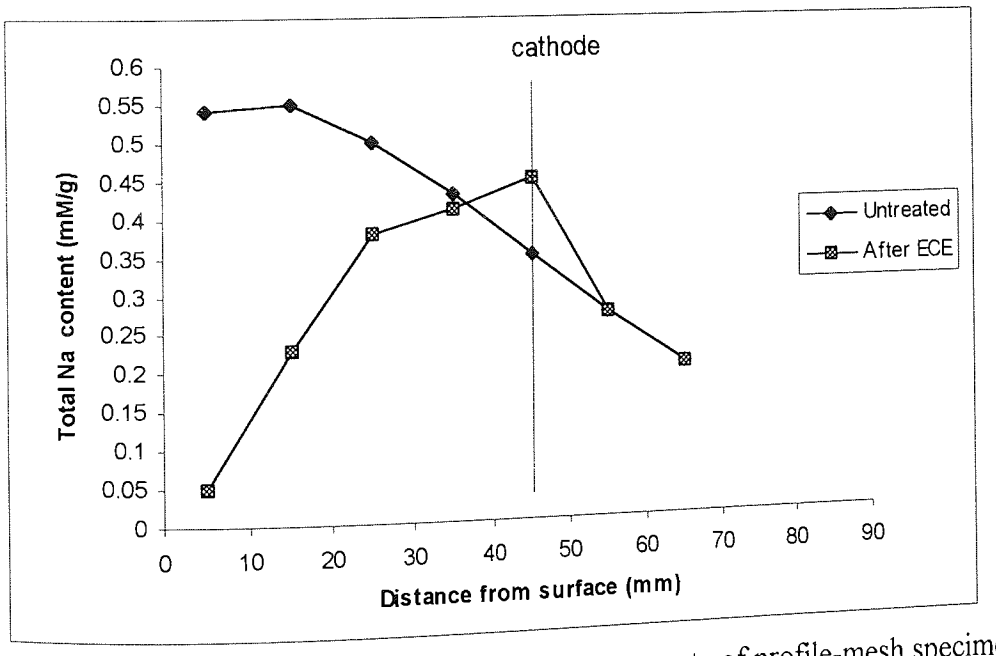

Figure 6.33: Total sodium content in hardened cement paste of profile-mesh specimens polarised at 5A/m^2 for 8 weeks

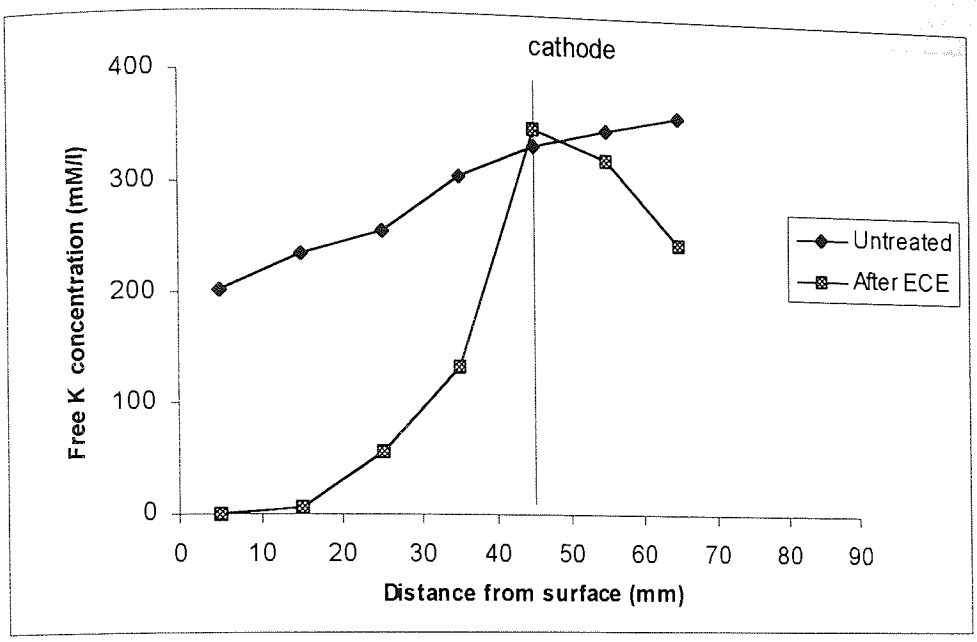

Figure 6.34: Free potassium concentration profile in pore solution of profile-mesh specimens polarised at 5 A/m^2 for 8 weeks

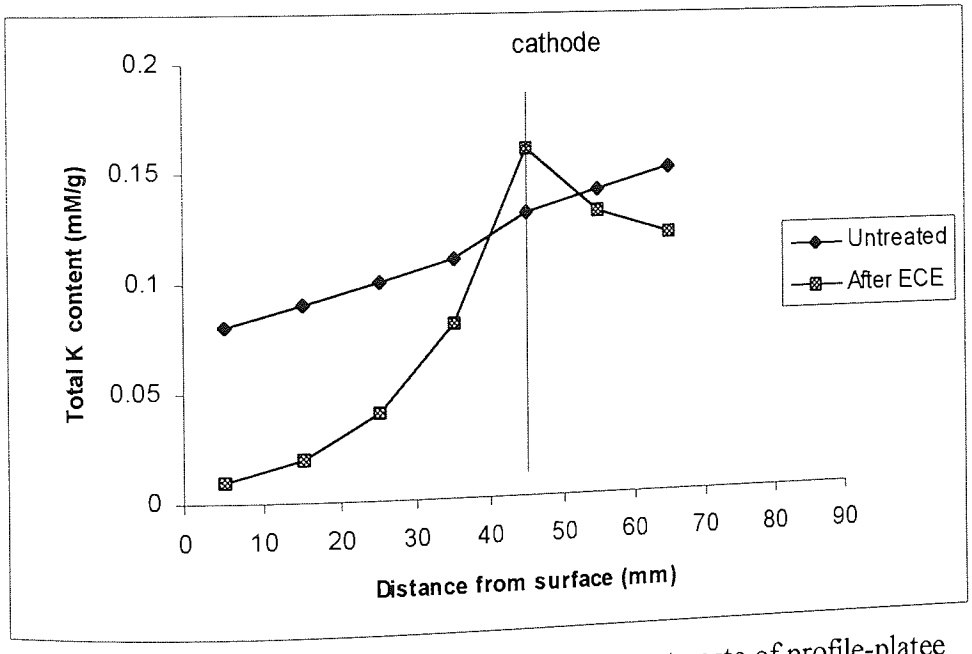

Figure 6.35: Total potassium content of hardened cement paste of profile-platee specimens polarised at 5 A/m^2 for 8 weeks

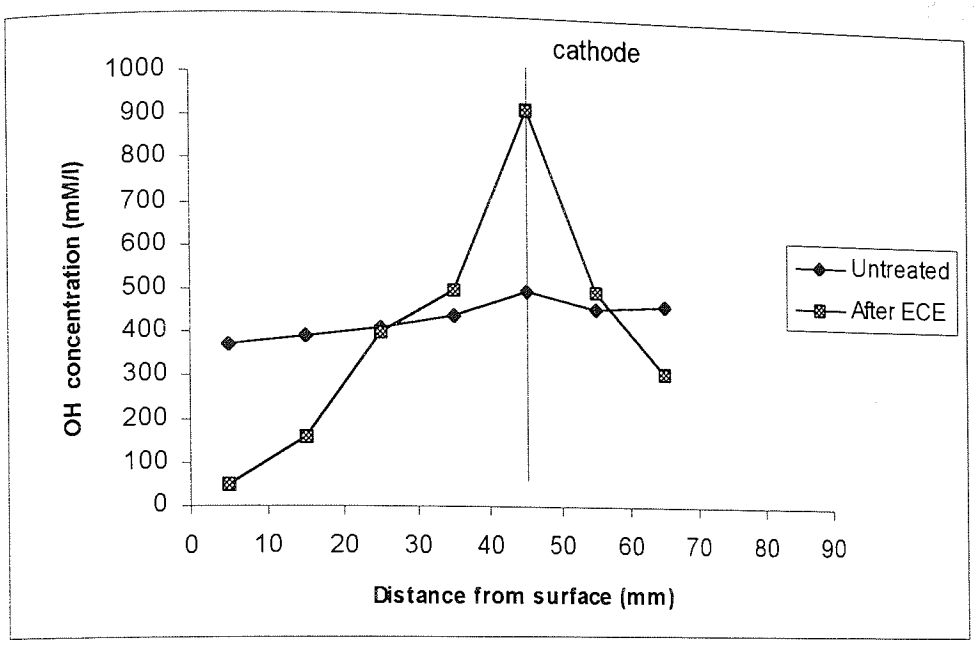

Figure 6.36: OH^- ionic concentration profile in pore solution of profile-mesh specimens polarised at 5 A/m^2 for 8 weeks

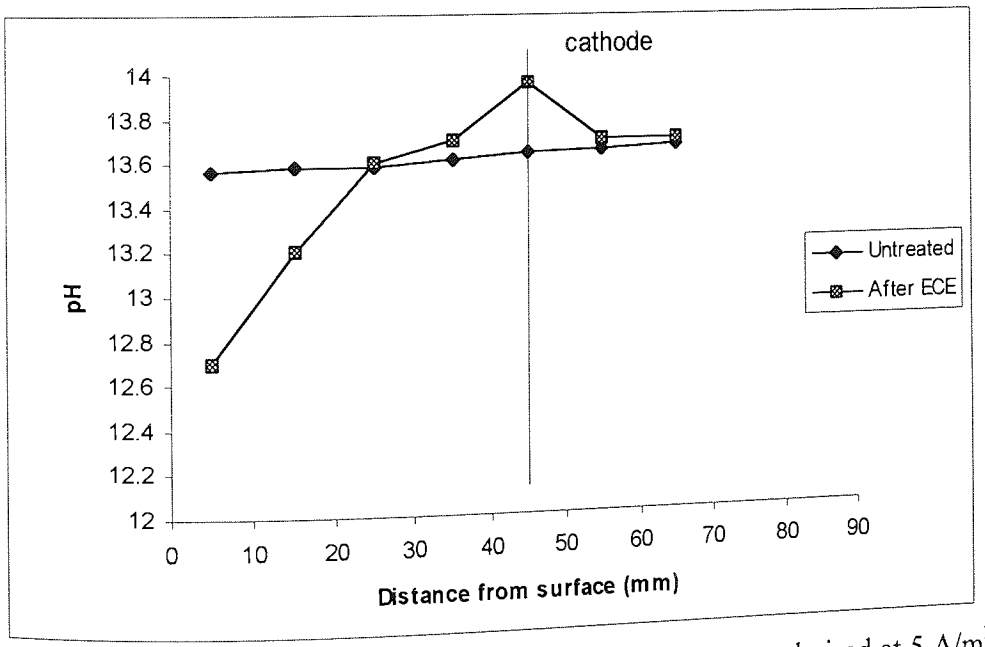

Figure 6.37: Pore solution pH profile of profile-mesh specimens polarised at 5 A/m^2 for 8 weeks

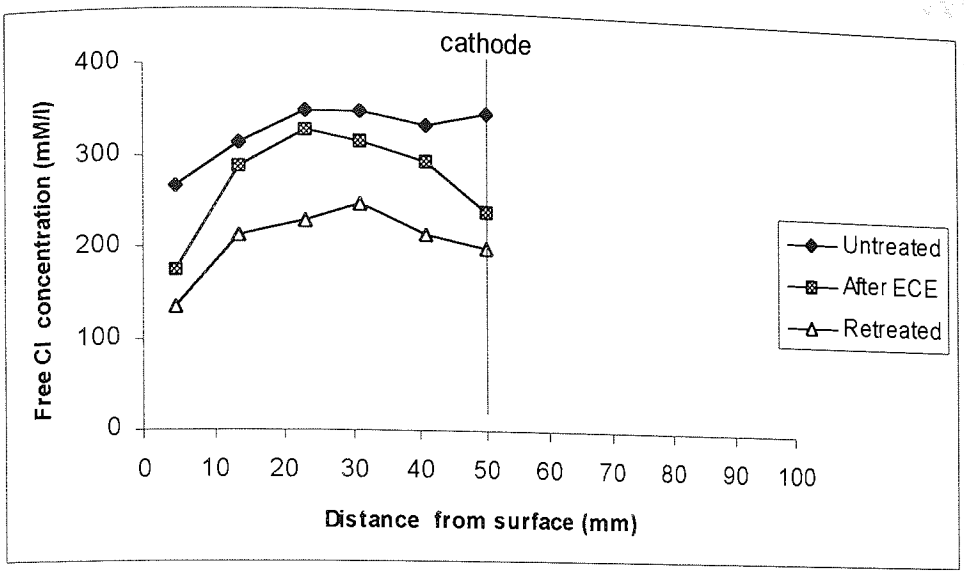

Figure 6.38: Free chloride concentration profile in pore solution of bulk-specimens polarised at 1A/m^2 for 12 weeks and retreated for 8 weeks after 9 months

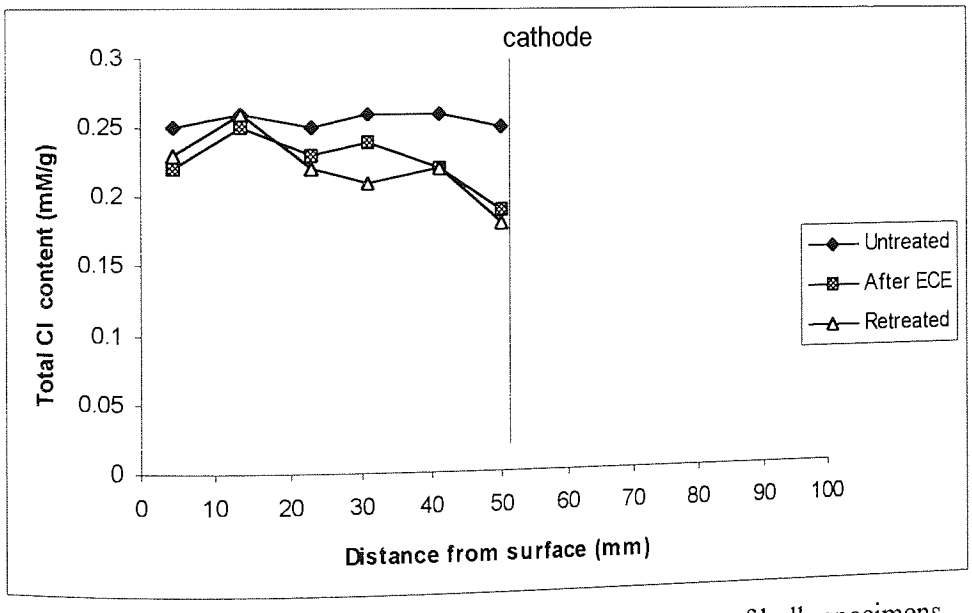

Figure 6.39: Total chloride content in hardened cement paste of bulk-specimens polarised at 1A/m^2 for 12 weeks and retreated for 8 weeks after 9 months

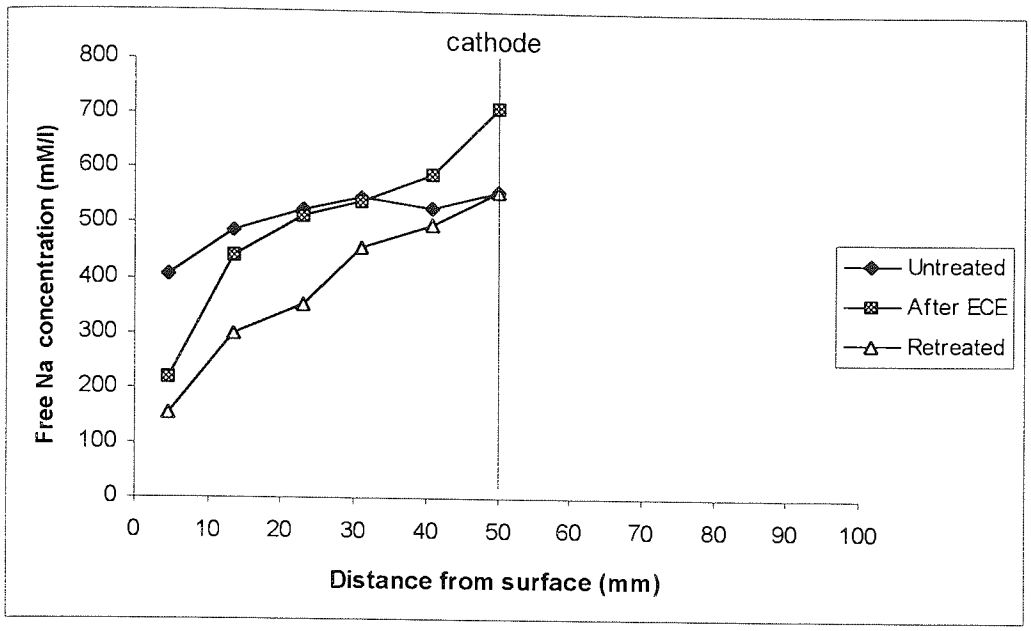

Figure 6.40: Free sodium concentration profile in pore solution of bulk-specimens polarised at 1 A/m^2 for 12 weeks and retreated for 8 weeks after 9 months

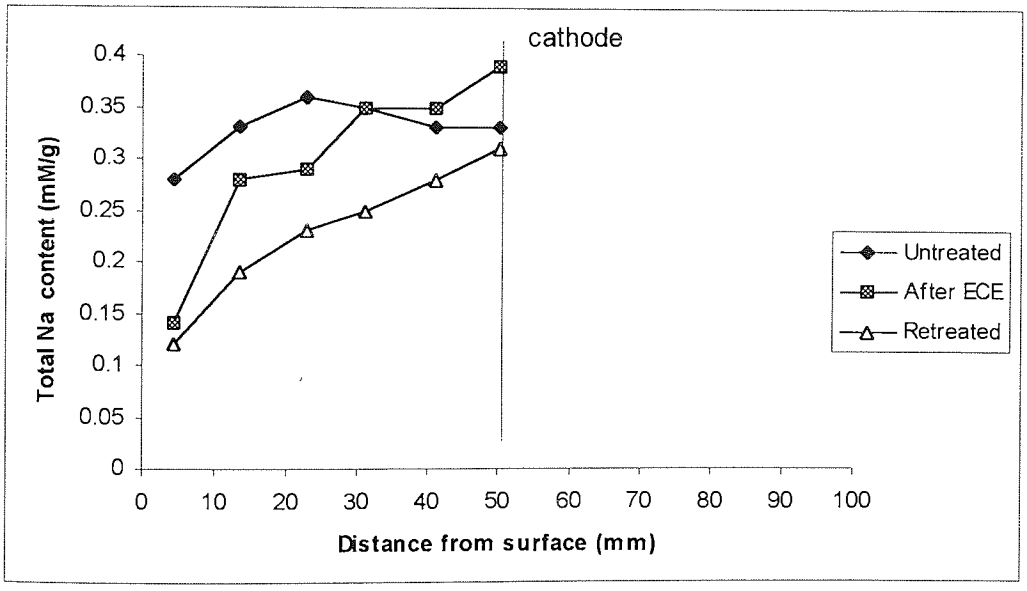

Figure 6.41: Total sodium content of bulk-specimens polarised at 1A/m^2 for 12 weeks and retreated for 8 weeks after 9 months

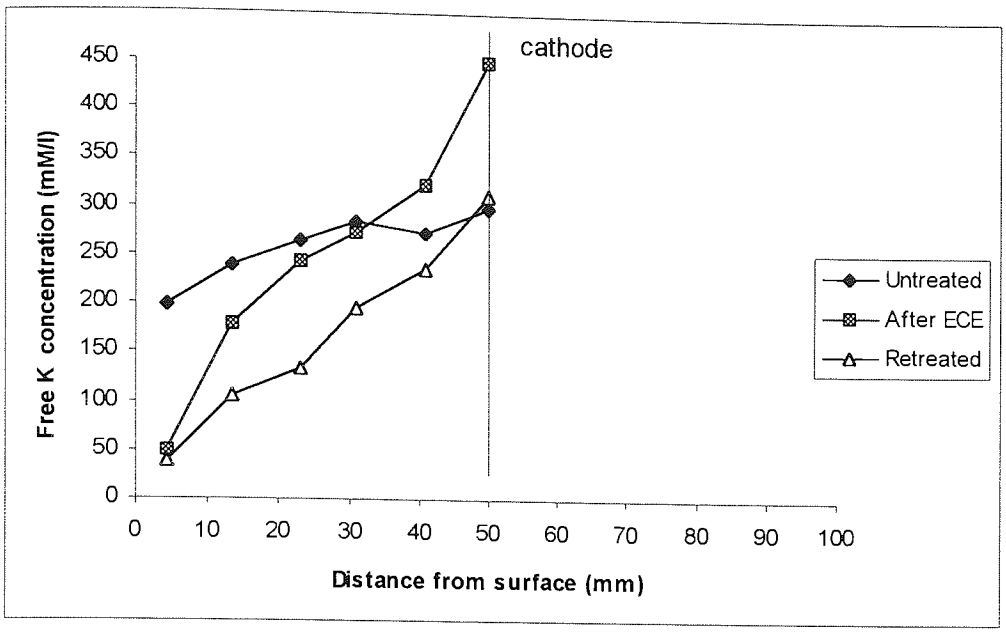

Figure 6.42: Free potassium concentration profile in pore solution of bulk-specimens polarised at 1A/m^2 for 12 weeks and retreated for 8 weeks after 9 months

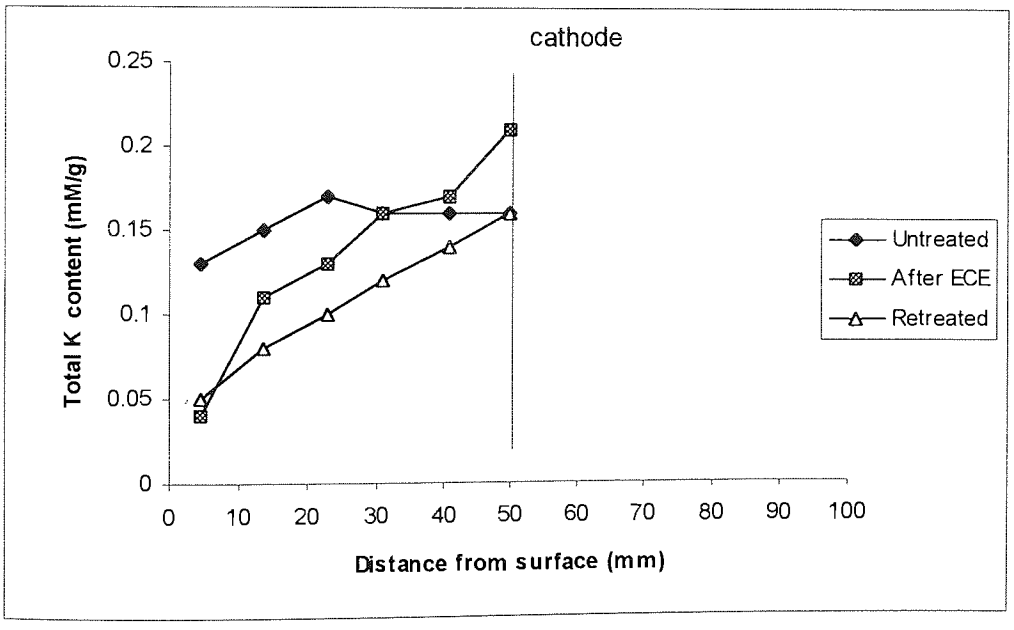

Figure 6.43: Total potassium content in hardened cement paste of bulk-specimens polarised at 1A/m^2 for 12 weeks and retreated for 8 weeks after 9 months

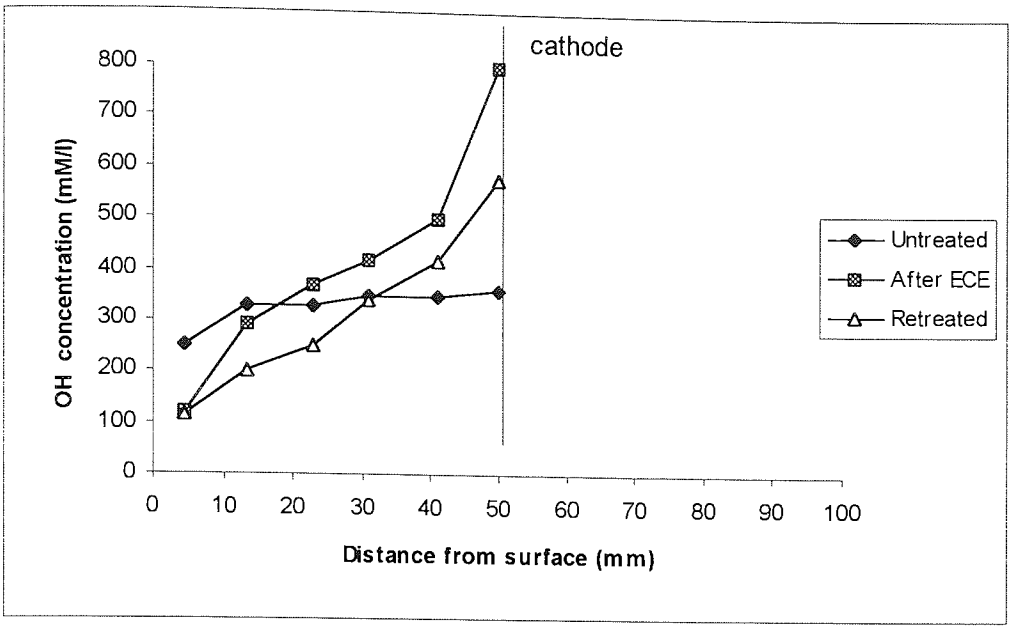

Figure 6.44: OH^- ionic concentration profile of Bulk-specimens polarised at 1 A/m^2 for 12 weeks and retreated for 8 weeks after 9 months

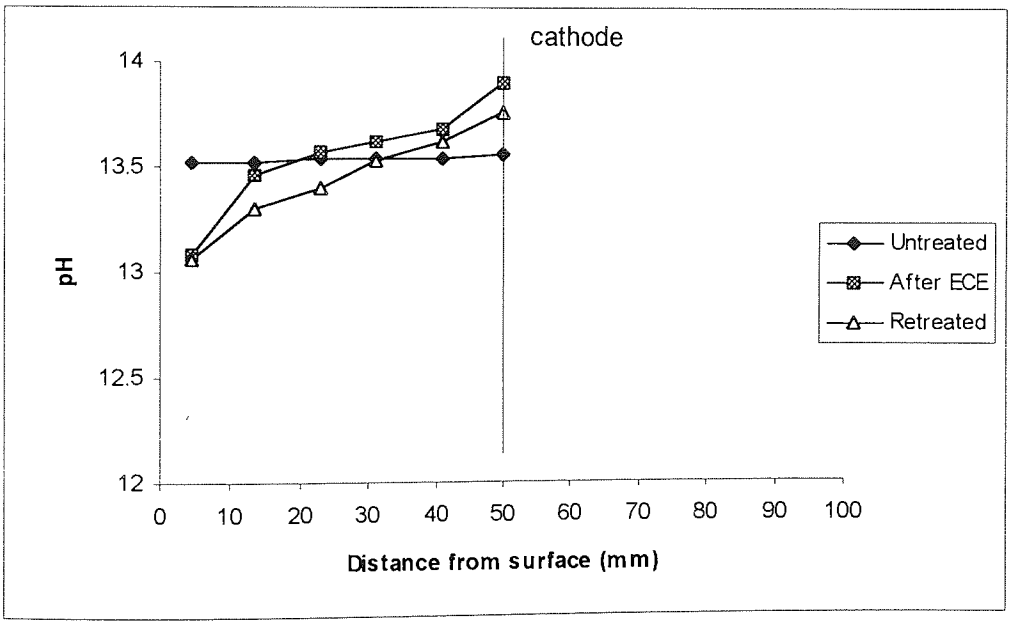

Figure 6.45: Pore solution pH profile of Bulk-specimens polarised at 1 A/m^2 for 12 weeks and retreated for 8 weeks after 9 months

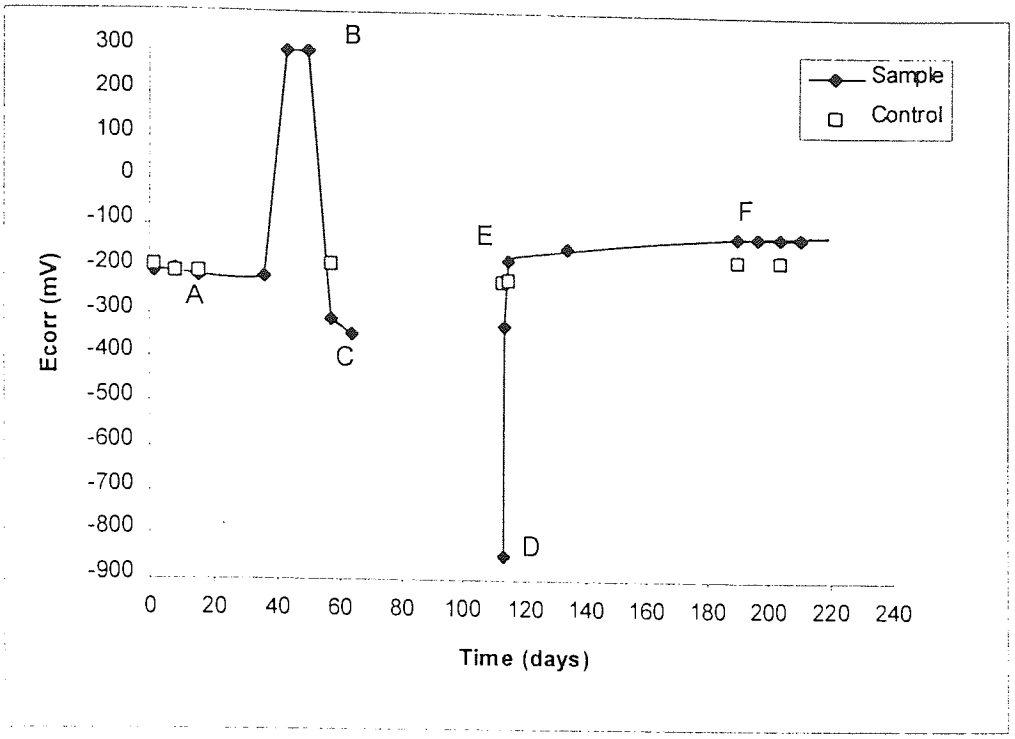

Figure 6.46: Change in corrosion potential before and after ECE

A = Before current is applied
B = Current applied potentiostatically +300 mV for 2 weeks
C = After current is switch off, before ECE
D = After ECE
E = Three days after ECE
F = Potential become more positive

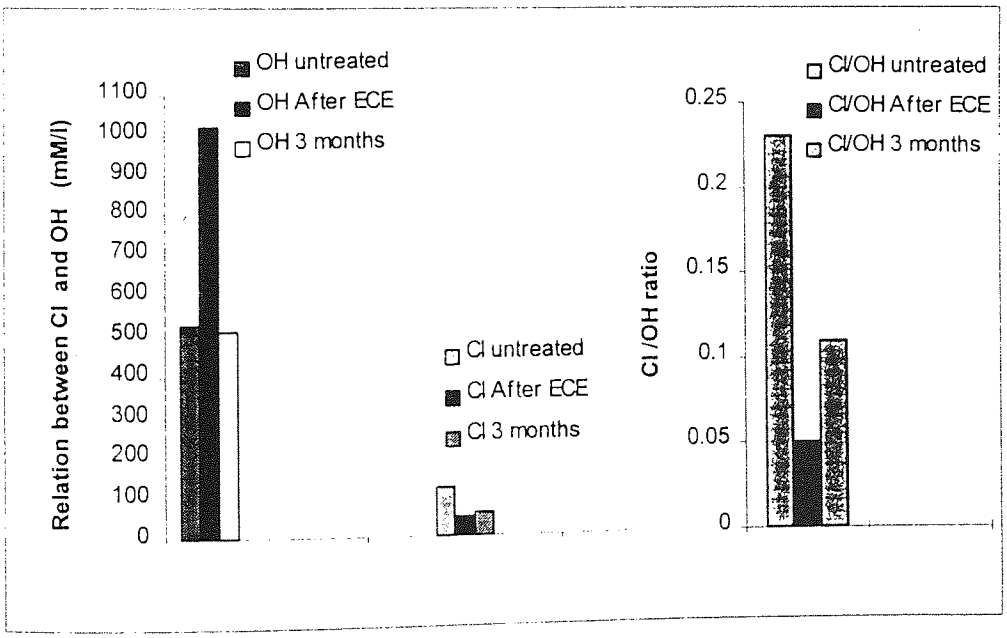

Figure 6.47: The change in chloride and hydroxyl ionic concentration around the cathode with time after ECE in a profile-plate specimens

CHAPTER 7

GENERAL CONCLUSIONS AND RECOMMENDATIONS FOR FURTHER WORK

This chapter summarizes the major findings in relation to the original aims of the investigation and identifies areas where further study is needed.

7.1 GENERAL CONCLUSIONS

The present work has shown that ECE is capable of removing chloride quite effectively. Equilibrium between free and bound chloride remains throughout the process allowing bound chlorides to be released and extracted. The efficiency of removal appears to be related to the transference number so, as the concentration of chloride is reduced, the proportion of chloride removed by a given quantity of charge diminishes. The removal of chloride ions from OPC specimens is more effective compared to that from blended cements.

The concentration of hydroxyl and alkali ions increased around the cathode during ECE. Sulphate ions were released from the solid phases as a result of the increased pH within the cement matrix. There was, however, no sign of significant change in the ettringite distribution within specimens during ECE treatment, though the investigation for this effect was somewhat limited.

The average microhardness measurements showed a slight apparent softening of the cement matrix close to the cathode after ECE, but this could not be confirmed statistically due to scatter in the results. The porosity of the cements around the cathode as determined from MIP measurements was found to increase slightly after the ECE treatment. However, these changes were very small and were likely to cause no significant effect to structures treated by ECE. The above small changes observed in OPC were not found in blended cements.

Remigration of chloride, especially for specimens where the original chloride level was significant at depths beyond the steel cathode, was observed to occur quite rapidly in this research. The pH of the treated specimens remained high for long periods. This high pH environment enhances the passivity of the steel and is therefore expected to delay the onset of corrosion re activation.

ECE was capable of removing some of the available chloride within the cover zone and from a small distance behind the reinforcement. The process is unlikely, however, to be successful in removing chlorides that have penetrated the structure significantly beyond the steel reinforcement or be present as internal chloride contaminants.

7.2 RECOMMENDATIONS FOR FURTHER WORK

The effect of cover thickness, quality of concrete and spacing of the reinforcement on the process of ECE needs to be assessed. These conditions, if studied further in the field, will clarify the capability of ECE as a rehabilitation option for heavily chloride-contaminated reinforced concrete.

As was suggested in chapter 6, removing chloride which was initially present in the form of $CaCl_2$ by ECE may be more difficult than NaCl because cements bind more $CaCl_2$ compared to NaCl. Since $CaCl_2$ has been used in some of the old structures as an accelerator, it would be of interest to look at the capability of the ECE system in removing this type of chloride and whether a similar equilibrium between free and bound chloride is maintained during treatment.

Preliminary work carried out in chapter 4 to look at the capability of ECE in removing chloride in blended cements was not very comprehensive. It is, therefore, suggested to look into this area in more detail by studying the efficiency of removal as well as side effects that might have occurred as a result of application of ECE to the structures made from these cements and possible remigration of chloride around the steel cathode. Work on SRPC cements is also suggested.

Further work is also needed to define the nature and the stability of the passive film which is formed around the reinforcement after the ECE treatment and also after storage of the specimens for a period of time. It would be useful to know the thickness and quality of the passive film as a result of the ECE treatment, for example, so that a better understanding of its passivating properties could be achieved.

Computer modeling is another promising technique which can be applied for the better understanding of ionic migration in concrete under the influence of current. Several models have been developed so far by Bennett and Turk, [1994], Andrade et al., [1995], Yu and Page, [1996] and Li and Page, [1998] which were moderately successful in modeling ionic redistribution and the removal of chloride. Among the problems encountered, however, in the work at Aston was that the concentration of OH^- ions was found in the main to be higher than concentrations determined experimentally. Modeling the remigration of chloride for the ECE process has so far only been carried out in a over-simplified manner by Stoop & Polder [1996]. However, this model needs to be refined by taking OH^- ions and alkali cations into consideration. Apart from the requirement of the charge balance in the pore solution, OH^- ions also play a major role in the ECE process by enhancing the pH around the steel cathode.

Long term studies on the durability of concrete structures after undergoing ECE treatment are also needed particularly with respect to the ability of surface coatings which may be applied after the treatment, to prevent further chloride ingress. Monitoring the Cl^-/OH^- ratio around the reinforcement as well as the potential of the steel will enable its corrosion activity to be better predicted thus leading to improved understanding of the long term effectiveness of the treatment.

REFERENCES

ALI, M.G. and RASHEEDUZZAFAR [1993], 'Cathodic Protection Current Accelerates Alkali Silica Reaction', ACI Material Journal, 90, 3, May-June.

ALI, M.G. and RASHEEDUZZAFAR, [1991], 'Bonding Problems with the Cathodic Protection of Steel in Reinforced Concrete Structures-Part 2', Corrosion Prevention & Control, 38, 6, pp 155-157.

ALVAREZ and GALVELE [1984], 'The Mechanism of Pitting of High Purity iron in 1 N NaCl solutions' Corrosion Science, Vol. 24, No.1, pp27-48.

AMERICAN CONCRETE INSTITUTE [1985], 'Corrosion of Metals in Concrete', Report no. ACI 222R-85, Detroit, USA.

ANDRADE, C., DIEZ, J.M., ALAMAN, A., and ALONSO, C. [1995], 'Mathematical Modelling of Electrochemical Chloride Extraction from Concrete', Cement and Concrete Research, Vol. 25, No. 4, pp727-740.

ANDRADE, C., SANJUAN, M..A., RECUERO, A. and RIO, O. [1994], 'Calculation of Chloride diffusivity in Concrete from Migration Experiments, in Non-Steady State conditions', Cement and Concrete Research, Vol. 24, No. 7, pp 1214-1228.

ARMSTRONG, K., GRANTHAM, M.G., Mc FARLAND, B. [1996], 'The Trial Repair of Victoria Pier St. Helier, Jersey using Electrochemical Desalination' Proc. 4th. International Symposium on Corrosion of Reinforcement in Concrete Construction, Eds C.L. PAGE, P.B. BAMFORTH and J.W. FIGG, SCI / Royal Society of Chemistry, Chambridge, ISBN 0-85404-731-X.

ARUP, H. [1983], 'The Mechanism of the Protection of Steel in Concrete Construction, ed A.P. Crane, Ellis Horwood, Chiester, pp151-158.

ARYA, C. and NEWMAN, J.B. [1990], 'Problem of Predicting risk of Corrosion of Steel in Chloride Contaminated Concrete', Proceeding of Inst. of Civil Engineers, Part 1- Design and Construction Vol. 88, pp 875-888.

ARYA, C., BUENFELD, N.R., AND NEWMAN, J.B. [1990], 'Factors Influencing Chloride Binding in Concrete', Cement and Concrete Research, Vol 20, No. 2, pp 291-300.

ARYA, C., SAID-SHAWQI and VASSIE, P.R.W. [1996], 'Factors Influencing Electrochemical Removal of Chloride from Concrete', Cement and Concrete Research, Vol. 26, No. 6, pp 851-860.

BAMFORTH, P.B. [1996], 'Predicting the Risk of Reinforcement Corrosion in Marine Structures, 3rd. CANMET/ACI International Conference on Performance of Concrete in Marine Environment, Aug. 4-9, pp 207-234.

BARNEYBACK, R.S., and DIAMOND, S. [1981], 'Expression and Analysis of Pore Fluid from hardened Cement Pastes and Morta', Cement and Concrete Research, Vol. 11, pp 279-285.

BENNETT, J. and SCHUE, T.J. [1993a], 'Chloride Removal Implementation Guide,' Strategic Highway Research Program, Report SHRP-S-347.

BENNETT, J., FONG, K.F. and SCHUE, T.J. [1993b], 'Electrochemical Chloride Removal and Protection of Concrete Bridge Component: Field Trial,' Strategic Highway Research Program, Report SHRP-S-669.

BENNETT, J., TURK, T., and SARINELL, R.F.[1994],'Mathematical Modelling of the Effect of Current Flow Through Concrete', paper no 285, corrosion 94. The Annual Conference and Corrosion Show Sponsored by NACE International.

BENNETT, J.E. & SCHUE, T.J. [1990], 'Electrochemical Chloride Removal from Concrete: A SHRP Contract Status Report', paper 316, Corrosion 90, NACE, USA.

BERTOLINI, L. [1993], 'Effect of Electrochemical Chloride removal on Structure and Mechanical Properties of Hardened Cement Paste', Report submitted to Aston University.

BERTOLINI, L., YU, S.W., and PAGE, C.L. [1996], 'Effect of Electrochemical Chloride Extraction on Chemical and Mechanical Properties of Hydrated Cement Paste', Advanced Cement Research, Vol. 8, pp 93-100.

BOAM, K. [1988], 'Concrete Highway Structures-Current Experience of Investigation and Repair,' Concete Repair Conference, Tara Hotel, London, 16 Mar. Palladian Publication Ltd.

BRITISH STANDARD [1970], 'Loss on Ignition,' No. 4550, part 2, section 13.2.

BROOMFIELD, J.P. [1997], 'Corrosion of Steel in Concrete: Understanding Investigation and Repair,' E & F N Spon,

BROWNE, R.D. [1982], 'Design Prediction of the life for Reinforced Concrete in Marine and other Chloride Environments',Durability of Building Materials, Jul, Vol 1, No2, pp 113-125.

BUENFELD, N. [1986], 'Chloride in Concrete,' Concrete Repair, Vol. 2. A Selection of Articles reprinted from the Journals CONSTRUCTION REPAIR & MAINTENANCE / CONCRETE, Palladian Publication Limited ISBN 0 86310 027 9.

BUENFELD, N.R. & BROOMFIELD, J.P. [1994], 'Effect of Chloride Removal on Rebar Bond Strength & Concrete Properties', Corrosion and Corrosion Protection of Steel in Concrete, ed. prof R.N.Swamy, Academic Press, Sheffield, ISBN 1 85075 723 2.

BURSTEIN, G.T. [1994], 'Passivity and Locallised Corrosion' in Shreir, L.L., Jarman, R.A. & Burstein, G.T. (eds), Corrosion, 3rd. edition, pp 1.118-1.1150.

BYFORS, K. [1986], 'Influence of Silica Fume and Fly Ash on Chloride Diffusion and pH values in Cement Paste, Cement and Concrete Research Vol. 17, No. 1, pp 115-130.

CATHODIC PROTECTION OF REINFORCED CONCRETE (Status Report), [1995], Society for Cathodic Protection of Reinforced Concrete, Report No. 001.95, ISBN 0 9525190 03.

COLLINS, F.G. AND FARINHA [1991], 'Repair of Concrete in the Marine Environment: Cathodic Protection vs Chloride Extraction', Australian Civil Engineering Transaction, 33, 1, Feb.

COLLINS, F.G. AND KIRKBY, G.A. [1992], 'Electrochemical Removal of Chlorides from Concrete', in Proceeding of the RILEM International Conference Rehabilitation of Concrete Structures, ed. D.W.S ho & F. Collins, Melbourne, Australia, 31 Aug-2 Sept. 1992, pp171-177.

CONCRETE SOCIETY TECHNICAL REPORT [1985], ' Permeability Testing of Site Concrete-A Review Methods and Experience', Permeability of Concrete and its Control, London.

CONCRETE SOCIETY TECHNICAL REPORT NO. 36 [1991], 'Cathodic Protection of Reinforced Concrete', The Concrete Society, Slough.

CUSSLER, E.L. [1984], 'Diffusion, Mass Transfer in Fluid System, Cambridge University Press. ISBN 0 521 29846 6

DAMIDOT, D. and GLASSER, F.P. [1993], 'Thermodynamic investigation of the CaO-Al_2O_3-$CaSO_4$-H_2O system at 25 °C and the Influence of Na_2O, Cement and Concrete Research, Vol 23, No1, pp221-228.

DAVEY, N. [1961], 'A History of Building Materials', Poenix House, London.

DIAMOND, S. [1976], 'Cement Paste Microstructure', Conf. on Hydraulic Cement Paste: their Structure and Properties, Proc., Cement and Concrete Association, Slough, Sheffield.

DIAMOND, S. [1981], 'Effect of Two Danish Fly Ashes on Alkali Content of Pore Solutions of Cement Fly Ash Pastes,' Cement and Concrete Research, Vol. 11, No. 3, pp 383-394

ELSENER, B. and BOHNI, H. [1994], 'Electrochemical Chloride removal Field Test', Proc. Corrosion and Corrosion Protection of Steel in Concrete, Ed. R.N. SWAMY, Academic Press.

ELSENER,B., MOLINA,M. & BOHNI, H. [1992], 'Electrochemical Removal of Chlorides from Reinforced Concrete', Int. Conf. Advances in Corrosion and Protection, UMIST, Manchester, 28 June-3 July 1992.

EVANS, U.R.,[1961], 'The Corrosion and Oxidation of Metals, Arnold, London.

FARINHA, P. and PEEK, A. [1991], 'Chloride Removal From Contaminatrd Reinforced Concrete', Concrete 91 Conference, Sydney, Australia.
FHWA-RD-74-5.

GALVELE [1981], 'Transport Process in Passivity Breakdown -II Full Hydrolysis of the Metal Ions', Corrosion Science, Vol 21, No. 8, pp551-579.

GJERP, P.J. & MILLER, J.B. [1990], 'Desalination of Concrete Roof Slab, House no 556. at Umm Said , Qatar. NCT Report, 09.04.94, OSLO (project report, vol 5 no.30).

GLASS G.K and BUENFELD N.R. [1997], 'Chloride Penetration into Concrete', RILEM publication Ed. L-O Nilsson and J.P Oliver

GRACE, W.R. [1991], 'Chloride Penetration in Marine Concrete-A Computer Model for Design and Service Life Prediction,' 3rd. International Regional Management Committee Symposium, Life prdiction of Corrodible Structures, Kayai, Hawaii, November.

GREEN, W.K. [1991], 'Electrochemical and Chemical Changes in Chloride Contaminated Reinforced Concrete Following Cathodic Polarisation', MSc Dissertation, UMIST, Nov. 1991.

GREEN, W.K., LYON, S.B. and SCANTLEBURY, J.B. [1993], 'Electrochemical Changes in Chloride-Contaminated Reinforced Concrete following cathodic Polarisation', Corrosion Science, Vol. 35, No. 5-8, pp 1627-1631.

HANCOCK, P. and MAYNE, J.E.O. [1958], 'The Effect of Inhibitors of the Corrosion of Iron on the air-formed film, Journal Chemical Society, pp 4172-4175.

HANNSON, C.M. and BERKE, N.S. [1988], 'Chloride in Concrete,' Proceeding Pore Structure and Permeability of Cementitious Materials, Material Research Society Symposium Proceedings, Vol. 137, Boston.

HANSSON, C.M. [1984], 'Comment on Electrochemical Measurement of the Rate of Corrosion of Steel in Concrete', Cement and Concrete Research Vol 14 pp 374-584.

HANSSON, I.L.H. and HANSSON, C.M. [1993], 'Electrochemical Extraction of Chloride from Concrete Part 1, A Qualitative model of the process', Cement and Concrete Research, 23, pp1141-1152, 1993.

HAUSMANN, D.A. [1967], 'Steel Corrosion in Concrete. How does it Occur ?', Material Protection, 6, 11, pp19-23.

HOBBS, D.W. [1988], 'Alkali-Silica Reaction in Concrete, Thomas Telford Ltd., London.

HOLDEN, W.R., PAGE, C.L. and SHORT, N.R. [1983], 'The Influence of Chloride and Sulphates on Concrete Durability,' Corrosion of Reinforcement in Concrete Contruction, Ed. Alan P. Crane, Society of Chemical Industry, London, pp 143-149.

HOPE, B.B., PAGE, J.A., and POLAND, J.S. [1985], 'The Determination of Chloride Content in Concrete,' Cement and Concrete Research Vol. 15, No. 5 pp 863-870.

HUSSAIN, S.E. and RASHEEDUZZAFAR [1993], 'Effect of Temperature on Pore Solution Composition in Plain Cements,' Cement and Concrete Research, Vol. 23, No. 6 pp 1357-1368.

IHEKWABA, N.M., HOPE, B.B., and HANSSON, C.M. [1996(a)], 'Carbonation and Electrochemical Chloride Extraction from Concrete', Cement and Concrete Research Vol 26, No. 7, pp 1095-1107.

IHEKWABA, N.M., HOPE, B.B., and HANSSON, C.M. [1996(b)], 'Pullout and Bond Degradation of Steel Rebars in ECE Concrete', Cement and Concrete Research, Vol 26, No. 2. pp 267-282.

IRASSAR, E.F., DAMIO, A and BATIC, O.R. [1996], 'Sulphate Attack on Concrete with Mineral Admixtures', Cement and Concrete Research, Vol 26, No. 1, pp113-123. ISBN 0 419 19630 7

JOHN, V. [1992], 'Introduction to Engineering Materials', 3rd. edition McMillan ISBN 0-333-56826-5

KARLSSON, F. [1990], 'Kloridutdrivning ur betong.' Nordisk Betong 4.

KEER, J.G, CHADWICK, J.R, THOMPSON, D.M. [1990], 'Protection of Reinforcement by Concrete Repair Materials against Chloride Induced Corrosion', Corrosion of Reinforcement in Concrete, Ed by Page C.L, Treadaway K.W.J, Bamforth P.B, Society of Chemical Industry pp 420-433.

LAMBERT, P. [1983], 'The Corrosion and Passivation of Steel in Concrete', PhD. Thesis, Aston University, UK.

LAMBERT, P., PAGE, C.L. and VASSIE, P.R.W. [1991], 'Investigation of Reinforcement corrosion 2. Electrochemical Monitoring of Steel in Chloride Contaminated Concrete', Material and Structures, 24, pp351-358.

LANKARD, D.R., SLATER, J.E., HEDDEN, W.A. and NIESZ, D.E. [1975], 'Neutralization of Chloride in Concrete', Report No. FHWA-RD-76-60, pp 1-143.

LEA, F.M. [1970], 'The Chemistry of Cement and Concrete,' 3rd edition Arnold

LI, L.Y., and PAGE, C.L. [1998], 'Modellingof Electrochemical Chloride Extraction from Concrete: Influence of Ionic Activity Coefficients', Journal of Computational Materials science, Vol. 9, pp 303-308.

LOCKE, C.E., DEHGHANIAN, C. and GIBBS, L. [1983], 'Effect of Impressed Current on Bond Strength between Steel Bar and Concrete', Corrosion 83, paper no 178, NACE, USA.

LONGUET, P., BURGLEN, L. and ZELWER, A. [1973], 'La phase liquid du ciment hydrate', Revue Materiaux de Construction et Travaux Publics, 676, pp 35-41.

LYSAGHT, V.E., and DEBELLIS, A. [1969], 'Hardness Testing Hand book' American Chain and Cable Company, USA.

MALLET, G.P. [1994], 'Repair of Concrete Bridges-State of the Art Review,' Thomas Telford, ISBN 0 7277 20074.

MANNING, D.G. and IP, A.K.C. [1993], 'Rehabilitating corrosion-damage bridges through the electrochemical migration of chloride ions', ACI Fall Convention, Minneapolis.

MASLEHUDDIN, M. [1994], 'The Influence of Arabian Gulf Environment on mechanisms of Reinforcement Corrosion', PhD Thesis submitted to Aston University.

MAYS, G. [1992], 'Durability of Concrete Structures, Investigation, Repair and Protection', E & FN SPON, ISBN 0 419 15620 8.

Mc FARLAND, B.J. [1995], 'Electrochemical Chloride Extraction, experience in The United States, UK and Europe', Strategic Highway Research Program & Federal Highways Administration Implementation Program, South Dakota.

MEITZ [1997], 'Draft State of the Art Report on Electrochemical Rehabilitation methods for Reinforced Concrete Structures'.

MILLER, J.B. [1989], 'Chloride Removal and Corrosion Protection of Reinforced Concrete', Conf. Strategic Highway Research Program and Traffic Safety on Two Continent', Gothenburg, September 1989.

MILLER, J.B. [1990]'Chloride Removal and Corrosion Protection of Reinforced Concrete', VTI Rapport 352A, p117-127.

MILLER, J.B. [1994], 'Structural Aspect of High Powered Electro-chemical Treatment of Reinforced Concrete'. Corrosion and Corrosion Protection of Steel in Concrete, ed. by Prof. R.N.Swamy, Academic Press, Sheffield, ISBN 1 85075 723 2.

MORRISON, G.L., VIRMANI, Y.P., and GILLILAND, W.J. [1976], 'Chloride Removal and Monomer Impregnation of Bridge Deck Concrete by Electro-Osmosis', report No. FHWA - KS - RD - 74-1, pp 1-41.

NATESAIYER, K.C. [1990], 'The Effect of Electric Current on Alakali Silica reactivity in Concrete', PhD Dissertation, cornell University, Ithaca, New York, January.

NEVILLE, A.M. [1995], 'Concrete Technology', Longman, ISBN 0-582-23070-5

NUSTAD, G.E. [1992], 'Laboratory Investigation of the Effects of Electrochemical Treatment of Reinforced Concrete on Bond Strength', Norwegian Concrete Technologies, Oslo, Norway (Unpublished).

NUSTAD, G.E. and MILLER, J.B. [1993], 'Effect of Electrochemical Treatment on Steel to Concrete Bond Strength', Paper no. 49, Engineering Solutions to Industrial Corrosion Problems, NACE, Sandefjord, Norway, June.

PAGE, C.L AND YU, S.W. [1995(a)], 'Potential Effects of Electrochemical Desalination of Concrete on Alkali Silica Reaction', Magazine of Concrete Research, 47, 170, Mar, p23-31.

PAGE, C.L. [1988], 'Basic Principle of Corrosion,' Corrosion of Steel in Concrete, ed. P. Schiessl, Report of the Technical Committee 60-CSC, RILEM, Chapman and Hall, London ISBN 0 412 321009

PAGE, C.L. [1991(a)], COMETT Short Course on the Corrosion of Steel in Concrete, University of Oxford.

PAGE, C.L. [1992], 'Interfacial Effects of Electrochemical Protection Methods Applied to Steel in Chloride-containing Concrete', in Rehabilitation of Concrete Structures, Proc. RILEM Int. Conf. on Rehabilitation of Concrete Structures, ed. D.W.S Ho & Frank Collins.

PAGE, C.L. [1995(b)], Personal Communication

PAGE, C.L. [1997(a)], 'Cathodic Protection of Reinforced Concrete-Principles and Applications,' Proceeding International Conference Repair of Concrete Structures, Ed. Blankvoll A. Norwegian Public Road Administration, Oslo, pp 123-131.

PAGE, C.L. [1997(b)], 'Degradation of Reinforced Concrete, Process, Investigation and Control', 5 day Post-Experience Course, Aston University, UK.

PAGE, C.L. [1998], 'Corrosion and its Control in Reinforced Concrete', The 6th. Sir Frederick Lea memorial Lecture, Paper presented at 26th. annual convention of the Institute of Concrete Technology, 6-8 April, Bosworth Hall, Market Bosworth, UK.

PAGE, C.L. and TREADAWAY, K.W.J. [1982], 'Aspect of the Electrochemistry of Steel in Concrete', Nature, 297, May 13.

PAGE, C.L., and VENNESLAND, Ø. [1983], 'Pore Solution Composition and Chlroride Binding Capacity of Silica Fume Cement paste', Materiaux Et. Construction, Part 16, pp19-25.

PAGE, C.L., LAMBERT, P., and VASSIE, P.R.W. [1991(b)], 'Investigation of Reinforcement Corrosion 1: The Pore Electrolyte Phase in Chloride Contaminated Concrete.2: Electrochemical Monitoring of Steel in Chloride-Contaminated Concrete Material and Structures, Vol 24, pp 243-252.

PAGE, C.L., SHORT, N.R. and ELTARRAS, A. [1981], 'Diffusion of Chloride Ions in Hardened Cement Paste', Cement and Concrete Research, Vol 11, No 3, pp 395-406.

PAGE, C.L., YU, S.W. and BERTOLINI, L. [1994], 'Some Potential Side Effects of Electrochemical Chloride Removal from reinforced Concrete', Proc. UK Corrosion and Eurocorr 94, Vol 3, The Institute of Materials London, pp 228-238.

PARKER, D. and HAYWARD, D. [1995], 'Ioning out Problems', New Civil Engineer, January.

POLDER, R.B. [1994], 'Electrochemical Chloride Removal from Reinforced Concrete Prisms containing Chloride from Sea Water Exposure. UK Corrosion and Eurucorr 94, 31 Oct.-3 Nov., Bornemouth, pp239-248. The Cameleon Press Ltd., London.

POLDER, R.B. and HONDEL, A.J VAN DEN.[1992], 'Electrochemical Realkalisation and Chloride Removal of Concrete-State of the Art, Laboratory and Field Experience',in Rehabilitation of Concrete Structures, eds. D.W.S. Ho & F. Collins, Melbourne, Australia, 31 Aug-2 Sept.1992, p135-148.

POURBAIX, M. [1966], 'Atlas of electrochemical Equilibria in Aqueous Solutions. Pergamon, Oxford.

RASHEEDUZAAFAR, ALI, M.G. and SULAIMANI, G.J.[1993] 'Degradation of Bond between Reinforcing Steel and Concrete due to Cathodic Protection Current', ACI Material Journal, 90,1.

RASHEEDUZZAFAR, HUSSAIN, S.E., and AL-SAADOUN, S.S. [1992], 'Effect of Tricalcium Aluminate Content of Cementon Chloride Binding and Corrosion of Reinforcing Steel in Concrete', ACI Materials Journal, Vol. 89, No. 1.

RILEM [1988], 'Corrosion of Steel in Concrete', Report of the Technical Comittee 60-CSC, ed. P. Schiessl, Chapman and Hall, ISBN 0 412 32100 9.

RILEM Report [1995], 'Performance Criteria for Concrete Durability,' Eds. J. Kropp and H.K Hilsdorf, E & FN Spon ISBN 0 419 19880 6

ROBERTS, M.H. [1962], 'Effect of Calcium Chloride on Durability of Pre-Tension Wire in Pre-stressed Concrete,' Magazine of Concrete Research, Vol. 14, No. 42, pp 143-152.

ROETHELI, B.E., COX, G.K., & LITTREAL, W.B. [1932], 'Metals and Alloys,' March, Vol. 3, No. 3 cited from Steel Corrosion in Concrete: Fundamentals and Civil Engineering Properties eds., Bentur, A., Diamond, S. and Berke, N.S.,1997. E & FN SPON, SBN 7131 2277 3

SCPRC/001.95 [1995], 'Cathodic Protection of Reinforced Concrete', Status Report published by The Society for the Cathodic Protection of Reinforced Concrete, ISBN 0952190 0 3.

SERGI, G, PAGE, C.L. and THOMSON, D.M. [1991], 'Electrochemical Induction of Alkali Silica Reaction in Concrete', Materials and Structures, 24, pp359-361.

SERGI, G., YU, S.W., and PAGE, C.L. [1992], 'Diffusion of Chloride and Hydroxyl Ions in Cementitious Materials exposed to a Saline Environment', Magazine of Concrete Research, Vol. 44, No. 158, pp 63-69.

SLATER, J.E. [1983], 'Corrosion of Metals in Association with Concrete', ASTM Special Technical Publication 818.

SLATER, J.E., LANKARD, D.R., and MORELAND, P.J. [1976], 'Electrochemical Removal of Chloride from Concrete Bridges Decks', Material Performance, Vol.15, part 11, pp 21-26.

SMITH, L.L., KESSLER, R.J. & POWERS, R.G. [1993], 'Corrosion of Epoxy Coated Rebar in a Marine Environment,' Transportation Research Circular No. 403, Transportation Research Board, National Research Council, pp 36-45.

STOOP, Ben T.J. and POLDER, R.B. [1996], 'Redistribution of Chloride After ECR from Reinforced Concrete Prism', 4th. International Symposium, Corrosion of Reinforcement in Concrete Construction Eds C.L. Page, P.B. Bamforth and J.W. FIGG, SCI, Cambridge, ISBN0-85404-731-X

STRATFUL, R.F. [1974], 'Experimental Cathodic Protection of a Bridge Deck', Transportation Research Record, No. 500.

STRECKER P.P. [1987], 'Corrosion Damaged Concrete, Assessment and Repair', CIRIA, ISBN 0-408-02556-5

The concrete Society [1985], 'Permeability of Concrete and its Control,' Papaer for a one day conference, London 12 Dec. ISBN 0 946691 13 4

THOMPSON, D.M. [1991], 'Concrete Repair in Highway Bridges,' Paper presented at a one day seminar on Corrosion and Deterioration in Concrete organised by the Institute of Corrosion, Crest Hotel Bristol, UK, 3 Sept.

THOMSON, D.M. [1989], 'Effectiveness of Repair of Reinforcement Corrosion in a Motorway Viaduct', Proc. 3rd. Int. Conf. Deterioration and Repair of Reinforced Concrete in The Arabian Gulf, Bahrain, 21-24 Oct. 1989, p157-171.

TREADAWAY, K.W.J. [1991], 'Corrosion Propagation', 'COMETT Short Course on the Corrosion of Steel in Concrete, University of Oxford.

TRITTHART, J. [1989(a)], 'Chloride Binding in Cement, 1: Investigations to Determine the Compositon of Pore Water in hardened cement', Cement and Concrete Research, Vol. 19, pp 586-594.

TRITTHART, J. [1989(b)], 'Chloride Binding in Cement, 2: The Influence of the Hydroxide concentration in the pore Solution of hardened Cement Paste on Chloride Binding', Cement and Concrete research, Vol. 19, pp 683-691.

TRITTHART, J. [1996], 'Electrochemical Chloride Removal - A Case Study and Laboratory Tests., Proc. 4th. International Symposium on Corrosion of Reinforcement in Concrete Construction, Eds C.L. PAGE, P.B. BAMFORTH and J.W. FIGG, ISBN 0-85404-731-X.

TUUTTI, K. [1982] 'Corrosion of Steel in Concrete,' Swedish Cement and Concrete Institute, S-100 44-CBI, Forskning Research, Stockholm.

UEDA. T et al. [1995],'Influence of Desalination on Bond Behaviour between Concrete and Reinforcing Steel', CONSEC 95: International Conference on Concrete under Severe Conditions.

VASSIE, P. [1984], 'Reinforcement Corrosion and the Durability of Concrete Bridges', Proc. Instn. of Civil Engineers, Vol 76, part 1, pp 713-723.

VENNESLAND AND OPHASL [1986], 'Removal of Chloride from Concrete', European Patent Application 0 200 428.

VOGEL, A.I. [1978], Vogel's Textbook of Quantative Inorganic Analysis, 3rd. edition, longmans 1978.

WALKER, R.J. [1994], 'Aspects of the Prevention and Repair of ChlorideInduced Corrosion of Steel in Concrete,' PhD Thesis, Aston University, Sept.

WALLBANK, E.J. [1989], 'The Performance of Concrete Bridges', HMSO, London

WINSLOW. D.N. and DIAMOND, S. [1970], 'A Mercury Porosimetry Studies of the Evaluation of porosity in Portland Cement', Journal of Materials, Vol. 5, No. 3, pp 564-585.

WOOD, J.G.M. [1994], 'Quantifying and Modelling Concrete Durability Performance,' Meeting at Building Research Establishment, November.

YONEZAWA. T, ASHWORTH, V., and PROCTOR, R.P.M. [1988], 'Pore Solution Composition and Chloride Effects on The Corrosion of Steel in Concrete', Corrosion (Houston), Vol. 44, No. 7, pp 489-494.

YU, S.W., and PAGE, C.L. [1996], 'Computer Simulation of Ionic Migration durind electrochemical Chloride Extraction from Hardened Concrete', British Corrosion Journal, Vol. 31, No. 1, pp 73-75.

APPENDICES

APPENDIX A: The calculation of hydroxyl ion concentration

OH^- in pore solution by acid titration. Specimens treated at 5 A/m^2 for 12 weeks.
Distance from surface: 52.5 mm

Volume of pore solution	=	0.1 ml
Molarity of acid (HNO_3)	=	0.01 M
Volume of acid added	=	6.65 ml
Concentration [OH^-]	=	Volume acid x Conc. H^+/ Vol. of pore solution
	=	6.65 x 0.01 x 1000/ 0.1
	=	665 mM/l
	=	Log [OH^-] + 14
	=	Log (665/1000) + 14
	=	13.823

APPENDIX B: The calculation of chloride ion concentration

A calibration curve was plotted from chloride standards. The equation of the curve was used to compute the chloride concentration using the net absorbance value. The calibration curve is as shown in Figure A1.

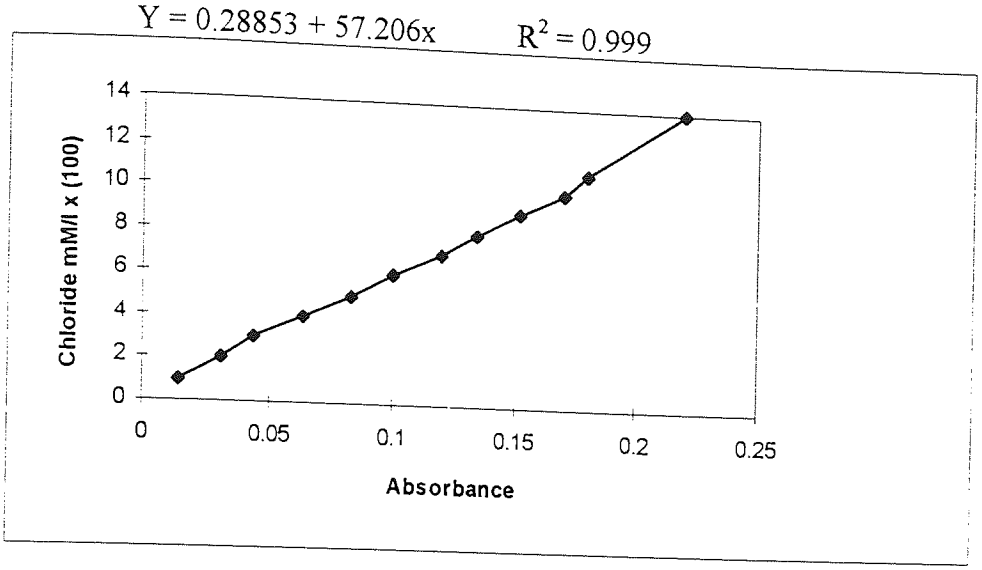

Figure A1: Chloride calibration curve

Example of calculation of free chloride; specimens treated at 5 A/m2 for 12 weeks. Distance from surface: 52.5 mm.

Dilution factor	=	2500
Absorbance value	=	0.096
Blank value	=	0.061
Net absorbance	=	0.035

Calculated chloride concentration Y	=	5727 mM/l
Pore solution chloride concentration	=	57.27 mM/l

Calculation of total chloride (acid soluble)

Mass of acid added Ma	=	50 ml
Dilution factor	=	500
Absorbance value	=	0.139
Blank	=	0.063
Net absorbance	=	0.076

Calculated chloride concentration 0.046 mM/l

Concentration of total chloride/g sample

= [conc. in (mM/l) x dilution] / [W_{950} x 1000]

= (0.046 x 500)/(0.42 x 1000)

= 0.060 mM/g

In some cases the chloride content as a percentage of sample weight was shown

Chloride concentration = total Cl x atomic mass x 100/1000
= 0.060 x 35.453 x 0.1
= 0.2 %

Calculation of bound chloride

Need to convert free chloride from mM/l to mM/g
Evaporable water (We) = 25.86 %

Free chloride (mM/g) = [Conc of soln (mM/l) x We] / (100 x 1000)
= 57.27 x 25.86 / (100/1000)
= 0.015 mM/g

Bound chloride = Total Cl - Free Cl
= 0.060 - 0.015
= 0.045 mM/g

APPENDIX C: The calculation of metal ion concentrations

The pore solution contained relatively high alkali metal ion concentrations. The calibration curve for sodium and potassium are as shown in Figure A2 and A3. The equation of the curve was used to calculate the ionic concentration from the intensity read from the spectrometer.

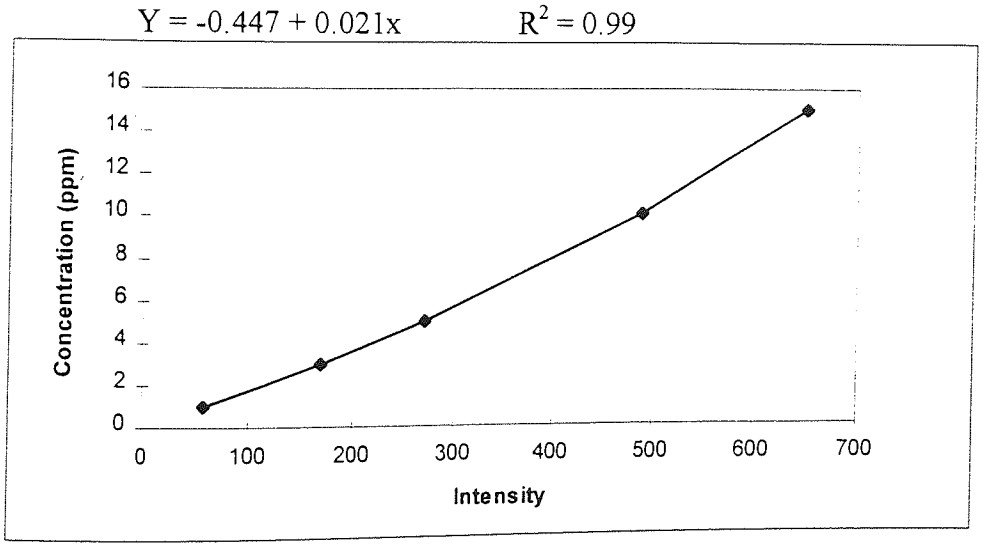

Figure A2: Calibration curve for sodium ions

Example of calculation of free sodium; specimens treated at 5 A/m^2 for 12 weeks.
Distance from surface: 52.5 mm.

Free sodium:

Max intensity 488	=	10 ppm
Sodium atomic mass A	=	22.989
Dilution	=	2500
Measured intensity	=	317
Concentration Y	=	6.21 ppm
Sodium concentration	=	[Conc (ppm) x dilution] / (atomic mass)
	=	(6.21 x 2500) / (22.989)
	=	675.34 mM/l

Total sodium:

Measured Intensity	=	419
Concentration Y	=	9.194 ppm
Sodium conc. (mM/g)	=	[Conc.(ppm) x dilution] / (A x W_{950} x 1000)
	=	[9.194 x 500] / [22.989 x 0.42 x 1000]
	=	0.48 mM/g

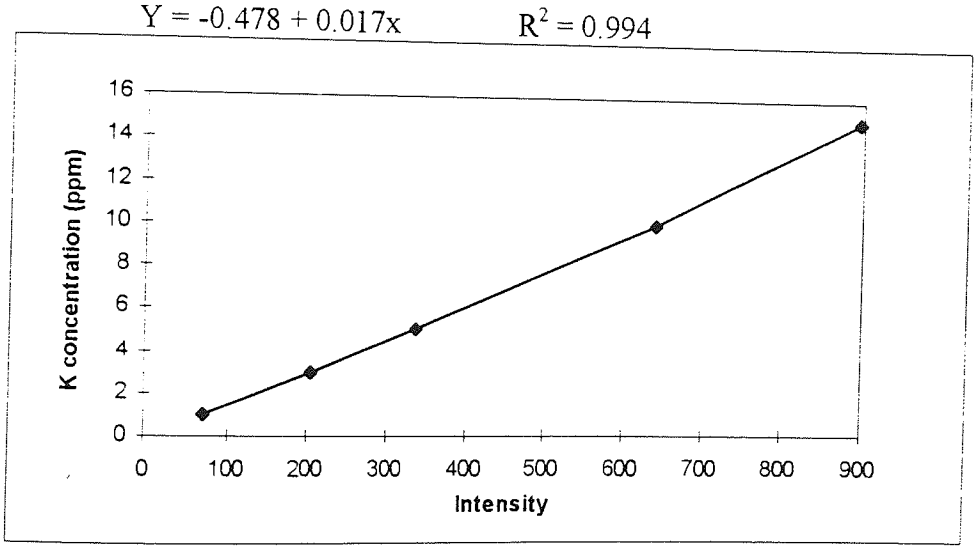

Figure A3: Calibration curve for potassium ions

Example of calculation of free potassium; specimens treated at 5 A/m^2 for 12 weeks.
Distance from surface: 52.5 mm

Free potassium:

Max intensity 895	=	15 ppm
Potassium atomic mass A	=	39.102
Dilution	=	2500
Measured intensity	=	438

Concentration Y	=	6.968 ppm
Potassium concentration	=	[Conc (ppm) x dilution] / (atomic mass)
	=	(6.968 x 2500) / (39.102)
	=	445.95 mM/l

Total potassium:

Measured Intensity	=	573
Concentration Y	=	13.482 ppm
Potassium conc. (mM/g)	=	[Conc.(ppm) x dilution] / (A x W_{950} x 1000)
	=	[13.482 x 500] / [39.102 x 0.42 x 1000]
	=	0.41 mM/g

APPENDIX D: The calculation of Sulphate ion concentrations

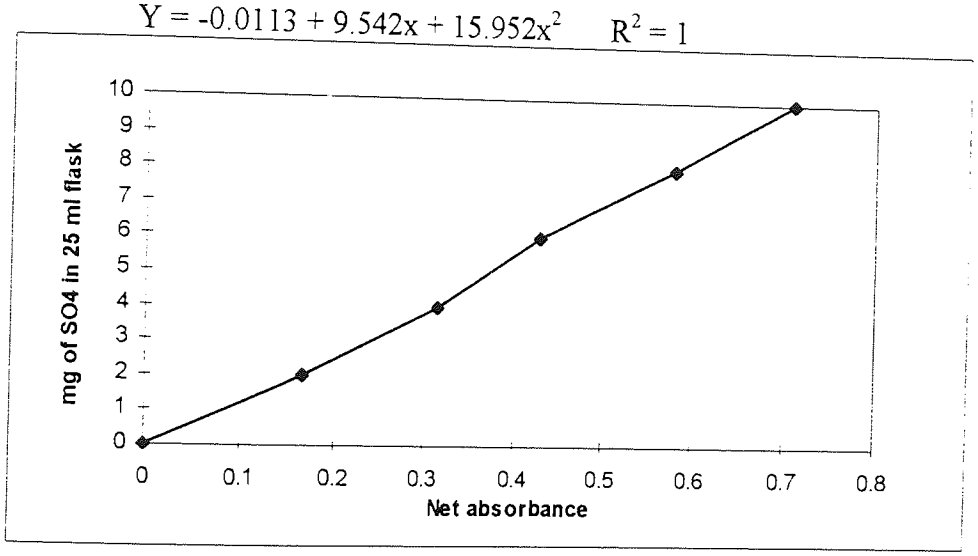

Figure A4: Calibration curve for sulphate ions

Example of calculation of sulphate; specimens treated at 5 A/m^2 for 12 weeks.
Distance from surface: 52.5 mm.

Free sulphate:

Sulphate atomic mass A	=	100
Volume of pore solution	=	0.5 ml
Absorbance value	=	0.645
Blank	=	0.017
Net absorbance	=	0.628
Concentration Y	=	8.940 Mg
Sulphate conc (mM/l)	=	[Conc (Mg) x 1000] / (A x Vol.)
	=	(8.940 x 1000) / (100 x 0.5)
	=	179 mM/l

APPENDIX E: The calculation of evaporable water

The equation below was used in the determination of evaporable water. The derivation of this equation is given elsewhere [Lambert, 1983]

Example of calculation of evaporable water; specimens treated at 5 A/m^2 for 12 weeks. Distance from surface: 52.5 mm.

Evaporable water = $(W_0 - W_{105})(100 - i + a) / (W_{950})$

Where W_0	=	2.54 g
W_{105}	=	2.09 g
W_{950}	=	1.74 g
Loss on ignition	=	0.77% g/g
Addition of NaCl	=	0.4% g/g

Evaporable water (E.W.%)	=	(2.54-2.09)x(100 - 0.77 - 0.4) / (1.74)
	=	25.8 %.

APPENDIX F: Data of Figures in Chapter 4

Table 1: Ionic concentration in pore solution after 4 weeks of desalination

Treatmentt ime (weeks)	Current density (mA/m^2)	Dis. from surface (mm)	OH^- (mM/l)	Cl^- (mM/l)	$SO_4^=$ (mM/l)	Na^+ (mM/l)	K^+ (mM/l)	Bal $\Sigma- + \Sigma+$
4	0	52.5	410	101.6	15	327.5	260.2	46.8
		45	400	203.1	12.1	412.6	260.2	45.4
		35	380	314.7	9	524.2	267.5	78.9
		25	340	452		638.7	252.9	99.6
		15	340	550		759.1	252.9	122
		5	230	431		600.5	147.1	86.6
4	1000	52.5	482	95.9	25.5	324.5	296.6	-7.8
		45	464	171.7	10.5	418.5	289.3	51.1
		35	430	300.4	10.7	521.2	282.1	51.4
		25	430	425		659.2	285.7	90
		15	400	545.0		776.7	278.4	110.2
		5	240	510.1		673.9	165.3	89.1
4	5000	52.5	520	77.3	28.1	377.3	322.2	46.1
		45	500	121.6	11.6	395.0	245.6	-4.35
		35	500	135.9	10.1	497.8	256.5	98.2
		25	520	297.5		647.5	245.6	75.5
		15	460	324.7		738.5	187	141
		5	140	201.7		350.9	19.4	28.6

Table 2: Evaporable water, pH in pore solution and free ionic content expressed as mM/g of hardened cement paste after 4 weeks of ECE

Treatment time (weeks)	Current density (mA/m^2)	Dis. From surface (mm)	We (%)	pH	Cl (mM/g)	Na (mM/g)	K (mM/g)
4	0	52.5	33.7	13.61	0.034	0.110	0.088
		45	34.4	13.60	0.070	0.142	0.089
		35	33.7	13.58	0.106	0.177	0.090
		25	35.3	13.53	0.159	0.225	0.089
		15	35.4	13.53	0.195	0.269	0.090
		5	36	13.36	0.155	0.216	0.053
4	1000	52.5	33.8	13.68	0.032	0.110	0.100
		45	31.9	13.67	0.055	0.133	0.092
		35	32.6	13.63	0.098	0.170	0.093
		25	33.2	13.63	0.141	0.219	0.095
		15	31.9	13.60	0.174	0.248	0.089
		5	33.3	13.38	0.170	0.225	0.055
4	5000	52.5	34.2	13.72	0.026	0.129	0.110
		45	33.0	13.70	0.040	0.130	0.081
		35	30.8	13.70	0.042	0.153	0.079
		25	32.8	13.72	0.098	0.212	0.081
		15	35.2	13.66	0.114	0.260	0.066
		5	31.1	13.15	0.063	0.109	0.006

Table 3: Total (acid soluble) content of chloride, sodium and potassium measured on samples of hardened cement paste after 4 weeks of ECE

Treatment time (weeks)	Current density (mA/m^2)	Dis. from surface (mm)	Cl (mM/g)	Na (mM/g)	K (mM/g)	Cl (%)
4	0	52.5	0.11	0.17	0.10	0.39
		45	0.15	0.21	0.12	0.52
		35	0.21	0.27	0.12	0.74
		25	0.25	0.29	0.11	0.88
		15	0.32	0.34	0.11	1.12
		5	0.36	0.39	0.11	1.27
4	1000	52.5	0.14	0.21	0.18	0.48
		45	0.15	0.21	0.13	0.54
		35	0.20	0.26	0.13	0.69
		25	0.23	0.31	0.13	0.81
		15	0.31	0.38	0.14	1.10
		5	0.30	0.39	0.12	1.07
4	5000	52.5	0.10	0.31	0.28	0.34
		45	0.13	0.22	0.13	0.47
		35	0.14	0.25	0.12	0.48
		25	0.19	0.31	0.13	0.66
		15	0.23	0.39	0.12	0.81
		5	0.25	0.37	0.09	0.89

Table 4: Ionic concentration in pore solution after 8 weeks of desalination

Treatment time (weeks)	Current density (mA/m^2)	Dist. from sufrace (mm)	OH^- (mM/l)	Cl^- (mM/l)	$SO_4^{=}$ (mM/l)	Na^+ (mM/l)	K^+ (mM/l)	Bal $\Sigma- + \Sigma+$
8	0	52.5	420	100.2	16.5	294	264.8	5.6
		45	400	207.4	22	410.4	276.7	35.5
		35	360	303.3	15.5	490.4	257.2	53.2
		25	330	466.3		647.9	264.8	116.4
		15	300	556.6		746.1	248.5	137.9
		5	240	423.4		574.9	129.9	41.3
8	1000	52.5	500	110.2	27.1	357.9	321.3	69.1
		45	420	177.4	21.3	403.6	258.2	64.4
		35	430	281.8	21.8	526.9	255	70.1
		25	390	380.5		609.1	218	56.6
		15	380	477.7		714.2	198.4	54.8
		5	170	344.7		461	67.8	13.8
8	5000	52.5	660	58.7	.85	.522.3	.399.7	.333.3
		45	540	84.4	30	460.7	222.5	-0.73
		35	620	137.4	30	613.7	225.6	22.11
		25	550	160.2	22	657.1	111.4	14.14
		15	230	131.6	11.6	337.3	24.3	-23.25
		5	160	45.8	2.5	47.3	12.8	-150.7

Table 5: Evaporable water, pH in pore solution and free ionic content expressed as mM/g of hardened cement paste after 8 weeks of ECE

Treatment time (weeks)	Current density (mA/m^2)	Dis. from surface (mm)	We (%)	pH	Cl (mM/g)	Na (mM/g)	K (mM/g)
8	0	52.5	30.3	13.62	0.030	0.089	0.080
		45	33.8	13.60	0.070	0.139	0.093
		35	33.8	13.56	0.102	0.166	0.087
		25	34	13.52	0.159	0.220	0.090
		15	31.5	13.48	0.175	0.235	0.078
		5	36.4	13.38	0.154	0.209	0.047
8	1000	52.5	29.7	13.70	0.033	0.106	0.096
		45	33.6	13.62	0.060	0.135	0.087
		35	33.1	13.63	0.093	0.174	0.084
		25	33.1	13.59	0.126	0.202	0.072
		15	32.9	13.58	0.157	0.235	0.065
		5	35.4	13.23	0.122	0.163	0.024
8	5000	52.5	25	13.82	0.015	0.131	0.100
		45	29.4	13.73	0.025	0.135	0.065
		35	29.4	13.79	0.040	0.180	0.066
		25	29.9	13.74	0.048	0.196	0.033
		15	30.5	13.36	0.040	0.103	0.007
		5	33.8	13.2	0.015	0.016	0.004

Table 6: Total (acid soluble) content of chloride, sodium and potassium measured on samples of hardened cement paste after 8 weeks of ECE

Treatment Time (weeks)	Current density (mA/m^2)	Dis. from surface (mm)	Cl (mM/g)	Na (mM/g)	K (mM/g)	Cl (%)
8	0	52.5	0.14	0.16	0.13	0.51
		45	0.17	0.17	0.11	0.60
		35	0.22	0.22	0.12	0.77
		25	0.30	0.27	0.12	1.07
		15	0.34	0.31	0.11	1.22
		5	0.35	0.34	0.09	1.25
8	1000	52.5	0.13	0.24	0.20	0.48
		45	0.14	0.24	0.15	0.48
		35	0.20	0.29	0.14	0.69
		25	0.23	0.35	0.14	0.82
		15	0.29	0.38	0.12	1.04
		5	0.30	0.33	0.09	1.06
8	5000	52.5	0.07	0.41	0.37	0.24
		45	0.11	0.29	0.14	0.38
		35	0.13	0.32	0.13	0.47
		25	0.16	0.39	0.09	0.56
		15	0.18	0.33	0.03	0.62
		5	0.17	0.04	0.01	0.61

Table 7: : Ionic concentration in pore solution after 12 weeks of desalination

Treatment Time (weeks)	Current density (mA/m^2)	Dis. from surface (mm)	OH^- (mM/l)	Cl^- (mM/l)	$SO_4^=$ (mM/l)	Na^+ (mM/l)	K^+ (mM/l)	Bal $\Sigma- + \Sigma+$
12	0	52.5	360	93	47.4	255.5	265.0	-27.4
		45	310	208.9	44.9	381.1	253.0	25.5
		35	280	353.3	37.4	504.4	254.1	50.4
		25	260	474.9	27.6	634.6	238.9	83.4
		15	230	541.6	56.7	728.2	220.4	63.6
		5	170	333.3	24.8	467.8	104.0	18.9
12	1000	52.5	500	98.7	47.4	373.9	323.0	3.3
		45	436	157.4	30.7	412.7	246.9	4.8
		35	440	244.6	28.6	499.5	246.9	4.5
		25	360	287.5	26.6	561.2	196.8	57.3
		15	300	341.9	31.5	629.7	141.3	66.2
		5	140	257.5	7.7	362.5	44.5	-5.9
12	5000	52.5	665	57.3	179	675.3	446.0	41.4
		45	510	73.0	92.2	584.0	181.6	-1.9
		35	410	90.2	74.5	538.3	86.9	-23.9
		25	320	91.6	69.0	435.5	22.7	-91.2
		15	80	34.4	6.8	47.3	11.8	-68.9
		5	60	34.4	4.3	13.1	3.1	-86.9

Table 8: Evaporable water, pH in pore solution and free ionic content expressed as mM/g of hardened cement paste after 12 weeks of ECE

Treatment time (weeks)	Current density (mA/m^2)	Dis. from surface (mm)	We (%)	pH	Cl (mM/g)	Na (mM/g)	K (mM/g)
12	0	52.5	29.9	13.56	0.028	0.076	0.079
		45	29.6	13.49	0.062	0.113	0.075
		35	30.2	13.45	0.107	0.152	0.077
		25	30.7	13.41	0.146	0.195	0.073
		15	31.2	13.36	0.169	0.227	0.069
		5	32.1	13.23	0.107	0.150	0.033
12	1000	52.5	31.5	13.70	0.031	0.118	0.102
		45	29.0	13.64	0.046	0.120	0.072
		35	32.3	13.64	0.079	0.161	0.080
		25	29.0	13.56	0.083	0.163	0.057
		15	38.5	13.48	0.131	0.242	0.054
		5	34.3	13.15	0.088	0.124	0.015
12	5000	52.5	25.9	13.823	0.015	0.175	0.115
		45	28.4	13.71	0.021	0.166	0.052
		35	30.4	13.61	0.027	0.164	0.026
		25	30.9	13.51	0.028	0.134	0.007
		15	29.2	12.90	0.010	0.014	0.004
		5	31.9	12.78	0.011	0.004	0.001

Table 9: Total (acid soluble) content of chloride, sodium and potassium measured on samples of hardened cement paste after 12 weeks of ECE

Treatment time (weeks)	Current density (mA/m^2)	Dis. from surface (mm)	Cl (mM/g)	Na (mM/g)	K (mM/g)	Cl (%)
12	0	52.5	0.13	0.15	0.18	0.47
		45	0.18	0.21	0.17	0.65
		35	0.23	0.27	0.16	0.81
		25	0.31	0.32	0.15	1.11
		15	0.31	0.33	0.13	1.10
		5	0.31	0.30	0.09	1.11
12	1000	52.5	0.11	0.25	0.21	0.40
		45	0.14	0.24	0.14	0.51
		35	0.18	0.27	0.14	0.63
		25	0.23	0.33	0.12	0.83
		15	0.26	0.35	0.10	0.92
		5	0.25	0.26	0.10	0.88
12	5000	52.5	0.06	0.48	0.41	0.20
		45	0.10	0.30	0.13	0.34
		35	0.12	0.35	0.09	0.44
		25	0.14	0.32	0.05	0.49
		15	0.15	0.15	0.02	0.54
		5	0.14	0.05	0.01	0.49

Table 10: Ionic concentration in pore solution for control samples

Curing time (weeks)	Current density (mA/m^2)	Dist. from surface (mm)	OH^- (mM/l)	Cl^- (mM/l)	$SO_4^=$ (mM/l)	Na^+ (mM/l)	K^+ (mM/l)	Bal $\Sigma- + \Sigma+$
8	0	52.5	528	120.2	24.2	380.5	337.6	21.4
		45	524	201.7	23.7	497.9	339.1	63.8
		35	516	293.2	23.5	598.9	336.1	78.8
		25	513	424.8	23.5	718.7	334.6	68.6
		15	510	500.3	23.2	829.1	336.1	108.5
		5	504	546.6	23.2	906.7	333.1	142.7

Table 11: Evaporable water, pH in pore solution and free ionic content expressed as mM/g of hardened cement paste for control samples

Curing time (weeks)	Current density (mA/m^2)	Dist. from surface (mm)	We (%)	pH	Cl (mM/g)	Na (mM/g)	K (mM/g)
8	0	52.5	33.8	13.72	0.041	0.129	0.114
		45	32.9	13.72	0.066	0.164	0.111
		35	30.8	13.71	0.090	0.184	0.103
		25	31.4	13.71	0.133	0.226	0.105
		15	31.6	13.71	0.158	0.262	0.106
		5	33.8	13.70	0.185	0.307	0.113

Table 12: Total (acid soluble) content of chloride, sodium and potassium measured on samples of hardened cement paste of control samples

Curing time (weeks)	Current density (mA/m^2)	Dist. from surface (mm)	Cl (mM/g)	Na (mM/g)	K (mM/g)	Cl (%)
8	0	52.5	0.13	0.17	0.14	0.46
		45	0.16	0.22	0.14	0.56
		35	0.20	0.24	0.13	0.71
		25	0.24	0.31	0.13	0.84
		15	0.29	0.38	0.13	1.04
		5	0.32	0.43	0.13	1.12

Table 13: Ionic concentration in pore solution of OPC (bulk-specimens)

Treatment time (weeks)	Current density (mA/m^2)	Dist. from surface (mm)	OH^- (mM/l)	Cl^- (mM/l)	$SO_4^=$ (mM/l)	Na^+ (mM/l)	K^+ (mM/l)	Bal $\Sigma- + \Sigma+$
12	0	52.5	360	347.6		555.7	300.3	148.4
		45	350	333.3		528.8	273.8	119.2
		35	350	347.6		548.3	284.1	134.8
		25	330	347.6		523.9	263.5	109.7
		15	330	313.3		487.2	239.9	83.8
		5	250	261.8		406.4	198.7	93.3
12	1000	52.5	800	240.3		713.0	449.6	122.2
		45	500	293.2		590.4	321.7	118.9
		35	420	316.1		540.4	273.8	78.1
		25	370	326.1		512.9	243.3	60.0
		15	290	287.5		440.4	177.9	40.7
		5	120	174.5		217.8	48.6	-28.2
12	5000	52.5	1400	130.2	203.7	1159.6	808.8	30.8
		45	500	121.6	45.1	514.9	218.8	21.9
		35	440	105.9	30.4	486.2	192.1	71.7
		25	400	130.2		491.4	118.9	80.2
		15	160	101.6		277.4	10.50	26.3
		5	50	44.4		0.76	3.14	-90.5

Table 14: Evaporable water, pH in pore solution and free ionic content expressed as mM/l of hardened cement paste (Bulk-specimens)

Time (weeks)	Current density (mA/m^2)	Dis. from surface (mm)	We (%)	pH	Cl (mM/g)	Na (mM/g)	K (mM/g)
12	0	52.5	35.5	13.56	0.123	0.197	0.107
		45	34.8	13.54	0.116	0.184	0.095
		35	34.7	13.54	0.121	0.190	0.099
		25	34.5	13.54	0.120	0.181	0.091
		15	33.8	13.52	0.106	0.165	0.081
		5	34.5	13.52	0.090	0.140	0.069
12	1000	52.5	35.7	13.90	0.086	0.254	0.160
		45	33.1	13.70	0.097	0.195	0.106
		35	34.3	13.62	0.108	0.185	0.094
		25	35.7	13.57	0.116	0.183	0.087
		15	34.0	13.46	0.098	0.150	0.061
		5	35.8	13.08	0.062	0.078	0.017
12	5000	52.5	34.5	14.15	0.045	0.400	0.279
		45	33.8	13.70	0.041	0.174	0.074
		35	34.3	13.64	0.036	0.167	0.066
		25	34.9	13.60	0.045	0.172	0.042
		15	33.8	13.20	0.034	0.094	0.004
		5	34.3	12.70	0.015	0.0003	0.001

Table 15: Total (acid soluble) content of chloride, sodium and potassium measured on samples of hardened cement paste (Bulk-specimens)

Treatment time (weeks)	Current density (mA/m^2)	Dist. from surface (mm)	Cl (mM/g)	Na (mM/g)	K (mM/g)	Cl (%)
12	0	52.5	0.25	0.32	0.16	0.88
		45	0.26	0.33	0.16	0.94
		35	0.26	0.35	0.16	0.94
		25	0.25	0.37	0.18	0.90
		15	0.26	0.33	0.15	0.93
		5	0.25	0.28	0.13	0.88
12	1000	52.5	0.19	0.39	0.21	0.69
		45	0.22	0.35	0.17	0.79
		35	0.24	0.35	0.16	0.86
		25	0.23	0.29	0.12	0.81
		15	0.25	0.28	0.11	0.89
		5	0.22	0.14	0.04	0.77
12	5000	52.5	0.14	0.64	0.35	0.51
		45	0.15	0.32	0.13	0.54
		35	0.16	0.32	0.12	0.55
		25	0.14	0.25	0.06	0.51
		15	0.18	0.15	0.01	0.64
		5	0.17	0.04	0.01	0.62

Table 16: Ionic concentration in pore solution of GGBS and PFA

Treatment time (weeks)	Current density (mA/m^2)	Dist. from surface (mm)	OH^- (mM/l)	Cl^- (mM/l)	$SO_4^{=}$ (mM/l)	Na^+ (mM/l)	K^+ (mM/l)	Bal $\Sigma- + \Sigma+$
12	GGBS 5000	50	540	164.5	38	680	175.1	74.8
		41	290	187.4	8.1	400.7	85.1	-7.77
		32	200	258.9	9.8	400.7	81	3.20
		23	180	251.8		385.1	74.3	27.6
		14	160	227.5		325.1	59.5	-2.88
		5	40	85.9		19.7	2.7	-103.5
12	PFA 5000	50	1200	130.2	135.4	1008.6	590.4	-2.07
		41	360	138.8	13	333.2	161.7	-29.8
		32	260	238.9	7.9	345.7	154.9	-13.97
		23	110	198.9		210.7	50.1	-48.1
		14	40	113		53.1	5.8	-94.21
		5	30	54.4		15.2	1.5	-67.7

Table 17: Evaporable water, pH in pore solution and free ionic content expressed as mM/g of hardened cement paste (GGBS & PFA)

Time (weeks)	Current density (mA/m^2)	Dist. from surface (mm)	We (%)	pH	Cl (mM/g)	Na (mM/g)	K (mM/g)
12	GGBS 5000	50	36.9	13.73	0.061	0.251	0.065
		41	36.9	13.46	0.069	0.148	0.031
		32	38.3	13.30	0.099	0.154	0.031
		23	36.9	13.26	0.093	0.142	0.027
		14	37.6	13.20	0.085	0.122	0.022
		5	38.9	12.60	0.033	0.008	0.001
12	PFA 5000	50	35.9	14.08	0.047	0.362	0.212
		41	38.5	13.56	0.053	0.120	0.062
		32	39.9	13.41	0.095	0.138	0.062
		23	38.4	13.04	0.076	0.081	0.019
		14	38	12.60	0.043	0.020	0.002
		5	39.7	12.48	0.022	0.006	0.001

Table 18: Total (acid soluble) content of chloride, sodium and potassium measured on samples of hardened cement paste (GGBS & PFA)

Treatment time (weeks)	Current density (mA/m^2)	Dist. from surface (mm)	Cl (mM/g)	Na (mM/g)	K (mM/g)	Cl (%)
12	GGBS 5000	50	0.19	0.56	0.20	0.66
		41	0.24	0.38	0.14	0.86
		32	0.24	0.32	0.11	0.87
		23	0.27	0.34	0.13	0.98
		14	0.26	0.29	0.11	0.94
		5	0.21	0.07	0.05	0.73
12	PFA 5000	50	0.19	0.53	0.33	0.68
		41	0.23	0.31	0.17	0.80
		32	0.26	0.30	0.16	0.92
		23	0.31	0.23	0.08	1.11
		14	0.27	0.08	0.04	0.97
		5	0.25	0.03	0.03	0.89

APPENDIX G: Microhardness Reading

Profile-specimens, 0 A/m^2 - 4 weeks						
Dist. from cathode (mm)	0.1	0.5	1.0	2.0	10.0	25.0
	43	29	37	31	37	40
	48	40	41	48	42	45
	34	40	47	36	25	31
	41	40	41	30	64	30
	34	39	46	39	37	37
	37	40	34	51	31	31
	28	35	44	33	31	29
	40	36	41	42	45	22
	39	30	47	46	40	32
	40	28	43	39	34	27
	42	34	32	34	40	32
	49	48	38	23	24	23
	43	33	37	25	27	39
	38	30	32	26	24	25
	33	39	61	34	55	36
	34	46	25	55	21	32
	31	30	54	26	43	22
	47	37	31	33	30	18
	37	37	38	24	24	37
	28	45	58	50	21	20
	46	35	41	27	26	40
	28	35	53	34	33	35
	27	45	35	59	20	24
	40	30	35	48	34	47
	34	27	27	27	26	28
	30	22	27	37	33	39
	29	36	32	24	45	29
	24	33	19	37	47	48
	41	35	33	27	31	28
	44	31	39	40	38	28

Profile-specimens, 1 A/m^2 - 4 weeks						
Dist. from cathode (mm)	0.1	0.5	1.0	2.0	10.0	25.0
	36	25	23	29	29	41
	36	29	34	27	26	46
	34	49	29	44	33	30
	21	25	23	39	43	22
	28	18	26	33	44	22
	23	25	33	43	31	29
	29	34	24	24	30	25
	37	24	21	33	30	42
	29	22	31	54	45	27
	43	31	42	29	18	41
	34	19	20	33	48	44
	27	22	23	22	30	37
	27	27	43	21	34	44
	37	21	24	25	37	34
	27	36	23	22	26	34
	20	21	32	49	20	37
	36	22	38	28	36	28
	26	30	45	23	30	46
	25	38	24	27	25	27
	27	27	24	30	35	31
	43	28	33	26	33	54
	20	25	34	32	24	25
	34	25	40	25	31	42
	25	30	24	33	32	29
	28	30	40	30	28	22
	23	33	24	21	32	36
	33	23	33	29	32	36
	42	24	21	21	29	44
	23	25	32	33	19	41
	20	33	30	28	50	33

$5A/m^2$ - 4 weeks						
Dist. from cathode (mm)	0.1	0.5	1.0	2.0	10.0	25.0
	42	25	35	42	23	47
	28	34	33	40	28	29
	29	29	30	45	51	50
	26	23	28	27	40	32
	31	25	26	33	38	39
	45	27	40	35	65	26
	25	34	43	52	50	31
	46	62	36	50	42	36
	19	23	40	31	27	27
	38	34	43	45	35	38
	17	33	26	29	43	54
	38	26	25	56	30	49
	26	23	23	25	34	40
	37	25	26	35	32	30
	27	25	12	30	25	23
	24	23	20	19	46	30
	35	24	36	24	32	33
	26	50	26	34	32	32
	26	21	19	28	28	28
	31	26	28	37	25	73
	27	31	30	30	32	62
	28	33	28	30	30	40
	31	27	36	24	33	32
	40	34	30	38	33	32
	31	35	41	24	31	39
	27	54	31	41	37	42
	25	33	29	33	35	66
	30	30	26	40	35	43
	34	27	23	39	45	42
	35	29	34	41	40	40

Profile-specimens, 0A/m^2 - 8 weeks						
Dist. from cathode (mm)	0.1	0.5	1.0	2.0	10.0	25.0
	35	34	31	28	36	32
	35	21	35	33	36	40
	41	47	41	37	41	50
	40	49	56	60	42	30
	42	19	30	17	44	40
	22	27	40	26	23	25
	63	33	35	50	42	36
	33	27	51	36	57	35
	25	65	46	55	40	35
	29	29	27	37	50	38
	37	30	56	44	29	25
	38	39	32	43	46	40
	26	49	43	31	30	23
	29	29	37	35	42	29
	51	39	41	30	41	25
	20	49	18	24	17	31
	32	42	54	33	35	53
	26	42	40	30	33	44
	32	32	56	32	25	66
	35	41	43	30	31	31
	34	34	35	27	36	39
	45	42	39	52	40	42
	44	62	27	49	48	26
	45	34	51	40	39	47
	44	62	22	25	29	42
	52	49	45	48	27	42
	52	44	26	39	37	36
	51	41	20	49	55	29
	41	59	51	36	51	29
	47	59	46	50	33	45

Profile-specimens, 1A/m^2 - 8 weeks						
Dist. from cathode (mm)	0.1	0.5	1.0	2.0	10.0	25.0
	34	29	42	36	21	54
	33	33	44	36	30	50
	41	49	66	32	40	28
	43	33	35	28	25	40
	42	36	48	45	35	46
	41	44	39	38	42	29
	47	50	40	32	37	35
	30	15	25	29	35	32
	30	22	29	45	25	50
	29	27	33	38	25	36
	46	46	30	30	27	25
	31	43	29	29	29	67
	35	37	19	19	60	36
	27	35	24	24	33	40
	34	16	50	50	48	43
	26	48	30	30	48	33
	34	39	41	41	50	37
	36	36	35	35	40	30
	42	29	33	33	24	31
	44	23	42	42	37	55
	29	26	29	24	22	21
	35	29	31	21	22	30
	31	25	30	21	24	38
	30	35	29	36	24	44
	40	24	26	28	32	44
	40	50	29	46	18	27
	30	33	44	40	15	22
	49	40	32	48	22	23
	42	30	34	23	22	51
	38	30	28	29	41	59

Profile-specimens, 5A/m^2 - 8 weeks						
Dist. from cathode (mm)	0.1	0.5	1.0	2.0	10.0	25.0
	29	29	28	31	28	25
	37	25	30	32	45	39
	31	38	42	27	30	31
	40	34	38	30	30	37
	26	25	37	32	22	36
	26	26	31	44	26	22
	40	30	30	18	67	34
	48	30	34	46	36	43
	33	33	29	60	23	20
	46	39	36	21	29	27
	29	41	31	59	42	40
	29	39	25	27	37	49
	37	37	32	31	44	36
	30	54	36	45	44	32
	34	46	36	29	44	59
	21	40	34	43	38	56
	23	27	33	25	39	36
	31	27	32	26	39	49
	28	37	33	33	57	28
	29	47	48	31	39	40
	33	41	21	25	49	28
	33	30	31	24	43	28
	33	27	36	25	15	27
	25	25	21	19	37	24
	15	31	23	26	22	23
	31	26	26	32	38	35
	22	23	28	35	38	25
	27	32	34	43	38	32
	27	28	31	31	21	32
	23	21	30	25	40	30

Profile-specimens, 0 A/m^2 - 12 weeks						
Dist. from cathode (mm)	0.1	0.5	1.0	2.0	10.0	25.0
	41	26	31	14	33	33
	19	42	29	22	29	33
	33	42	57	35	24	30
	16	39	48	35	61	30
	26	25	50	37	48	21
	36	45	56	50	42	40
	43	30	38	28	59	31
	16	43	30	38	29	24
	19	50	27	38	58	26
	24	54	25	34	58	33
	49	38	44	66	37	28
	55	35	71	49	37	35
	32	41	30	34	37	18
	38	28	30	34	28	41
	66	44	49	41	49	45
	43	44	28	16	69	64
	25	45	41	21	33	50
	39	46	34	42	29	32
	32	30	49	33	28	60
	69	31	44	41	28	32
	43	56	31	32	50	36
	23	36	57	41	23	33
	40	63	26	39	30	34
	27	49	38	38	54	37
	36	45	44	47	27	42
	25	31	27	43	33	47
	43	45	39	49	39	32
	32	41	61	27	37	36
	52	41	51	26	35	35
	52	60	28	26	31	53

Profile-specimens, 1 A/m^2 - 12 weeks						
Dist. from cathode (mm)	0.1	0.5	1.0	2.0	10.0	25.0
	20	36	36	38	30	28
	23	53	40	36	33	23
	36	38	35	37	40	30
	32	42	37	49	34	32
	27	34	32	39	47	50
	30	57	39	30	44	31
	30	34	46	39	29	57
	38	40	38	31	39	29
	22	45	33	26	42	57
	42	56	45	34	25	46
	38	36	38	26	33	38
	26	42	24	31	41	25
	29	30	34	22	33	38
	25	21	34	27	41	23
	34	41	27	50	30	23
	23	29	36	36	58	23
	27	29	54	33	58	34
	45	38	22	30	36	42
	27	47	27	25	55	33
	27	25	39	30	27	38
	11	47	44	24	34	29
	38	47	34	41	34	37
	41	18	59	61	30	37
	43	32	33	30	21	44
	23	44	22	52	47	36
	18	28	38	35	29	35
	31	46	35	41	45	65
	27	37	27	41	53	43
	45	52	38	35	53	36
	30	54	43	30	31	35

Profile-specimens, 5 A/m^2 - 12 weeks						
Dist. from cathode (mm)	0.1	0.5	1.0	2.0	10.0	25.0
	22	31	24	28	33	31
	21	24	29	28	37	18
	24	31	24	15	30	23
	22	23	19	21	39	26
	44	28	14	24	21	35
	17	21	27	20	21	31
	45	17	19	20	21	35
	31	37	25	16	37	29
	30	27	25	31	38	41
	27	20	19	17	24	37
	19	19	30	35	45	40
	58	30	17	32	40	24
	29	31	24	24	34	25
	21	39	33	24	33	39
	14	20	19	20	36	71
	20	21	35	24	58	52
	35	21	27	20	41	31
	19	23	20	20	26	26
	21	20	21	23	26	26
	26	20	26	20	33	37
	34	39	23	28	46	50
	31	40	37	32	32	30
	29	26	33	38	37	28
	25	33	33	39	26	43
	30	34	38	21	31	29
	36	45	30	38	52	25
	31	28	32	22	40	25
	31	29	32	44	30	42
	15	41	48	49	35	42
	27	39	40	44	40	29

Bulk-specimens, OPC, 5 A/m^2 - 12 weeks						
Dist. from cathode (mm)	0.1	0.5	1.0	2.0	10.0	25.0
	21	26	22	25	26	23
	24	20	24	26	21	41
	20	24	20	25	24	31
	32	22	23	26	43	33
	14	29	22	25	23	22
	16	20	19	22	23	34
	20	26	18	29	31	23
	12	27	22	34	25	23
	14	15	20	22	24	28
	34	23	22	34	22	25
	23	22	34	21	23	25
	25	17	19	27	22	32
	20	29	24	40	39	27
	22	27	25	33	20	28
	32	24	29	18	22	29
	14	21	20	30	18	29
	19	18	16	34	21	25
	23	18	21	20	24	37
	37	23	23	17	39	25
	15	23	21	15	30	28
	17	27	25	35	36	36
	20	25	24	32	35	35
	31	25	21	21	27	32
	21	22	19	21	28	21
	34	19	15	27	34	31
	22	20	28	19	20	20
	18	22	20	18	16	26
	16	26	20	28	25	26
	13	23	28	27	18	28
	28	19	21	36	20	29

Bulk-specimens, OPC, (untreated) - 12 weeks						
Dist. from cathode (mm)	0.1	0.5	1.0	2.0	10.0	25.0
	32	29	31	28	38	59
	23	33	36	31	39	50
	47	30	45	43	68	39
	54	35	45	41	43	54
	23	39	38	30	43	38
	30	41	58	39	40	46
	41	51	48	35	42	35
	24	37	33	56	39	33
	36	39	33	37	43	35
	45	53	42	46	43	35
	31	46	24	32	35	36
	22	21	23	35	34	44
	22	28	26	30	47	36
	21	31	31	28	40	45
	31	20	33	35	36	58
	22	34	31	27	36	34
	22	38	34	25	49	37
	19	36	28	37	42	49
	27	45	22	32	41	29
	26	50	34	31	35	56
	16	40	28	33	47	47
	27	37	34	40	34	45
	26	35	34	32	40	32
	28	35	36	38	43	37
	35	37	35	36	39	35
	36	34	39	43	38	45
	27	36	41	45	42	44
	31	39	40	40	45	48
	35	37	25	43	48	45
	37	39	38	46	42	47

PFA, 5 A/m^2 - 12 weeks						
Dist. from cathode (mm)	0.1	0.5	1.0	2.0	10.0	25.0
	26	14	39	39	36	32
	29	15	29	35	24	16
	29	29	19	24	26	28
	29	21	23	40	28	28
	45	17	20	36	23	22
	33	26	30	29	22	26
	27	21	42	49	28	23
	24	26	32	35	23	27
	32	40	15	38	20	32
	25	25	28	35	40	34
	12	21	15	27	35	33
	28	25	30	35	39	34
	16	38	26	20	21	33
	27	32	26	27	51	47
	14	20	32	31	46	26
	14	13	25	29	38	21
	49	19	19	29	26	34
	32	19	12	27	35	36
	23	33	45	34	45	30
	18	34	28	31	44	26
	14	19	38	48	42	32
	29	34	30	42	31	34
	28	27	29	26	22	21
	26	25	20	23	22	27
	20	20	16	25	29	24
	45	16	20	30	26	30
	34	29	22	28	38	35
	20	25	35	26	41	25
	20	34	39	37	42	35
	29	15	21	41	30	30

PFA, Untreated - 12 weeks						
Dist. from cathode (mm)	0.1	0.5	1.0	2.0	10.0	25.0
	33	21	27	38	34	43
	37	25	25	33	46	32
	45	38	16	36	34	46
	23	32	16	26	29	29
	30	20	23	42	24	22
	26	13	35	24	41	29
	29	19	21	60	22	29
	25	19	24	49	20	36
	17	33	40	29	28	36
	21	34	26	34	17	36
	25	27	29	45	38	26
	32	24	46	35	40	46
	28	23	32	28	16	44
	22	27	35	31	26	38
	33	18	35	31	25	26
	28	32	34	31	38	45
	12	36	34	34	26	31
	32	24	24	32	25	36
	25	24	32	32	37	19
	20	18	30	37	15	36
	29	32	38	38	33	30
	34	30	29	34	32	35
	26	21	26	26	30	34
	21	25	26	24	25	36
	20	18	23	30	21	39
	30	15	29	36	16	28
	32	19	34	38	30	36
	21	38	21	38	32	37
	30	30	30	46	38	30
	30	28	36	44	35	39

GGBS, 5 A/m2 - 12 weeks						
Dist. from cathode (mm)	0.1	0.5	1.0	2.0	10.0	25.0
	41	45	38	25	22	38
	40	31	29	36	31	18
	50	39	39	33	29	24
	21	29	29	27	16	35
	39	27	40	50	13	28
	44	54	33	26	14	35
	35	33	36	56	14	18
	38	44	39	20	14	44
	46	30	45	36	36	30
	34	43	26	19	30	25
	36	27	38	18	28	31
	35	19	26	19	32	27
	27	48	44	31	12	32
	30	27	39	17	24	16
	36	32	26	22	33	42
	27	38	23	21	16	26
	41	39	27	21	23	32
	25	36	22	21	29	21
	34	23	27	24	23	29
	36	28	45	18	69	16
	36	36	45	28	45	20
	34	35	40	25	42	24
	35	34	30	34	20	28
	35	50	26	31	24	26
	27	29	25	45	25	37
	34	29	29	35	15	34
	36	28	29	40	22	38
	37	25	39	32	23	30
	38	37	35	27	20	25
	46	42	40	23	19	22

GGBS, untreated - 12 weeks						
Dist. from cathode (mm)	0.1	0.5	1.0	2.0	10.0	25.0
	13	41	16	14	32	40
	20	16	21	20	25	40
	15	17	16	25	17	36
	20	15	21	25	23	26
	18	36	39	15	26	30
	33	24	20	19	44	47
	36	24	13	12	15	28
	44	34	20	12	20	47
	29	26	22	12	16	37
	46	78	17	15	21	32
	19	30	29	39	19	44
	22	49	23	42	18	27
	50	26	22	33	16	27
	34	25	27	41	27	27
	25	22	21	24	28	31
	40	18	34	16	27	19
	31	21	28	48	31	26
	35	12	27	20	25	31
	24	30	36	22	26	31
	35	39	26	23	15	45
	28	29	15	14	40	45
	30	39	32	20	27	35
	35	37	33	25	30	32
	38	32	24	29	25	28
	25	22	27	37	22	20
	23	25	21	21	23	29
	28	20	16	17	19	29
	25	30	36	25	20	37
	30	25	20	20	16	40
	35	34	15	27	14	43

APPENDIX H: Assignment of XRD peaks that are typically found in hydrating portland cement at ambient temperatures

COMPOUND	DEGREES 2-THEETA ANGLES				
AFt type					
$C_3A.3CaCl_2.H_{30}$		8.70	24.30	34.88	17.51
Ettringite $C_3A.3CS.H_{32}$		9.08	15.78	22.90	35.05 40.8
Afm type					
C_4AH_{19}	8.18	32.05	36.04	31.03	
C_2AH_8		8.26	15.62	17.65	18.80
Monosulphate $C_3A.CS.H_{12}$		9.93	19.94	40.41	22.26
Friedel's salt $C_3A.CaCl_2.H_{10}$ alpha		11.21	22.55	23.08	31.14
beta		11.32	22.78	31.14	38.96
Sulphates					
Gypsum $CaSO_4.2H_2O$		11.70	29.16	20.79	33.41
Anhydrite $CaSO_4$		12.75	31.36		
Hemihydrate $CaSO_4.1/2H_2O$	29.76	14.73	31.94	25.58	
Sodium Sulphate Thenadrite		32.17	19.03	28.04	33.80
Calcium silicate hydrates					
Type I		7.07	29.38	31.96	51.12
Type II		9.21	27.10	28.61	29.09
C-S-H gel		28.80	29.38	31.96	50.72
Other					
Hydrogarnet C_3AH_6		17.17	39.13	19.85	26.43
Calcite $CaCO_3$		29.36	35.89	39.34	43.07
Calcium Hydroxide $Ca(OH)_2$		34.06	18.09	28.68	47.64
Iron (III) Hydroxide $Fe(OH)_3$		35.02	30.81		

APPENDIX I: Data of Figures in Chapter 6

Table 19: Ionic concentration in pore solution of Bulk-OPC treated with 1 A/m^2

Treatment time (weeks)	Current density (mA/m^2)	Dist. from surface (mm)	OH^- (mM/l)	Cl^- (mM/l)	$SO_4^=$ (mM/l)	Na^+ (mM/l)	K^+ (mM/l)	Bal $\Sigma- + \Sigma+$
Untreated	0	50	360	347.6		555.7	300.3	148.4
		41	350	333.3		528.8	273.8	119.2
		32	350	347.6		548.3	284.1	134.8
		23	330	347.6		523.9	263.5	109.7
		14	330	313.3		487.2	239.9	83.8
		5	250	261.8		406.4	198.7	93.3
After 12 weeks ECE	1000	50	800	240.3		713	449.6	122.2
		41	500	293.2		590.4	321.7	118.9
		32	420	316.1		540.4	273.8	78.1
		23	370	326.1		512.9	243.3	60
		14	290	287.5		440.4	177.9	40.7
		5	120	174.5		217.8	48.6	-28.2
Retreated for 8 wks after 9 mths of storage	1000	50	580	200.3		557.6	312.9	90.2
		41	420	214.6		498.5	236.7	100.6
		32	340	246.1		455.5	195.5	64.9
		23	250	228.9		353.4	133.6	8.1
		14	200	211.7		299.7	105	-7
		5	114	133.1		154.7	38.3	-54.1

Table 20: Evaporable water, pH in pore solution and free ionic content of Bulk-OPC treated with 1 A/m^2 expressed as mM/g of hardened cement paste

Treatment time (weeks)	Current density (mA/m^2)	Dist. from surface (mm)	We (%)	pH	Cl (mM/g)	Na (mM/g)	K (mM/g)
Untreated	0	50	35.5	13.56	0.123	0.197	0.107
		41	34.8	13.54	0.116	0.184	0.095
		32	34.7	13.54	0.121	0.190	0.099
		23	34.5	13.54	0.120	0.181	0.091
		14	33.8	13.52	0.106	0.165	0.081
		5	34.5	13.52	0.090	0.140	0.069
After 12 weeks ECE	1000	50	35.7	13.90	0.086	0.254	0.160
		41	33.1	13.70	0.097	0.195	0.106
		32	34.3	13.62	0.108	0.185	0.094
		23	35.7	13.57	0.116	0.183	0.087
		14	34	13.46	0.098	0.150	0.061
		5	35.8	13.08	0.062	0.078	0.017
Retreated for 8 wks after 9 mths of storage	1000	50	33.3	13.76	0.067	0.186	0.104
		41	31.3	13.62	0.067	0.156	0.074
		32	32.0	13.53	0.079	0.146	0.062
		23	32.9	13.40	0.075	0.116	0.044
		14	34.2	13.30	0.072	0.103	0.036
		5	36.8	13.06	0.049	0.057	0.014

Table 21: Total (acid soluble) content of chloride, sodium and potassium of Bulk-OPC treated with 1 A/m^2 measured on samples of hardened cement paste

Treatment time (weeks)	Current density (mA/m^2)	Dist. from surface (mm)	Cl (mM/g)	Na (mM/g)	K (mM/g)	Cl (%)
Untreated	0	50	0.25	0.32	0.16	0.88
		41	0.26	0.33	0.16	0.94
		32	0.26	0.35	0.16	0.94
		23	0.25	0.37	0.18	0.90
		14	0.26	0.33	0.15	0.93
		5	0.25	0.28	0.13	0.88
After 12 weeks ECE	1000	50	0.19	0.39	0.21	0.69
		41	0.22	0.35	0.17	0.79
		32	0.24	0.35	0.16	0.86
		23	0.23	0.29	0.12	0.81
		14	0.25	0.28	0.11	0.89
		5	0.22	0.14	0.04	0.77
Retreated for 8 wks after 9 mths of storage	1000	50	0.18	0.31	0.16	0.68
		41	0.22	0.28	0.14	0.77
		32	0.21	0.25	0.12	0.87
		23	0.22	0.23	0.10	0.93
		14	0.25	0.19	0.08	0.96
		5	0.22	0.12	0.05	0.93

Table 22: Ionic concentration in pore solution of Bulk-OPC treated with 5 A/m^2

Treatment time (weeks)	Current density (mA/m^2)	Dist. from surface (mm)	OH^- (mM/l)	Cl^- (mM/l)	$SO_4^{=}$ (mM/l)	Na^+ (mM/l)	K^+ (mM/l)	Ca^{2+} (mM/l)	Bal $\Sigma- + \Sigma+$
After 8 weeks of curing	0	86	330	347.6	22.7	506.7	262.0		45.7
		77	330	346.2	22.7	509.2	272.3		59.8
		68	350	344.7	25.2	536.1	279.7		70.5
		59	350	347.6	22.7	553.2	291.4		101.6
		50	360	347.6	25.2	555.7	300.3		97.8
		41	350	333.3	22.7	528.8	273.8		73.8
		32	350	347.6	25.2	548.3	284.1		84.3
		23	330	347.6	25.2	523.9	263.5		59.2
		14	330	313.3	24.5	487.2	240.0		34.8
		5	250	261.8	24.7	406.4	199.0		43.8
After 12 weeks of ECE	5000	86	420	334.7	56.4	606.3	317.4		52.2
		77	490	346.2	59.0	634.9	327.3		8.11
		68	550	321.9	65.8	710.7.2	393.5		50.5
		59	780	293.2	72.9	765.5	479.4		25.8
		50	1400	130.2	203.7	1159.6	808.8		30.8
		41	500	121.6	45.1	514.9	218.8		21.9
		32	440	105.9	30.4	486.2	192.1		71.6
		23	400	130.2	16.7	491.4	118.9	0	48.2
		14	160	101.6	6.2	277.4	10.5	7.41	28.8
		5	50	44.4	3.9	0.76	3.14	12.45	-73.5
After 8 months of storage	5000	86	480	320.4	26.5	697.6.1	283.0		127.8
		77	540	326.1	30.4	739.4	303.4		115.8
		68	590	320.4	28.3	773.3	337.2		136.3
		59	660	283.2	39.3	802.0	341.4		121.7
		50	760	198.9	64.7	862.1	342.8		116.6
		41	680	150.2	36.5	723.7	279.4		99.8
		32	630	161.7	20.3	674.1	228.7		70.7
		23	500	166.0	14.3	598.5	152.7		56.5
		14	360	147.4	15.5	468	92.2		21.7
		5	220	105.9	18.6	314	3.14		-45.9

Table 23: Evaporable water, pH in pore solution and free ionic content of Bulk-OPC treated with 5 A/m^2 expressed as mM/g of hardened cement paste

Treatment time (weeks)	Current density (mA/m^2)	Dist. from surface (mm)	We (%)	pH	Cl (mM/g)	Na (mM/g)	K (mM/g)
After 8 weeks of curing	0	86	34.8	13.52	0.121	0.176	0.091
		77	34.7	13.52	0.120	0.177	0.094
		68	34.5	13.54	0.119	0.185	0.097
		59	33.8	13.54	0.118	0.187	0.099
		50	35.5	13.56	0.123	0.197	0.107
		41	34.8	13.54	0.116	0.184	0.095
		32	34.7	13.54	0.121	0.190	0.099
		23	34.5	13.52	0.120	0.181	0.091
		14	33.8	13.52	0.106	0.165	0.081
		5	34.5	13.40	0.090	0.140	0.069
After 12 weeks of ECE	5000	86	34.5	13.62	0.115	0.209	0.109
		77	32.9	13.69	0.114	0.209	0.108
		68	32.9	13.74	0.122	0.234	0.129
		59	32.5	13.89	0.095	0.249	0.156
		50	34.5	14.15	0.045	0.400	0.279
		41	33.8	13.70	0.041	0.174	0.074
		32	34.3	13.64	0.036	0.167	0.066
		23	34.9	13.60	0.045	0.172	0.042
		14	33.8	13.20	0.034	0.094	0.004
		5	34.3	12.70	0.015	0.0003	0.001
After 8 months of storage	5000	86	33.8	13.68	0.108	0.236	0.096
		77	32.6	13.73	0.106	0.241	0.099
		68	35.0	13.77	0.112	0.271	0.116
		59	32.9	13.82	0.093	0.264	0.112
		50	36.7	13.88	0.073	0.316	0.126
		41	34.8	13.83	0.052	0.252	0.097
		32	34.3	13.80	0.055	0.231	0.079
		23	32.6	13.70	0.054	0.195	0.050
		14	34.1	13.56	0.050	0.159	0.031
		5	37.5	13.34	0.040	0.118	0.001

Table 24: Total (acid soluble) content of chloride, sodium and potassium of Bulk-OPC treated with 5 A/m^2 measured on samples of hardened cement paste

Treatment time (weeks)	Current density (mA/m^2)	Dist. from surface (mm)	Cl^- (mM/g)	Na^+ (mM/g)	K^+ (mM/g)	Cl (%)
After 8 weeks of curing	0	86	0.25	0.36	0.15	0.90
		77	0.25	0.36	0.15	0.90
		68	0.26	0.35	0.16	0.91
		59	0.25	0.33	0.16	0.87
		50	0.25	0.32	0.16	0.88
		41	0.26	0.33	0.16	0.94
		32	0.26	0.35	0.16	0.94
		23	0.25	0.37	0.18	0.90
		14	0.26	0.33	0.15	0.93
		5	0.25	0.28	0.13	0.88
After 12 weeks of ECE	5000	86	0.21	0.28	0.13	0.74
		77	0.24	0.32	0.14	0.87
		68	0.24	0.35	0.15	0.86
		59	0.20	0.34	0.16	0.70
		50	0.14	0.64	0.35	0.50
		41	0.15	0.32	0.13	0.54
		32	0.16	0.32	0.12	0.55
		23	0.14	0.25	0.06	0.51
		14	0.18	0.15	0.01	0.64
		5	0.17	0.04	0.01	0.62
After 8 months of storage	5000	86	0.22	0.39	0.12	0.79
		77	0.23	0.41	0.14	0.83
		68	0.25	0.40	0.14	0.90
		59	0.22	0.42	0.16	0.79
		50	0.15	0.48	0.16	0.53
		41	0.17	0.43	0.14	0.60
		32	0.17	0.41	0.12	0.61
		23	0.14	0.33	0.08	0.51
		14	0.19	0.26	0.05	0.67
		5	0.18	0.17	0.04	0.65

Table 25: Ionic concentration in pore solution of profile-MESH treated with 5 A/m^2

Treatment time (months)	Current density (mA/m^2)	Dist. from surface (mm)	OH^- (mM/l)	Cl^- (mM/l)	$SO_4^{=}$ (mM/l)	Na^+ (mM/l)	K^+ (mM/l)	Bal $\Sigma- + \Sigma+$
After 8 months of curing	0	65	470	285.6		491.2	372.0	107.6
		55	460	393.4		676.3	350.4	173.4
		45	500	525.0		799.6	335.2	109.8
		35	440	616.1		927.6	306.3	177.8
		25	410	668.3		1031.9	256.0	209.6
		15	390	682.4		1195.9	233.1	250.7
		5	370	616.1		1010.6	201.2	225.7
After 2 months of ECE	5000	65	310	296.1		418.3	247.8	59.96
		55	500	353.3		630.6	323.1	100.4
		45	920	223.2		993.8	349.2	199.78
		35	500	269.1		735.7	134.1	100.73
		25	400	267.6		651.2	55.8	39.4
		15	160	191.3		299.5	9.7	-42.1
		5	50	77.3		7.2	3.6	-116.5

Table 26: Evaporable water, pH in pore solution and free ionic content of profile-MESH treated with 5 A/m^2 expressed as mM/g of hardened cement paste

Treatment time (months)	Current density (mA/m^2)	Dist. from surface (mm)	We (%)	pH	Cl (mM/g)	Na (mM/g)	K (mM/g)
After 8 months of curing	0	65	30.2	13.67	0.086	0.148	0.110
		55	32.4	13.66	0.127	0.219	0.114
		45	30.0	13.70	0.157	0.240	0.101
		35	30.2	13.64	0.186	0.280	0.092
		25	34.8	13.61	0.232	0.359	0.089
		15	33.6	13.59	0.229	0.368	0.078
		5	34.9	13.57	0.215	0.352	0.070
After 2 months of ECE	5000	65	28.8	13.70	0.107	0.191	0.098
		55	30.3	13.70	0.107	0.191	0.098
		45	30.6	13.96	0.068	0.304	0.107
		35	31.3	13.70	0.084	0.230	0.042
		25	31.3	13.60	0.084	0.204	0.017
		15	32.8	13.20	0.063	0.098	0
		5	34.0	12.70	0.026	0.002	0

Table 27: Total (acid soluble) content of chloride, sodium and potassium of profile-MESH treated with 5 A/m^2 measured on samples of hardened cement paste

Treatment time (months)	Current density (mA/m^2)	Dist. from surface (mm)	Cl (mM/g)	Na (mM/g)	K (mM/g)	Cl (%)
After 8 months of curing	0	65	0.19	0.20	0.15	0.67
		55	0.22	0.27	0.14	0.76
		45	0.27	0.35	0.13	0.97
		35	0.31	0.43	0.11	1.10
		25	0.37	0.51	0.10	1.30
		15	0.38	0.55	0.09	1.34
		5	0.37	0.54	0.08	1.30
After 2 months of ECE	5000	65	0.22	0.20	0.12	0.77
		55	0.24	0.27	0.13	0.85
		45	0.18	0.45	0.16	0.64
		35	0.22	0.41	0.08	0.77
		25	0.25	0.38	0.04	0.90
		15	0.28	0.23	0.02	0.98
		5	0.25	0.05	0.01	0.90

Table 28: Ionic concentration in pore solution of profile-PLATE treated with 5 A/m^2

Treatment time (weeks)	Current density (mA/m^2)	Dis. from surface (mm)	OH^- (mM/l)	Cl^- (mM/l)	$SO_4^=$ (mM/l)	Na^+ (mM/l)	K^+ (mM/l)	Ca^{2+} (mM/l)	Bal $\Sigma- + \Sigma+$
After 8 weeks of curing	0	55	528	120.2	24.2	380.5	337.6		21.4
		45	524	201.7	23.7	497.9	339.1		63.8
		35	516	293.2	23.5	598.9	336.1		78.8
		25	513	424.8	23.5	718.7	334.6		68.6
		15	510	500.3	23.2	829.1	336.1		108.5
		5	504	546.6	23.3	906.7	333.1		142.7
After 8 weeks of ECE	5000	55	1020	47.3	209.3	835.17	627.65		-23
		45	400	38.7	15.9	297.0	147.8		-26
		35	330	54.4	7.7	251.9	102.1		-46
		25	300	91.6	3.5	308.9	74.7	0	-13
		15	200	115.9	1.5	266.2	13.8	4.4	-24
		5	100	34.4	0.7	14.9	4.7	10.8	-94.7
After 3 months of storage	5000	55	510	57.3	52.6	342.7	281.6		-48
		45	430	83	27.8	325.7	181.8		-61
		35	420	103	12.3	351.2	145.3		-51
		25	350	128.8	9.4	351.2	83.8		-62.5
		15	290	138.8	5.5	351.2	22.4		-66
		5	100	63	3.7	34.5	8.9		-126.9

Table 29: Evaporable water, pH in pore solution and free ionic content of profile-PLATE treated with 5 A/m^2 expressed as mM/g of hardened cement paste

Treatment time (weeks)	Current density (mA/m^2)	Dist. from surface (mm)	We (%)	pH	Cl (mM/g)	Na (mM/g)	K (mM/g)
After 8 weeks of curing	0						
		55	33.8	13.72	0.041	0.129	0.114
		45	32.9	13.72	0.066	0.164	0.111
		35	30.8	13.72	0.090	0.184	0.103
		25	31.4	13.71	0.133	0.226	0.105
		15	31.6	13.71	0.158	0.262	0.106
		5	33.8	13.71	0.185	0.307	0.113
After 8 weeks of ECE	5000						
		55	26.9	14.01	0.013	0.224	0.168
		45	31.9	13.60	0.012	0.095	0.047
		35	31.3	13.52	0.017	0.079	0.032
		25	30.3	13.48	0.028	0.094	0.023
		15	31.5	13.30	0.036	0.084	0.004
		5	31.2	13.00	0.011	0.005	0.0
After 3 months of storage	5000						
		55	29.2	13.71	0.017	0.100	0.082
		45	32.4	13.63	0.027	0.105	0.059
		35	32.1	13.62	0.033	0.113	0.047
		25	32.5	13.54	0.042	0.114	0.027
		15	32.1	13.46	0.045	0.113	0.007
		5	31.7	13.0	0.020	0.011	0.0

Table 30: Total (acid soluble) content of chloride, sodium and potassium of profile-PLATE treated with 1 A/m^2 measured on samples of hardened cement paste

Treatment time (weeks)	Current density (mA/m^2)	Dist. from surface (mm)	Cl (mM/g)	Na (mM/g)	K (mM/g)	Cl (%)
After 8 weeks of curing	0					
		55	0.13	0.17	0.14	0.46
		45	0.16	0.22	0.14	0.56
		35	0.20	0.24	0.13	0.71
		25	0.24	0.31	0.13	0.84
		15	0.29	0.38	0.13	1.04
		5	0.32	0.43	0.13	1.12
After 8 weeks of ECE	5000					
		55	0.09	0.36	0.25	0.31
		45	0.12	0.24	0.13	0.43
		35	0.14	0.22	0.10	0.51
		25	0.18	0.27	0.09	0.64
		15	0.19	0.29	0.06	0.69
		5	0.20	0.12	0.02	0.73
After 3 months of storage	5000					
		55	0.11	0.27	0.18	0.38
		45	0.13	0.24	0.15	0.45
		35	0.16	0.25	0.12	0.55
		25	0.17	0.26	0.08	0.60
		15	0.20	0.30	0.06	0.70
		5	0.20	0.11	0.01	0.72